UNIVERSITY NOVI SAD

FACULTY OF MEDICINE

TARGETING STAT3-DRIVEN BREAST CANCER CELLS USING POLY-L-GLUTAMIC ACID-COATED LAYER-BY-LAYER NANOPARTICLES

DOCTORAL DISSERTATION

Mentors:
Prof. dr Karmen Stankov
Prof. dr Momir Mikov

Candidate:
Isidora Tošić, MPharm

Novi Sad, 2021

UNIVERZITET U NOVOM SADU

MEDICINSKI FAKULTET

UTICAJ *IN VITRO* IZLAGANJA STAT3-AKTIVIRANIH MALIGNIH ĆELIJA DOJKE VIŠESLOJNIM NANOČESTICAMA OBLOŽENIM POLI-L-GLUTAMINSKOM KISELINOM

DOKTORSKA DISERTACIJA

Mentori:
Prof. dr Karmen Stankov
Prof. dr Momir Mikov

Kandidat:
mag. farm. Isidora Tošić

Novi Sad, 2021. godine

UNIVERZITET U NOVOM SADU
MEDICINSKI FAKULTET

Obrazac - 5a

KLJUČNA DOKUMENTACIJSKA INFORMACIJA

Vrsta rada:	Doktorska disertacija
Ime i prezime autora:	Isidora Tošić
Mentor (titula, ime, prezime, zvanje, institucija)	Prof. dr Karmen Stankov, redovni profesor, Medicinski fakultet Novi Sad. Prof. dr Momir Mikov, redovni profesor, Medicinski fakultet Novi Sad
Naslov rada:	Uticaj *in vitro* izlaganja STAT3-aktiviranih malignih ćelija dojke višeslojnim nanočesticama obloženim poli-L-glutaminskom kiselinom.
Jezik publikacije (pismo):	Engleski jezik Srpski jezik (latinica)
Fizički opis rada:	Stranica: 165 Poglavlja: 8 Referenci: 290 Tabela: 4 Slika: 50 Grafikona: 105 Priloga: 0
Naučna oblast:	Medicina
Uža naučna oblast (naučna disciplina):	Biohemija i farmakologija
Ključne reči / predmetna odrednica:	STAT3 transkripcioni faktor; transkripcioni faktori; neoplazme dojke; trostruko negativni karcinom dojke; nanočestice; molekularna ciljana terapija; lipidomika; poliglutaminska kiselina

Rezime na srpskom jeziku:

Karcinom dojke je na globalnom nivou najučestalije maligno oboljenje kod žena. Prema procenama, svakoj osmoj ženi će u nekom momentu života biti dijagnostikovan karcinom dojke. Savremeni medicinski pristupi su unapredili metode lečenja i dijagnostike u zbrinjavanju pacijenata sa neoplazmom dojke, značajno poboljšavajući kvalitet života i rezultate terapije. Uprkos napretku, karcinom dojke je trenutno drugi vodeći uzrok smrtnosti uzrokovane malignitetom. Dva molekularna podtipa karcinoma dojke, hormon receptor (HR) i humani epidermalni faktor rasta 2 (HER2) pozitivni karcinomi dojke, poseduju specifične strukture na površini maligne ćelije koje su uspešno iskorišćene za dizajniranje ciljanih terapija. Date terapije omogućavaju diferencijaciju između malignog i normalnog tkiva, što rezultira selektivnom indukcijom apoptoze u malignim ćelijama. Stoga je razvoj ciljanih terapija značajno doprineo poboljšanju prognoze za pacijente sa navedenim podtipovima maligniteta dojke. Treći tip karcinoma dojke, trostruko-negativni karcinom dojke (TNBC) predstavlja njegov najagresivniji oblik, koji karakteriše izražen metastatski potencijal i visoka stopa recidiva. Pored toga, trenutno nisu poznati receptori na površini ćelijske membrane koji bi mogli razlikovati TNBC od normalnih ćelija i efikasno bili upotrebljeni za razvoj ciljanih terapija. Stoga se ovaj maligni oblik leči isključivo nespecifičnim pristupima, kao što su hemioterapija, radioterapija i hirurški zahvati. Usled svega navedenog, TNBC predstavlja tip karcinoma dojke sa najvećom potrebom za daljim rasvetljavanjem patoloških mehanizama na kojima zasniva maligno ponašanje kao i istraživanje novih strategija lečenja koje bi mogle iskoristiti dato znanje.

Prenosilac signala i aktivator transkripcije 3 (STAT3) je onkogeni transkripcioni faktor koji reguliše ekspresiju gena uključenih u esencijalne ćelijske procese, uključujući ćelijski rast, preživljavanje, proliferaciju, diferencijaciju, migraciju i imunološki odgovor. Konstitutivna aktivacija STAT3 je zabeležena u širokom spektru malignih bolesti, uključujući solidne i hematološke malignitete. Značaj STAT3 signalizacije u karcinomu dojke se odlikuje njegovom patološkom aktivacijom u 70% svih karcinoma dojke, i praktično svim trostruko-negativnim karcinomima dojke. Stoga, terapije selektivno usmerene na STAT3 imaju veliki potencijal u lečenju takvih malignih oboljenja. STAT3 je intracelularni protein koji se fiziološki aktivira kao odgovor na spoljašnje stimuluse, poput citokina i faktora rasta. Kada je aktiviran, STAT3 se translocira iz citoplazme u jedro, gde se vezuje za svoju konsenzus sekvencu od devet baznih parova u promoteru ciljnih gena i reguliše njihovu transkripciju. Budući da faktori transkripcije poput STAT3 imaju velike i relativno ravne molekularne površine kako bi omogućili interakcije sa drugim proteinima i DNK, istovremeno takva molekulska struktura je poprilično problematična za direktno vezivanje malih molekula. S obzirom na poteškoće u direktnom ciljanom delovanju na STAT3, u okviru ove disertacije smo razmotrili mogućnost da metaboličke promene

uzrokovane konstitutivnom aktivacijom STAT3 mogu predstavljati vulnerabilnost ćelija karcinoma dojke koja se može terapijski iskoristiti. Imajući u vidu da je maligna transformacija povezana sa promenama različitih ćelijskih metabolita, istražili smo kako STAT3 utiče na kvantitativnu i kvalitativnu distribuciju lipida u epitelnim ćelijama karcinoma dojke.

Kako bismo ispitali efekte konstitutivne STAT3 aktivacije na metabolički profil ćelija karcinoma dojke, inhibirali smo ili aktivirali STAT3 u dva komplementarna ćelijska sistema i potom analizirali lipidni profil korišćenjem masene spektrometrije. Otkrili smo da STAT3 vrši modulaciju nekoliko klasa lipida, sa najizraženijom redukcijom ćelijskog nivoa N-acil taurina (NAT) i arahidonske kiseline (AA). Da bismo ispitali da li je aktivacija STAT3 praćena datim metaboličkim promenama kod pacijenata, izvršili smo in silico analize obogaćivanja gena pomoću javno dostupnih podataka RNK mikromatrica od 129 pacijenata obolelih od karcinoma dojke. Potvrdili smo da je STAT3 genska signatura značajno obogaćena u uzorcima pacijenta sa niskom ekspresijom cistein dioksigenaze (CDO1) i cistationin gama liaze (CTH), dva enzima potrebna za biosintezu taurina iz homocisteina. Suprotno tome, STAT3 genska signatura je značajno obogaćena u uzorcima pacijenata sa visokom ekspresijom metaboličkih enzima AA ciklooksigenaze 2 (COX-2) i 5-lipoksigenaze (5-LOX), dok ekspresija enzima koji oslobađa AA iz plazma membrane, fosfolipaze A2 (PLA2G4A), nije u korelaciji sa STAT3 aktivnošću. Ovi nalazi ukazuju na to da aktivacija STAT3 rezultira smanjenjem ćelijskog nivoa AA i taurina modulacijom ekspresije enzima koji su uključeni u njihov metabolizam. Kako su i taurin i arahidonska kiselina uključeni u modeliranje plazme membrane, ispitali smo korišćenje datih STAT3-uzrokovanih metaboličkih promena u identifikovanju selektivnih nanonosača lekova koji bi mogli da iskoriste date lipidne karakteristke.

Analizirali smo ćelijsko vezivanje biblioteke od 12 višeslojnih (Layer-by-Layer, LbL) nanočestica (NP) koje se razlikuju u površinskom sloju, s obzirom da omotač modulira njihovu interaktivnost sa ćelijskom membranom. Otkrili smo da se NP obložene poli-L-glutaminskom kiselinom (PLE) vezuju za ćelije karcinoma dojke sa aktiviranim STAT3 sa 50% većom efikasnošću nego za netransformisane ćelije. Navedena pojava ne predstavlja nespecifičnu posledicu maligne transformacije, jer nanočestice presvučene drugim strukturama nisu pokazale dati efekat. Pored toga, svojstvo ciljanog delovanja PLE-NP nestaje kada se inhibira fosforilacija ili transkripciona aktivnost STAT3 korišćenjem ruksolitiniba i pirimetamina. S obzirom da je STAT3 konstitutivno aktiviran u gotovo svim trostruko-negativnim karcinomima dojke, ispitali smo korišćenje PLE-NP kao seletivnog pristupa ovom tipu karcinoma dojke zasnovanog na ciljanom delovanju na STAT3. Nanočestice obložene sa PLE pokazale su povećano vezanje za TNBC ćelijske linije MDA-MB-231 i SUM159PT, koje se značajno smanjuje inhibicijom STAT3 ekspresije korišćenjem dve različite kratke interferirajuće RNK (siRNK). Kako naši mikroskopski podaci visoke rezolucije pokazuju da se date nanočestice pretežno vezuju za ćelijsku membranu i ne moraju

nužno biti internalizovane u citoplazmu, dodatno smo ispitali svojstva penetracije PLE-NP u trodimenzionalne strukture organoida ćelija dojke. Rast STAT3-transformisanih organoida pokazuje izraženo veću ćelijsku gustinu uz formiranje većeg broja masivnih kolonija, te se mogla očekivati otežana penetracija nanočestica kroz tako guste ćelijske strukture. Međutim, PLE-NP su pokazale afinitet prema ćelijama sa aktiviranim STAT3 čak i u trodimenzionalnom modelu karcinoma dojke i distribuciju u dubini STAT3 transformisanih tumorskih organoida. Nakon datih otkrića, evaluirali smo translacioni potencijal ovih nalaza. Uzimajući u obzir da STAT3-transformisane ćelije pokazuju veću otpornost na citotoksične agense, ispitali smo da li bi poboljšana ciljana isporuka lekova putem PLE-NP-a pružila terapijsku prednost. Otkrili smo da PLE-NP ispunjene sa cisplatinom indukuju apoptozu ćelija karcinoma dojke sa aktiviranim STAT3, uključujući TNBC, u nižim koncentracijama u poređenju sa ćelijama kojima nedostaje STAT3 aktivnost, uključujući nemaligne ćelije dojke. Suprotno tome, STAT3-aktivirane ćelije su pokazale značajno veću apoptotsku otpornost na slobodan cisplatin kao i na nanočestice ispunjene cisplatinom koje nemaju ciljni sloj ili su obložene neciljajućim dekstran sulfatom (DXS). Ovi nalazi dodatno ističu terapijski potencijal selektivnog delovanja na maligne ćelije sa aktiviranim STAT3, korišćenjem PLE obloženih LbL nanočestica. Konačno, s obzirom da se terapija gama zračenjem često koristi u lečenju maligniteta dojke i može delovati na ćelijsku distribuciju lipida, analizirali smo njen uticaj na ćelijsko vezivanje PLE-NP. Ozračivanje ćelija poboljšalo je selektivna svojstva PLE-NP ka STAT3-transformisanim ćelijama na dozno zavisan načina, sugerišući potencijalnu sinergiju između datih terapijskih modaliteta. Rezultati ove disertacije ukazuju da ćelijske lipidne promene uzrokovane aktiviranim STAT3 mogu biti terapijski iskorišćene LbL nanočesticama obloženim površinskom poli-L-glutaminskom kiselinom. Navedene nanočestice imaju veliki potencijal za isporuku lekova malignim ćelijama dojke, uključujući trostruko-negativne ćelije karcinoma dojke, uz smanjenu toksičnost ka normalnom tkivu. Kombinovani tretman sa radioterapijom može ponuditi sinergiju sa PLE-nanočesticama i povećati njihov afinitet ciljanog delovanja. U zaključku, rezultati ove doktorske disertacije ukazuju na potencijalni novi pristup lečenju trostruko-negativnog karcinoma dojke, kome trenutno nedostaju ciljani terapijski modaliteti.

Datum prihvatanja teme od strane nadležnog veća:	23.03.2021.
Datum odbrane: (Popunjava odgovarajuća služba)	

Članovi komisije: (titula, ime, prezime, zvanje, institucija)	Predsednik: Član: Član: Član:
Napomena:	Nema

UNIVERSITY OF NOVI SAD
FACULTY OF MEDICINE

KEY WORD DOCUMENTATION

Document type:	Doctoral dissertation
Author:	Isidora Tošić
Mentor: (title, first name, last name, position, institution)	Prof. dr Karmen Stankov, full professor, Faculty of Medicine Novi Sad Prof. dr Momir Mikov, full professor, Faculty of Medicine Novi Sad
Thesis title:	Targeting STAT3-driven breast cancer cells using poly-L-glutamic acid-coated Layer-by-Layer nanoparticles
Language of text: (script)	English language Serbian language (latin script)
Physical description:	Pages: 165 Chapters: 8 References: 290 Tables: 4 Illustrations: 50 Graphs: 105 Appendices: 0
Scientific field:	Medicine
Scientific subfield (scientific discipline):	Biochemistry and pharmacology
Subject, Key words:	STAT3 Transcription Factor; Transcription Factors; Breast Neoplasms; Triple Negative Breast Neoplasms; Nanoparticles; Molecular Targeted Therapy; Lipidomics; Polyglutamic Acid

Abstract in language of publication:

Breast cancer is the most prevalent malignancy in women worldwide. It is estimated that every eight women in the world will be diagnosed with breast cancer at some moment of life. The modern medical approaches have reshaped treatment and diagnostic strategies in management of patients with breast neoplasms, significantly improving quality of life and therapy outcomes. Despite these advances, breast cancer is currently the second leading cause of all cancer-related mortality. Two of the breast cancer subtypes, hormone receptor (HR) and human epidermal growth factor receptor 2 (HER2) positive breast cancers, have specific entities on their surface successfully employed in designing targeted therapies. Such treatments enable distinction between malignant and normal tissue, resulting in selective induction of apoptosis in cancer cells. Therefore, development of targeted therapies strongly advanced the prognosis for patients with these breast cancer subtypes. The third type of breast cancers, triple-negative breast cancer (TNBC) represents its most aggressive form, characterized by substantial metastatic potential and higher recurrence rates. In addition, thus far there are no known cell surface receptors that could differentiate the TNBC from normal cells which could be efficiently employed for targeted therapy desing. Thus, this subset is treated with non-specific approaches alone, such as chemotherapy, radiotherapy and surgical procedures. Therefore, TNBC represents a subset of breast cancers with the greatest need for further elucidation of the pathological mechanisms underlying the malignant behavior and investigation of the novel treatment strategies that could exploit this knowledge.

Signal transducer and activator of transcription 3 (STAT3) is an oncogenic transcription factor that regulates the expression of genes involved in essential cellular processes including cell growth, survival, proliferation, differentiation, migration and immune response. Constitutive activation of STAT3 has been reported in a wide spectrum of malignant diseases, including both solid and hematological malignancies. The importance of STAT3 signaling in breast cancer is displayed by its abnormal activation in 70% of all breast cancers, accounting for essentially all triple-negative breast cancers. Therefore, targeting STAT3 holds a great potential in treatment of such malignancies. STAT3 is an intracellular protein that is physiologically activated in response to external stimuli, such as cytokines and growth factors. Upon activation, it shuttles from cytoplasm to nucleus, where it binds to its nine base pair consensus sequence in the promoter of its target genes to regulate their transcription. Since transcription factors like STAT3 have large and relatively flat molecular surfaces to allow protein-DNA and protein-protein interactions, it makes it challenging to directly target these proteins using small molecules. Given the difficulties in direct targeting, we considered whether metabolic changes driven by constitutive activation of STAT3 could provide vulnerability in breast cancer cells that can be exploited therapeutically. Recognizing that malignant transformation is associated with changes in a variety of cellular metabolites, we investigated how STAT3 affects lipid distribution in mammary epithelial cells, in both qualitative and quantitative manner.

To evaluate the metabolic architecture resulting from persistent STAT3 activation, we inhibited or activated STAT3 in two complementary mammary epithelial cellular systems and performed mass spectrometry-based lipid profiling. We found that STAT3 prominently modulated several lipid classes, with most profound

reduction of N-acyl taurine (NAT) and arachidonic acid (AA). To investigate if STAT3 activation was accompanied by these metabolic changes in patients, we performed in silico gene set enrichment analyses using publicly available microarray data of 129 breast cancer patients. We confirmed that STAT3 gene expression signature was significantly enriched in patient's samples with low expression of cysteine dioxygenase (CDO1) and cystathionine gamma lyase (CTH), the two enzymes required for taurine biosynthesis from homocysteine. On the contrary, STAT3 signature was highly enriched in patients' samples with high expression of AA metalytic enzymes cyclooxygenase 2 (COX-2) and 5-lipoxygenase (5-LOX), whereas enzyme that releases AA from plasma membrane, phospholipase A2 (PLA2G4A) did not correlate with STAT3 activity. These findings indicate that STAT3 activation results in reduction of cellular AA and taurine levels by modulating the expression of enzymes involved in their metabolism. As both of taurine and arachidonic acid are involved in plasma membrane remodeling, we examined utilizing these STAT3-driven metabolic alterations in identifying selective nano-size drug carriers that could exploit these lipid properties.

We screened a library of 12 layer-by-layer (LbL) nanoparticles (NP) differing in the surface layer that modulates interactivity with the cell membrane. We found that poly-L-glutamic acid (PLE)-coated NPs bind to STAT3-transformed breast cancer cells with 50% greater efficiency than to non-transformed cells. This was not a non-specific consequence of malignant transformation, as nanoparticles coated with other surface chemistries did not display such an effect. Furthermore, the targeting property of PLE-NPs was lost when STAT3 was abrogated using phosphorylation or transcriptional inhibitors, ruxolitinib and pyrimethamine. As STAT3 is constitutively activated in almost all triple-negative breast cancers, we investigated utilizing PLE-NPs as a STAT3-targeting approach for this subset of breast cancers. The nanoparticles terminally layered with PLE showed potent binding to TNBC cells MDA-MB-231 and SUM159PT, and the heightened NP-cell binding was attenuated when STAT3 expression was diminished using two different small interfering RNAs (siRNAs). As our high-resolution microscopy data indicates that these nanoparticles predominantly bind to cell membrane and might not necessarily be internalized into the cytoplasm, we further examined the tumor penetrating properties of PLE-NPs in three-dimensional breast cell organoids. STAT3-transformed organoids grew at much higher cellular density and formed greater numbers of massive colonies, which could have been expected to impede penetrating ability of nanoparticles through such dense cellular structures. However, PLE-NPs displayed affinity towards STAT3-driven cells even in the three-dimensional breast cellular model and distributed in depth of the STAT3-transformed tumor organoids.

Next, we examined the translational potential of these findings. As STAT3-transformed cells show greater resistance to cytotoxic agents, we evaluated if enhanced targeted delivery via PLE-NPs would provide a therapeutic advantage. We found that cisplatin-loaded PLE-NPs induced apoptosis of STAT3-driven breast cancer cells, including TNBC, at lower concentrations compared to cells lacking activated STAT3. On the contrary, these cells showed significantly greater resistance to apoptosis induced by either un-encapsulated cisplatin or cisplatin-loaded NPs lacking the targeting layer or coated with a non-targeting dextran sulfate (DXS). These findings further emphasize the therapeutic potential of targeting STAT3-driven cells using

PLE-coated LbL nanoparticles. In addition, since radiation is commonly used in breast cancer treatment and may alter cellular lipid distribution, we analyzed its effect on PLE-NP-cell binding. Irradiation of cells enhanced the STAT3-targeting properties of PLE-NPs in a dose-dependent manner, suggesting potential synergies between these therapeutic modalities.

These findings suggest that cellular lipid changes driven by activated STAT3 may be exploited therapeutically using uniquely designed LbL nanoparticles complemented with surface poly-L-glutamic acid. These nanoparticles hold great potential for the delivery of anticancer agents to breast malignant cells, including triple-negative breast cancer cells, with decreased toxicity in normal tissue. The combination treatment with radiotherapy may offer synergy with PLE-nanoparticles and enhance their targeting affinity. Taken together, the results of this dissertation indicate a potential novel treatment approach to triple-negative breast cancers, which currently lack targeted therapeutic options.

Accepted on Scientific Board on:	23.03.2021.
Defended: (Filled by the faculty service)	
Thesis Defend Board: (title, first name, last name, position, institution)	President: Member: Member: Member:
Note:	None

I would like to thank my mentors, Professor dr Karmen Stankov and Professor dr Momir Mikov for the support, help and knowledge they devoted to me through my professional education. Their support during my doctoral studies and preparation of my doctoral dissertation is a part of much greater picture – shaping a young professional in pharmacy and medical sciences.

I am immensely grateful to Professor dr David Frank, who gave me the opportunity of conducting this exceptional research in Frank's laboratory. Thank you for your generous support throughout these years and teaching me how to think scientifically. By continually giving a personal example of a patient, kind and professional mentor, David helped me grow as a scientist but also as a person. I could not have asked for a better teacher.

My gratitude goes to my committee members, Professor dr Viktorija Dragojević Simić, Profesor dr Velibor Vasović and Ass. Professor dr Jasmina Katanić for their critical feedback and support through the preparation of my dissertation.

I would like to thank my lab coworkers for their knowledge sharing, endless experimental discussions and providing me the pleasure of working with a smile. It would not have been so if I was not surrounded by great people with such wonderful ambitions and personalities. I am particularly grateful to Sarah Walker, who despite her extremely busy schedule invested her time to teach me as much as possible. I could only return such a favor by passing it on to the future generations of scientist to come.

I am grateful to all of my dearest friends, both from my wonderful hometown Novi Sad and from my today's home Boston, who kept me smiling during all these years. They take an important part in this milestone, which I would hardly reach without so much love, laugh and support.

I would not be here without having a perfect soulmate by my side through all these years. I would like to thank Vanja for his infinite patience, love and joy he is giving me every day. Every challenge is an adventure with you.

Finally, I would like to thank my dearest family, mom, dad and Miloš, for always being there for me. They taught me that family matters the most and is the foundation of each individual. Nothing can break our dreams when we support and care for each other.

These people are the root of my strength and enthusiasm. They all contributed to achieving this goal and share a significant part in it. Most importantly, they helped me become the person I am today and will always be the source of my happiness and aspirations.

Isidora Tošić

Table of Contents

1. Introduction

1.1. *Breast malignancies*

1.1.1. Epidemiology of breast cancer

Breast malignant neoplasm is the most frequently diagnosed malignancy in women worldwide, including both developing and developed countries (Figure 1). It was estimated that more than 2 million patients were newly diagnosed with breast cancer in 2018, accounting for 25-30% of total malignancy incidence in 185 investigated countries (1). The incidence of breast cancer had a rising trend in the last decade (0.4% yearly), likely due to the increasing obesity epidemic, changes in reproductive factors and use of menopausal hormone therapy (2,3). Furthermore, breast cancer is the leading cause of cancer-related mortality in women in the majority of world countries, with estimated 600 000 deaths in 2018 (Figures 2 and 3) (1). Analogical statistical observations were reported in the Republic of Serbia, with breast cancer comprising 26% of incidence and 17.5% of total cancer-associated mortality, with similar statistical trends reported in Vojvodina region (4,5). Development of new diagnostic and therapeutic strategies in the last decades had a significant impact on the treatment outcomes, as evidenced by increased breast cancer patient's five-year survival from 75% (1975-1977) to 90% (2005-2011) (3,6). Patients diagnosed during the early stages of the disease have promising chances for a successful therapy. However, based on the 2019 USA National Center for Health Statistics report, less than 25% of newly diagnosed patients are discovered as *in situ* tumors (3,7). Although majority of breast cancers have not developed metastases at the moment of diagnosis, almost one third of the patients diagnosed with *in situ* tumor will encounter metastatic dissemination eventually (7,8). If the disease is diagnosed when tumor has already disseminated to distant tissue, therapeutic options are limited and five-year survival decreases to only 26% (3). The most frequent mortality cause of breast cancer is metastatic dissemination in lymph nodes, bones, liver, lung and CNS (8).

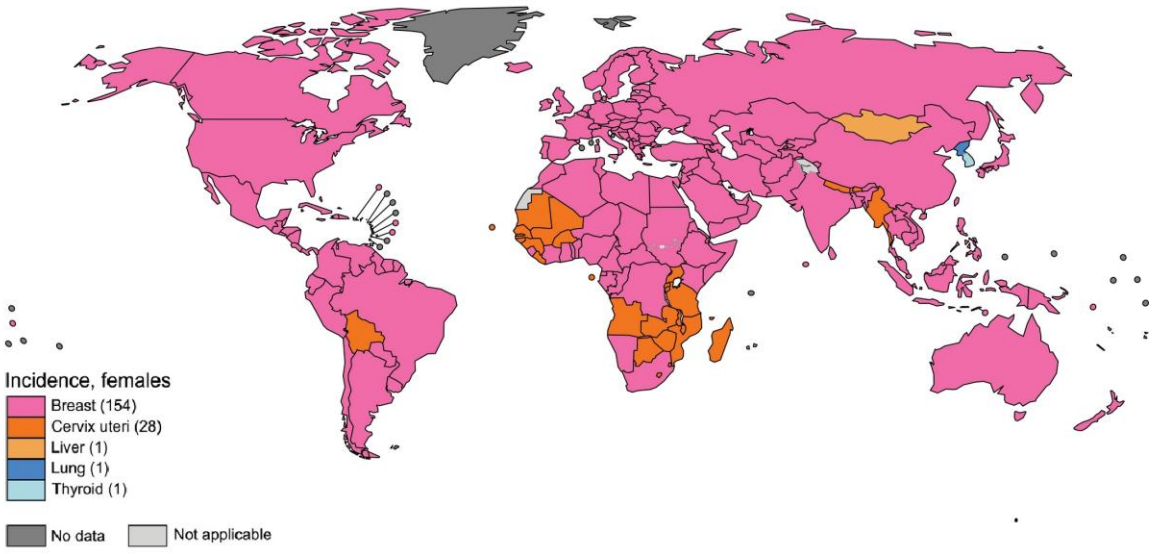

Figure 1. World map of estimated malignancy types with the highest incidence in each of the 185 investigated countries in female population. Breast cancer is most frequently diagnosed malignancy in 154 of 185 investigated countries. (1).

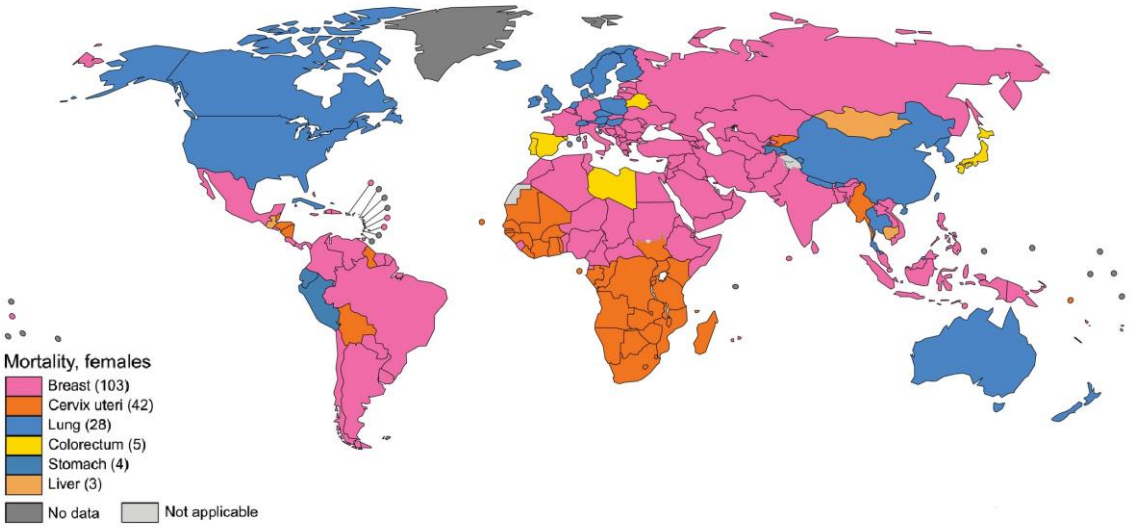

Figure 2. World map of estimated malignancy types with the highest mortality in each of the 185 investigated countries in female population. Breast cancer is the leading cause of cancer-related mortality in 103 of 185 countries. (1)

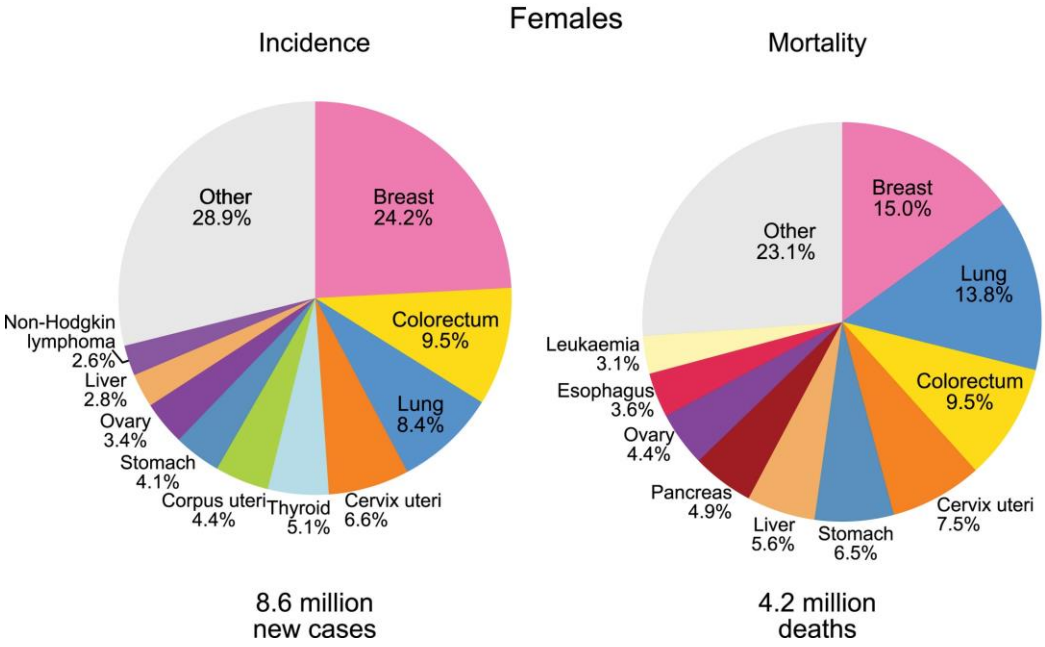

Figure 3. Estimated incidence and mortality of the most common malignancies in women worldwide in 2018. Breast cancer is the most frequently diagnosed and the leading cause of cancer-related mortality in women comprising 24.2% and 15% of all malignant cases, respectively. (1)

1.1.2. Treatment approaches

The strategy for treatment of breast cancer is most commonly multimodal and includes combination of surgical methods and/or radiotherapy as local treatments; and systemic therapy that comprises of chemotherapy, hormonal and targeted therapy (6). Since the proper therapy choice highly depends on the type of breast cancer, breast cancer classification is continuously being improved according to the disease stage, anatomical region and molecular basis of malignant cells.

1.1.3. Breast cancer classifications

Traditional classification of breast cancers systemizes them in accordance with their anatomic region into ductal, lobular, nipple and not otherwise specified breast cancers.

TNM classification of malignant tumors by The Union for International Cancer Control (UICC) classifies the tumors based on the extent of malignant spread, focusing on tumor size (T), lymph node status (L) and occurrence of metastasis (M). The diagnosis is based on clinical, radiological and laboratory screening of the patient. According to TNM, breast cancers can be sorted into 4 phases. The tumor is classified into the first stage when it is localized in the breast tissue, which is categorized as the second or third phase if spread to surrounding tissue and adjacent lymph nodes. The last, forth stage represents a tumor that has disseminated and metastasized to distant organs. Local therapy achieves better results in treatment of early stages malignancies. Thus, all patients with non-metastatic breast cancer are recommended a surgical tumor resection and considered for postsurgical radiation. Additionally, adjuvant chemotherapy is recommended for patients with high risk of postoperative disease recurrence (7,9). At advanced stages, the effect of localized treatment is attenuated and systemic approaches are more desirable, thus the treatment of stage four breast cancer mainly comprises of pharmacological approaches (8). The metastatic breast cancer is hardly curable and the management of patients with advanced and metastasized disease is focused on extending the life while minimizing disease symptoms and therapy side effects. The adequate choice of systemic therapy for all disease stages, using targeted agents or non-specific chemotherapy, greatly depends on the molecular characteristics of breast cancer cells.

Determination of appropriate therapy for breast cancer patients strongly depends on the molecular type of cancer cells. Pathological proliferation and survival of cancer cells commonly depends on the specific molecule that acts as an oncogenic driver, thus its suppression results in apoptosis. These specific molecules can serve as targets for both distinction of malignant cells among non-malignant tissue and for efficient induction of apoptosis in malignant cells. Therefore, determining molecular basis of breast cancer cells by molecular biology methods, such as immunohistochemistry, provides prediction of the therapy that the cancer cells is susceptible to respond to (10).

1.1.4. Molecular types of breast cancer

There are three molecular types of breast malignant cells. Based on the expression of hormone receptors (HR) for estrogen (ER) and progesterone (PR), and human epidermal growth factor receptor 2 (ERBB2, also known as HER2), breast cancers can be sorted into three groups: hormone receptor positive (70% of patients), ERBB2 positive (15-20%) and triple-negative tumors that do not express any of the three molecular markers (15-20%) (8).

Luminal breast cancers express hormone receptors for estrogen and/or progesterone,

and can be divided into subtypes A and B. Luminal A type is the most common type of breast cancer worldwide and usually develops and grows slowly. The subtype B is more aggressive than A, and in addition to hormone receptors, it can be characterized by HER2 overexpression. Therefore, the treatment for both subtypes includes hormonal therapy, whereas subtype B can be additionally complemented with HER2-targeted agents and chemotherapy for prevention and management of possible metastatic developments (8,11).

ERBB2 positive breast cancers cells are defined by overexpression of the ERBB2 transmembrane receptor tyrosine kinase or by detection of gene copy amplification of this oncogenic driver (12). This molecular subtype can be both hormone receptor positive and negative, with approximately equal allocations (8). HER2 signaling results in aggressive malignant phenotype, with higher tendency for metastatic development than HR positive breast cancers. However, development of HER2-targeted approaches significantly improved patient prognosis, resulting in survival of patients with metastatic cancer of approximately 5 years, while 75% of all HER-2 positive patients achieve a pathological complete response (8). The most widely used targeted therapy against HER2 receptor is monoclonal antibody trastuzumab (Herceptin®). Other used inhibitors include pertuzumab (Perjeta®), also HER2 antibody, as well as lapatinib (Tykerb®) and neratinib (Nerlynx®) that are dual inhibitors of tyrosine kinases. Lapatinib and neratinib dysregulate signaling pathways of both HER2/neu and epidermal growth factor receptor (EGFR), which is also commonly overexpressed in breast cancers (13). The combination of targeting agents towards HER2 and/or EGFR with chemotherapy showed favorable outcomes in these patients resulting in augmented response rates, extended progression-free survival and prolonged overall survival in comparison with chemotherapy alone (14). Compliant with current treatment recommendations, targeted therapy is given in addition to non-specific chemotherapy, including taxanes (paclitaxel, docetaxel), doxorubicin, cyclophosphamide and platinum-based antineoplastic such as carboplatin (8).

Basal or triple-negative breast cancer (TNBC) represents a heterogeneous form of breast cancer whose cells do not express ER, PR nor overexpress HER2 receptor (15). In spite of the relatively low prevalence (15-20%), this is the most aggressive and most challenging breast cancer type to treat, therefore representing a substantial fragment of the total breast cancer patient mortality (13). Triple-negative breast cancers have a high tendency for metastatic development and even if the patient achieves remission, risk of relapse is higher than in other molecular types. In case of metastatic TNBC development, the overall median survival is drastically shorter than for the same stage disease of the other two subtypes, which is approximately one year versus five years, respectively (8). TNBCs are particularly difficult to treat due to the absence of known molecular target such as previously described membrane receptors in other types. Standard treatment comprises of nonspecific

therapy such as surgical methods, radiation and chemotherapy which generally involves taxanes, anthracyclines and cyclophosphamide (15). Therefore, this is the breast cancer type with the vital requirement for development of novel therapeutic modalities.

Other molecular characteristics, such as EGFR, androgen and folate receptor expression, mutations in *PTEN* or *PIK3CA* genes encoding phosphatase and tensin homolog (PTEN) and phosphoinositide 3-kinase (PI3K) proteins, are being evaluated in attempts to design more specific cancer-directed therapies (16). However, the current predictive factors for effective targeted therapy remain HER2 overexpression and hormone receptor status solely. Although therapeutic options such as hormonal therapy and antibodies possess beneficial targeting properties and specificity, other approaches are characterized by lack of selectiveness with following insufficient efficacy, along with systemic toxicity and damage to healthy tissue (17). Therefore, better understanding of etiology of breast and other malignancies through elucidating their biologic and genomic backgrounds might provide a novel target for distinction of malignant cells as the basis of selective therapy. Along with development of novel technologies to exploit these malignant features, such researches may improve treatment of this highly prevalent and frequently lethal disease.

1.2. *Etiology of malignant transformation*

Etiology of malignant diseases is most commonly multifactorial, comprising of hereditary, environmental and life style factors mutually interacting to initiate and drive the tumor development. Unraveling the molecular aspects is highly important for understanding the biology of malignant cells, identification of patients with predisposition for cancer development and thus application of prevention measures, determination of appropriate patient-specific therapy and establishment of new therapeutic modalities.

Human genome is characterized by high level of diversity resulting in specific genotype and phenotype of each individual. The human genome contains 19,116 protein-encoding genes and a similar number of genes encoding non-coding ribonucleic acids (ncRNA) (18). Along with studying the sequences of gene-coding segments of genome or exons, major role is played by the non-coding regions, which are the regulatory regions or introns. The transcriptional products that do not translate into the functional proteins, such as micro RNA (miRNA) and long non-coding RNA (lncRNA) delicately modulate the transcription levels of other genes and may recruit chromatin regulators to DNA regions whose transcription they modulate (19). Genome sequence variants in both exons and introns can result in alteration of final protein synthesis and function (20). In addition, elements that regulate the processes of gene transcription, translation and posttranslational modifications

strongly affect the consequential phenotypical manifestations without alteration of DNA sequence. Gene expression control is one of the fundamentals for normal development, differentiation and function of cells and its impairment is often the cause of various pathophysiological manifestations, which is particularly profound in etiology of malignant disorders (21). Therefore, epigenetics, transcriptomics, proteomics and metabolomics, or rather their combination studied by multi-omics gained increasing attention when studying the biological backgrounds of malignant pathogenesis as well as strategies to prevail them. Multi-omics approach has thus far revealed great number of key mutations, signaling pathways, proteins, metabolites and other molecules which may represent potential targets for therapeutic intervention (22). Therefore, it can provide a foundation for development and application of personalized medicine for treatment of diverse number of malignant neoplasms, including breast cancer.

1.2.1. Genetic background of malignant development

Oncogenesis represents a multistep process in alteration of genes and their products of transcription involved primarily in cell growth, proliferation, differentiation, apoptosis, angiogenesis and immune response, as the essential cellular processes whose impairment characterizes malignant cells. According to their role in the context of their physiological activities, genes implied in the tumorigenesis can be sorted into three groups: tumor suppressors, oncogenes and genes involved in DNA repair mechanisms (20).

- Proto-oncogenes are genes which are controlling normal cell growth, differentiation and proliferation by stimulating them to a physiological extent, thus can become major oncogenic drivers in case of mutation or aberrant hyper-stimulation. Upon activation, proto-oncogenes become oncogenes, and are assorted generally within the major protein classes of protein kinases, G-protein coupled receptors, transcription factors, cytokines and growth factors.
- Tumor suppressors are genes whose active role involves inhibition of cell growth, proliferation and other vital processes in oncogenesis. In malignant manner, the normal function of these genes is frequently suppressed, either by loss-of-function mutation, reduction of expression, for instance by pathological epigenetic silencing of their expression, or some other means of inhibition.
- Genes involved in DNA damage repair have a vital function in maintenance of genome integrity, thus their impairments result in expanding the DNA damage with each new replication. While impairment of each of these genes may initiate malignant transformation, combined disruption of multiple genes within these three groups additionally increases the risk for malignant development (20,23).

1.2.2. Hereditary predispositions for tumorigenesis

Human malignancies can be hereditary or sporadic. Hereditary malignancies are caused by mutated gene in germline epithelial cells, commonly in terms of cell cycle regulation and DNA repair and are expressed ubiquitously. They represent the basis for 5-10% of all malignancies. Even if the mutation occurs, it often requires additional factors for the disease to manifest, such as DNA damage in somatic cells or other somatic mutations and impairments (24). The likelihood of malignancy development depends both on the penetrance of each of the mutated genes together with their interactions, along with interactions with the environmental factors. However, significant percent of the mutation carriers will eventually develop the malignancy, and thus it is important for individuals with family history of malignancy to investigate their genetic background. Identification of patients with high risk for tumor development can have a strong impact through preventive measures. With that regards, preventive salpingo-oophorectomy in patients with risk of ovarian cancer, or tamoxifen treatment in patients with risk of breast cancer development, as determined by presence of breast cancer 1 or 2 (*BRCA1/2*) gene mutations, reduce the risk of cancer development by 85 and 60%, respectively (25-27). Among the frequent drivers of hereditary malignancies are mutations of *BRAF* gene in lymphoblast leukemia, *KRAS* in stomach cancer, *MET* in kidney cancer, *PTEN* and *P53* in various multi-organ malignancies and *BCRA1/2* which represents 80-90% of all hereditary breast and ovarian cancers (20).

More common are sporadic tumors, representing 90-95% of prevalence of all malignancies. Sporadic malignancies occur as a result of acquired somatic mutations without an obvious hereditary pattern. These mutations may be triggered during the course of life time by the environmental exposure to carcinogens, such as radiation, tobacco smoke and asbestos. Such agents are known to induce DNA damage, which if not successfully repaired by the DNA damage repair machinery, result in potentially tumorigenic mutation. Additionally, chronic inflammation and/or increased and prolonged hormone levels create a favorable environment for tumor development, as a number of cell cycle controlling factors are regulated by cytokines and hormones (28). For instance, high estrogen levels, originating from endogenous or exogenous sources, are a major factor in development of breast malignancies, as it stimulates mammary cell proliferation (29). Malignant transformation may be facilitated through altered function of specific modulators of vital cellular functions, commonly through transcriptional regulation of genes governing these essential mechanisms (19,30). Regulation of gene expression represents a complex and tightly controlled process which leads to manifestation of function and maintenance of cell homeostasis (19). Gene expression regulation provides a wide range of cell-specific features and functions specifying the cell type and controlling specific pathways (30). Therefore, transcriptomics and epigenetics have an inevitable importance, as alterations of transcription factors, cofactors,

chromatin regulators and non-coding RNAs have crucial roles in manifesting a certain phenotype. The gene expression regulation is particularly important in malignant transformation and concomitant events governing malignant behavior and maintaining survival of these cells, including angiogenesis, migration and immune evasion. The focus of this dissertation will be on the role of transcription factors in malignant behavior of breast cancer cells. In particularly, we will focus on the oncogenic signal transducer and activator of transcription 3 (STAT3), the transcription factor commonly upregulated in breast cancers and initiator of tumorigenesis and aggressive malignant cellular behavior.

1.2.3. Transcription factors

Transcription of the genetic information from DNA to mRNA is a fundamental cellular process, displayed by the complex mechanisms and apparatus of intertwined elements required for manifestation of transcription and providing its tight control. The enzyme that catalyzes mRNA synthesis based on the DNA sequence is RNA polymerase II (Pol II) (30). In order to perform its activity, Pol II needs to gain access to the gene core promoter sequence, which is adjacent to the transcription start site responsible for transcription initiation (31). The access to promoter is restrained by chromatin, thus Pol II admission is dependent on nucleosome shifting and chromatin opening, which is differently regulated for various promoter sites, such as by chromatin modelling, DNA methylation, demethylation, acetylation and deacetylation as well as by transcription factors (19).

The human genome encodes more than 1600 transcription factors (TFs), whose function is often cell-type specific to assure the proper expression of genes in a tissue-specific manner (19). Transcription factors, also known as *trans* factors, are proteins interacting with the *cis*-regulatory elements residing principally in the 5’ region of the gene promoter upstream of their specific target genes to initiate or suppress their transcription (32). Promoters are defined as DNA regions closely localized to the protein-coding regions of genes whose transcription they regulate in interaction with other elements of the regulatory machinery. In addition to binding to gene promoters, transcription factors can regulate the expression of genes by binding to the DNA enhancer region. Whereas gene enhancer sequence can be found very distant, a million base pairs away or more from its target gene sequence in a linear manner, it is spatially close to it due to the DNA highly coiled and dynamically organized structure (30). They contain binding sites for transcription factors and are cooperating this complex process without a direct contact with promoter region.

Other than the *trans*-domain required for DNA-binding, TFs contain a domain which

may interact with various co-regulator (CoR) proteins to enhance or suppress their activity (33). Co-regulators, or co-activators, do not necessarily have DNA-binding affinity, but rather affect DNA-bound TF stability or activity to cooperate with it and coordinate the transcription process (Figure 4). Forming of a co-activator-activator complex facilitates or impedes the transcription by recruitment of other general transcription factors, or by enabling other functions of co-activators: certain members of this class of proteins induce conformational changes to TFs, which may allow TFs to bind to its target sequence in gene promoter or enhancer, while a number of known functions of these transcriptional regulators are manifested through a direct histone acyltransferase activity and chromatin remodeling (34). When bound to the promoter, transcription factors can enable local chromatin opening, which commonly includes recruitment of chromatin modeling complexes and histone acetyltransferases. Additionally, chromatin opening as an isolated event is not a sufficient factor for Pol II to bind to the DNA, as the polimerase is unable to recognize the promoter sequence itself. Instead, Pol II binding to DNA depends on transcription factor forming a bridge between the cognate promoter and the polymerase. Therefore, TFs initiate or suppress the recruitment of RNA polymerase II (35) to the specific gene to regulate transcription process (30,35). In addition to regular transcription factors, general transcription factors (GTF) regulate transcription by binding to their cognate gene sequence commonly found 25-35 base pairs upstream of transcription starting site of most genes, such as TATA box, generally regulating transcription in a non-specific manner (36).

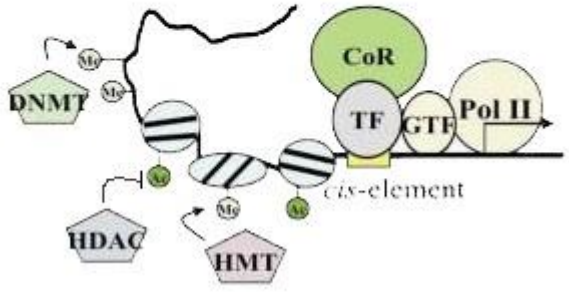

Figure 4. Transcription complex bound to the *cis*-element in the gene promoter.

TF - transcription factor; GTF - general transcription factor; Pol II - RNA polymerase II; CoR - transcription co-regulator; DNMT - DNA methyltransferase; HDAC - histone deacetylase; HMT - histone methyltransferase (33).

Considering the importance of transcription factors in regulation of gene transcription and thus defining the fundamental cellular processes, it is evident that impairment of TF

activity is a common event in cancer development (35). Dysregulation of TF activity can both initiate and promote manifestation of malignant phenotype. Alteration of TF activity can result from mutations of genes encoding them, such as deletion, amplification, gain-of-function, loss-of-function and translocation, with the examples of *TP53* (usually single nucleotide substitution resulting in missense mutation) (37) and *MYC* genes (usually amplification or translocation), that are encoding tumor protein 53 (p53) and c-Myc, found mutated in various malignancies (38). However, TF deregulation is more frequently manifested as an inappropriate activation, signaling or posttranslational modification of a wild-type (WT) transcription factor (39). In addition, aberrant activity of a wild-type TF can be a consequence of a mutation in its binding site or in the protein responsible for its activation, commonly a kinase which functions upstream of a TF. This dissertation focuses on the signaling and therapeutic utilization of knowledge on the transcription factor signal transducer and activator of transcription (STAT) 3, whose abnormal activation is a common event and a driver of various malignant types, including majority of breast cancers.

1.2.4. Signal transducer and activator of transcription family of proteins

Signal transducers and activators of transcription (STAT) are a family of proteins consisting of seven structurally related transcription factors. STAT family comprises of proteins termed STAT1 to STAT6, including closely related STAT5A and STAT5B (40). Under physiological conditions, STATs reside in the cellular cytoplasm and their activation is dependent on the external stimuli, such as cytokine or growth factor. Once stimulated by the specific stimuli, they are phosphorylated at the tyrosine residue by the upstream kinases, resulting in forming a homo- or heterodimer. In the dimerized condition, STATs translocate from cytoplasm to nucleus where they bind their consensus sequences at the target gene promoters to regulate their transcription. Although an un-phosphorylated monomer of STAT molecule is capable of shuttling to nucleus, this process is inefficient and vastly accelerated by phosphorylation and consequent dimerization. The genes whose transcription is regulated by the STAT family of proteins are involved in the essential cellular processes of cell survival, proliferation, differentiation, angiogenesis and immune response (41). Along with their transcriptional activity, STAT proteins lay at the convergence point of various signaling pathways. As they interact with these pathways and their mediators, STATs represent intracellular signaling mediators and transducers of the external cellular stimuli (42).

1.2.5. Molecular structure of STAT proteins

Members of the STAT family of proteins share a similar molecular structure, each of

them comprising of six domains (Figure 5). N- or amino-terminal domain mediates the non-essential ability of STATs dimers to assemble into tetramer, which additionally stabilizes DNA-binding. The coiled-coil domain is responsible for interactions with other regulatory proteins, transcription factors and co-activators of transcription. DNA-binding domain is the segment of STAT molecule which directly interacts and binds to its cognate DNA sequence which is, in general, TT(N4–6)AA. SRC-homology 2 (SH2) domain of one STAT molecule binds to the phosphorylated tyrosine residue of another one during the formation of an active dimer, which facilitates the cytoplasmic-nuclear translocation. The transactivation domain interacts with other proteins in the nucleus, such as histone acetyltransferases, to regulate the gene transcription (41). The carboxy-terminal domain contains a site of serine phosphorylation (pS), whose function is yet not completely elucidated. Phosphorylation of the serine residue has shown to enhance the transcriptional functionality of certain STATs, such as STAT1 and STAT3. However, serine phosphorylation status provides regulation of transcriptional activity only to a certain degree, which is most likely cell type- and promoter-specific (43). In some STATs serine phosphorylation is associated with non-canonical STATs activity in mitochondria (41,44), with implication of STAT3 phosphorylated at serine residue 727 in control of electron transport chain and generation of reactive oxygen species (ROS), promoting tumor growth of breast cancers (45).

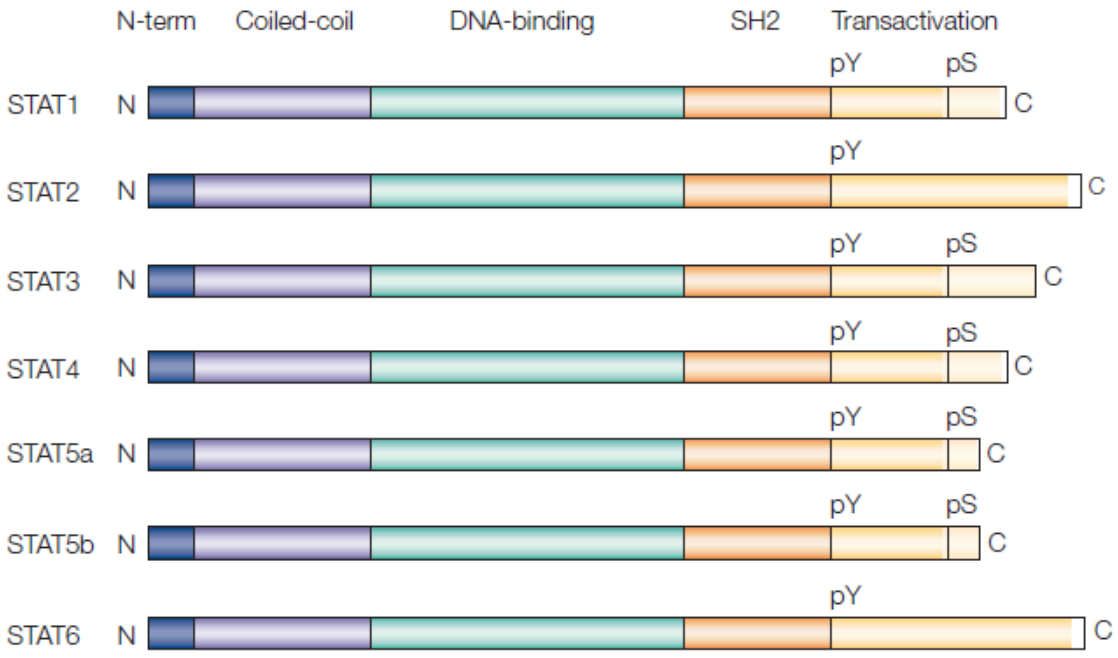

Figure 5. The domain structures of STAT family of proteins. The seven protein members of STAT family share a similar structure and consist of six domains, including amino-terminal, coiled-coil, DNA-binding, SH2, transactivation and carboxy-terminal domain (41).

1.2.6. STAT family members involved in oncogenesis

Of the seven family members, STAT1, STAT3 and STAT5 have been shown to have the most relevant implications in cancer initiation and development.

STAT1 is primarily activated by interferons (IFN), such as IFNα, IFNβ and IFNγ and is generally described as an anti-tumorigenic transcription factor (46). It initiates transcription of genes that induce apoptosis and growth arrest, as well as the ones involved in immune response and immunological mechanisms for tumor and virus eradication (47). Based on its canonical function in mediating interferon cell response and anti-cancer immunity, it was widely believed that STAT1 primarily acts as a tumor suppressor. However, continuous STAT1 activation has also been described in a variety of cancer cell lines, as well as in some patients with certain types of malignant tumors such as breast cancer, leukemia and head and neck malignancies (48). Thus, its tumor suppressor role is complex and might be tissue specific, whereas exact circumstances, such as interactions with other mediators of cellular processes which are further to be elucidated, might affect its function. One of the proposed hypotheses explaining STAT1 pro-tumorigenic effect involves its ability to upregulate various proinflammatory cytokines, such as tumor necrosis factor alpha (TNFa), cyclooxygenase 2 (COX-2) and production of inducible nitric oxide synthase (iNOS). Thereupon, STAT1 activity may contribute chronic inflammation, creating a favorable microenvironment for tumorigenesis and metastatic development (49).

STAT5 is activated by interleukin (IL)-2, granulocyte macrophage colony-stimulating factor (GM-CSF), IL-15, IL-7, IL-3, IL-5 and prolactin, which is particularly important in breast cancer pathogenesis (50). STAT5 is reported as a key mediator in pathogenesis of various hematological malignancies, such as in genetic fusion of breakpoint cluster region protein (BCR) and Abelson leukaemia protein (ABL) - BCR-ABL-driven chronic myeloid leukemia (CML) as well as in acute myeloid leukemia (AML) containing FMS-like tyrosine kinase 3 (FLT3) internal tandem duplication (51). However, its role in breast cancer pathogenesis is proven complex. Although impaired STAT5 activity is considered a tumor promoting effect in breast cancers, it has favorable manifestations in cancers which are also attributed with high STAT3 activity. In this tissue, it is evidenced that STAT5 and STAT3 compete with each other for binding the similar DNA sequence of target genes, finally producing opposing effects (52). Thus, co-activation of STAT3 and STAT5 results in a milder phenotype of breast cancer when compared with the upregulated STAT3 activation alone (53,54). Other than the competing mechanism due to the structural similarity with STAT3, STAT5 is enhancing the expression of genes involved in differentiation process, which might limit the aggressiveness of tumor cells.

1.3. *Signal transducer and activator of transcription 3*

The human *STAT3* gene is a 75,245 base pair linear DNA region located on chromosome 17q21.2, and comprising of 24 exons and 23 introns. It is ubiquitously expressed in many human tissues, as one of the four so far identified isoforms, namely STAT3α (92 kDa), STAT3β (83 kDa), STAT3γ (72 kDa) and STAT3δ (64 kDa), which result from alternative splicing or proteolytic processing. The STAT3α is the full length and major isoform of human STAT3 comprising of 770 amino acid (55). STAT3β is a result of alternative splicing of exon 23, which lacks the C-terminal transactivation domain and is considered a dominant-negative regulator of STAT3 (56). The last two isoforms result from proteolytic processing, and are less common that the previously mentioned isoforms. STAT3γ is a result of a limited proteolysis of the full length major isoform STAT3α, which similarly to the β-isoform, lacks the C-terminus domain and is also considered a dominant negative isoform (57). Another product of proteolytic processing, STAT3δ, is as well reported as unable to regulate the transcription of the target genes, however, knowledge about its physiological and potentially pathophysiological functions is currently limited.

1.3.1. STAT3 signaling pathway

STAT3 pathway is stimulated by the interleukin family of cytokines, including IL-6, IL-10, IL-23, IL-21, IL-11, oncostatin M (OSM), leukemia inhibitory factor (LIF) and growth factors such as epidermal growth factor (EGF), platelet-derived growth factor (PDGF) and others (41,50). Upon their binding to the corresponding plasma membrane receptor, receptor oligomerizes bringing membrane-associated kinases into close proximity to initiate their transphosphorylation. The family of such kinases that further phosphorylate STATs are Janus kinases (JAK), with JAK2 being the principal STAT3 kinase (58). JAKs then phosphorylate receptors intracellular domain, forming a docking site for inactivated cytoplasmic STAT3. Following STAT3 recruitment, JAKs phosphorylate it at tyrosine 705 (Y705) residue. In addition to membrane receptor kinases, non-receptor cytoplasmic kinases that signal through STATs include ABL and Src-related kinases, which are frequently persistently active, for instance in CML with BCR-ABL fusion (41,59). Tyrosine phosphorylation further initiates phosphotyrosine residue of one STAT molecule to interact with the SH2 domain of another one, leading to conformational change and forming of an active dimer. Most frequently, STAT3 forms a homodimer, however, formation of heterodimers is also possible with STAT1. Dimerization facilitates its translocation to the nucleus and binding to the promoter of its target genes (Figure 6) (60).

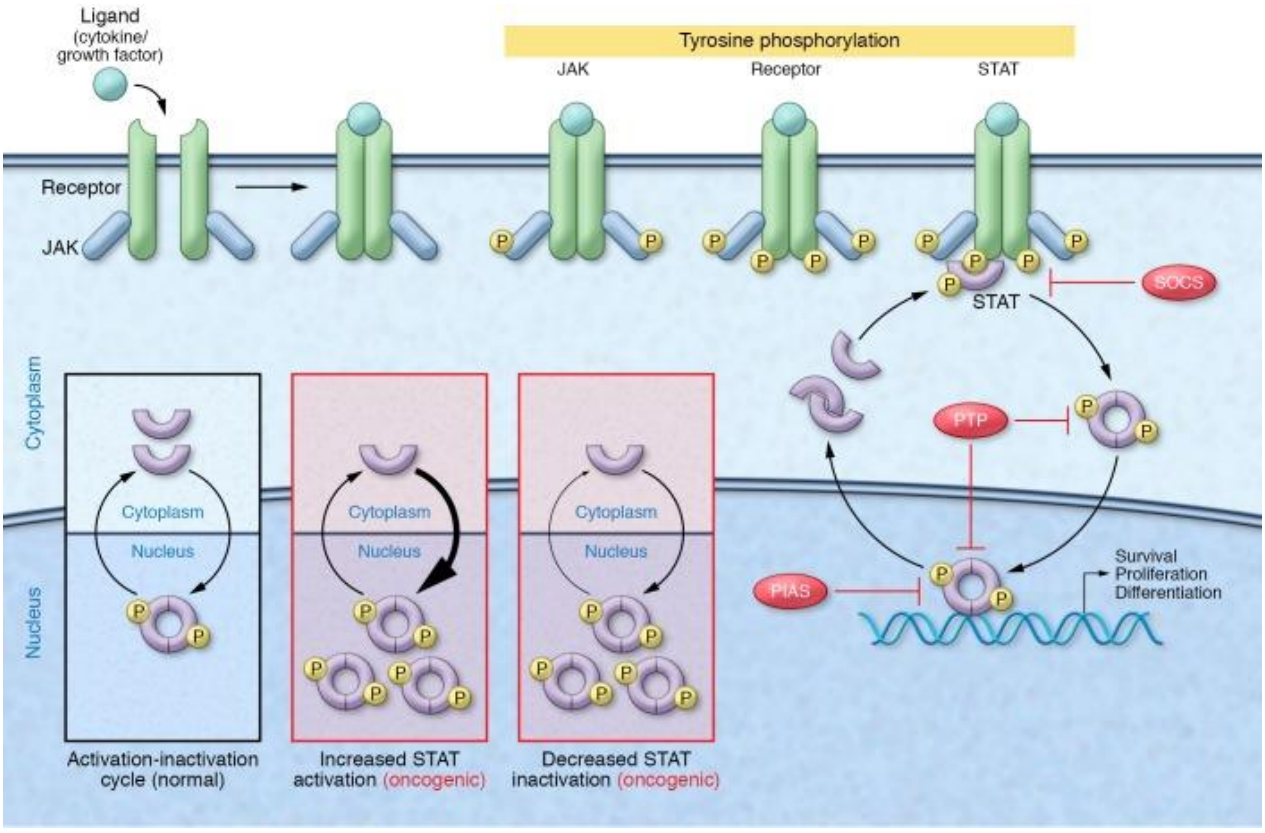

Figure 6. Signaling pathway of STAT proteins. Upon stimulation by a cytokine or growth factor, corresponding membrane receptor oligomerizes and transphosphorylate membrane associated kinases such as JAKs. JAKs than phosphorylate receptor intracellular domain, forming a docking site for cytoplasmic STATs. JAKs then phosphorylate STAT proteins, facilitating their dimerization and translocation to nucleus, where they bind their consensus DNA sequence to regulate transcription of target genes. Physiological negative regulators of this patway include SOCS, PIAS and PTP (50).

JAK – Janus kinase; STAT – signal transducer and activator of transcription; SOCS – suppressor of cytokine signaling; PTP – protein tyrosine phosphatase; PIAS – protein inhibitor of activated STAT.

In nucleus, STAT3 binds to the nine base pair sequence TTCN3GAA in the promoter of its target genes to modulate their transcription (Figure 7). Genes whose transcription is regulated by STAT3 are the key mediators of cell cycle, and promote oncogenic cell behavior including cell survival, proliferation, migration, angiogenesis and immune response. Such pro-tumorigenic genes whose transcription is activated by STAT3 include regulators of cell survival and suppressors of apoptosis, such as B-cell lymphoma (*BCL*)-2, *BCL-6*, *BCL-xL*, myeloid cell leukemia (*MCL*)-1, survivin (member of the inhibitor of apoptosis (IAP) family); regulators of proliferation such as *MYC* and cyclin D1; promoters of migration and metastasis including matrix metalloproteinases (*MMP*s); mediators of

angiogenesis such as vascular endothelial growth factor (*VEGF*) and pro-inflammatory cytokines such as *IL-6* (50,54,59).

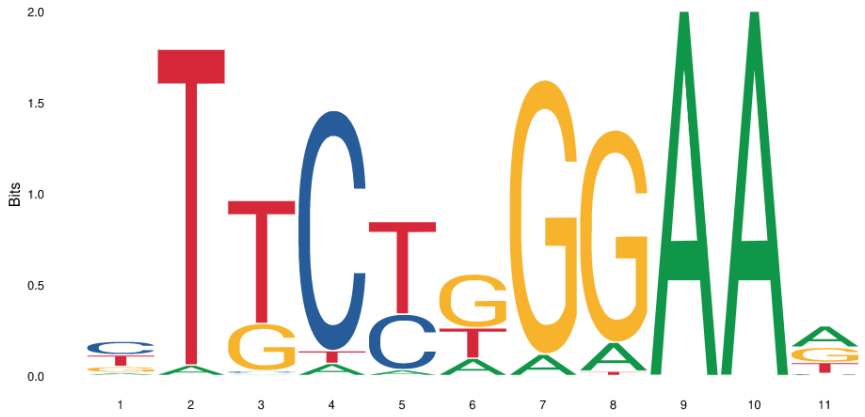

Figure 7. STAT3 DNA-binding consensus site. Graphical representation of frequency of nucleotide sequence that STAT3 has affinity to bind (JASPAR Database v8, Creative Commons Attribution, July 2020)

1.3.2. Dysregulation of STAT3 activity

Given its role in essential cellular events, STAT3 function is tightly regulated by endogenous inhibitors including suppressors of cytokine signaling (SOCS), protein tyrosine phosphatases (PTPs) and protein inhibitors of activated STATs (PIAS) (50). Whereas stimuli-dependent phosphorylation of STAT3 is rapid and transient in normal cells, it is frequently constitutively activated in a variety of malignant disorders driving the proliferation, self-renewal, angiogenesis and chemoresistance of malignant cells. STAT3 can be constitutively active as a result of mutation, in which case they are most frequently occurring in the SH2 domain (Figure 8). However, much more common are other means of STAT3 persistent phosphorylation, such as cytokine overstimulation due to paracrine or autocrine sources in tumor microenvironment; hyper-activation of JAKs due to genetic, epigenetic alterations or overexpression; or by downregulation of STAT3 physiological inhibitors (50,59). Impairment of STAT3 signaling pathway alone is capable of triggering malignant transformation, and is associated with aggressive malignant types and poor prognosis (61). Primarily STAT3, but also STAT5 are frequently constitutively activated in large number of human solid and hematological malignancies, including acute and chronic myeloid leukemia, various forms of lymphomas, breast, ovarian, lung, head and neck, prostate and other malignancies (62). Constitutive STAT3 activation is commonly reported

in association with excessive IL-6 paracrine or autocrine secretion in a number of malignant types, such as in myeloma, prostate, ovarian, breast, colorectal cancer and head and neck squamous malignancies (63-5). The extent to which STAT3 enhances oncogenic potential of a cell varies between the tissue types, suggesting that cell-type specific interactions with other proteins, such as co-regulators of transcription and other transcription factors, modulate the potency of STAT3 activity (59).

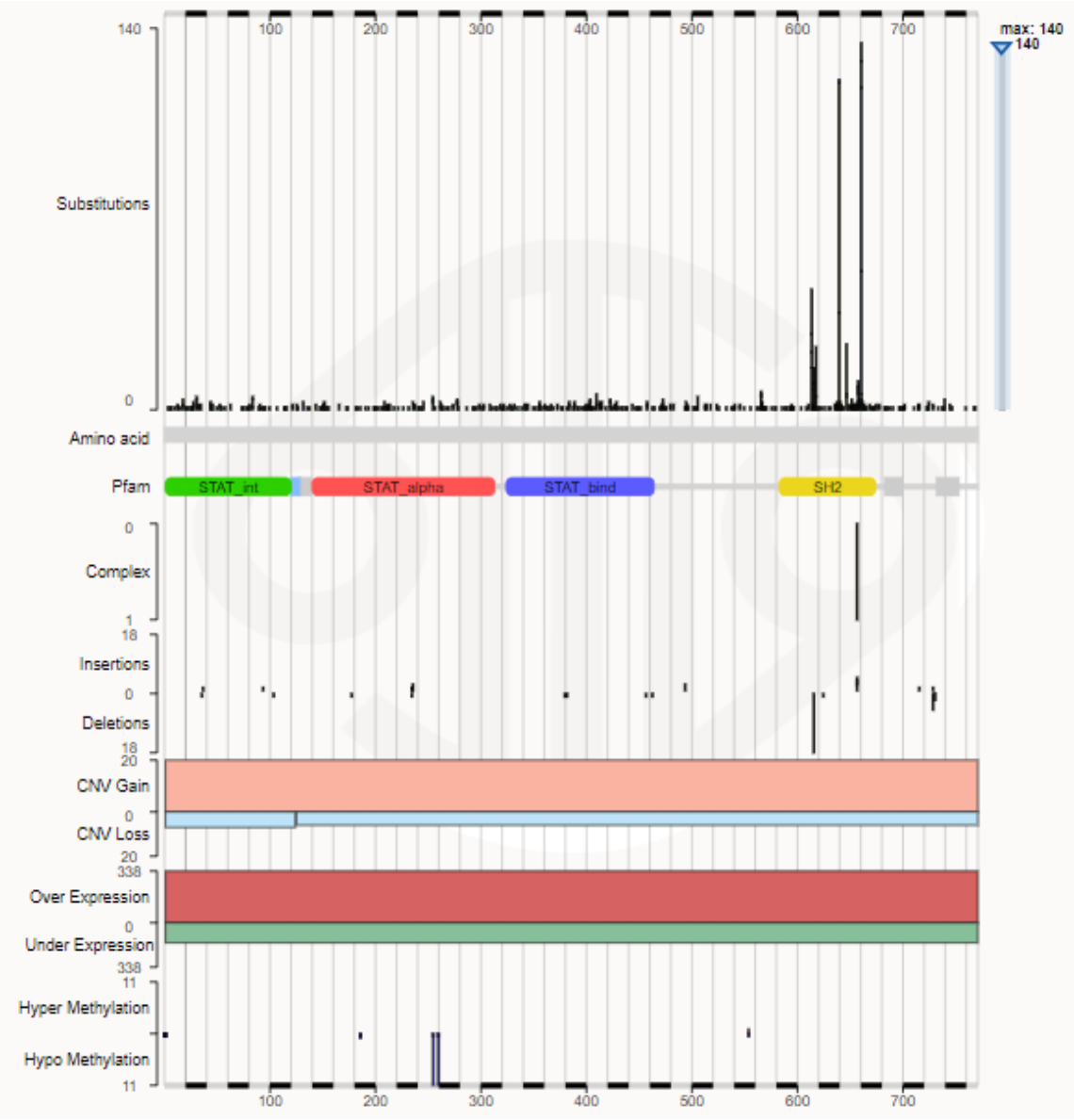

Figure 8. Alterations in the *STAT3* gene. Distribution of genetic abnormalities in STAT3 across its 770 amino acids in 59 231 unique samples (1 287 unique samples with mutations) (COSMIC Database v91, Sanger Institute, July 2020).

1.3.3. STAT3 in immune regulation

One of the paramount properties and indicator of tumor persistence is its ability to evade detection by immune surveillance system. Roles of immune system in regulating tumor growth have been identified in the past decades, with a number of novel treatment strategies involving the administration of immunomodulatory therapies (66,67). Tumor microenvironment is generally characterized by excessive secretion of pro-inflammatory cytokines and chemokines which further facilitate tumor growth. On the other hand, tumors often secrete signals which suppress the immunological ability to detect and induce apoptosis in malignant cells. The specific factors and biological mechanisms of suppressing the anti-tumor immunity are being intensively investigated and one of the factors that plays important roles in escaping the immune-surveillance is STAT3. STAT3 signaling actively intertwines with the nuclear factor kappa B (NFκB) pathway, which is highly associated with both inflammatory processes and cytokine stimulation as well as suppression of anti-tumor immunity (68). Several genes whose expression is stimulated by NFκB activity, such as *IL-6*, are potently activating STAT3. In addition, there is a feedback loop between these two oncogenic transcription factors, as STAT3 was shown to directly associate with RELA, a member of NFκB family of proteins (69). RELA is the functional component of NFκB participating in its hetero-dimerization and translocation to nucleus, where activated STAT3 traps it and contributes its persistent activity (69). Both of these proteins can additionally stimulate the transcription of genes governing inflammation and suppression of anti-tumor immune response. For instance, both were shown to enhance the expression of programmed death ligand 1 (PD-L1) on tumor cells, the key suppressor of T-cell specific tumor-directed immunity and a negative prognostic marker in many malignant types (70-72). Additionally, STAT3 transcriptional activity stimulates the expression of IL-6, IL-10, transforming growth factor β (TGFβ) and previously mentioned VEGF, while downregulating IFNγ, IFNβ and IL-12 to promote the immune evasion (73). IL-6, IL-10 and VEGF further stimulate the activation of STAT3, propagating a positive feedback loop between cancer and immune cells in tumor microenvironment, impacting both innate and adaptive immunity (73,74). Furthermore, IL-12 plays a role in activation and maturation of dendritic cells which bridge innate and adaptive immunity by presenting the antigen to naive antigen-specific T cells, initiating their proliferation and tumor infiltration. STAT3-mediated suppression of IL-12 thus leads to the state of a tolerant immunity, and blocking STAT3 restores the immune physiological function and tumor antigen-specific CD8+ T cell activity *in vivo* (74). Additionally, STAT3 stimulates transcriptional expression of FOXP3 in CD4+ T cells, which is a crucial mediator of conversion of naive CD4+T cells into the CD4+ CD25+ Foxp3+ T regulatory (Treg) cells. The Treg cells further attenuate CD8+ T-cell activation via secretion of IL-10 and TGF-β, thus suppressing anti-tumor immunity and maintaining immunosuppressed environment (73-75).

1.3.4. STAT3 in formation of metastases

The metastatic dissemination of cancer is the most severe complication of malignant diseases and the primary cause of cancer-related death, being responsible for 90% of mortality causes in patients with solid malignant tumors (76). It is defined by a complex multi-step process of malignant cell invading a tissue localized distantly from the primary tumor. At first, tumor infiltrates in adjacent tissue, then access the blood circulation, followed by extravasation into an anatomically distant tissue and its adaptation to the new microenvironment, including formation of new blood vessels to support its growth (77). STAT3 is involved in each of these steps, promoting the final occurrence of metastases (78). The invasion of cancer cells to the extracellular matrix (ECM) is one of the first prerequisite steps and thus initiates the metastatic process. It is commonly promoted by matrix metalloproteases (MMPs), which remodel the ECM by degrading its proteins to enable tumor movement into the neighboring stroma. The STAT3 activity enhances the expression of these enzymes, including MMP-2 (79), MMP-9 (80) and MMP-7 (78). In addition, STAT3 promotes tumor metastasis by upregulating the expression of other transcription factors such as TWIST (81-83), which is involved in tumor invasion, migration as well as epithelial to mesenchymal transition (EMT). If the tumor cell surmounts the physical obstacles and enters the blood or lymphatic stream, it encounters several obstacles, such as mechanical stress, hemodynamic turbulence and recognition and elimination by the immuno-surveillance system. Using previously described mechanisms of anti-tumor immunosuppression, activation of STAT3 helps cancer cell evade the clearance by immune system in circulation (74,84).

1.3.5. STAT3 in tumor angiogenesis

Malignant cells have augmented needs for nutrients and oxygen to support their survival and excessive growth. At early stages of solid tumor development while it still remains small by volume, the majority of tumor cells are in close proximity to normal blood vessels, from which they are supplied. Along with the tumor growth, less cells of the neoplastic tissue are in direct contact with the blood vessels, limiting its necessary nutrient supply and resulting in hypoxic environment of the tumor (85). To survive, malignant tissue requires development of new vascularization, and thus factors that facilitate angiogenesis are crucial mediators of tumorigenesis (86). Pathological angiogenesis, as one of the hallmarks of cancer, is driven by the extensive expression of angiogenic factors. The most potent known angiogenic factor that strongly induces formation of new blood vessels is VEGF, which is highly secreted by malignant cells (87). One of the well-established STAT3 direct target genes is VEGF, whose expression is stimulated by abnormal STAT3 activity (88). In

addition, aberrant STAT3 activation contributes the expression of hypoxia-inducible transcription factor (HIF) 1α target genes, the second major component of angiogenesis (89). In this case, STAT3 was shown not to directly regulate the expression of HIF1α, yet rather serves as its co-activator by binding to the promoter site of its target genes and recruiting other co-activating proteins and Pol II (90). HIF1α and HIF2α both induce the expression of genes highly involved in neovascularization, including VEGF (91). Taken together with previously mentioned STAT3-mediated suppression of IL-12, IFNβ and IFNγ secretion which regularly attenuate neovascularization (92), STAT3 plays an important role in this process essential for survival and cancer growth.

1.3.6. STAT3 in metabolic modeling

1.3.6.1. Effects of STAT3 in regulation of glucose and energy metabolism

Since cancer cells are commonly supplied by insufficient vascularization, they are often hypoxic and have fewer nutrient resources compared to normal cells. As a compensatory mechanism, they are generally characterized by alterations of metabolic pathways to satisfy their distinct needs. In addition, many enzymes in glucose metabolism exert other cellular functions, including transcriptional activity, and therefore might be shifted in cancer cells to promote pathological growth (93). The crucial role of metabolic regulation in cancer development and progression has recently been recognized (94-6). For instance, pentose phosphate, generated in the same name pathway, supports the high rates of nucleic acids synthesis, thus malignant cells modulate its flux to enhance their proliferation abilities (97). In addition, due to the hypoxic states of cancer cells, they are likely to shift from aerobic to anaerobic glycolysis resulting in production of lactate. This is observed even when the oxygen level is sufficient to support the more efficient production of ATP through oxidative phosphorylation and electron chain system in mitochondria, likely due to the fluctuating levels of oxygen supply. This effect is known as Warburg effect, and partially explains cancers high demands for glucose (98).

Raising evidence suggests that STAT3 plays diverse roles in metabolism of proliferating breast cancer cells, by its involvement in energy metabolism, metabolism of glucose and lipids (93). STAT3 transcriptional activity was shown to promote the aerobic glycolysis to enhance energy production and proliferation of breast cancer (99). One of the non-canonical functions of STAT3, associated with serine phosphorylation, relates to its localization in mitochondria. As opposed to Warburg effect, STAT3 in mitochondria stimulates oxidative phosphorylation and respiration through the electron transport chain (ETC) (100,101). The first observations of pSer STAT3 activity in mitochondrial activity

came from the observation that a component of ETC complex I, GRIM-19, directly binds to STAT3 (102) and is likely responsible for its transport into mitochondria (103). Mitochondrial STAT3 enhances the activity of both Complex I and II of the ETC, and its inhibition attenuates their functional activity (104,105). This results in increased production of ATP, providing additional energy needed for rapid oncogenic growth and division (99,104). Consequently, substitution of serine 727 residue for alanine or aspartate significantly suppressed tumor growth and activity of the electron transport system in breast cancer cells (45).

1.3.6.2. Effects of STAT3 activation on lipid metabolism

Previous studies have suggested a crosstalk between STAT3 signaling and lipid metabolism, including lipolysis, beta oxidation and membrane lipid raft modeling in various cancer types (106-8). In addition, STAT3 pathway is interconnected with leptin, the hormone secreted predominantly by adipocytes and enterocytes in small intestine to regulate energy metabolism by suppressing appetite. Besides binding to its receptor OBR on plasma membrane, which can itself mediate downstream signaling through STAT3 (109), leptin was shown to bind to IL-6 receptor glycoprotein 130 (GP130), initiating a cascade of events that lead to phosphorylation of STAT3 (110,111). It is suggested that continuous leptin stimulation induce the STAT3-mediated expression of its major endogenous inhibitor and target gene SOCS3, which further decreases leptin-induced signal transduction and finally facilitates leptin resistance (112). Wang et al. further unraveled the consequences of leptin- or otherwise mediated activation of STAT3 signaling axis (108). They showed that STAT3 transcriptionaly upregulates the expression of carnitine palmitoyltransferase 1B (CPT1B) which mediates fatty acid oxidation (FAO). This pathway is shown crucial for self-renewal of breast cancer stem cells and promotes their chemoresistance. FAO results in production of NADH and $FADH_2$ which can both reduce oxidative stress in these cells and enhance ATP production by electron transport system (113). Another product of JAK/STAT3-mediated FAO is acetyl-CoA, which may be later utilized for energy production through Krebs cycle, fatty acid synthesis and protein acetylation, which promotes tumor growth and was demonstrated to be necessary for maintaining survival of breast cancer stem cells (108). Accordingly, acetyl-CoA supplementation partially reversed the detrimental effects of silencing STAT3 on proliferation and survival of breast cancer stem cells (108).

When observing the STAT3-mediated changes in general lipid status of an organism, pharmacological inhibition of STAT3 phosphorylation significantly reduced the plasma levels of total cholesterol content, triacylglycerol (TAG) and low-density lipoprotein cholesterol (LDL-C) and increased the levels of high-density lipoprotein cholesterol (HDL-

C) in diet-induced obese and atherosclerotic rabbits and mice (114,115). Along with STAT3 immune effects, these findings support the hypothesis that STAT3 inhibition might be beneficial in treatment of atherosclerosis (116). Finally, STAT3 was shown to be an important factor in preadipocyte differentiation into adipocytes and promotor of mitotic clonal expansion and lipid accumulation in adipocytes (117), as well as fatty acid uptake in cancer cells (118).

1.3.7. Role of STAT3 in breast cancer

The importance of STAT3 in breast cancer is displayed by its aberrant activation in 70% of all cases, which has been detected in each of the molecular types (119). In particular STAT3 is constitutively phosphorylated in essentially all triple-negative breast cancers, the most aggressive type of breast cancers characterized by poor prognosis, substantial metastatic potential and high recurrence rate (8). The aberrant activation of STAT3 in TNBC is highly associated with the cell survival, proliferation, invasion, metastatic potential, angiogenesis and suppression of immuno-surveillance system (120). Activation of STAT3 is driving these oncogenic behavior of breast cancers by various previously described manners. First, transcriptional targets of STAT3 are highly involved in the essential cellular processes including survival, proliferation, migration and immune response. Also, by interacting with other oncogenic factors or tumor suppressors, such as Glioma-Associated Oncogene Homolog 1 (GLI1) (121), NFκB, FoxO1/3 (122); and oncogenic pathways such as PI3K/AKT and PTEN (123), STAT3 facilitates the oncogenic cellular behavior.

Unlike the other subtypes, TNBCs currently lack targeted therapy and are commonly treated using non-specific methods comprising of chemotherapy, radiation and surgical procedures. Along with limited effectiveness, non-targeting approaches are harmful to normal tissue, emphasizing the need for development of novel treatment strategies (124). As STAT3 is abnormally activated in nearly all TNBC, it might serve as a prominent target in designing selective therapies for this breast cancer type.

1.3.8. STAT3 as a target in cancer treatment

Various pathological signaling pathways converge on a number of transcription factors, which are the final regulators of the malignant gene expression patterns. Therefore, novel research is focused on designing therapies directed towards these oncogenic transcription factors, with STAT3 presenting an appealing target due to its biological and clinical relevance (33). Development of therapeutic strategies focused on suppressing STAT3 hold merit for several reasons. Firstly, although playing crucial roles in essential

cellular processes, normal cells can endure STAT3 depletion as it is not necessary for survival of normal cells (125). On the other hand, malignant cells driven by this oncogenic event commonly show the effect of "oncogene addiction", meaning that they can hardly recover the loss of their principal driver, and thus its inhibition results in growth arrest and cellular death. While normal cells do not display such a dependency, this phenomenon creates a basis for a favorable therapeutic window of STAT3 inhibitors (50). Another aspect of STAT3 targeting relates to the fact that it is a converging point of multiple oncogenic signaling pathways. Therefore, targeting a single protein is advantageous compared to targeting several upstream kinases, as STAT3-specific inhibition could prevent development of drug resistance associated with activation of collateral signaling pathways (50, 120). Due to the high therapeutic index deriving from these properties, number of approaches have been taken in designing and development of STAT3 therapeutic inhibitors (125-7).

Some of the chemicals have been established for targeting upstream mediators of STAT3, such as Janus kinase, with example of ruxolitinib, which is currently tested in clinical trials for treatment of pancreatic, colorectal and breast cancer, including TNBC (ClinicalTrials.gov,126,128). The limitations of kinase inhibitors commonly relate to the absence of a single driver kinase and resistance development by kinase mutation or bypassing the inhibition through collateral signaling pathways (129). On the other hand, direct inhibition of STAT3 has proven difficult due to the following challenges in designing efficient and clinically translatable inhibitor (130). Due to these obstacles, only a few of them have been successfully implemented, and STAT3 is commonly termed as "undruggable".

- STAT3 as other transcription factors, has a relatively large and flat molecular surface suitable for protein-protein and protein-DNA interactions, albeit challenging for direct targeting by small molecules due to a lack of a sterically available hydrophobic binding pocket in proximity with the regions of interest such as SH2 domain required for dimerization, Y705 residue or DNA-binding domain.
- Specificity and potency of the developing molecules is limited, as a number of novel STAT3-inhibiting agents are identified by large scale screening strategies and thus may exert off-target effects.
- Peptide inhibitors might be developed to obtain high specificity and potency, however, they are characterized by limited ability to cross the biological membranes. Therefore, their intracellular stability and bioavailability *in vivo* is commonly suboptimal due to their physiological degraders (131)
- DNA-decoys represent an interesting approach to bind activated STAT3 in nucleus and consequently prevent its DNA-binding. Also, dominant-negative expression vectors and small interfering RNAs (siRNA) provide an effective inhibition of

STAT3 protein expression and activity in cell cultures, however, their *in vivo* bioavailability and cellular delivery is often suboptimal (132,133).

For all the above, there is a growing need for development of new therapeutic strategies which could overcome the listed restrains. Novel researches are directed towards overcoming these limitations and one of the emerging promising tool is the development of nanomedicine, which has the potential of overcoming a number of the listed constraints (134,135).

Nanotherapies are defined by highly modifiable features, from which numerous advantageous characteristics could be derived (Figure 9). By means of incorporating a compound into a nanoparticle with beneficial pharmacokinetic (PK) properties, one can surmount drugs suboptimal absorption and permeability through biological membranes, short elimination half-life and low bioavailability, insufficient biodistribution in the tissue of interest and nonspecific effects with notable toxicity in healthy tissue. Most importantly, modifications of the nanosystem's surface chemistry commenced a whole new area of targeted nanotherapeutic development (136).

1.4. *Nanomedicine*

Nanomedicine represents a novel compelling form of pharmaceutics designed for treatment and diagnosis of a number of common diseases including diabetes, cardiovascular diseases, infective diseases and has gained particular attention in oncology (134, 137). Nanotherapies are abundantly investigated in treatment of breast cancers, with currently 77 ongoing clinical trials testing new nanoscale formulations and considerably more studies testing nanotechnologies in the preclinical setting (ClinicalTrials.gov). So far, several nanomedicines gained approval by the US Food and Drug Administration (FDA), most of which are indicated in oncology. Three of the liposomal formulations, Doxil®, Abraxane® and MyoCet® are already widely used in the treatment of breast cancer.

Nanomedicine is defined as biomedical application of materials with at least one dimension being 100-200nm (138). Versatile types of nanomedicines are being developed, investigated and some of them clinically applied, with liposomes and nanoparticles representing two major groups with various mutual features, thus often subjects of overlapping terminologies. Whereas liposomes represent spherical particles with a hydrophilic core and a membranous lipid bilayer surface, nanoparticles can be different in shape and structure such as micelles, capsules, colloids, and dendrimers; and composition,

with examples of polymeric, lipid, carbon and metal nanoparticles (17).

1.4.1. Potentials of nanomedicine application

Nanocarriers have the ability of encapsulating various drugs and pharmaceutic agents, providing them with favorable pharmacokinetic properties. This enables *in vivo* administration of different molecules with extremely poor PK profile, such as siRNA, miRNA, genes and peptides, whose systemic administration is otherwise impossible (139). Other agents that have modest but applicable PK profile, including a variety of chemotherapeutic agents characterized by narrow therapeutic window, can also greatly benefit from nanosystem-based drug delivery. In this manner, nanocarriers protect the pharmaceutic agent from degradation in circulation and enable its controlled release, remarkably affecting stability of the active substance (140). As a consequence, very high serum concentrations of therapeutics are avoided, and elimination half-life is prolonged (141). With that regard, the maximum tolerated dose of mertansine, a chemotherapeutic clinically used for TNBC treatment, is increased 8-fold when encapsulated into a nanoparticle (142). Furthermore, drug incorporation into a nanocarrier can improve endo- and transcytosis of otherwise suboptimally permeable substances, providing augmented intracellular drug concentration (143,144). In addition, nanoformulations that integrate certain metals with good conductivity and electrical properties, such as gold, platinum and silver, are used to deliver a sensitizing agent during radiotherapy or as contrast enhancers. Thus, they might serve for improving radiosensitivity or as imaging and diagnostic tools (145). Interestingly, certain carbon nanoparticles, such as fullerenol-derived ones, are distinguished for their antioxidant activity and therefore might enhance the safety profile of drugs whose side effects are related to induction of oxidative stress, including doxorubicin, commonly used in breast cancer treatment (146-8). Importantly, modifications of nanosystem surface chemistry provide the possibility of directing the chemotherapeutic agents to malignant cells based on the differential expression of molecules on the plasma membrane (Figure 9) (149). Consequentially, greater drug concentrations are obtained at the site of interest, while delivery to healthy tissue is reduces, minimizing the overall toxicity of cytotoxic agents (10,149,150).

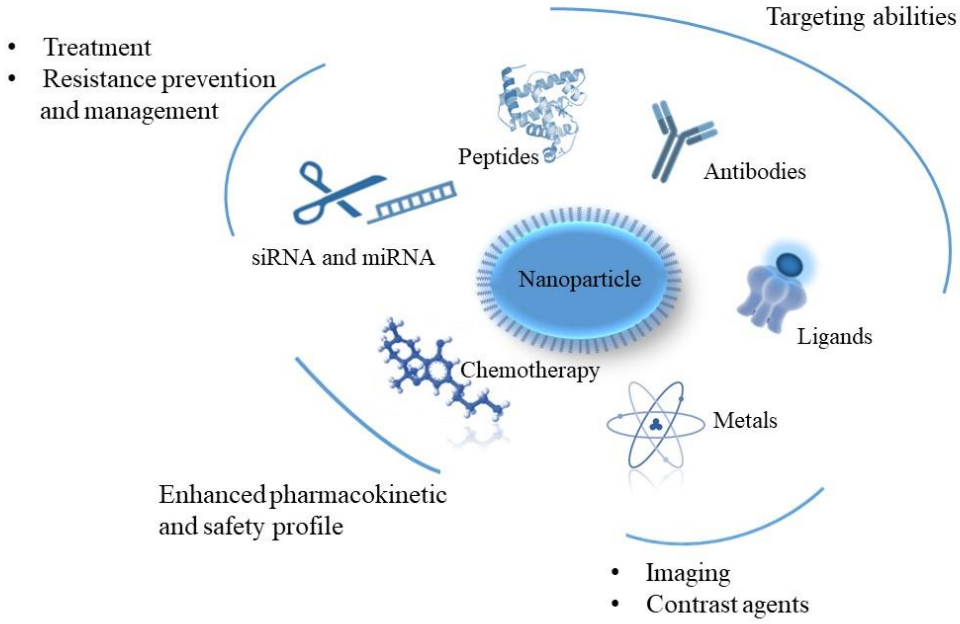

Figure 9. Schematic presentation of potential conjugates and contents of nanoparticles and following features that they may provide to such assembly.

1.4.2. Tumor targeting properties of nanotherapeutics

1.4.2.1. Passive targeting of breast cancer using nanotherapy

Accumulation of drug-carrying nanosystems at the malignant site can be achieved by active or passive tumor targeting. A typical example of passive targeting is the retention of nanoforms in vasculature of tumor tissue. Solid tumors including breast cancers develop new vascularization which differs from the physiological blood vessels and displays greater permeability (151). Thus, the leaky vessels make the cancer cells easily reachable by nanosize particles (152). As the lymphatic drainage in tumors is reduced, nanosystems retain in the malignant environment for prolonged periods (153). This nonspecific phenomenon, although simple, results in significantly higher concentrations of nanotherapeutics in tumor tissue, and is known as the enhanced permeability and retention effect (EPR) (154). An exemplary utilization of such an effect is Abraxane®, the FDA approved liposomal paclitaxel which efficiently targets breast cancer cells. It is noteworthy that EPR effect highly depends on the abnormal tumor vessel development. Although neovascularization begins during initial stages of tumorigenesis, early lymphogenic metastasis are unlikely to be

targeted using this approach (155). Another mechanism for nonspecific targeting grounds on the hypoxic microenvironment of solid malignancies, including breast cancers. Hypoxic microenvironment might further trigger the occurrence of somatic mutations and thus promote invasive behavior and metastatic progression. Additionally, the low oxygen environment is known to contribute development of resistance patterns to various antineoplastic therapeutics (156,157). Anaerobic cellular metabolism driven by the hypoxic state of cancers results in lower pH of the malignant formation and adjacent tissue. Nanoformulations can be designed to have preferential affinity and reduced stability at acidic pH conditions, hence decomposing and releasing the drug at the tumor site, while being stable and maintaining integrity at physiological pH levels (158-60).

1.4.2.2. Active targeting of breast cancer using nanocarriers

Active tumor targeting strategies using nanotherapeutics involve supplementing the nanocarrier surface with a molecular entity that shows a binding affinity towards molecules abnormally expressed on the plasma membrane of malignant cells. This advanced type of tumor targeting attains better specificity than passive targeting, followed by improved selectiveness and drug accumulation in the malignant tissue. Common molecules used for obtaining nanosystems targeting affinity are monoclonal antibodies and ligands of the receptors of interest. An example of such highly expressed receptor on breast and other malignant cells is cell surface adhesion receptor cluster of differentiation 44 (CD44). Thus, nanoparticles conjugated with CD44 ligand, hyaluronic acid, are widely tested for their tumor-targeting ability (161,162). Likewise, breast cancers overexpressing HER2 can be effectively targeted using nanosystems terminally containing trastuzumab (163). Despite the great specificity and selectiveness of antibody-conjugated nanotherapeutics, their potential limitation might derive from possible nanoparticle physiochemical alterations induced by association with a large molecular structure of the antibody. In avoiding such unfavorable effects to PK profile of a nanosystem, a number of researchers are focused on developing surface targeting agents that comprise of peptides and amino acids (164-6). The tumor targeting properties of nanosystems are highly investigated as a tool for breast cancer treatment. Such an approach has particular significance for TNBC treatment, which urgently requires development of targeted therapeutic modalities. The targets that nanoparticles could be directed against can be derived from membrane properties and expression profiles of these cancers. For instance, approximately 50% of TNBC cells are characterized by high EGFR expression, making it an attractive target for selective nanoparticle-mediated TNBC treatment. Therefore, numerous approaches utilize drug nanocarriers complemented with anti-EGFR peptides and antibodies (167-9). Similarly, folate receptor alpha (FRα) represents a promising candidate for targeting TNBC cells, as 50-85% of metastatic TNBC express it on their membrane (170-2). In contrast, only certain epithelial cells express FRα

physiologically, with distribution localized at the apical tissue margins hardly reachable by blood circulation (173).

The oncogenic transcription factor STAT3 is abnormally activated in most of the malignantly transformed cells, inclusive of 70% of breast cancers and almost all TNBC cases (120). Therefore, STAT3-mediated properties of cancer cells might provide a distinction between malignant and normal cells. Thus, targeting STAT3 in treatment of these tumors poses a strong therapeutic index, and might serve as a potential target for designing selective nanomedicinal therapy for this aggressive neoplastic disorder. To investigate the ability of targeting STAT3-driven cells, we evaluated utilizing Layer-by-Layer (LbL) nanoparticles (NPs) as novel drug delivery systems.

1.4.3. Layer-by-Layer Nanoparticles

LbL nanoparticles are nanoscale systems consisting of multiple ultrathin alternatingly charged layers (Figure 10). Their components are highly modifiable providing a possibility of customized design and nature and enabling multi-functionality. The composing layers can be generated of synthetic polyions and natural biomacromolecules, by sequential deposition of alternatingly charged polyelectrolytes onto the colloidal core (174). Such alternating assembly creates an ionically crosslinked thin film membrane which regulates discharge of the drug from the core or intermediate films. Different charge layers allow encapsulation of versatile types of molecules with highly controlled release, including drugs, peptides, nucleic acids and diagnostic agents (175,176). Incorporation of compounds into different layers of this assembly enables packaging of combination of agents into a single nanoparticle, even in case they are otherwise incompatible. This unique structure provides high therapeutic loading capacity within the layers, with encapsulation of molecules weighting 10% to 50% of NP mass, while other similar polymer films typically enable 1-10% loading capacity (174,177).

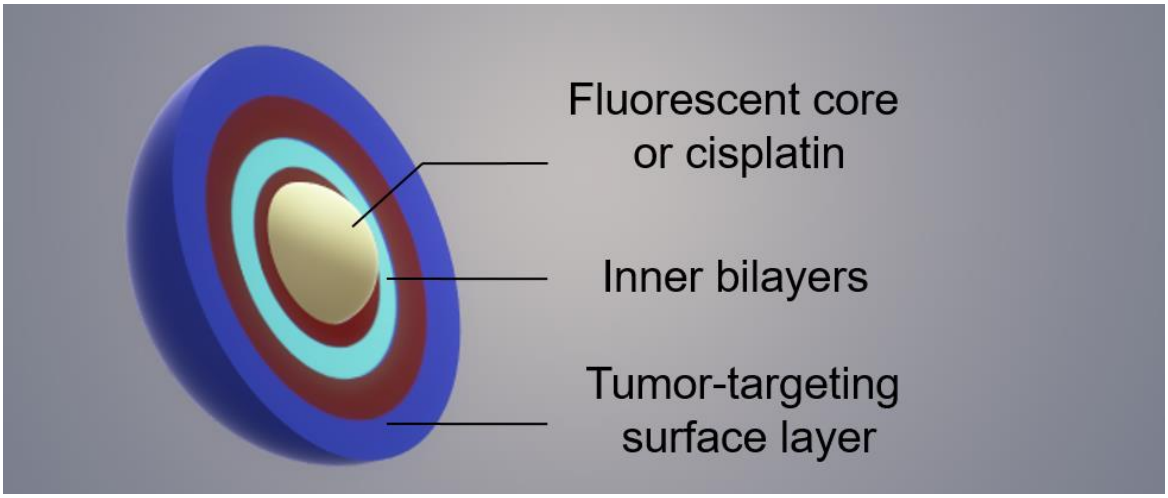

Figure 10. Schematic illustration of Layer-by-Layer nanoparticles. Multilayer LbL nanoparticles consist of a core incorporating fluorescent dyes or drugs; inner layers are suitable for drug incorporation, while structure of the outmost layer is responsible for NP-cell interaction and thus may be utilized for development of targeting abilities.

The colloidal core of the particles is a carboxy-modified latex, which can itself carry the therapeutic payload or fluorescent dye for NP detection. The surrounding layers, thick only a few tens of nanometers, are composed of cationic poly-L-arginine (PLR), with polyanions as the terminal layer. Most importantly, the surface layer is responsible for the NP interaction with the plasma membrane, which enables the design of LbL NPs with tumor-targeting properties (164,174). To investigate utility of these nanosystems in targeting STAT3-driven breast cancer cells, we screened a library of NPs coated with different modifications of the surface chemistry. The negative charge of the outmost layer is chosen for advanced biocompatibility and systemic circulation compared to the cationic NPs (178). For instance, positively charged constructs have affinity towards the negatively charged luminal surface of blood vessels, the kidney globular basement membrane, epithelial cell membrane surface and erythrocytes, which may cause off-target effects of drug-loaded NPs (179). Polyanionic electrostatically stabilized NPs are capable of relatively long circulation, however, may also interact with components of extracellular matrix, such as collagen type I. The surface layer was constructed of polyanions containing sulfated or carboxylated functional groups with either previously known ligand-receptor interactions such as sodium hyaluronate (HA) and heparin-folate conjugate (HF), or those without known interactions, including poly-L-glutamic acid (PLE) and poly-L-aspartic acid (PLD) (Figure 11). The average hydrodynamic diameters of all NPs range from 100 to 155 nm (164,180), average polydispersity indices from 0.04 to 0.13 and zeta potentials < -30 mV (164). In addition, these NP systems have been proven capable of encapsulating both hydrophobic and hydrophilic substances, thus improving cellular delivery and permeability through biological membranes of variety of molecules (174). They are generated from biodegradable materials,

and tested for safety in *in vivo* setting, exerting a favorable pharmacokinetic profile (164,181).

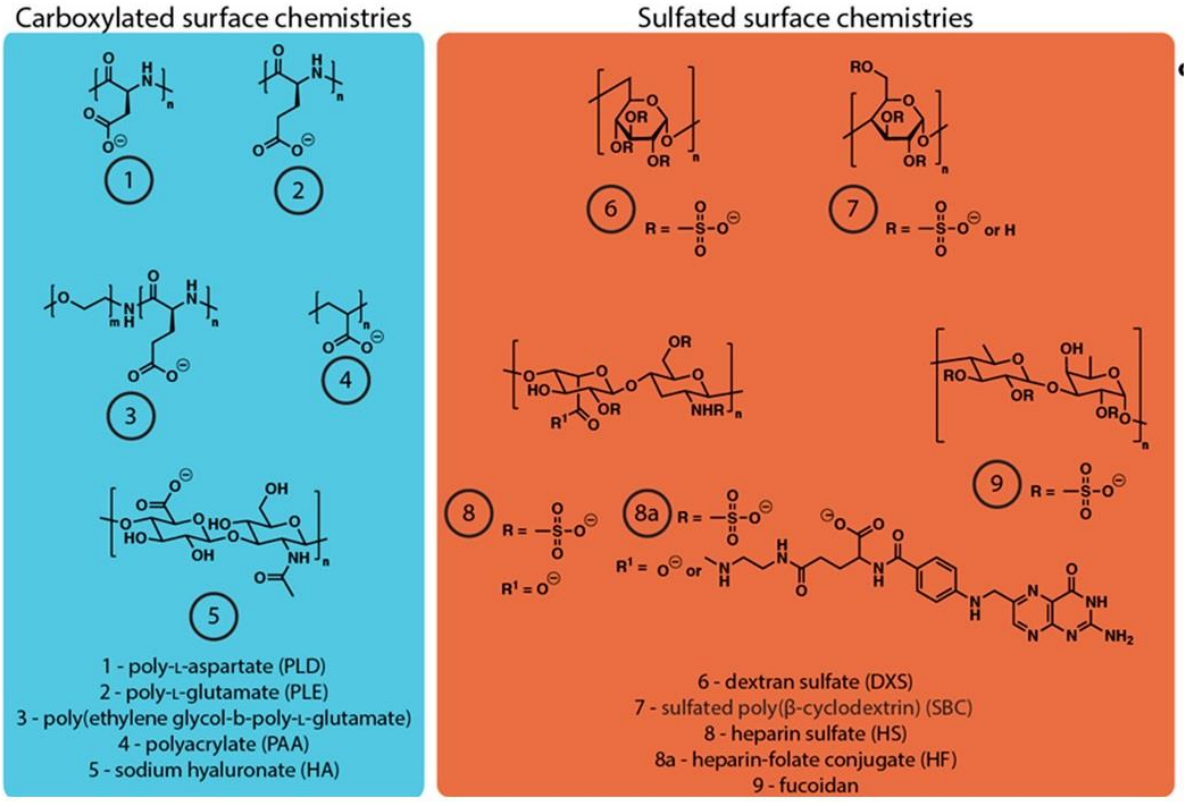

Figure 11. Layer-by-layer modifications used to develop a panel of nanoparticles exploring diverse anionic surface chemistries. Scheme of LbL functionalization; 100 nm cores were coated with poly-L-arginine followed by one of 10 different anionic polymers (164).

2. Aims and hypotheses

2.1. *Study need rationale*

The aberrant activity of the oncogenic transcription factor STAT3 is a common event in breast cancer, characterizing two third of all cases and almost all triple-negative breast cancers. Therefore, it represents a promising target for treatment of this malignancy. As malignant transformation is associated with changes in number of metabolic enzymes and their substrates, we investigated how STAT3 activation qualitatively and quantitatively affects metabolic architecture of cells. We tested exploiting these lipid alterations in designing selective therapy directed towards cancer cells characterized by constitutive STAT3 activity. Thus, we evaluated utilizing Layer-by-Layer nanoparticles in exploiting these differences between malignant cells and normal cells, which are characterized by low and transient STAT3 activity. As radiotherapy is commonly used in treatment of breast cancer patients, we have evaluated the effect of irradiation on STAT3-dependent cell-binding capability of the most promising STAT3-targeting LbL nanoparticle.

2.2. *Main aims of the study and anticipated results*

1. Investigation of STAT3-modulated cellular lipid architecture by performing mass spectrometry following induction or inhibition of STAT3 in two different breast cellular systems, including a TNBC cell line.
2. Identification of the optimal NP modification with targeting affinity towards STAT3-driven cells by screening a library of LbL nanoparticles using fluorescent microscopy.
3. Quantification of the STAT3-targeting NP-cell binding by flow cytometry and validation in three breast cell lines.
4. Characterization of NP penetration into the three-dimensional breast cellular organoids by confocal microscopy.
5. Evaluation of the translational potential of these findings by testing the effects of cisplatin-loaded NP treatment on cellular apoptosis by Annexin V/DAPI staining and flow cytometric analysis.
6. Investigation of the effect of acute gamma radiation therapy to NP-cellular binding.

2.3. *Main hypotheses*

1. By evaluating of a total of 220 metabolites by mass spectrometry-based lipid profiling analysis in two cellular systems following STAT3 activation or suppression and comparison of the metabolites with consistent alterations across the tested conditions and models, we expect to detect the lipid metabolites directly regulated by STAT3 transcriptional activity.
2. Screening a library of LbL nanoparticles differing in their surface layer will result in identification of the NP modification with STAT3-targeting properties, as time-lapse fluorescent microscopy enables real-time evaluation of the degree of nanoparticle cellular binding.
3. Flow cytometry enables precise quantification of the NP cellular binding. Therefore, we expect to accurately quantify the level of the cellular binding of NPs targeting STAT3-driven cancer cells using this method. Validation of the NP targeting ability is achieved by testing three breast cell lines (nonmalignant breast cells with inducible STAT3 construct and two TNBC cell lines) and inhibiting STAT3 genetically (using siRNA) and pharmacologically (pyrimethamine and ruxolitinib).
4. Three-dimensional organoids might provide a better model for investigating malignant phenotype of breast cancers. Characterization and quantification of the STAT3-targeting NP penetration throughout all three dimensions provides a more precise simulation of the mechanism of NP-tumor interaction in solid cancers.
5. Based on the previous findings, it is expected that cisplatin-loaded STAT3-targeting NPs will induce apoptosis in STAT3-driven cells to a greater extent than in cells with diminished STAT3 activity.
6. We expect a statistically significant increase in STAT3-dependent differential cellular binding of STAT3-targeting NPs following acute gamma irradiation in a dose dependent manner.

3. Methods, samples and place of experimental research

3.1. *Materials and Methods*

3.1.1. Cell lines

MDA-MB-231 and MDA-MB-468 cells (kindly provided by Myles Brown, Dana-Farber Cancer Institute) were maintained in Dulbecco's modified Eagle's medium (DMEM) with 10% fetal bovine serum (FBS). SUM159PT cells (received from Kornelia Polyak, Dana-Farber Cancer Institute) were maintained in Ham's F-12 medium supplemented with 5% heat inactivated FBS, 10 mM HEPES (Gibco), 1 µg/mL hydrocortisone (Sigma) and 5 µg/mL insulin (Sigma). MCF-10A cells (ATCC, crl-10317) were stably engineered to express STAT3C (with a FLAG epitope) under an inducible promoter, and were maintained in DMEM/F12 containing 5% horse serum, 20 ng/mL EGF (Peprotech, Rocky Hill, NJ), 0.5 µg/mL hydrocortisone (Sigma), 100 ng/mL cholera toxin (Sigma) and 10 µg/mL insulin (Sigma). STAT3C is a mutated form of STAT3 protein, with introduction of two cysteine residues 662 and 664 in a C-terminal loop of the SH2 domain. These mutations stabilize the dimerization of two STAT3C molecules and result in formation and accumulation of transcriptionaly active dimer complexes. Although tyrosine phosphorylation is still essential for its function, STAT3C remains dimerized for vastly prolonged time following phosphorylation compared to the wild-type STAT3 (39,182). Thus, STAT3C is a constitutively active mutated form of STAT3 that activates the transcription of STAT3 target genes (182-4). To induce STAT3C expression, cells were incubated with 2 µg/mL doxycycline (Sigma) for 24 hours prior to treatment with nanoparticles. Induction of STAT3C is a sufficient oncogenic factor to induce the malignant transformation of MCF-10A cells.

All cells were maintained in a humidified incubator at 37 °C with 5% CO_2 and passaged for less than three months after thawing. All cells were authenticated by short tandem repeat DNA profiling, and were routinely tested for the presence of *Mycoplasma* by PCR.

3.1.2. Immunoblot analyses

Cells for immunoblot analyses were lysed on ice for 15 minutes in RIPA lysis buffer (Boston BioProducts) with phosphatase inhibitor cocktail (Cell Signaling Technology) and

complete protease inhibitors (Roche). The protein quantity was detected using Bradford reagent on spectrophotometer. They were denatured on 101.4℃ for 5 minutes in the presence of beta-mercaptoethanol, which breaks the disulfide bridges of the teriary protein structure, and sodium-dodecyl sulfate (SDS), that provides proteins with negative charge needed in further electrophoretic separation. 25 μg of proteins from each sample were applied on polyacrylamide gel and separated by size using gel electrophoresis (polyacrylamide gel electrophoresis, PAGE). The proteins from gel were transferred to nitrocellulose membrane and incubated in milk solution to block non-specific binding of the antibody. Immunoblots were probed overnight with primary antibodies to phospho-STAT3 (Y705) (9131, Cell Signaling Technology), STAT3 (sc-482, Santa Cruz), FLAG (F1804, Sigma), tubulin (T5168, Sigma-Aldrich) and washed in TBST for 30'. Then the membrane was probed for 1 hour with the secondary anti-mouse or anti-rabbit antibodies (Life Technologies), conjugated with chemiluminescent horseradix peroxidase (HRP), when the protein bands were detected using charge-coupled device (CCD) camera. Tubulin was used as an endogenous loading control for all samples.

3.1.3. mRNA expression analyses by reverse transcriptase polymerase chain reaction (RT-PCR)

Total cellular RNA was isolated using Qiagen RNeasy Mini kits. RNA quality and quantity were evaluated on a NanoDrop 8000 spectrophotometer (Thermo Fisher Scientific). For each sample 4 μg of RNA was reverse transcribed with TaqMan (Applied Biosystems) to generate cDNA. Quantitative polymerase chain reaction (qPCR) was performed in quadruplicates using Power SYBR master mix (Applied Biosystems) on a QuantStudio 6 Flex Real-Time PCR System (Applied Biosystems). Specificity of amplification was confirmed by melt curve analysis. Cycle threshold (Cτ) values for target genes were normalized to the endogenous reference gene glyceraldehyde 3-phosphate dehydrogenase (GAPDH), and the fold change was determined by dividing the expression in each sample by that of the untreated control sample. Primer sequences (Table 1) were designed from the UCSC genome browser reference mRNA sequences using Primer3.

Table 1. Primer sequences used for quantitative reverse transcriptase PCR analysis (RT-qPCR) of mRNA expression.

Gene	Forward Sequence	Reverse Sequence
GAPDH	AATCCCATCACCATCTTCCA	TGGACTCCACGACGTACTCA
BCL3	CCTCTGGTGAACCTGCCTAC	TACCCTGCACCACAGCAATA
BCLAF1	GGAAGCATACCCGTTTAGCA	TTCTACGGCGATCAATGTCA
IL6	GAAAGCAGCAAAGAGGCACT	TTTCACCAGGCAAGTCTCCT
JUNB	AAATGGAACAGCCCTTCT	TGTAGAGAGAGGCCACCA
MCL1	GAGACCTTACGACGGGTT	TTTGATGTCCAGTTTCCG
SOCS3	TCAAGACCTTCAGCTCCAAG	TGACGCTGAGCGTGAAGAAG
STAT3	ACCGGCGTCCAGTTCACTACT	CCGGGATCCTCTGAGAGCTGC

3.1.4. RNA interference

Cells were transfected using Lipofectamine RNAiMAX with 10 nM of siRNA targeting STAT3 #2 or STAT3 #3 (D-003544-02-0010 and D-003544-03-0010, respectively; Dharmacon), or non-targeting siRNA control (sc-37007, Santa Cruz). Cells were transfected with siRNA for 48 hours, when analyzed by liquid chromatography coupled to tandem mass spectrometry. In case of nanoparticle treatment, the media was changed following 48-hour transfection to remove lipofectamine, and the cells were then incubated for an additional 24 hours (MDA-MB-231) or 72 hours (SUM159PT) prior to nanoparticle treatment.

3.1.5. Mass spectrometry-based lipidomic profiling

Prior to mass spectrometry analysis, MDA-MB-468 cells were transfected with siRNA targeting STAT3 #3 or non-targeting siRNA control as previously described, or treated with 10 μM pyrimethamine (or dimethyl sulfoxide (DMSO) control) for 24 hours, and MCF-10A cells were treated for 24 hours with 2 μg/mL DOX (or DMSO control). Liquid chromatography coupled to tandem mass spectrometry (LC-MS/MS) was performed with five replicates per condition, as described in detail in the following protocol.

Cell pellets were extracted into 3 ml of 2:1 chloroform/methanol and 1 ml of phosphate-buffered saline (PBS) along with the internal standards pentadecanoic acid (PDA) (10 nmol, Sigma-Aldrich) and monoalkylglycerol ether (MAGE) (10 nmol, Santa Cruz Biotechnology) for negatively and positively charged metabolites, respectively. Centrifugation was used to separate organic and aqueous layers (1000 x g for 5 min); the organic layer was collected, dried under nitrogen, and re-dissolved in 120 µl chloroform. Metabolomes were separated with reverse-phase chromatography using a Luna C5 column (50 mm x 4.6 mm with 5 µm diameter particles, Phenomenex). The mobile phase A was a ratio of 95:5 water/methanol, and the mobile phase B was a ratio of 60:35:5 2-propanol/methanol/water. Solvent modifiers – 0.1 % ammonium hydroxide, and 0.1% formic acid with 5 mM ammonium formate – were used in both negative and positive ionization modes, respectively. The flow rate was initially at 0.1 ml/min for 5 min to alleviate backpressure associated with chloroform injection. Beginning at 0% B, the gradient increased linearly to 100% B over the course of 45 minutes at a flow rate of 0.4 ml/min, followed by an isocratic gradient of 100% B for 17 minutes at 0.5 ml/min before equilibrating for 8 minutes at 0% B with a flow rate of 0.5 ml/min.

Mass spectrometry was performed using an electrospray ionization (ESI) source on an Agilent 6430 or 6460 QQQ LC-MS/MS (Agilent Technologies). The capillary voltage was set to 3.0 kV, and the fragmentor voltage to 100 V. The drying gas temperature was 350°C, the flow rate was 10 l/min, and nebulizer pressure was at 35 psi. Metabolites were identified via Selective Reaction Monitoring (SRM) of the transition from precursor to product ions at associated optimized collision energies and retention times as previously described (185). Metabolites were then quantified by integrating the area under the curve, and normalized to the internal standard values.

3.1.6. Nanoparticles

The Layer-by-Layer nanoparticle library was synthesized and characterized by Hammond laboratory, Koch Institute for Integrative Cancer Research, Massachusetts Institute of Technology, Cambridge, MA, USA, using previously described methods (164,180). The list of investigated nanoparticles is shown in Table 2.

3.1.6.1. Cisplatin (CDDP) loading into anionic liposomes

Lipids and cholesterol were purchased from Avanti Polar Lipids. Cyanine dyes were purchased from Lumiprobe. All other reagents and solvents were purchased from Sigma or

VWR unless noted otherwise. Water used for the experiments below was purified using a Milli-Q Lab Water Purification System (Millipore Sigma) unless noted otherwise. Passive loading was employed for cisplatin (CDDP) encapsulation into the nanoparticles. 1,2-distearoyl-sn-glycero-3-phosphoglycerol (DSPG, 25mg/mL in 65:35:8 chloroform/methanol/water by volume) and 1,2-distearoyl-sn-glycero-3-phosphocholine (DSPC, 25 mg/mL in chloroform) and cholesterol (25 mg/mL in chloroform) were combined in a 1:1:1 mole ratio in a round bottom flask. The solvent was evaporated using a rotary evaporator until a dry lipid film was obtained. A Branson sonicator was filled with reverse-osmosis water and heated to 80 °C. The cisplatin solution used for loading was prepared by adding cisplatin (Tokio Chemical Industry) to water (8.5 mg/mL) and heating to 80 °C to solubilize the drug. Under sonication, the cisplatin solution was added to the lipid film to give a final lipid + cholesterol concentration of 5 mg/mL. The solution was sonicated at 80 °C for 3 minutes with manual shaking. Following, the solution was allowed to cool to room temperature and unencapsulated cisplatin in the form of insoluble precipitates was removed via centrifugation (1 minute at 200 rcf), after which the supernatant was removed and centrifugation repeated. To obtain uniform particles, the cisplatin + liposome solution was extruded (186), making sure to keep the solution at or above 80 °C to prevent drug precipitation.

3.1.6.2. Cisplatin (CDDP) quantification

A modified version of a previously published protocol was utilized (186). Sodium diethyldithiocarbamate trihydrate (Sigma Aldrich 71480, lot# BCBS9779V) was used for cisplatin derivatization as described in the representative protocol below. In a 1.5 mL tube, 225 µL of CDDP liposome sample and 225 µL of methanol were mixed with 50 µL water and 100 µL diethyldithiocarbamate (DDTC, 0.1 g/mL in 0.1N NaOH) followed by incubation for 30 minutes at 37 °C. Then, 300 µL chloroform were added, the tube was mixed via vortexing to extract the DDTC-CDDP complex and centrifuged for 5 minutes at 1000 rpm to separate the two layers. 100 µL of the organic phase were removed, solvent was evaporated, and the sample was resuspended in 100 µL dimethylformamide (DMF) for high performance liquid chromatography (HPLC) analysis (Agilent). A Sunfire C18 5 µm 4.6 x 150 mm column was utilized to analyze cisplatin derivatives using an isocratic method of 20% H_2O + 80% MeOH over 10 minutes at a flow rate of 1 mL/min. The peak area corresponding to the DDTC-CDDP complex at 254 nm was integrated and compared to a standard curve prepared from free cisplatin derivatized as described above to obtain CDDP loading in the liposomes.

Table 2. Types of nanoparticles used in this research and their abbreviated symbols

Nanoparticle	Abbreviation
CML core coated with dextran sulfate	DXS-NP
CML core coated with sulfated poly(β-cyclodextrin)	SBC-NP
CML core coated with heparin-folate conjugate	HF-NP
CML core coated with fucoidan	Fuc-NP
CML core coated with poly-L-aspartate	PLD-NP
CML core coated with poly(ethylene glycol-block-poly-L-glutamate)	PLE-b-PEG-NP
CML core coated with poly-L-glutamic acid	PLE-NP
CML core coated with polyacrylic acid	PAA-NP
CML core coated with hyaluronic acid	HA-NP
1:1 blend ratio of hyaluronic and poly-L-aspartic acid	1:1 HA/PLD
1:3 blend ratio of hyaluronic and poly-L-aspartic acid	1:3 HA/PLD
3:1 blend ratio of hyaluronic and poly-L-aspartic acid	3:1 HA/PLD
Cisplatin-loaded NP without coating layer	CDDP-CML
Cisplatin-loaded NP coated with DXS	CDDP-DXS
Cisplatin-loaded NP coated with PLE	CDDP-PLE

3.1.7. Drug treatment

MCF-10A cells were plated and allowed to adhere overnight. Then they were pre-incubated with 5 μM pyrimethamine (46706, Sigma Aldrich) or 2.5 μM ruxolitinib (ab141356, Abcam) for 4.5 hours. They were then induced with doxycycline (or DMSO vehicle control) for 24 hours, prior to nanoparticle treatment.

3.1.8. Nanoparticle treatment

After the indicated treatments, cells were incubated with 100 ng/mL fluorescently-labeled nanoparticles or H_20 vehicle control for 24 hours prior to flow cytometric analysis or microscopic imaging. Following treatment with CDDP-loaded nanoparticles or free CDDP, the cells were washed with PBS, replenished with fresh media and incubated for a total of three days, after which viability was detected by flow cytometry.

3.1.9. Nanoparticle library screening

MCF-10A cells were incubated with doxycycline (to induce STAT3C) or vehicle control for 24 hours, after which the membrane was stained red using Wheat Germ Agglutinin (W11262, Life Technologies), and nuclei were stained blue using Hoechst stain (4082S, Cell Signaling Technology). The stains were washed with PBS and the cells were treated with differently coated nanoparticles (100 ng/mL) in phenol red-free media and images were taken on CellObserver (Zeiss) every 30 minutes for a total of 8 hours. The membrane and nuclear nanoparticle binding were analyzed with custom pipelines created in CellProfiler 2.2.0 software (Broad Institute of Harvard and MIT).

3.1.10. Deconvolution microscopy

Chambered cover glass (ThermoFisher Scientific) was coated with rat tail collagen (300 μL of 50 μg/mL in 0.02N acetic acid). After 5 minutes, the wells were washed with room temperature PBS and allowed to dry in a sterile environment. Wells were stored at 4 °C up to one week prior to seeding MCF10A cells at 8,000 cells/well in DOX- or DMSO-containing media (n=3). The cells were allowed to adhere for 24 hours prior to treatment with 100 ng/mL sulfoCy3 labeled PLE-NP solution. The cells were incubated for either 2 or 24 hours, at which time they were washed 3x with PBS and fixed in 4% methanol free formaldehyde prepared in PBS (15 min, room temperature). This was followed by three washes of ice-cold Hank's Balanced Salt Solution (HBSS, ThermoFisher) at 5 min/wash. Solutions and cover glass/wells were kept covered with aluminum foil for the following steps to prevent photo bleaching of the fluorophores. 300 μL of wheat germ agglutinin-AF647 (10 μg/mL in HBSS) were added to each well and incubated at room temperature for 10 min. Cells were washed 3x with room temperature PBS (5 min/wash) before fixing again with 4% formaldehyde for 2 min followed by another 3x PBS wash (5 min/wash). 300 μL of 1.25 μg/mL Hoechst in PBS were added to each well for 2 min at room temperature before washing with 3x with room temperature PBS (5 min/wash). Finally, the wells were filled with ~5 drops of Vectashield (H-1000) to prevent photobleaching and stored at 4 °C protected from light. The cells were imaged with the Applied Precision DeltaVision Ultimate Focus Microscope with TIRF Module (Inverted Olympus X71 microscope) equipped with 405, 488, 512, and 568 nm lasers. Images were acquired with 60 and 100x objectives. All images were acquired under the same illumination settings and then processed with OMX softWoRx software (Applied Precison/GE). Image LUTs were linearly adjusted to improve contrast on FIJI.

3.1.11. Flow cytometry

Cells were induced with doxycycline (MCF-10A) or transfected with siRNA (SUM159PT and MDA-MB-231), and treated with fluorescently-labeled non-loaded or CDDP-loaded nanoparticles as described above. After incubation with nanoparticles, the cells were washed with PBS, trypsinized and neutralized with corresponding media, and washed again with PBS.

3.1.11.1. Analyzing the cellular binding of non-loaded nanoparticles

Cells were then resuspended and incubated with live/dead stain (L34975, Life Technologies) for 30 minutes at 4°C in the dark. When the cell integrity is compromised, the stain interacts with the free amines on the intracellular side and on the cell surface, emitting fluorescence of near infrared spectrum 50-fold greater compared with when the cells are intact and viable. The stain was removed by centrifugation (5 minutes at 1500 rpm), the cells were resuspended in PBS, and centrifuged again using the same parameters. Then the cells were carefully resuspended in PBS containing 3% FBS to obtain a single cell suspension, when analyzed on flow cytometer.

The gating strategy was first set according to the forward (FSC) and side (SSC) scatter of the laser, whose detection recapitulates the diameter and granularity of the cells. Accordingly, we focused on the homogenous cell population and avoided apoptotic cells and debris displayed by low laser intensity of FSC and SSC (Figure 12). Then, we looked into the height and area of the forward scatter signal (FSC-H and FCS-A, respectively) of the homogenous population of cells. By identifying the cells with the proportional FSC-H and FSC-A, the previous population was filtered to include only the single cells, and the cell aggregates were excluded from further analysis (Figure 12).

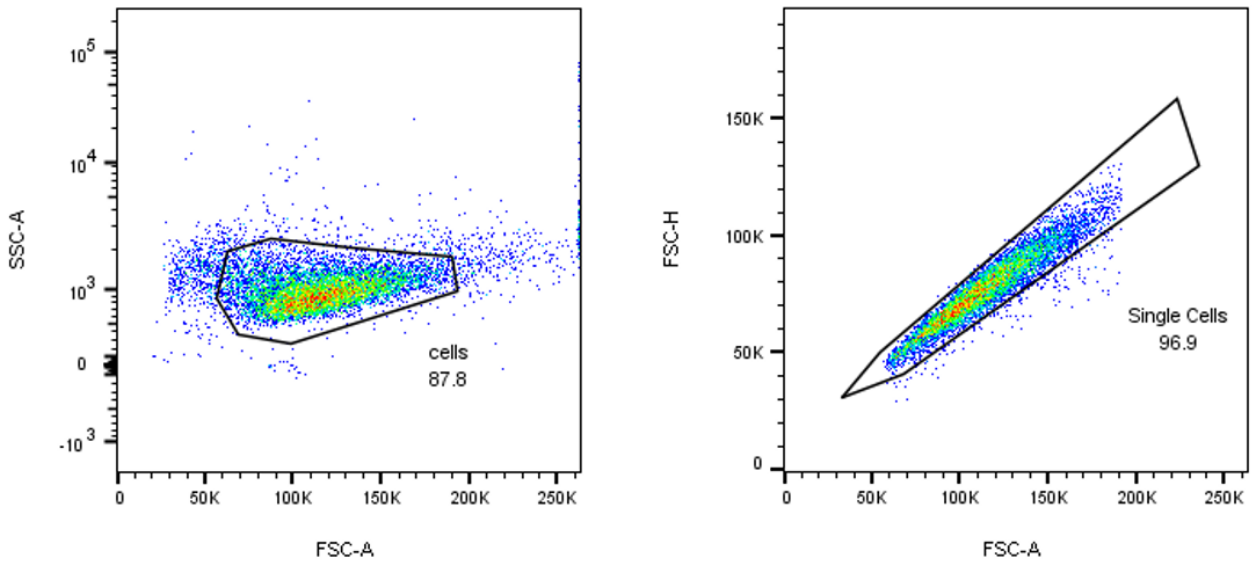

Figure 12. Determining populations of cells and single cells in flow cytometric analyses. The gating strategy for homogenous cell population determination was based on cell side scatter (SSC) and forwards scatter (FSC) laser signal, and FSC height and area for determining single cells.

Further, this population was refined by removing from analysis the population of cells that stained positive for live/dead stain (Figure 13). The nanoparticle-cell binding was measured by yellow-green (FITC) fluorescence of the nanoparticles attached to the cells in the population of viable single cells. Prior to recording fluorescence intensities, the laser wavelengths were set according to the vehicle-treated negative controls (Figure 13). The median fluorescence intensities of each sample containing at least 1000 cells were taken into further statistical analysis.

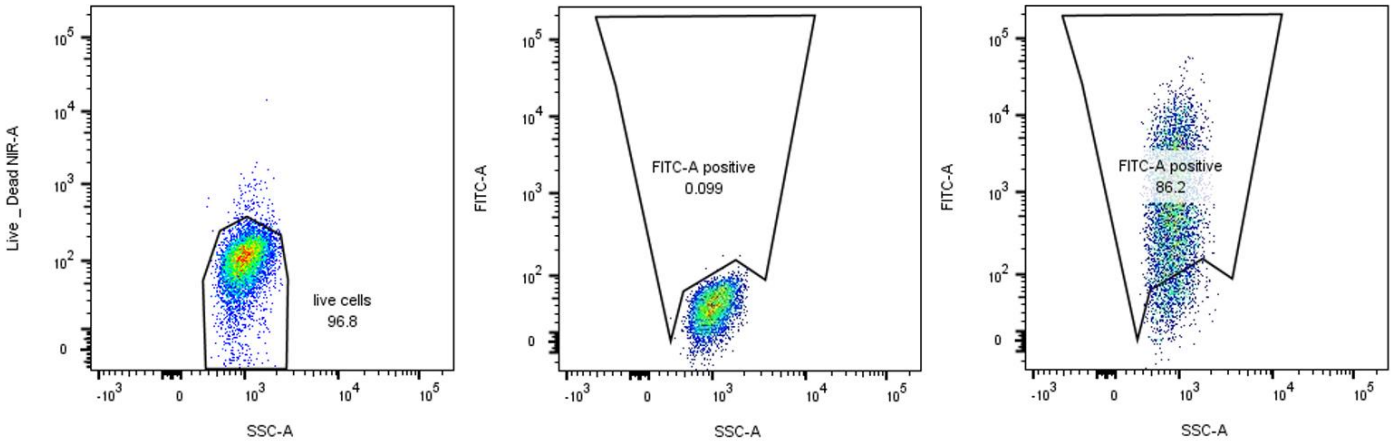

Figure 13. Determining population of live cells and gating strategy for nanoparticle fluorescence in flow cytometric analyses. Determining population of live/dead negative cells (left). Gating of NP-bound cell fluorescence (FITC-A) is set according to the vehicle H_2O treated control (middle). Nanoparticle-cell binding fluoresce is shown in right panel.

3.1.11.2. Analyzing the viability after CDDP-loaded NP treatment

Previously trypsinized, neutralized with corresponding media, and washed cells were resuspended in PBS containing Annexin V/4′,6-diamidino-2-phenylindole (DAPI) staining. This was performed using Apoptosis Detection Kit I (BD Biosciences). In addition to samples stained with both Annexin V and DAPI which were taken into further analyses, each condition included samples stained with Annexin V only, DAPI only and non-stained controls to assure that there is no signal overlaps between the different lasers. The cells were then analyzed on flow cytometer and Annexin V/DAPI fluorescence of the cells was measured. Annexin V binds to phosphatidylserine, an intracellular molecule. Soon after initiation of apoptosis, phosphatidylserine is translocated to the cell surface, thus allowing detection of early apoptotic cells using Annexin V staining. DAPI intercalates between the two DNA strands and emits fluorescence when integrated into the cells with abrogated integrity, therefore allowing detection of the late apoptotic or necrotic cells.

When analyzing the data, we first determined the cell populations of interest using previously described gating methods for detecting cell population and single cells. Then we analyzed both Annexin V and DAPI fluorescence of each cell in the remaining population. Based on this, the percentage of viable cells for each sample, defined as both Annexin V and DAPI negative, were taken into further statistical analysis. Each sample contained at least 1000 cells.

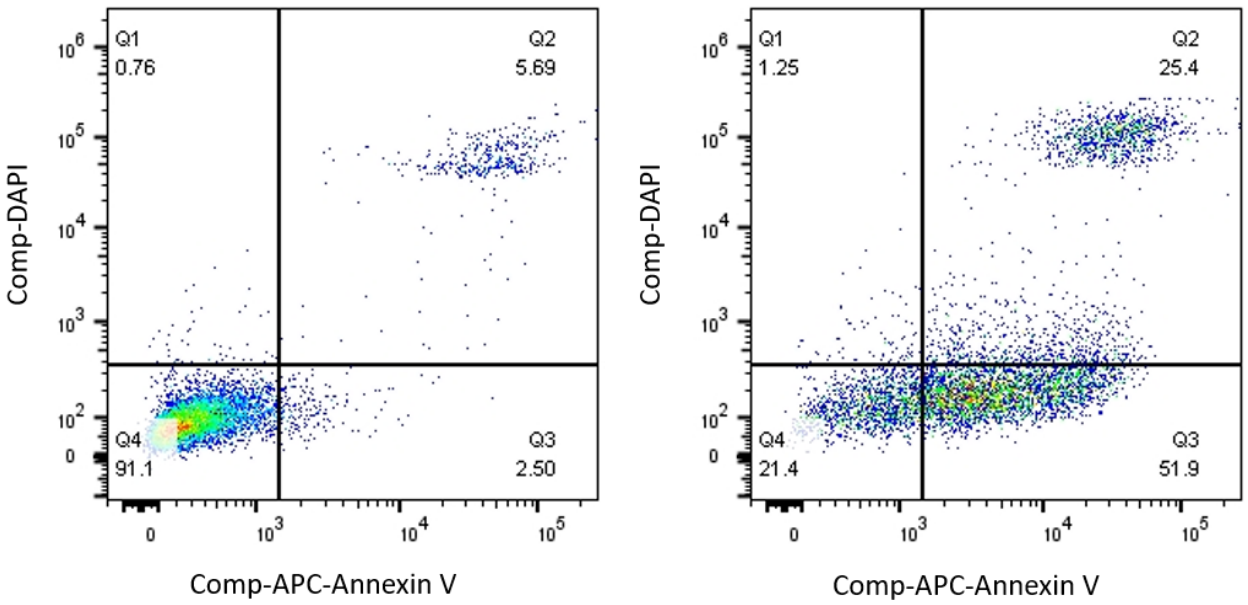

Figure 14. Determining viable, early and late apoptotic and necrotic cells based on the Annexin V and DAPI cell staining using flow cytometry. Vehicle treated controls (left) were used to setup the gating strategy for CDDP and CDDP-NP treated cell analyses (right).

All of the samples for flow cytometric analyses were prepared in at least three replicates, and each assay was performed in at least two independent biological experiments. Fluorescence distribution was acquired on a BD LRSFortessa instrument and analyzed with FlowJo software (Treestar). The gating strategy for fluorescence intensity determination is set according to vehicle-treated controls.

3.1.12. Three dimensional organoid culturing

Cells were cultured for three to ten days in Nanoculture plates (MBL International). The bottom of these plates allows adherence, and is coated with a non-adherent honeycomb or microsquare pattern structure, to allow adherence of a single cell to the bottom of the well. Remaining cells would attach to the cell adherent to the well bottom, forming a spherical three-dimensional structure (Figure 15). In our research, honeycomb pattern surface film plates were used.

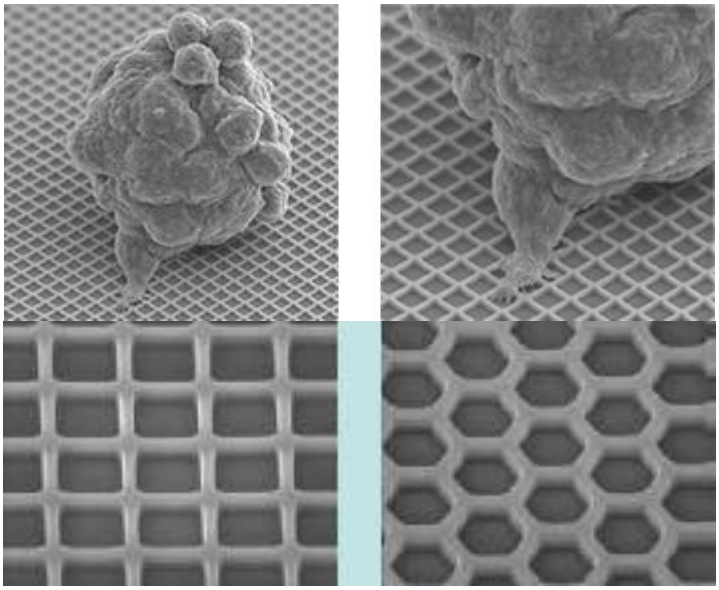

Figure 15. Patterns of 3D cell culture plates and cell adhesion in forming an organoid. HeLa cell spheroid attaching to the nano-scale microsquare structure of film (top). Microsquare and honeycomb microfilm surface patterns (bottom) (MBL International).

The MCF-10A cells were cultivated to form three-dimensional spheroids using their corresponding media with heat-inactivated horse serum. First, the plates were filled with 50% of media (containing 4µg/mL doxycycline or same volume DMSO), centrifuged 5 minutes at 1000 x g and incubated at 37℃ for 30 minutes. Then, the single cell suspension containing the remaining 50% of media was added to the corresponding wells, and incubated at room temperature for 15 minutes, when moved to the incubator and incubated for three to ten days. To preserve STAT3C induction, the MCF-10A cells were replenished with 2 µg/mL doxycycline (or DMSO control) every three days of culturing. The MDA-MB-231 and MDA-MB-468 cells were cultured in the same manner, however, these cell lines were proven unable to grow three-dimensional organoids using this approach.

3.1.12.1. Confocal microscopy of three-dimensional organoids

MCF-10A organoids were stained with 2 µM Lox1 hypoxia stain (#Lox1, MBL International) and treated with 100 ng/mL nanoparticles for 24 hours prior to confocal microscopy imaging with Zeiss LSM 880+ Airyscan microscope. All images were acquired under the same illumination settings using 10x objective. Image LUTs were linearly adjusted to improve contrast in ImageJ software (National Institutes of Health). Yellow-green (NP) and red (Lox1) fluorescence were quantitated in unprocessed Z-stack three-dimensional images with a custom macro script written in ImageJ software (National Institutes of Health).

3.1.12.2. Macro for fluorescence quantification through organoids

```
rename("Original");
run("Duplicate...", "title=channel_2 duplicate channels=2");
run("Add Slice");
run("Add Slice");
setSlice(nSlices);
run("Add Slice");
run("Add Slice");
run("Despeckle", "stack");
run("Mean...", "radius=35 stack");
run("Auto Threshold", "method=Otsu white stack use_stack_histogram");
run("Invert LUT");
run("Dilate", "stack");
run("Close-", "stack");
run("Fill Holes", "stack");
selectImage("Original");
run("Duplicate...", "title=channel_1 duplicate channels=1");
run("Add Slice");
run("Add Slice");
setSlice(nSlices);
run("Add Slice");
run("Add Slice");
selectImage("channel_2");
run("3D OC Options", "volume nb_of_obj._voxels integrated_density
mean_gray_value centroid dots_size=10 font_size=40 show_numbers white_numbers
store_results_within_a_table_named_after_the_image_(macro_friendly)
redirect_to=channel_1");
run("3D_Objects_Counter", "threshold=128 slice=26 min.=90000 max.=192136448
exclude_objects_on_edges objects statistics summary");
```

3.1.13. Gamma irradiation

MCF-10A cells were cultured with DMSO- or DOX-containing media for 24 hours to induce the expression of STAT3C. Then, the cells were irradiated with a ^{137}Cs source as a single administration of the following doses: 0; 0.5; 1; 2; 4; 6; 8 or 10 Gy. Relative viable cell number was determined after 1 to 3 days of incubation by measuring ATP-dependent bioluminescence (Cell Titer-Glo; Promega) on a Luminoskan Ascent luminometer. For nanoparticle-cell association experiments, the cells were treated for 24 hours with 100 ng/mL PLE-NP following single dose irradiation, after which NP-cell binding was quantified using flow cytometry, as described above.

3.1.14. Gene set enrichment analysis

The previously published GSE5460 microarray dataset of 129 breast cancer patient samples (187) and GSE3526 normal tissue microarray dataset (353 samples) were downloaded from the Gene Expression Omnibus. The breast cancer patient samples data was sorted according to the mRNA expression of genes of interest, namely cysteine dioxygenase (CDO1), cystathionine gamma lyase (CTH), phospholipase A2 (PLA2G4A), cyclooxygenase 2 (COX-2), 5-lipoxygenase (5-LOX) and the housekeeping gene GAPDH. The 30 samples with the highest and lowest mRNA expression for each gene were analyzed for expression of validated STAT3 gene expression signatures (188). For comparison of STAT3 activation profile between normal and breast cancer samples, the two expression datasets were compared for enrichment of STAT3 gene expression signatures. Gene set enrichment analysis was performed using xapps.gsea from the Broad Institute of MIT and Harvard (http://software.broadinstitute.org). Statistical significance is presented as normalized p-value and normalized enrichment score (NES).

3.2. *Means of selection, size and construction of models*

In assuring robust evaluation of the biological effects, testing each of the hypotheses included different methodological approaches and mechanistic evaluation in different cell lines. For mass spectrometric lipid analyses three different approaches and two cellular systems for STAT3 inhibition or activation were used, with each of the conditions tested in five replicates. The relevance of the metabolic changes was observed through statistical significance and consistency of metabolic alterations across the tested models. For LbL NP screen, 12 NPs with different shell layers were evaluated, each of which tested in duplicates.

Flow cytometric analyses: To exclude the possibility that increased binding to STAT3-driven cells is a non-specific effect of malignant transformation, NPs coated with non-targeting modification were used in parallel with the STAT3-targeting NPs. To assure robust detection of STAT3-dependent NP cellular binding, three different cellular systems were used. In MCF-10A cells STAT3-dependency was evaluated by performing STAT3C induction, and inhibition of STAT3 phosphorylation (ruxolitinib) and transcriptional activity (pyrimethamine). For TNBC cell line testing, two distinct single sequences siRNA (and scramble siRNA control) were used for cell transfections to exclude the possibility of off-target siRNA effects on NP-cell binding. In evaluating the effects of cisplatin-loaded NPs, each cell condition was treated with cisplatin-loaded targeting NPs, non-targeted NPs, non-coated NPs and unencapsulated cisplatin. Each of the experimental conditions was tested in at least triplicates unless otherwise indicated. Each biological experiment was separately done at least twice.

3.3. *Statistical Analyses*

Following generation of data, the results were analyzed using method-appropriate software as previously stated, which required generation of computational pipelines and macros. Final data was analyzed with Excel version 2013 (Microsoft) and GraphPad Prism software version 8.4 (La Jolla, CA) for evaluation of statistical significance of the proposed hypothesis. Thereby, the descriptive statistical methods and methods for the statistical testing of the hypothesis were used. Among the descriptive methods, central tendency measures such as arithmetic mean and median; and measures of variability (standard deviation and standard error) were used. For statistical significance validation, Students T-tests and two-way ANOVA were performed. The analyzed data is presented in tabular and graphical form. Values of $p<0.05$ are considered significant (*, $p < 0.05$; **, $p < 0.01$; ***, $p < 0.001$; ****, $p < 0.0001$).

3.4. *Place and time of experimental research*

Preparation of samples, validations of methodology, experimental work and data analysis were performed in the period 2018-2020. The research was performed at the following institutions:

- Department of Medical Oncology, Dana-Farber Cancer Institute, Boston, MA, USA
- Harvard Center for Biological Imaging, Harvard University, Cambridge, MA, USA
- Koch Institute for Integrative Cancer Research, Massachusetts Institute of Technology, Cambridge, MA, USA

4. Results

4.1. *Effect of STAT3 activation on lipid metabolism in breast cancer cells*

STAT3 is aberrantly activated in the majority of breast cancers and represents a crucial mediator in pathogenesis of this disease. Since STAT3 is difficult to target directly, we investigated whether metabolic changes driven by constitutive activation of STAT3 could provide a therapeutic opportunity (189). Recognizing that malignant transformation is associated with changes in a variety of cellular metabolites, we examined how STAT3 qualitatively and quantitatively affects lipid distribution in mammary epithelial cells using two complementary systems (189). First, we used non-transformed MCF-10A cells in which an activated form of STAT3 can be expressed with an inducible doxycycline (DOX)-responsive promoter, and is sufficient to induce tumorigenesis *in vivo* (190). Induction of the promoter increased STAT3 protein expression and phosphorylation, followed by enhanced mRNA expression of target genes including *SOCS3*, *BCL-3*, BCL2-associated transcription factor 1 (*BCLAF1*), and a positive autoregulation of its own expression (Figure 16) (189).

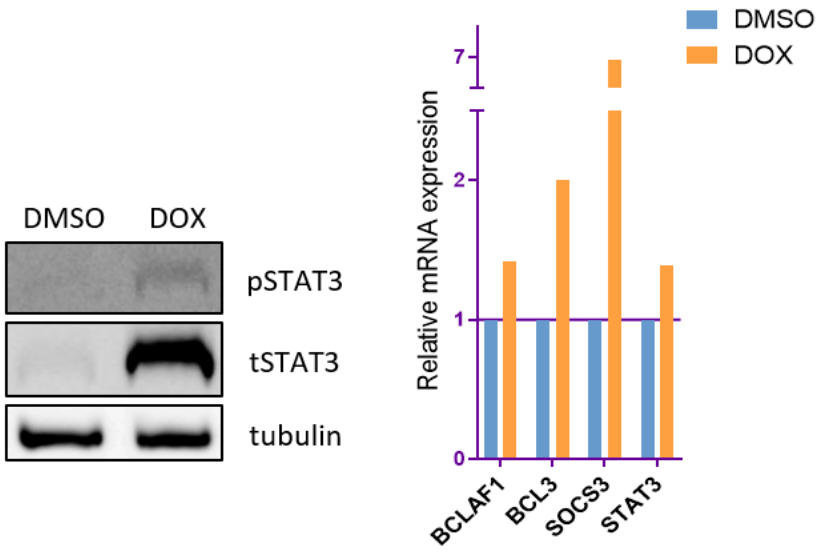

Figure 16. Induction of STAT3C in MCF-10A cells. MCF-10A cells were incubated for 24 hours in DMSO- or DOX-containing media to induce the expression of STAT3C. Then, cells were lysed and protein and mRNA were analyzed by Western blot (left, n=2) and qRT-PCR (right, n=4).

We also used a triple-negative breast cancer cell line, MDA-MB-468, characterized

by constitutive STAT3 tyrosine phosphorylation, in which we inhibited STAT3 activity genetically (with RNA interference) or pharmacologically (with the small molecule inhibitor pyrimethamine (PYR) (Figure 17) (189,191).

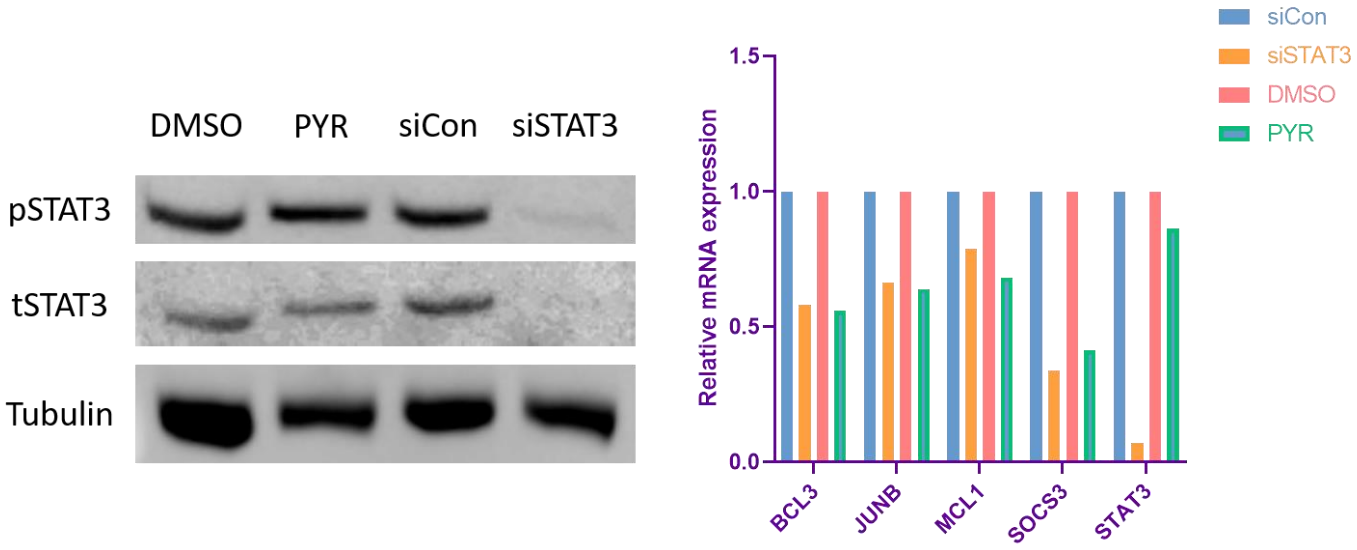

Figure 17. Inhibition of STAT3 activity in MDA-MB-468 cells. MDA-MB-468 cells were transfected with siSTAT3#3 or non-targeting siRNA control for 48 hours; or were treated with 10μM pyrimethamine (PYR) or DMSO control for 24 hours. Then the cells were lysed and protein and mRNA were analyzed by immunoblotting (left, n=2) and qRT-PCR (right, n=4). Genetical inhibition of STAT3 reults in reduction of mRNA and protein expression of STAT3, followed by reduced mRNA expression of its target genes. Pyrimethamine does not affect phosphorylation or protein expression of STAT3, and inhibits STAT3 transcriptional activity, as evidenced by reduction of its target genes expression.

We then performed liquid chromatography coupled to tandem mass spectrometry (LC-MS/MS)-based profiling to evaluate a total of 220 lipid molecules, which we have classified into negatively and positively charged metabolites (189). We have presented the results as the cumulative data of all metabolites significantly altered with STAT3 activity in either of the conditions (Tables 3 and 4). Then, we evaluated which of the alterations are consistent across different approaches in activating or suppressing STAT3 activity and summarized the findings in Figures 18 and 19. The inclusion criteria for such summary were statistically significant alterations with minimally 20% difference and same type of alteration within at least two of the tested conditions. In the summary figures, we also included the metabolites belonging to the same group of molecules if there was statistical significance in any of the conditions. The data of the metabolites that do not display statistically significant modification by any of the three means of modulation of STAT3 activity are not shown.

Table 3. Cumulative data on STAT3-induced alterations of positively charged metabolites in MDA-MB-468 cells and MCF-10 cells.

Metabolite	siSTAT3		PYR		DOX	
	fold change	p-value	fold change	p-value	fold change	p-value
C16:0/C16:0/C16:0 TAG	**0.561**	**0.023**	**0.765**	**0.062**	1.135	0.107
C16:0/C20:4/C16:0 TAG	0.912	0.642	**0.624**	**0.002**	**1.381**	**0.003**
C18:0/C18:0/C18:0 TAG	**0.540**	**0.016**	1.042	0.762	1.067	0.536
C18:0/C18:1/C18:0 TAG	**0.492**	**0.012**	**0.717**	**0.040**	1.116	0.256
C18:0/C20:4/C18:0 TAG	0.787	0.220	**0.645**	**0.002**	**1.249**	**0.038**
16:0 MAG	0.781	0.438	**1.269**	**0.017**	1.046	0.722
C18:1 MAG	0.890	0.757	**1.399**	**0.021**	1.273	0.065
C20:4 MAG	0.930	0.867	1.022	0.858	**1.724**	**0.001**
C16:0e/C2:0 MAGe	0.896	0.788	**1.774**	**0.012**	**1.242**	**0.028**
C18:0e MAGe	0.772	0.487	0.952	0.637	**1.139**	**0.012**
C18:1e/C2:0 MAGe	0.953	0.904	**0.825**	**0.040**	1.116	0.423
C16:0/C18:1 PG	**0.606**	**0.003**	2.503	0.202	-	-
C18:0e/C18:1 PGe	1.109	0.545	0.976	0.858	**1.522**	**0.014**
C16:0/C20:4 PC	0.842	0.305	0.843	0.139	**1.175**	**0.012**
C18:0/C18:1 PC	0.738	0.081	0.892	0.195	**1.200**	**0.006**
C18:0/C20:4 PC	0.921	0.647	0.862	0.131	**1.118**	**0.049**
C16:0e/C18:1 PCe	0.778	0.203	1.142	0.186	**1.254**	**0.001**
C16:0e/C20:4 PCe	**0.622**	**0.027**	0.955	0.662	**1.171**	**0.012**
C18:0e/C18:1 PCe	0.846	0.371	1.084	0.490	**1.199**	**0.011**
C18:0e/C20:4 PCe	**0.681**	**0.033**	0.984	0.830	**1.216**	**0.005**
C16:0p/C20:4 PCp	0.825	0.284	0.953	0.700	**1.180**	**0.002**

Metabolite	siSTAT3		PYR		DOX	
	fold change	p-value	fold change	p-value	fold change	p-value
C18:0p/C20:4 PCp	0.733	0.113	0.969	0.753	**1.186**	**0.003**
C18:0 LPC	0.828	0.691	1.088	0.339	**1.326**	**0.022**
C16:0e LPCe	0.519	0.229	**1.564**	**0.004**	**1.306**	**0.030**
C18:0e LPCe	0.745	0.492	**1.584**	**0.001**	**1.485**	**0.007**
C18:1e LPCe	0.862	0.699	**1.443**	**0.004**	1.259	0.242
C16:0 LPS	1.113	0.826	**1.716**	**0.016**	1.156	0.594
C18:1 LPS	0.837	0.683	**1.238**	**0.031**	1.200	0.467
C18:0 LPS	0.955	0.910	**1.326**	**0.036**	1.323	0.086
C18:0 LPE	0.682	0.422	**1.545**	**0.002**	1.291	0.057
C16:0/C20:4 PE	0.947	0.765	0.875	0.236	**1.200**	**0.006**
C18:0/C18:1 PE	0.861	0.420	0.963	0.784	**1.163**	**0.047**
C16:0/C18:1 PS	0.976	0.912	**1.306**	**0.007**	1.296	0.109
C16:0/C20:4 PS	1.138	0.590	**1.710**	**0.000**	1.162	0.244
C18:0/C18:1 PS	0.774	0.248	**0.887**	**0.050**	1.178	0.135
C16:0e/C18:1 PSe	0.966	0.886	**1.377**	**0.001**	**1.284**	**0.001**
C16:0 Ceramide	0.733	0.350	**0.571**	**0.000**	1.291	0.132
C18:0 Ceramide	0.466	0.070	**0.546**	**0.000**	**1.643**	**0.018**
C18:1 Ceramide	0.708	0.289	**0.631**	**0.002**	-	-
C16:0/C18:1 DAG	0.844	0.642	**1.850**	**0.002**	1.047	0.445
C18:0/C18:1 DAG	0.674	0.267	1.312	0.197	**1.189**	**0.039**
C16:0 AC	0.843	0.704	**0.750**	**0.001**	**1.705**	**0.002**
sphingosine	0.606	0.088	**1.479**	**0.001**	1.323	0.071
Estradiol sulfate	0.737	0.440	1.096	0.684	**1.300**	**0.010**

Metabolite	siSTAT3		PYR		DOX	
	fold change	p-value	fold change	p-value	fold change	p-value
C16:0 SM	0.970	0.878	**1.229**	**0.002**	**1.223**	**0.023**
C18:0 SM	1.018	0.922	**1.267**	**0.003**	**1.206**	**0.004**
C18:1 SM	0.930	0.635	1.104	0.079	**1.295**	**0.013**
C20:4 SM	0.869	0.515	0.913	0.152	**1.282**	**0.007**

STAT3 was inhibited in MDA-MB-468 cells using siRNA to STAT3 (siSTAT3) or pyrimethamine (PYR); and activated in MCF-10A cell using doxycycline (DOX), when the cell metabolic profile was analyzed by LC-MS/MS. The metabolic alterations are shown as a fold change between activated and inactivated STAT3 (siCon/siSTAT3; DMSO/PYR and DOX/DMSO). Statistically significant changes are indicated in bold, and names of metabolites are bolded if consistent within at least two conditions.

C16:0 – palmitic acid; C18:0 – stearic acid; C18:1 – oleic acid; C20:4 – arachidonic acid; TAG – triacylglycerol; MAG – monoacylglycerol; PG – phosphatidylglycerol; PC – phosphatidylcholine; PCp – phosphatidylcholine plasmalogen; LPC – lysophosphatidylcholine; LPS – lysophosphatidylserine; LPE – lysophosphatidylethanolamine; PE – phosphatidylethanolamine; PS – phosphatidylserine; DAG – diacylglycerol; SM – sphingomyelin. “e” at the end of the symbol indicates an ether linkage.

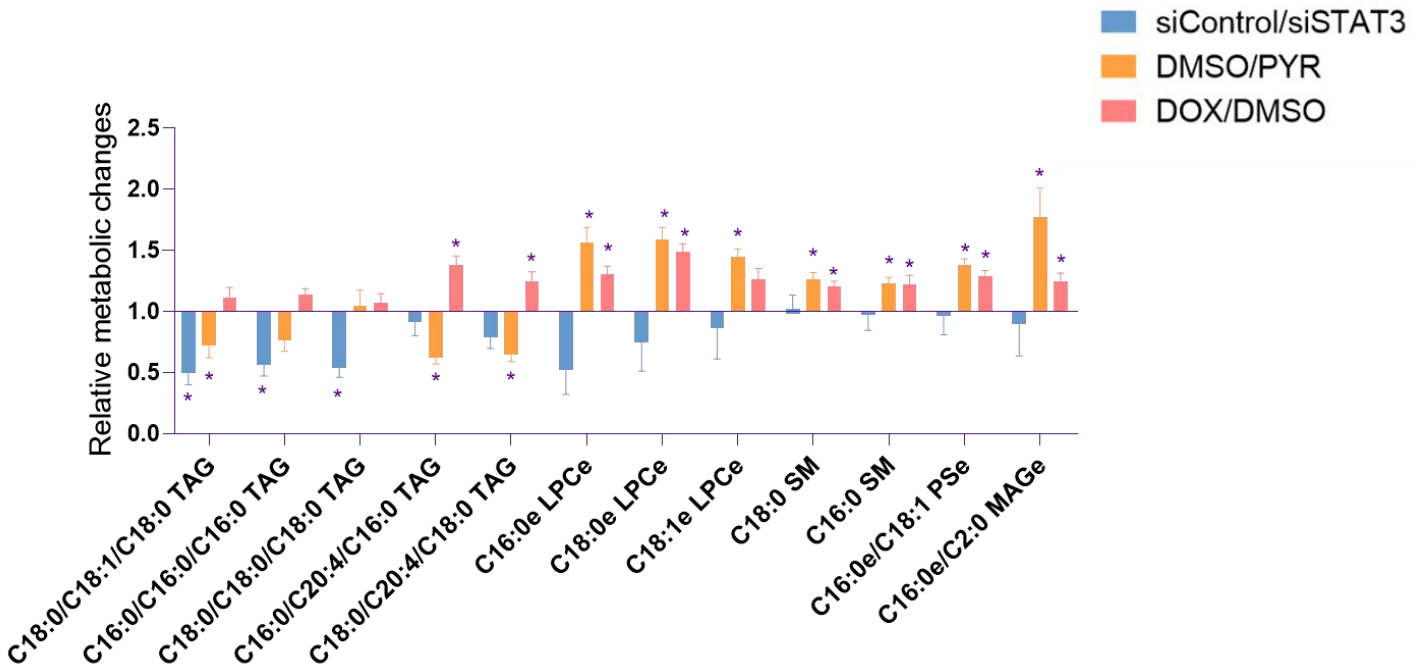

Figure 18. Summary of the most consistent STAT3-dependent alterations of positively charged lipids in MDA-MB468 cells and MCF-10A cells. Data is presented as mean values of fold change between active and inactive STAT3 ±SEM. *, p value < 0.05.

C16:0 – palmitic acid; C18:0 – stearic acid; C18:1 – oleic acid; C20:4 – arachidonic acid; TAG – triacylglycerol; MAG – monoacylglycerol; LPC –lysophosphatidylcholine; PS – phosphatidylserine; SM – sphingomyelin. “e” at the end of the symbol indicates an ether linkage.

Table 4. Cumulative data on STAT3-induced alterations of negatively charged metabolites in MDA-MB-468 cells and MCF-10 cells.

Metabolite	siSTAT3		PYR		DOX	
	fold change	p-value	fold change	p-value	fold change	p-value
C16:0 NAT	**0.540**	**0.000**	**0.602**	**0.002**	0.609	0.250
C18:0 NAT	**0.577**	**0.002**	**0.384**	**0.001**	0.614	0.245
C18:1 NAT	**0.753**	**0.017**	**0.262**	**0.000**	1.509	0.448
C20:4 NAT	**0.714**	**0.014**	0.450	0.166	**0.383**	**0.018**
C16:0/C16:0 PI	**0.494**	**0.000**	1.004	0.961	0.986	0.925
C16:0/C18:1 PI	**0.837**	**0.005**	**1.201**	**0.005**	1.005	0.970
C16:0/C20:4 PI	1.073	0.247	**0.678**	**0.001**	1.065	0.622
C18:0/C18:1 PI	**0.813**	**0.001**	**1.204**	**0.031**	0.979	0.857
C18:0/C20:4 PI	**1.176**	**0.010**	0.960	0.572	1.049	0.664
C16:0e/18:1 PIe	**0.656**	**0.000**	1.113	0.214	0.978	0.876
C16:0e/20:4 PIe	**0.832**	**0.015**	**0.634**	**0.001**	1.060	0.607
C18:0e/C18:1 PIe	**0.742**	**0.000**	1.090	0.346	1.020	0.874
C18:0e/C20:4 PIe	**0.739**	**0.000**	**0.725**	**0.013**	1.016	0.879
C20:4e LPIe	1.087	0.570	**1.863**	**0.004**	1.125	0.810
C16:0/C20:4 PA	**0.525**	**0.001**	0.728	0.202	0.771	0.659
C16:0/C18:1 PA	**0.597**	**0.000**	**1.345**	**0.025**	1.027	0.833
C18:0/C20:4 PA	**0.668**	**0.001**	0.867	0.572	0.974	0.879
C16:0e/18:1 PAe	**0.634**	**0.002**	**1.158**	**0.077**	0.973	0.827
C18:0e/C18:1 PAe	**0.833**	**0.023**	1.816	0.256	0.800	0.683
C18:0e/C20:4 PAe	**0.697**	**0.038**	**0.562**	**0.043**	1.675	0.224
C16:0 LPA	**0.458**	**0.001**	1.239	0.206	**1.628**	**0.005**

Metabolite	siSTAT3		PYR		DOX	
	fold change	p-value	fold change	p-value	fold change	p-value
C18:1 LPA	**0.599**	**0.012**	0.939	0.688	**1.573**	**0.025**
C20:4 LPA	**0.538**	**0.005**	0.758	0.170	1.164	0.611
C16:0e LPAe	-	-	**3.110**	**0.009**	0.763	0.491
C16:0 FFA	**0.911**	**0.020**	1.187	0.051	0.953	0.450
C20:4 FFA	**0.906**	**0.002**	1.016	0.832	0.952	0.541
C24:0 FFA	**0.803**	**0.021**	1.043	0.594	0.998	0.984
18:0/C16:0 C1P	0.887	0.074	**1.167**	**0.009**	0.980	0.883
Cardiolipin C18:1/18:1/18:1/18:1 T1	**0.877**	**0.027**	0.952	0.907	0.795	0.769
Cardiolipin C18:1/18:1/18:1/18:1 T2	**0.872**	**0.027**	1.032	0.839	1.051	0.710
lanosterol	**0.770**	**0.036**	1.331	0.333	0.989	0.906

STAT3 was inhibited in MDA-MB-468 cells using siRNA to STAT3 (siSTAT3) or pyrimethamine (PYR); and activated in MCF-10A cell using doxycycline (DOX), when the cell metabolic profile was analyzed by LC-MS/MS. The metabolic alterations are shown as a fold change between activated and inactivated STAT3 (siCon/siSTAT3; DMSO/PYR and DOX/DMSO). Statistically significant changes are indicated in bold, and names of metabolites are bolded if consistent within at least two conditions.

C16:0 – palmitic acid; C18:0 – stearic acid; C18:1 – oleic acid; C20:4 – arachidonic acid; NAT – N-acyl taurine; PIe – phosphatidylinositol; PA – phosphatidic acid; LPA – lysophosphatidic acid; FFA – free fatty acid; C1P – ceramide -1- phosphate. “e” at the end of the symbol indicates an ether linkage.

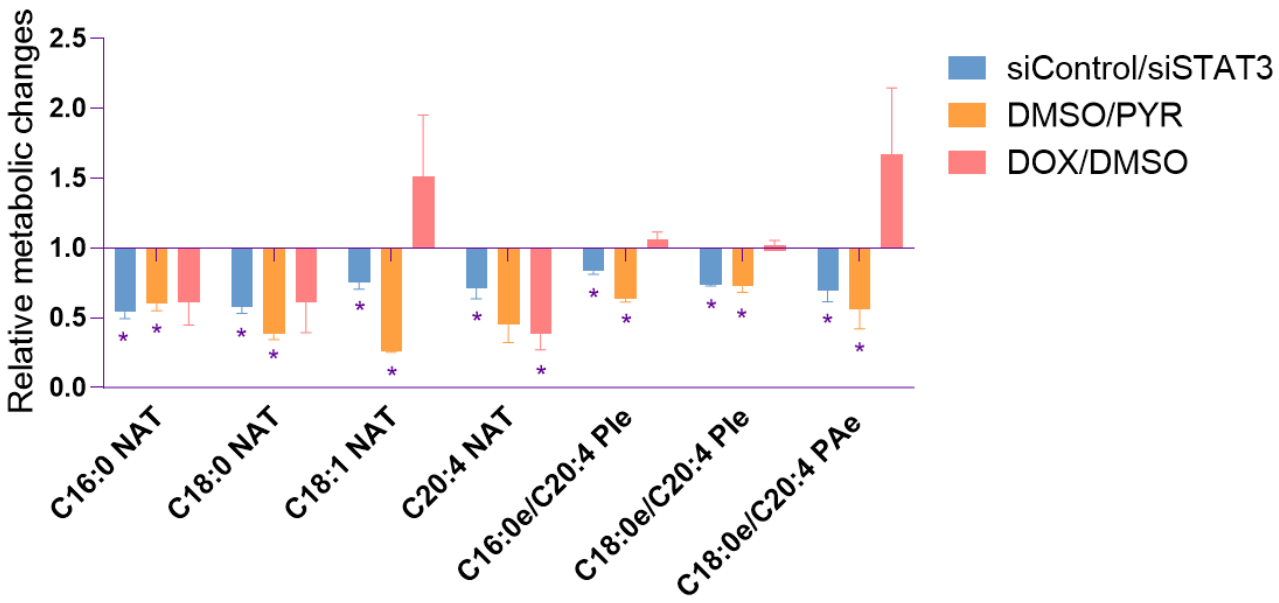

Figure 19. Summary of the most consistent STAT3-dependent alterations of negatively charged lipids in MDA-MB468 cells and MCF-10A cells. Data is presented as mean values of fold change between active and inactive STAT3 ±SEM. *, p value < 0.05.

C16:0 – palmitic acid; C18:0 – stearic acid; C18:1 – oleic acid; C20:4 – arachidonic acid; NAT – N-acyl taurine; PIe – phosphatidylinositol; PA – phosphatidic acid. “e” at the end of the symbol indicates an ether linkage.

We found several classes of lipid molecules that were significantly changed by activated STAT3 (Figures 18 and 19) (189). Four distinct but similar N-acyl-taurine (NAT) metabolites were decreased in MDA-MB-468 cells with activated STAT3 (189). Similarly, the presence of N-arachidonoyl taurine (C20:4 NAT), which has been reported to induce apoptosis of prostate cancer cells (192,193), was diminished when STAT3C was induced in MCF-10A cells (189). Two other taurine derivates, N-palmitoyl (C16:0) and N-stearoyl (C18:0) taurine, were strongly reduced when STAT3 is constitutively active in MDA-MB-468 cells, and showed an analogous trend with STAT3C induction (189). Interestingly, several lipid metabolites that were negatively modulated by STAT3, including taurine, were conjugated with arachidonic acid (AA, C20:4), the precursor for eicosanoid synthesis (Figures 18 and 19) (189). Both taurine and AA metabolites are actively involved in plasma membrane remodeling (194,195), providing a potential molecular distinction of STAT3-driven cancer cells (189). In addition, cellular abundance of two of the investigated triacylglycerols and phosphatidylinositol derivates decreases with activation of STAT3 in MDA-MB-468 cells, however analogy was not observed in STAT3-inducible system. For other metabolites such as sphingomyelin, lysophosphatidylcholine ether, monoacylglycerol

ether and phosphatidylserine overlapping correlation was found between PYR inhibition and STAT3 stimulation, although no significant effect was observed with STAT3 silencing. While these changes may be important, they may also be cell context dependent.

These consistent and large decreases in AA and taurine may be directly related to transcriptional changes mediated by activated STAT3 (189). To further investigate if such correlation is detectable in breast cancer patients, we performed Gene set enrichment analysis (GSEA) using microarray data from 129 primary breast cancer patient samples (187), and compared the expression of enzymes involved in AA and taurine metabolism with the expression of STAT3 gene expression signatures. STAT3 gene expression signatures were highly enriched in patients' samples with low expression of both cystathionine gamma lyase (CTH) and cysteine dioxygenase (CDO1), the two enzymes required for taurine synthesis from homocysteine (Figure 20) (189).

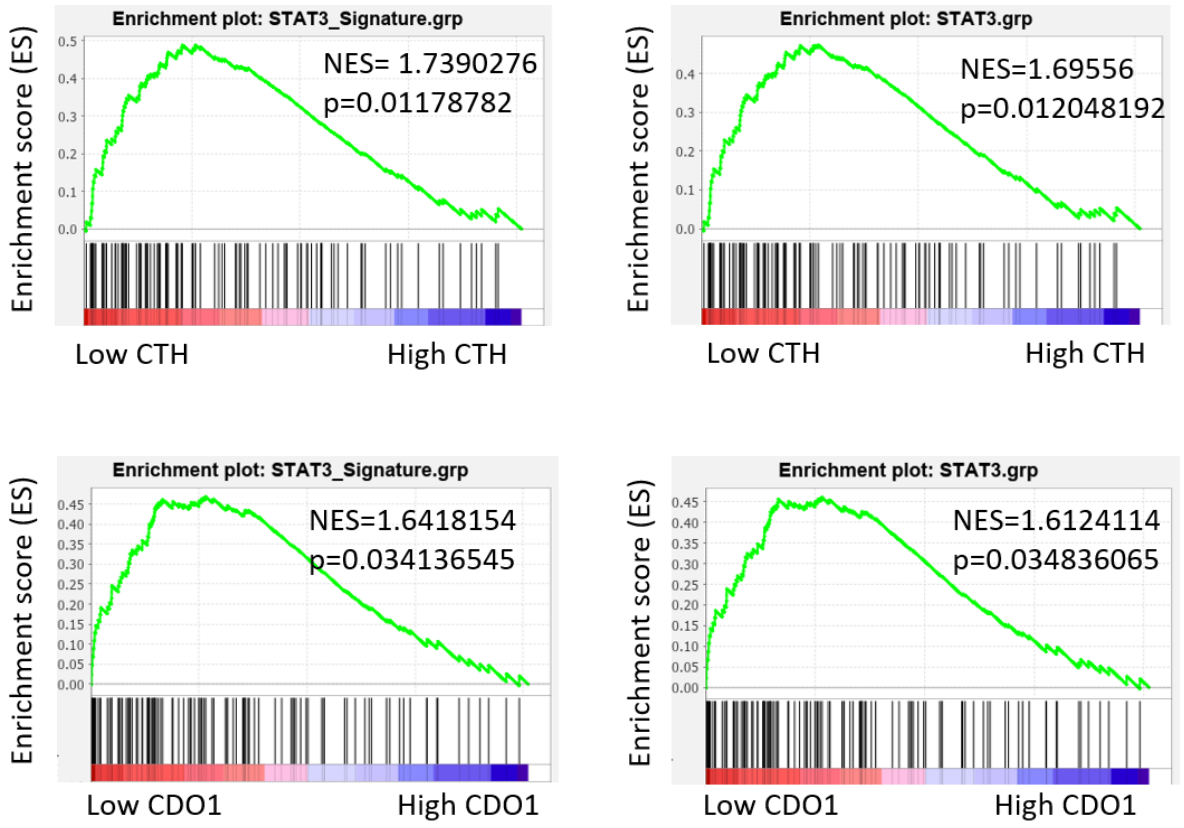

Figure 20. Correlation of enzymes involved in taurine synthesis with STAT3 gene expression signatures in breast cancer patient samples. Expression of enzymes cystathionine gamma lyase (CTH) and cysteine dioxygenase (CDO1) negatively correlates with the presence of STAT3 gene expression signature in the dataset of 129 breast cancer patient samples.

To investigate if STAT3 activity correlates with AA metabolism, we tested the correlation between STAT3 gene expression signature and expression of enzymes involved in AA membrane release and metabolism. STAT3 gene expression signatures were highly associated with mRNA expression of AA metabolic enzymes cyclooxygenase 2 (COX-2, PTGS2) and 5-lipoxigenase (5-LOX, ALOX5) (Figure 21) (189).

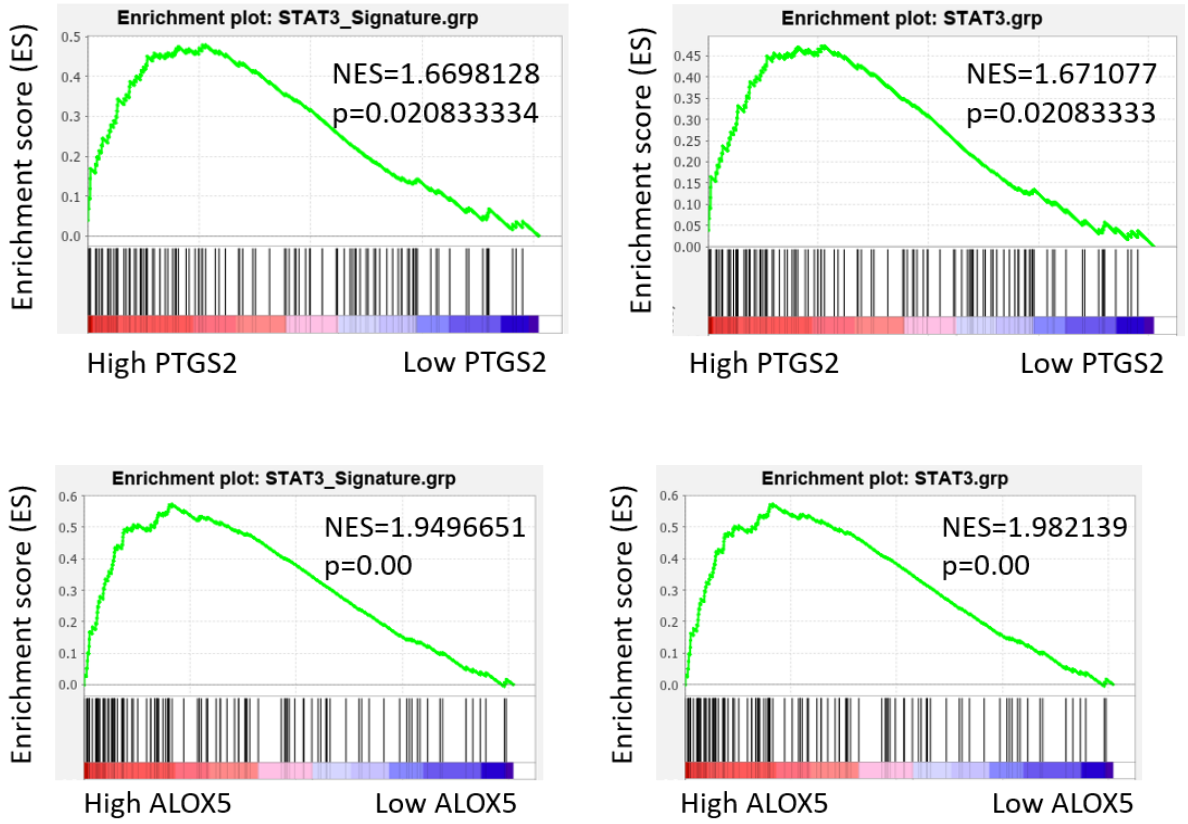

Figure 21. Correlation of enzymes involved in arachidonic acid metabolism with STAT3 gene expression signatures in breast cancer patient samples. Expression of enzymes cyclooxygenase 2 (PTGS2) and 5-lipooxygenase (ALOX5) positively correlates with the presence of STAT3 gene expression signature in the dataset of 129 breast cancer patient samples.

By contrast, phospholipase A2 (PLA2G4A), which is necessary for AA release from the membrane, did not show a significant relationship (Figure 22) (189).

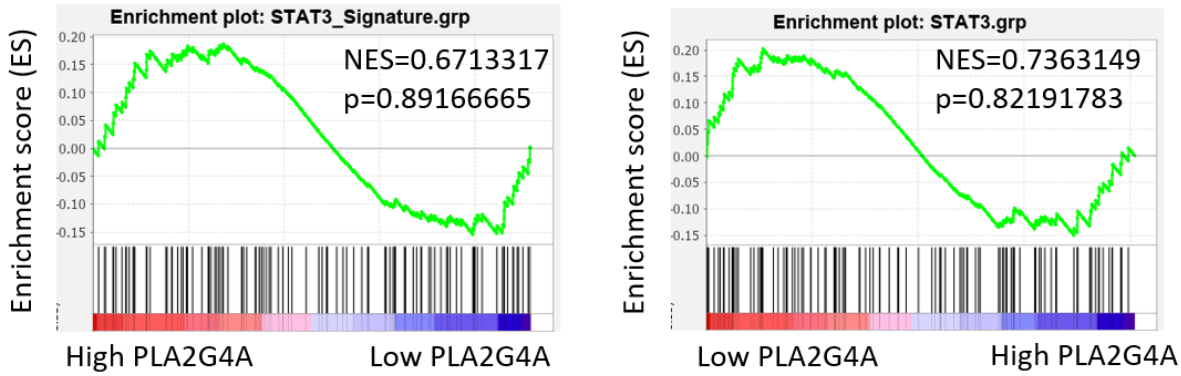

Figure 22. Correlation of enzyme responsible for arachidonic acid membrane release with STAT3 gene expression signatures in breast cancer patient samples. Expression of enzyme phospholipase A2 (PLA2G4A) does not correlate with the presence of STAT3 gene expression signature in the dataset of 129 breast cancer patient samples.

Similarly, the STAT3 signatures showed no correlation with the housekeeping gene GAPDH in the same breast cancer patient datasets (Figure 23) (189).

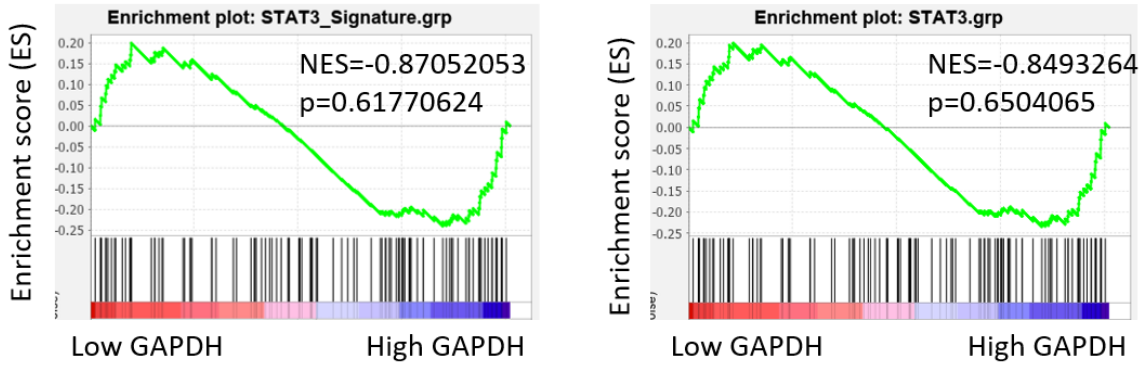

Figure 23. Correlation of housekeeping gene with STAT3 gene expression signatures in breast cancer patient samples. Expression of a housekeeping gene, glyceraldehyde 3-phosphate dehydrogenase (GAPDH), does not correlate with the presence of STAT3 gene expression signature in the dataset of 129 breast cancer patient samples.

Consistent with previous findings (196-9), these data indicate an intriguing crosstalk between STAT3 signaling and enhanced eicosanoid synthesis associated with inflammatory processes and cancer progression (189,200). The fact that both taurine derivates and AA are involved in plasma membrane remodeling (194,195) provides a basis for how changes in the metabolic architecture resulting from aberrant STAT3 activation can provide specificity for a tumor-targeting approach employing surface-directed nanoparticles (189).

4.2. *LbL nanoparticle library screen to identify STAT3-targeting drug carriers*

Given these prominent changes in lipid composition driven by activated STAT3, we investigated targeting STAT3-driven cancer cells using novel nanoparticles that can exploit these differences (189). Layer-by-layer (LbL) nanoparticles (NP) consist of a colloidal template as a core, surrounded by multiple ultrathin alternatively charged layers (189). Different charge layers allow packaging of a variety of therapeutic molecules with controlled release of the active substance (189). Most importantly, the surface layer is responsible for the NP interaction with the plasma membrane, thus determining its cell association and enabling targeting abilities (164,174,189). Therefore, we screened a library of 12 LbL NPs differing in their external layer to determine the surface composition that allowed the highest binding to cells characterized by the STAT3-induced lipid profile relative to non-malignant cells (189). The LbL coatings of surface layer contained either carboxylated or sulfated functional groups. The NPs carboxylated coating were the following: poly-L-aspartic acid (PLD), poly-L-glutamic acid (PLE), poly-L-glutamic acid – block – poly-ethylene glycol (PLE-b-PEG), polyacrylate (PAA) and sodium hyaluronate (HA), whereas dextran sulfate (DXS), sulfated poly(β-cyclodextrin) (SBC), heparin sulfate folate conjugate (HF) and fucoidan (Fuc) were the coating containing sulfated groups. We have also tested three blends of ratios 1:1; 1:3 and 3:1 combining hyaluronic acid and poly-L-aspartic acid coatings.

MCF-10A cells were induced with doxycycline (or treated with DMSO control) for 24 hours, when stained for membrane and nuclei and treated with differently coated nanoparticles. Then they were imaged every 30 minutes for a total of 8 hours, and the nuclear and membrane co-localization were analyzed by CellProfiler, using a custom pipeline for uniform NP detection. The quantification of membrane and nuclear co-localization of each of these particles are shown in Figures 24-35, and summarized in Figure 36.

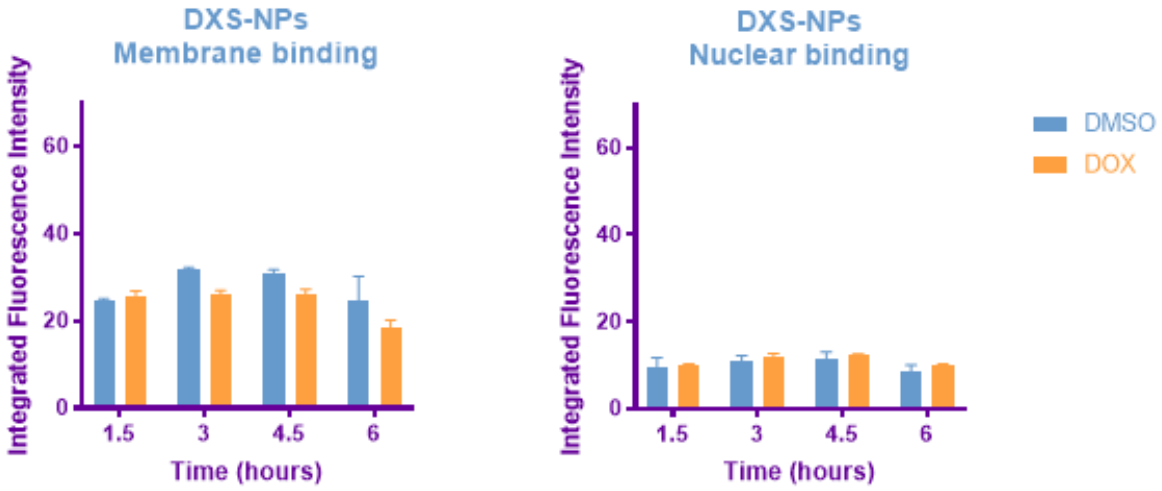

Figure 24. Dextran sulfate (DXS)-coated NPs binding to MCF-10A cells. Co-localization with membrane (left) and nuclei (right) of STAT3C-induced (orange) and non-induced (blue) MCF-10A cells over the course of time, as recorded by microscopy (mean value ±SD, n=2). The difference in NP-cell association between DOX-induced and DMSO-treated cells is not statistically significant, as evaluated by 2-way ANOVA test.

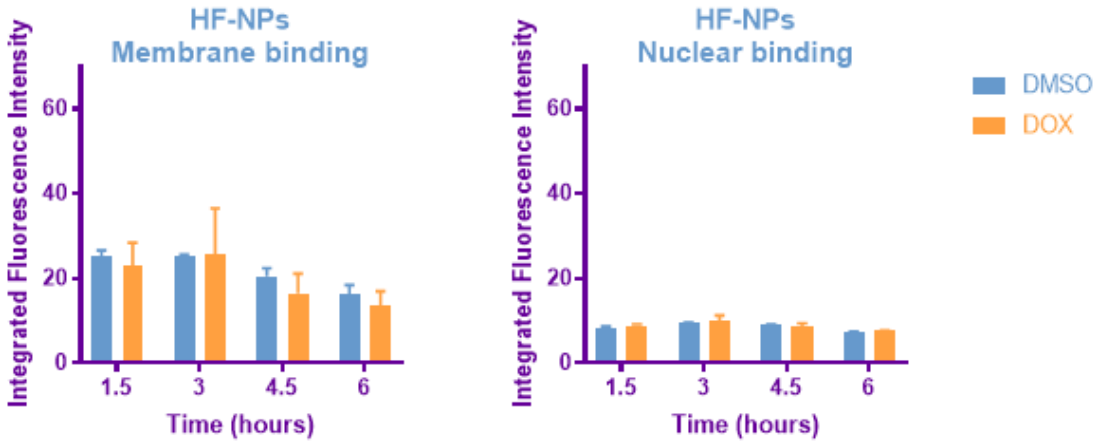

Figure 25. Heparin sulfate folate conjugate (HF)-coated NP binding to MCF-10A cells. Co-localization with membrane (left) and nuclei (right) of STAT3C-induced (orange) or non-induced (blue) MCF-10A cells over the course of time, as recorded by microscopy (mean value ±SD, n=2). The difference in NP-cell association between DOX-induced and DMSO-treated cells is not statistically significant, as evaluated by 2-way ANOVA test.

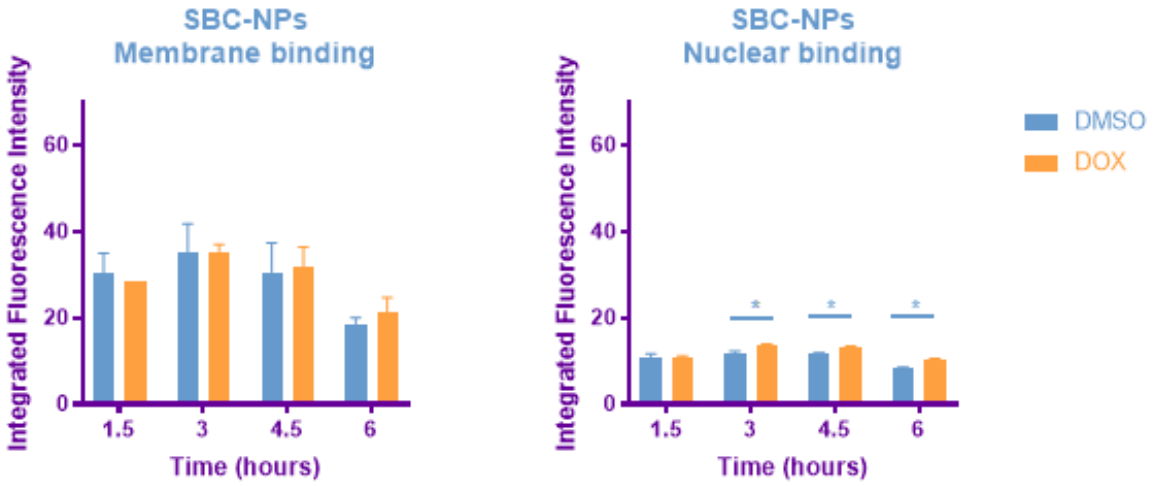

Figure 26. Sulfated poly (β-cyclodextrin) (SBC)-coated NP binding to MCF-10A cells. Co-localization with membrane (left) and nuclei (right) of STAT3C-induced (orange) and non-induced (blue) MCF-10A cells over the course of time, as recorded by microscopy (mean value ±SD, n=2). The difference in NP-nuclei co-localization between DOX-induced and DMSO-treated cells is statistically significant, as evaluated by 2-way ANOVA test.

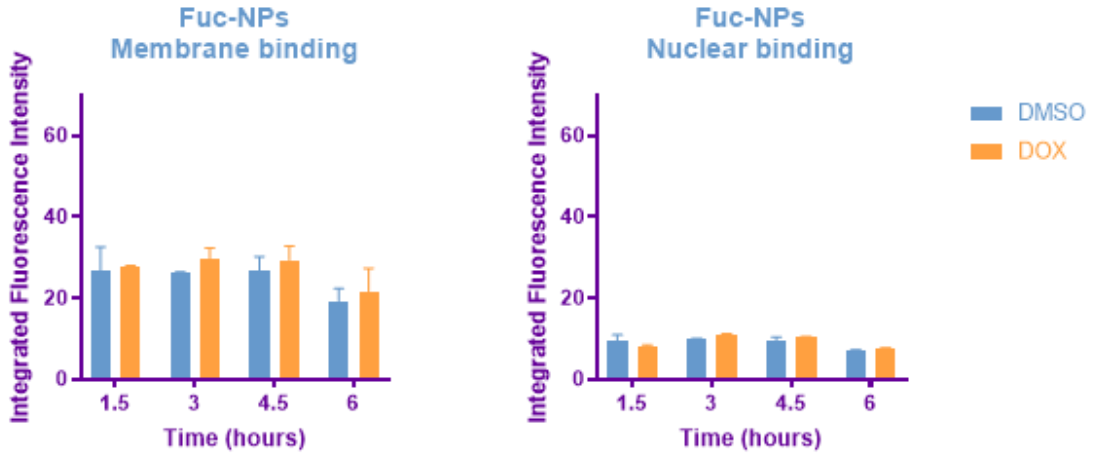

Figure 27. Fucoidan (Fuc)-coated NP binding to MCF-10A cells. Co-localization with membrane (left) and nuclei (right) of STAT3C-induced (orange) and non-induced (blue) MCF-10A cells over the course of time, as recorded by microscopy (mean value ±SD, n=2). The difference in NP-cell association between DOX-induced and DMSO-treated cells is not statistically significant, as evaluated by 2-way ANOVA test.

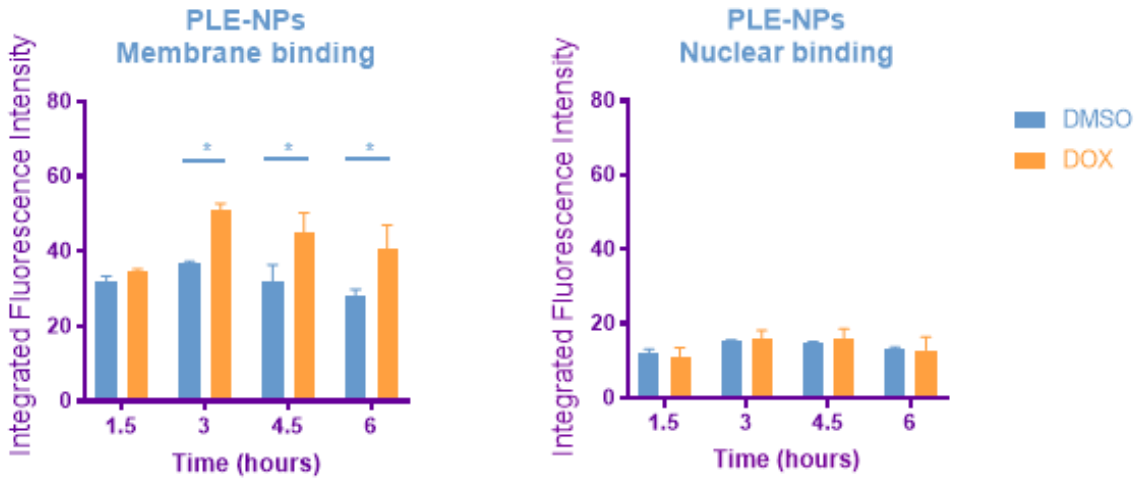

Figure 28. Poly-L-glutamic acid (PLE)-coated NP binding to MCF-10A cells. Co-localization with membrane (left) and nuclei (right) of STAT3C-induced (orange) and non-induced (blue) MCF-10A cells over the course of time, as recorded by microscopy (mean value ±SD, n=2). The difference in NP-membrane binding between DOX-induced and DMSO-treated cells is statistically significant, as evaluated by 2-way ANOVA test.

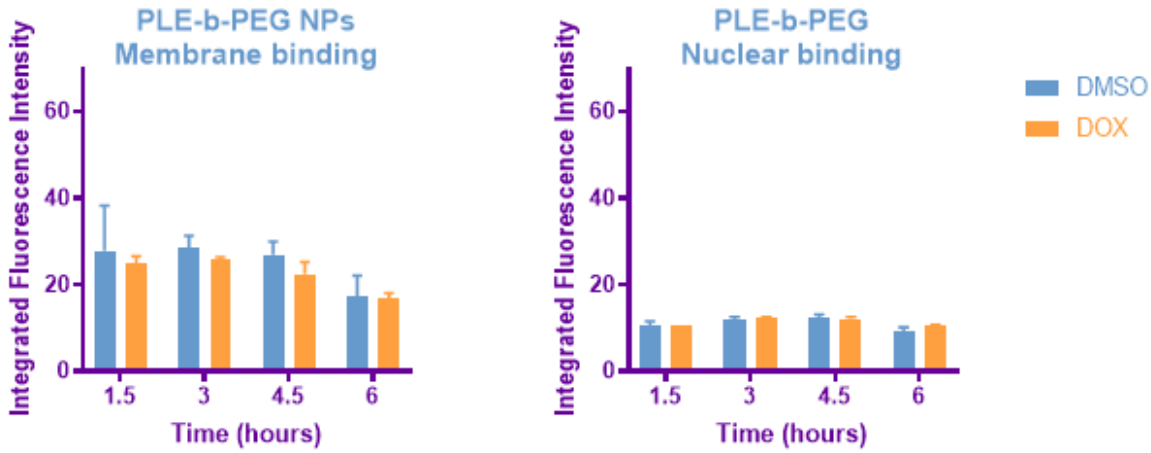

Figure 29. Poly-L-glutamic acid-block-poly-ethylene glycol (PLE-b-PEG)-coated NP binding to MCF-10A cells. Co-localization with membrane (left) and nuclei (right) of STAT3C-induced (orange) and non-induced (blue) MCF-10A cells over the course of time, as recorded by microscopy (mean value ±SD, n=2). The difference in cell-association between DOX-induced and DMSO-treated cells is not statistically significant, as evaluated by 2-way ANOVA test.

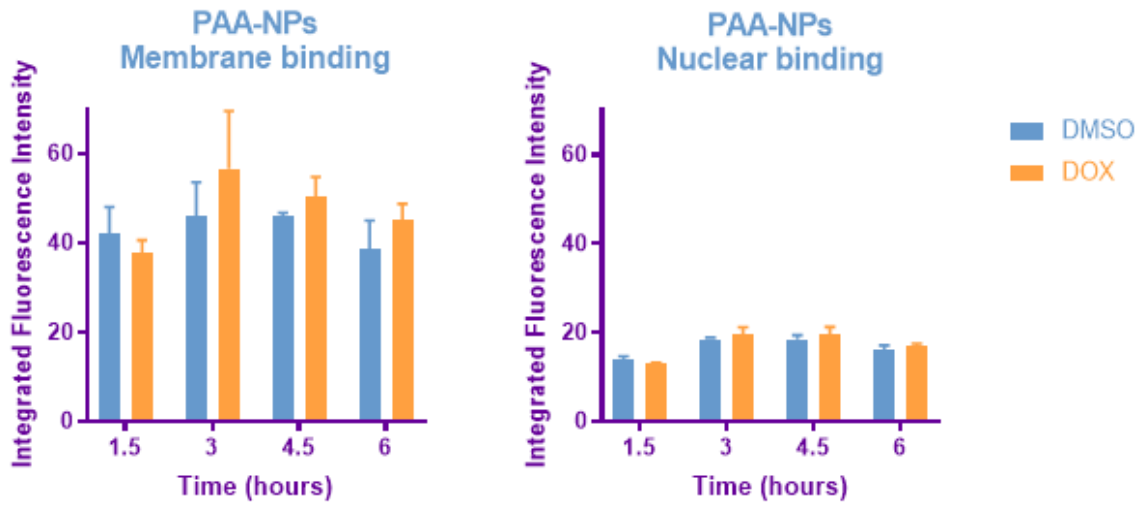

Figure 30. Polyacrylic acid (PAA)-coated NP binding to MCF-10A cells. Co-localization with membrane (left) and nuclei (right) of STAT3C-induced (orange) and non-induced (blue) MCF-10A cells over the course of time, as recorded by microscopy (mean value ±SD, n=2). The difference in cell-association between DOX-induced and DMSO-treated cells is not statistically significant, as evaluated by 2-way ANOVA test.

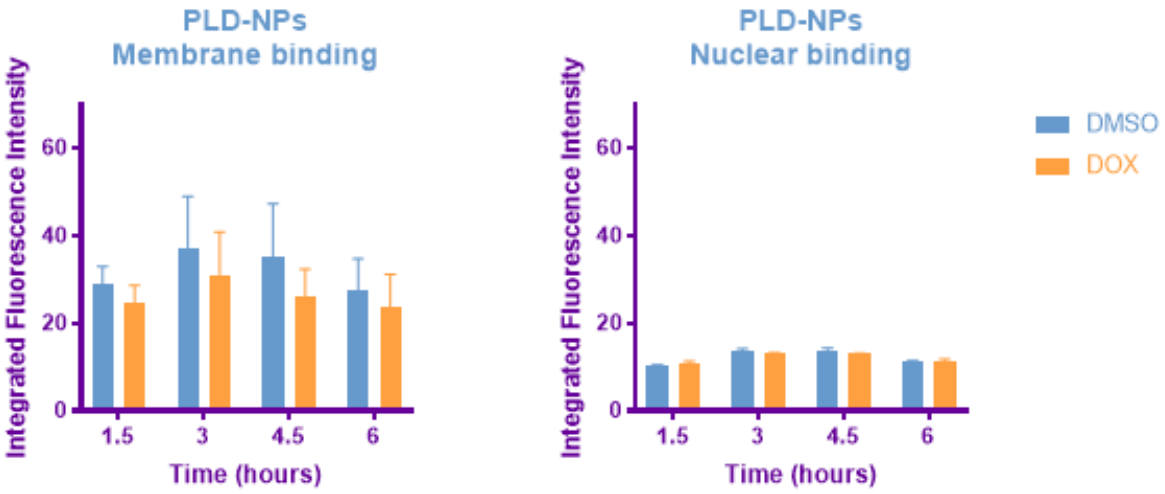

Figure 31. Poly-L-aspartic acid (PLD)-coated NP binding to MCF-10A cells. Co-localization with membrane (left) and nuclei (right) of STAT3C-induced (orange) and non-induced (blue) MCF-10A cells over the course of time, as recorded by microscopy (mean value ±SD, n=2). The difference in cell-association between DOX-induced and DMSO-treated cells is not statistically significant, as evaluated by 2-way ANOVA test.

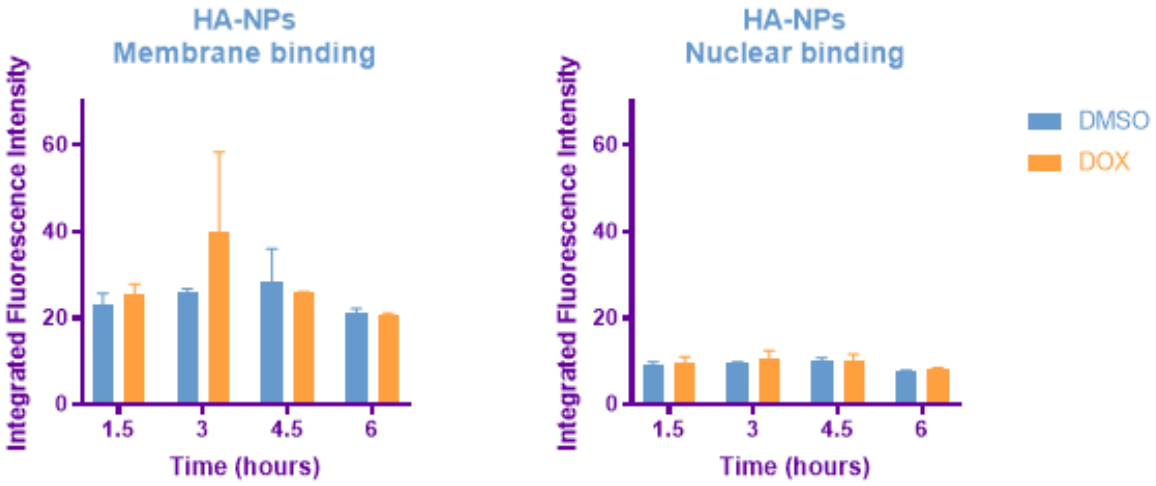

Figure 32. Hyaluronic acid (HA)-coated NP binding to MCF-10A cells. Co-localization with membrane (left) and nuclei (right) of STAT3C-induced (orange) and non-induced (blue) MCF-10A cells over the course of time, as recorded by microscopy (mean value ±SD, n=2). The difference in cell-association between DOX-induced and DMSO-treated cells is not statistically significant, as evaluated by 2-way ANOVA test.

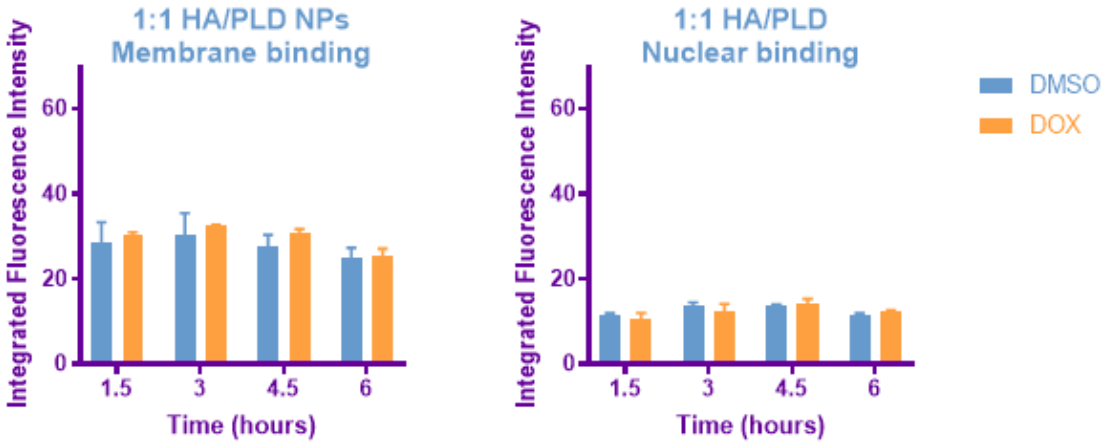

Figure 33. 1:1 blend ratio of hyaluronic and poly-L-aspartic acid (HA/PLD)-coated NP binding to MCF-10A cells. Co-localization with membrane (left) and nuclei (right) of STAT3C-induced (orange) and non-induced (blue) MCF-10A cells over the course of time, as recorded by microscopy (mean value ±SD, n=2). The difference in cell-association between DOX-induced and DMSO-treated cells is not statistically significant, as evaluated by 2-way ANOVA test.

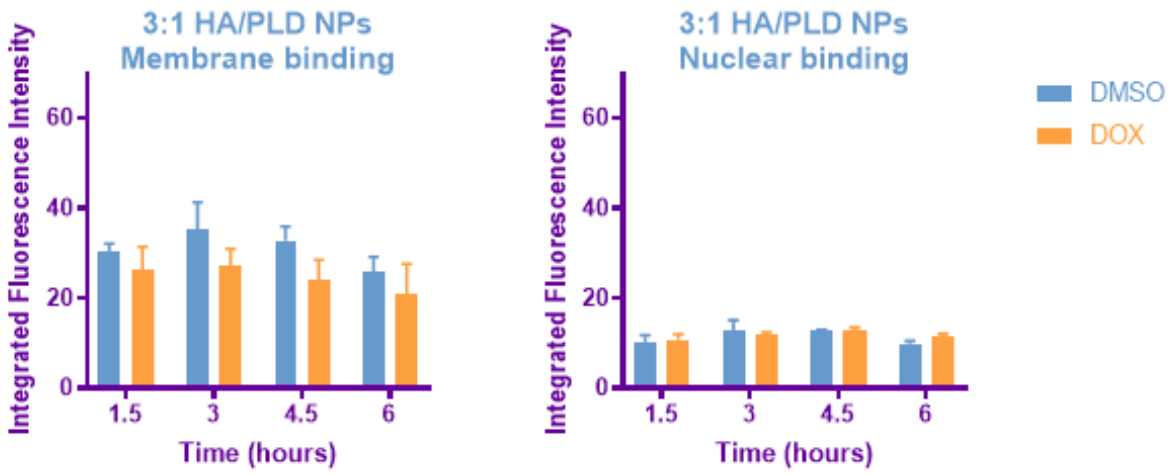

Figure 34. 3:1 blend ratio of hyaluronic and poly-L-aspartic acid (HA/PLD)-coated NP binding to MCF-10A cells. Co-localization with membrane (left) and nuclei (right) of STAT3C-induced (orange) and non-induced (blue) MCF-10A cells over the course of time, as recorded by microscopy (mean value ±SD, n=2). The difference in cell-association between DOX-induced and DMSO-treated cells is not statistically significant, as evaluated by 2-way ANOVA test.

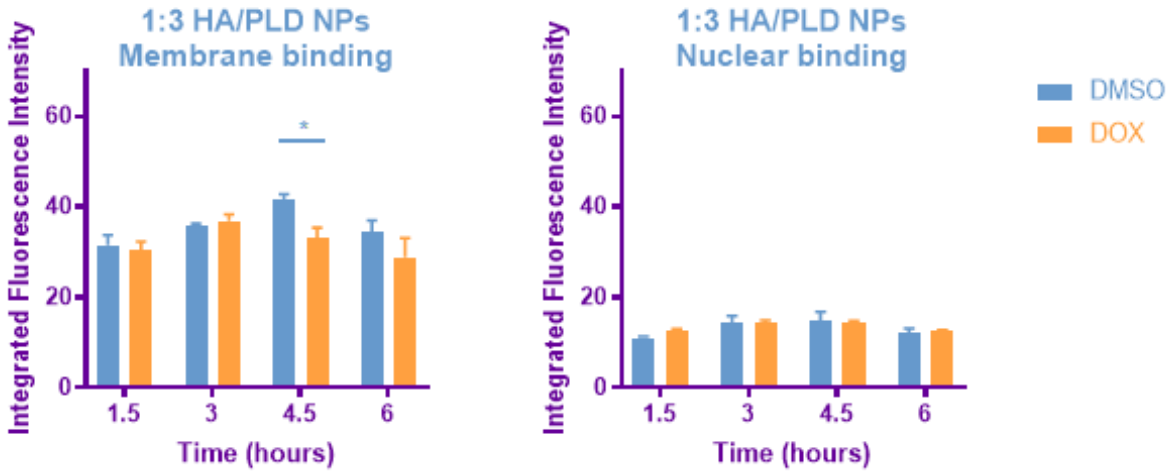

Figure 35. 1:3 blend ratio of hyaluronic and poly-L-aspartic acid (HA/PLD)-coated NP binding to MCF-10A cells. Co-localization with membrane (left) and nuclei (right) of STAT3C-induced (orange) and non-induced (blue) MCF-10A cells over the course of time, as recorded by microscopy (mean value ±SD, n=2). The difference in cell-association between DOX-induced and DMSO-treated cells is not statistically significant, as evaluated by 2-way ANOVA test.

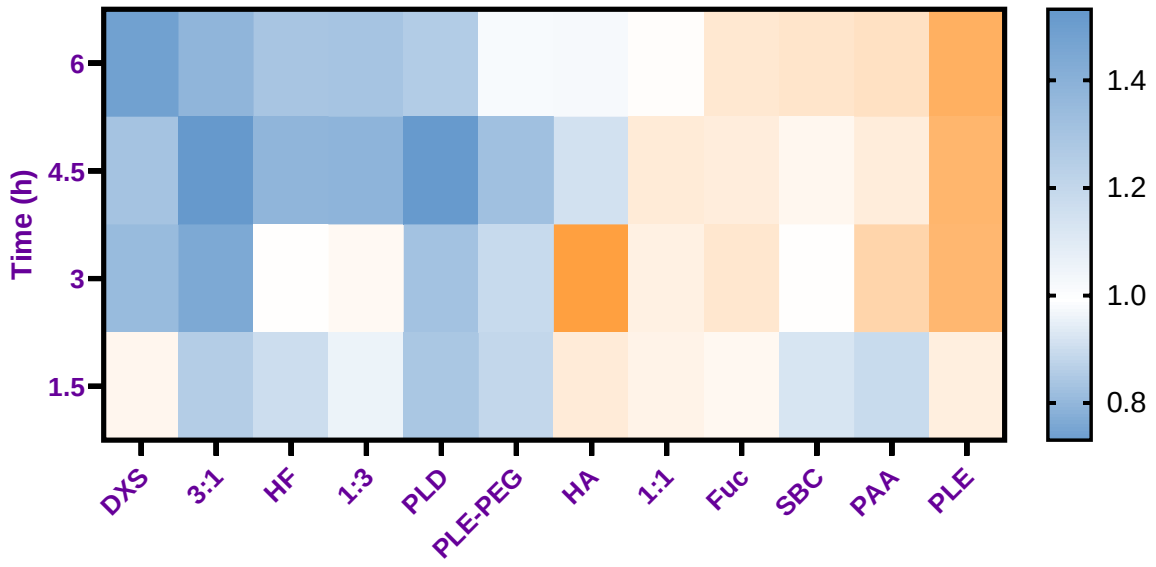

Figure 36. Heatmap of nanoparticle-membrane association comparing the ratio in STAT3-transformed and non-transformed cells.

MCF-10 cells were plated for 24 hours with DOX- or DMSO-containing media. Then the cells were treated with 100 ng/mL differently coated NPs for 24 hours, when membrane and nuclei were stained using Wheat Germ Agglutinin and Hoechst stain, respectively. The NP-cell association was imaged every 30 minutes using CellObserver microscope and analyzed using a custom pipeline created in CellProfiler. Heatmap of NP-cell membrane association ratio between non-transformed and STAT3-transformed cells is shown for indicated time points (n=2).

DXS – dextran sulfate; HA – hyaluronic acid; PLD – poly-L-aspartic acid; Fuc – fucoidan; SBC - sulfated β-cyclodextrin; HF - heparin sulfate folate conjugate; PAA - polyacrylic acid; PLE – poly-L-glutamic acid; PLE-PEG - poly-L-glutamic block-polyethylene glycol; 1:1, 1:3 and 3:1 – indicated ratio blend of hyaluronic acid and poly-L-aspartic acid.

We found that the poly-L-glutamic acid-coated NPs (PLE-NPs) showed significantly greater membrane binding to STAT3-driven cells compared to non-transformed counterparts (Figures 28 and 36) (189). The representative microscopic images of PLE-NP cell recruitment are shown in Figure 37. In addition, poly-L-glutamic acid – block – poly-ethylene glycol particles, in which PEG covers the glutamic acid, did not show a similar effect, suggesting importance of the terminal PLE layer in this targeting ability (Figure 29). This preferential cellular binding of PLE-NPs did not reflect a non-specific effect of neoplastic transformation, as LbL NPs coated with other modifications showed no difference in cell membrane association (Figures 24-36) (189). The differential NP-cell association was detected within the membrane, however, the co-localization with nuclei was minimal for all

investigated NPs in both conditions (Figures 24-35) (189). In addition, sulfated β-cyclodextrin-coated nanoparticles (SBC-NPs) showed statistically significant difference in nuclear co-localization between non- and STAT3-transformed cells (Figure 25). However, the differential SBC-NP binding was not observed within the cell membrane. As by using this method, we detect all the NPs whose fluorescence is co-localized with the nuclear stain fluorescence, it is possible that this is a result of non-specific nanoparticle binding on the membrane directly above the nucleus and not a consequence of direct NP binding to cell nuclei. Taken together with the generally low levels of nuclear co-localization, we did not further focus on dissecting the mechanism and evaluating these effects.

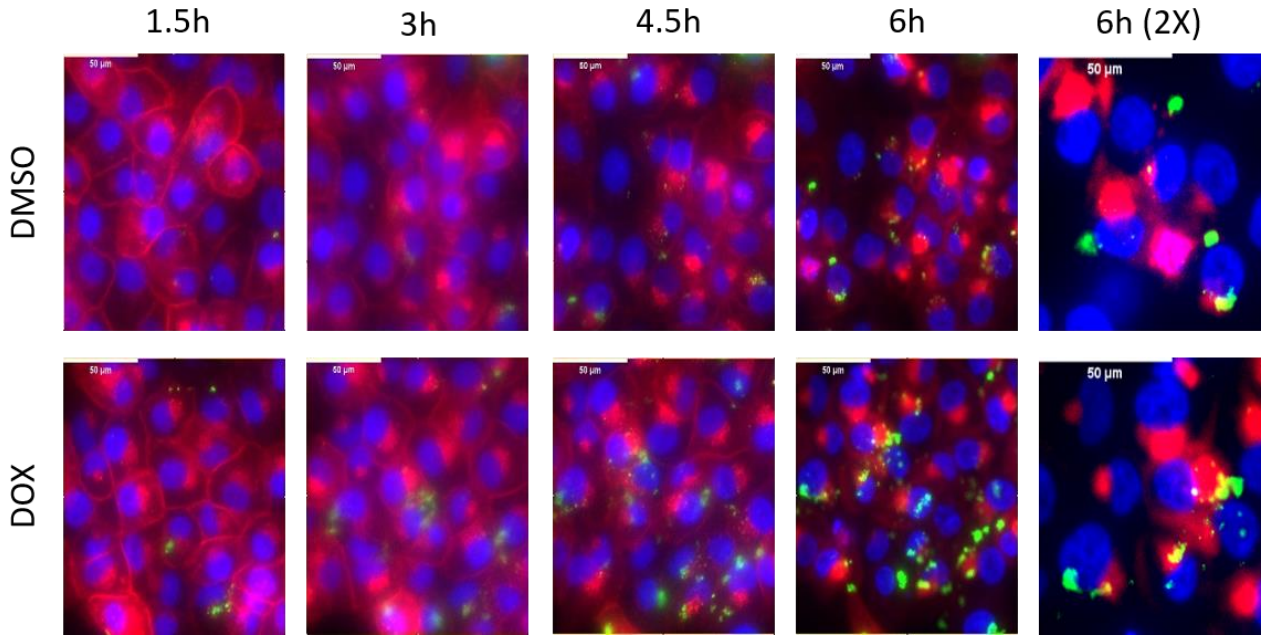

Figure 37. Representative images of PLE-NP-treated MCF-10A cells at indicated time points (n=2). MCF-10 cells were plated for 24 hours with DOX- or DMSO-containing media. Then the cells were treated with 100 ng/mL PLE- NPs for 24 hours, when membrane and nuclei were stained using Wheat Germ Agglutinin (red) and Hoechst stain (blue), respectively. The NP fluorescence is shown in green. NP-cell association was detected using CellObserver microscope and representative images at indicated time points are shown (n=2).

To further characterize the PLE-NP subcellular distribution we performed deconvolution microscopy in MCF-10A cells following 2 or 24 hours of incubation with PLE-coated NPs (Figures 38 and 39, respectively). Whereas PLE-NPs associated to a low extent with non-transformed MCF-10A cells, induction of STAT3 led to recruitment of considerably greater numbers of these NPs (189).

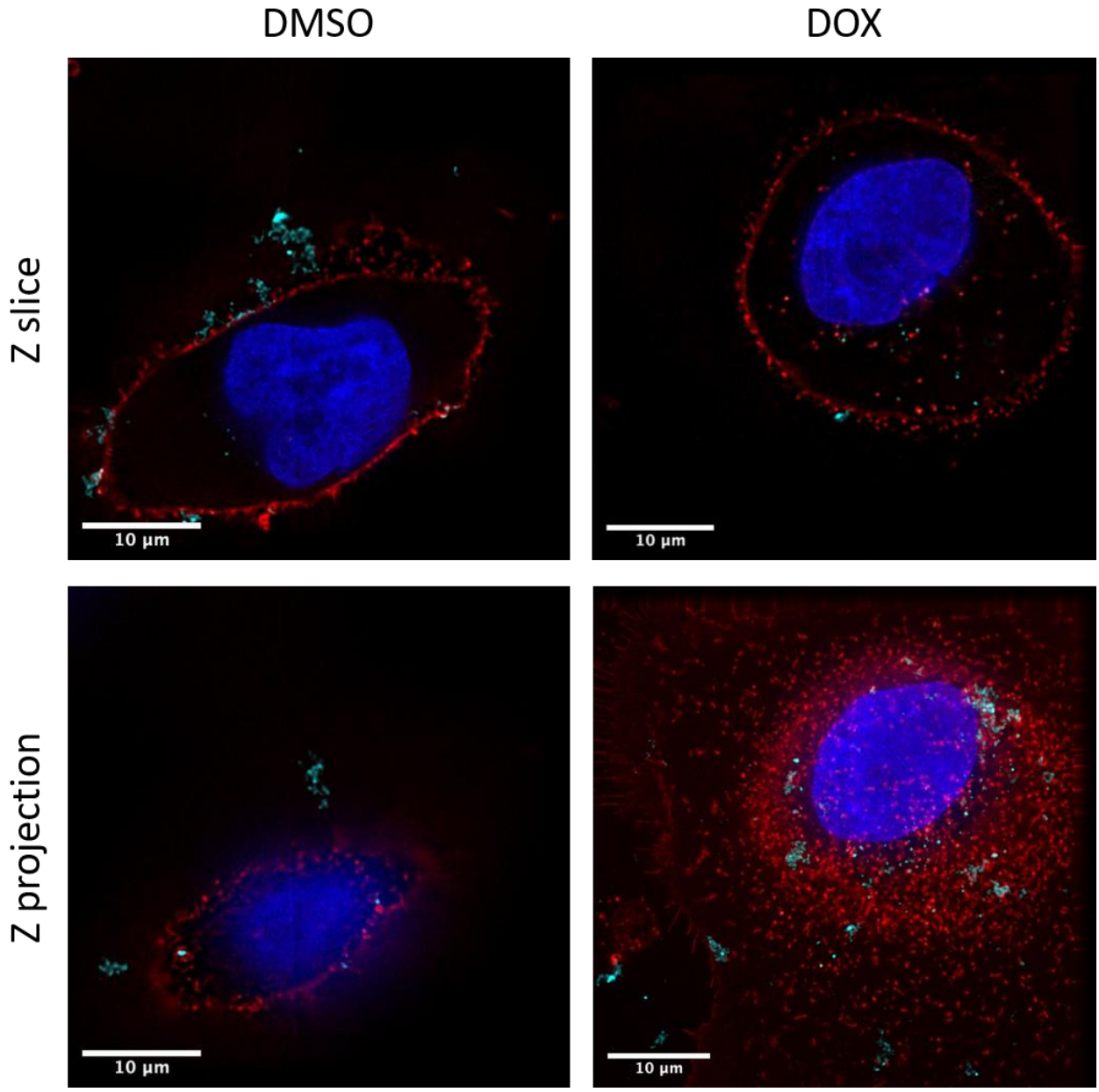

Figure 38. Deconvolution microscopy Z slice and Z projection images of MCF-10A cells following 2 hour treatment with 100 ng/ml PLE-NPs. Prior to NP treatment, cells were treated for 24 hours with DOX or DMSO control (n=3). The cells were stained red for membrane using Wheat Germ Agglutinin and blue for nucleus using Hoechst stain. The nanoparticles are shown in cyan.

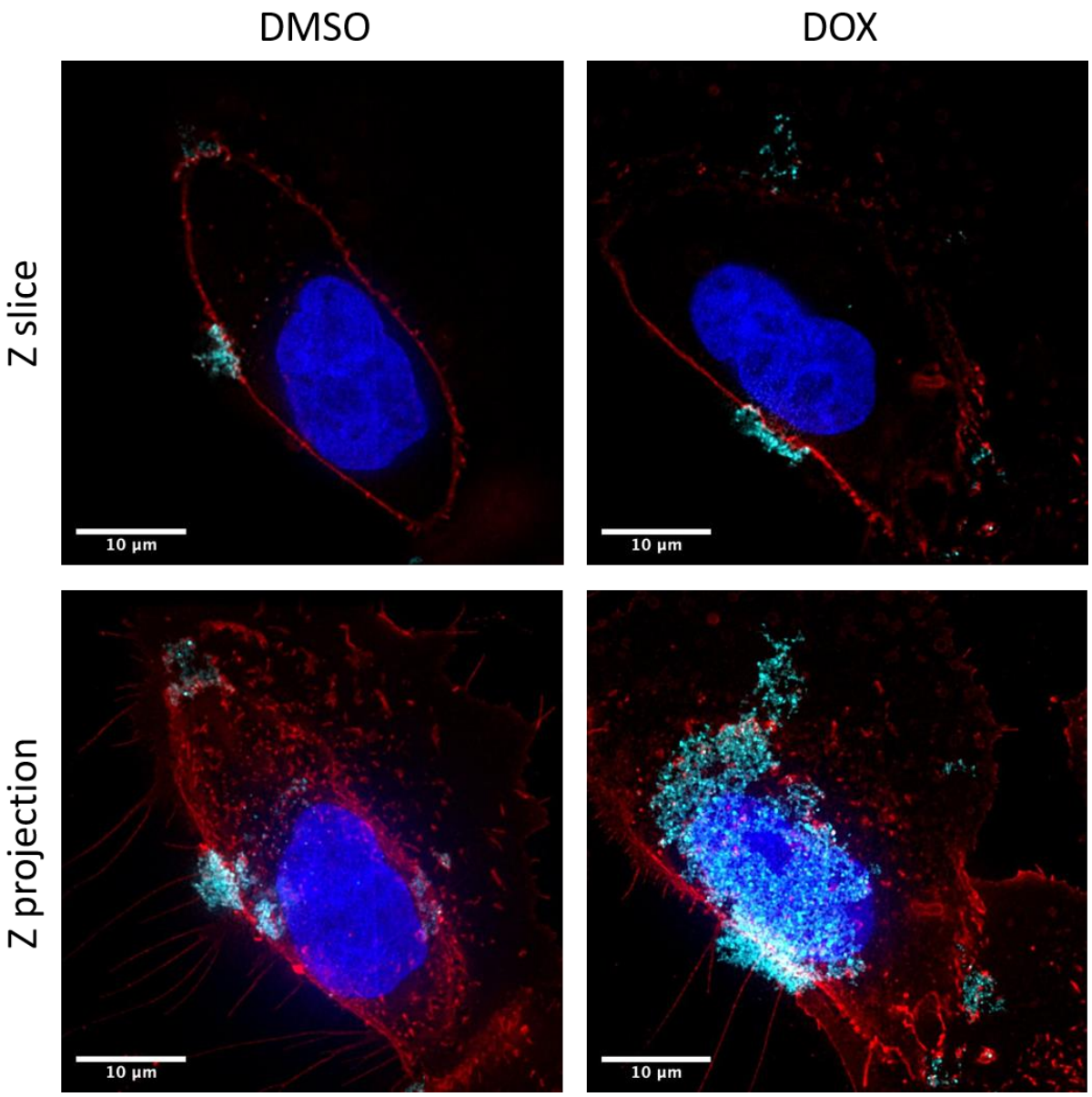

Figure 39. Deconvolution microscopy Z slice and Z projection images of MCF-10A cells following 24 hour treatment with 100 ng/ml PLE-NPs. Prior to NP treatment, cells were treated for 24 hours with DOX or DMSO control (n=3). The cells were stained red for membrane using Wheat Germ Agglutinin and blue for nucleus using Hoechst stain. The nanoparticles are shown in cyan.

Consistent with previous report (164), high resolution microscopy suggests that these nanoparticles bind and potentially integrate within the plasma membrane (Figures 38 and 39), further supporting the importance of cellular lipid composition in their targeting

specificity. Although they may not necessarily be internalized into the cytoplasm, PLE- NPs retain the ability to accumulate preferentially in tumor tissue *in vitro* and *in vivo* (164,189,201,202). Thus, we further investigated STAT3-dependency of these tumor-targeting properties of poly-L-glutamic acid coated LbL nanoparticles and its utility in treatment of breast cancers.

4.3. *Quantification of STAT3-dependent PLE-NP cell binding*

To quantify the differential cell binding of PLE-NPs in breast cellular systems, we first used MCF-10A cells with doxycycline-inducible expression of STAT3C (189). Using quantitative flow cytometry, we found that these nanoparticles preferentially associate with the cells with activated STAT3, displaying 50% greater cell-associated nanoparticle fluorescence compared to their non-transformed counterparts (Figure 40) (189). To confirm the specificity of PLE-NPs targeting ability, we also used non-targeting DXS-NPs which did not display such an effect.

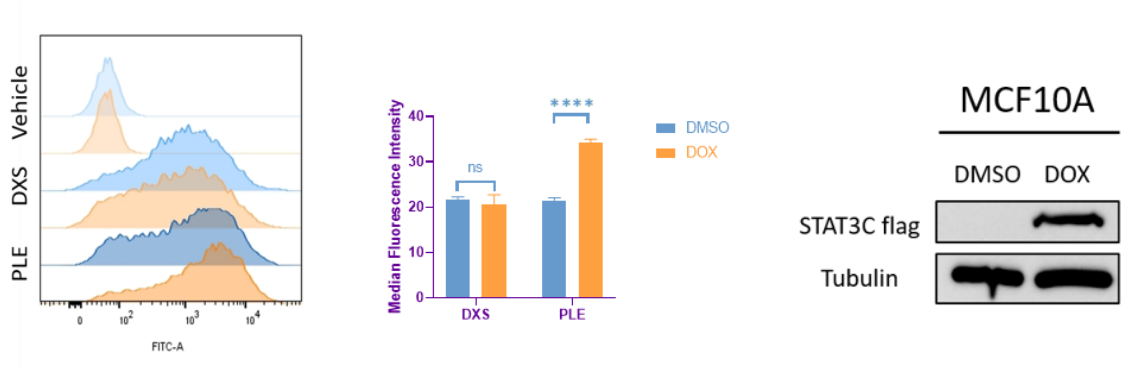

Figure 40. Quantification of PLE-NP and DXS-NP cell binding to MCF-10A cells. MCF-10A cells were cultured with DOX- or DMSO-containing media for 24 hours, then treated with 100 ng/ml PLE-NP, DXS-NP or H_2O vehicle control for additional 24 hours, when analyzed by flow cytometry. Representative histograms are shown in left panel. Quantification of NP-cell associated fluorescence (middle) is presented as mean ±SEM (n=4). In parallel, MCF-10A cells were cultivated in the same setting, and proteins were analyzed by immunoblot for confirmation of STAT3C induction (right).

To independently assess whether these differences were STAT3-dependent, we inhibited STAT3 phosphorylation with the JAK kinase inhibitor ruxolitinib (RUX) or STAT3 transcriptional activity with pyrimethamine (Figure 41) (189). Both treatments led to

a 50% reduction in cell-associated nanoparticle fluorescence.

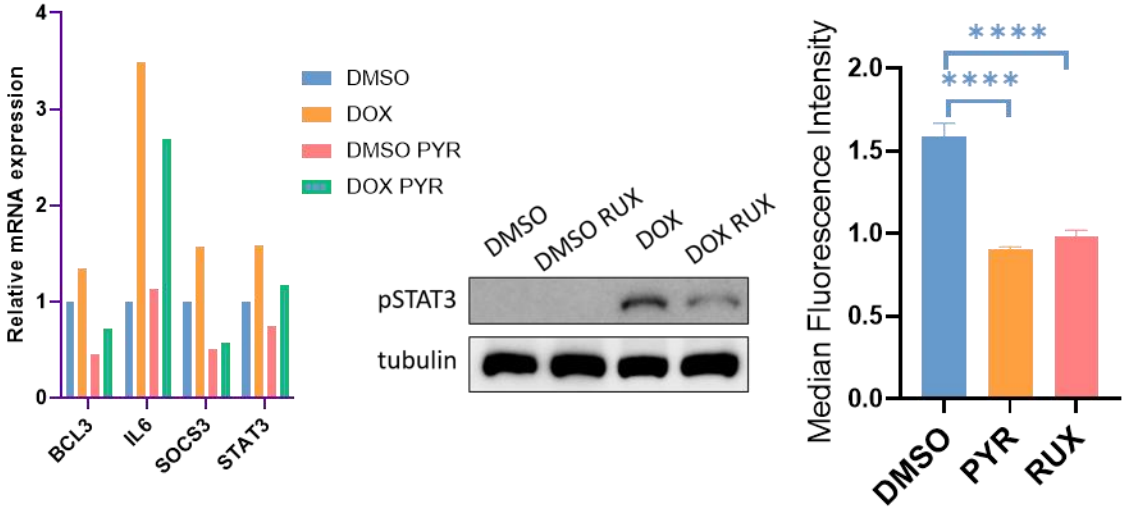

Figure 41. PLE-NP binding to MCF-10A cells is attenuated with pharmacological inhibition of STAT3. MCF-10A cells plated and allowed to adhere for 24 hours. Then, they were pre-incubated for 4.5 hours with STAT3 inhibitors pyrimethamine or ruxolitinib (or DMSO control), when STAT3C was induced with DOX (or DMSO control) for 24 hours. The effect of transcriptional inhibition of STAT3 by PYR was confirmed by RT-PCR (left), and inhibition of phosphorylation by RUX was determined by immunoblot analysis (middle). Cells were then incubated with 100 ng/ml PLE-NP for 24 hours, and analyzed by flow cytometry (right). NP association with STAT3-transformed cells was normalized to the mean values of the non-transformed counterparts for each of the treatments (n=4).

To confirm the safety of Layer-by-Layer nanoparticles and exclude the possibility of their cytotoxic effect, we evaluated the viability of cells following NP treatment by examining the numbers of cells that stained negative for live/dead stain. Representative flow cytometry dot plots are shown for non-transformed MCF-10A cells treated with DXS-NPs and PLE-NPs as compared with H_2O-treated vehicle controls (Figure 42).

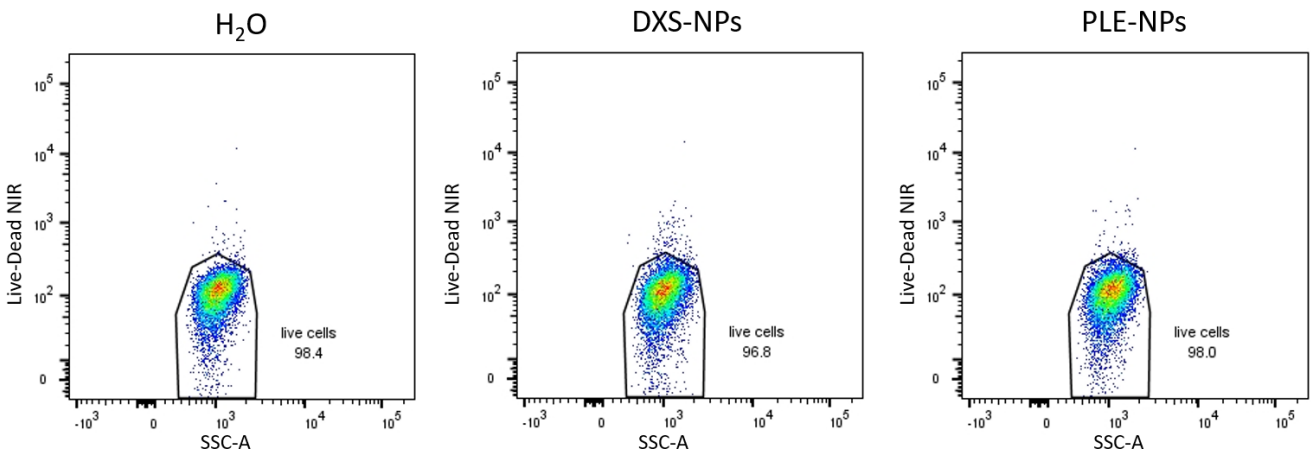

Figure 42. Viability of MCF-10A cells following treatment with DXS-NPs and PLE-NPs. Representative dot plots of flow cytometric analysis of non-induced MCF-10A cells stained with live/dead NIR staining following 24 hour treatment with 100 ng/ml DXS-NPs, PLE-NPs or H_2O vehicle control.

We quantified the percentages of viable cells following NP or vehicle treatment and concluded that the DXS- and PLE-coated nanoparticles do not induce cytotoxicity to MCF-10A cells, as compared to H_2O-treated controls (Figure 43).

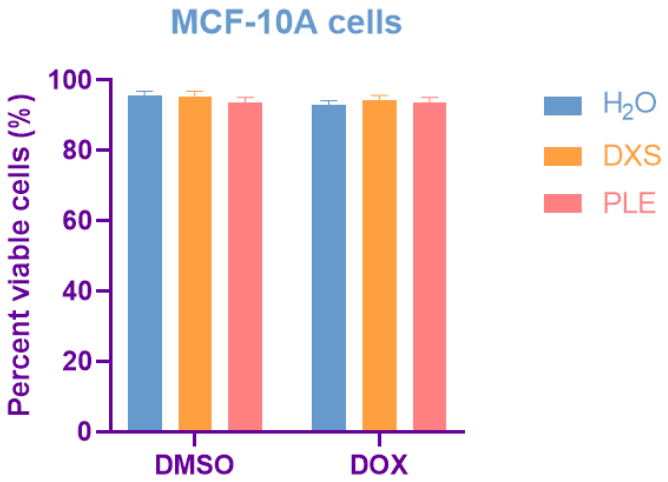

Figure 43. Percent of viable MCF-10A cells following treatment with PLE-NPs and DXS-NPs. Cells were induced for 24 hours with DOX (or DMSO control) and treated for additional 24 hour with 100 ng/ml DXS-NPs, PLE-NPs or vehicle control, when percentage of viable cells was determined by cell fluorescence of live/dead staining using flow cytometry.

4.4. *Evaluation of employing PLE-NPs in targeting STAT3-driven TNBC cells*

Since STAT3 is activated under basal conditions in most TNBCs, we investigated whether PLE-NPs could be used as a STAT3-targeted approach for this subset of breast cancers (189). We used the TNBC cell lines SUM159PT and MDA-MB-231 cells, as they both show constitutive tyrosine phosphorylation of STAT3 (Figure 44) (189).

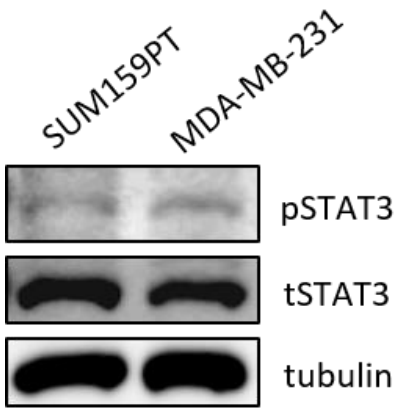

Figure 44. STAT3 phosphorylation under basal conditions in TNBC cells. Immunoblot analyses of triple-negative breast cancer cell lines SUM159PT and MDA-MB-231 cells show constitutive phosphorylation of STAT3 on Y705 under basal conditions.

Furthermore, these cells are dependent on STAT3 for long term survival, as it was not possible to derive STAT3 null clones of these lines by method of gene sequence alteration using the activity of Cas9 enzyme to clustered regularly interspaced short palindromic repeats/CRISPR-associated protein 9, CRISPR/Cas9. Therefore, we performed RNA interference-mediated silencing in these systems to determine STAT3-dependent interactions with NPs (189). We found that the TNBC cell lines MDA-MB-231 and SUM159PT showed robust binding of PLE-NPs, which was attenuated by depletion of STAT3 using two different siRNAs (189). This mechanism was specific for PLE-NPs, as DXS-coated NPs displayed either no difference or showed increased accumulation on cells lacking activated STAT3 (Figures 45 and 46) (189).

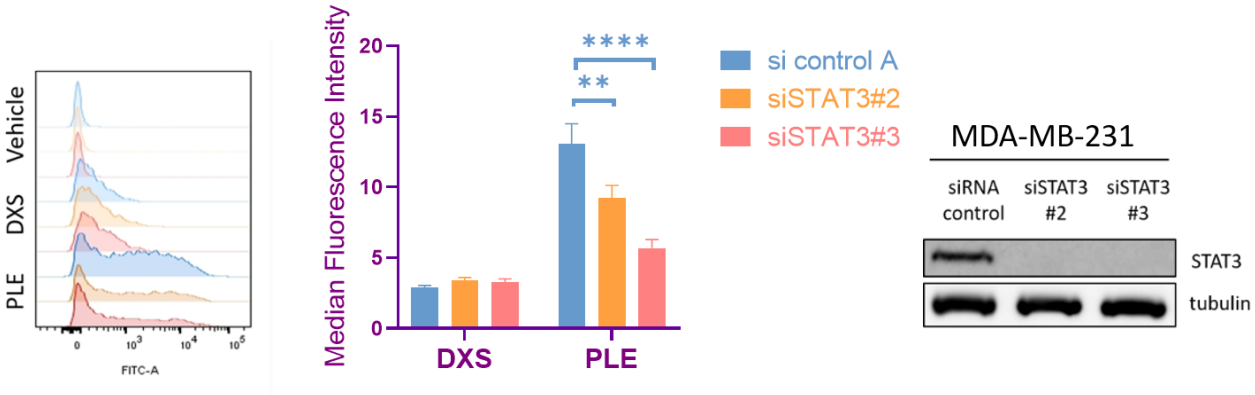

Figure 45. Quantification of PLE-NP and DXS-NP cell binding to MDA-MB-231 cells. MDA-MB-231 cells were transfected with two different siSTAT3 (or non-targeting siRNA control). Cells were then treated with 100 ng/ml PLE-NPs, non-targeting DXS-NPs (or vehicle H_2O control) for 24 hours and analyzed by flow cytometry. Representative histograms of cell-associated PLE-NP, DXS-NP and vehicle control fluorescence are shown (left) and median fluorescent intensity was quantitated and presented as mean ±SEM (middle; n=3). In parallel, MDA-MB-231 cells were cultivated in the same setting, and proteins were analyzed by immunoblot for confirmation of siRNA effectiveness (right).

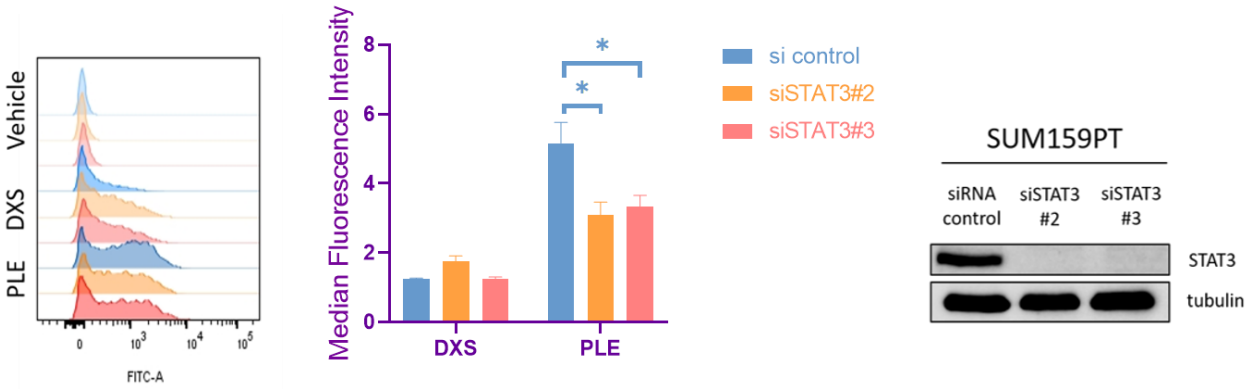

Figure 46. Quantification of PLE-NP and DXS-NP cell binding to SUM159PT cells. SUM159PT cells were transfected with two different siSTAT3 (or non-targeting siRNA control). Cells were then treated with 100 ng/ml PLE-NPs, non-targeting DXS-NPs (or vehicle H_2O control) for 24 hours and analyzed by flow cytometry. Representative histograms of cell-associated PLE-NP, DXS-NP and vehicle control fluorescence in are shown (left) and median fluorescent intensity was quantitated and presented as mean ±SEM (middle; n=3). In parallel, SUM159PT cells were cultivated in the same setting, and proteins were analyzed by immunoblot for confirmation of siRNA effectiveness (right).

We further evaluated the kinetics of PLE-NP cell-binding properties in TNBC cells. We have cultivated MDA-MB-231 and SUM159PT cells as previously described and transfected them with siRNAs to STAT3 and non-targeting control, when treated with 100 ng/ml PLE-NPs. Following 15 minutes to 24 hour incubation with the nanoparticles, the cells were prepared for flow cytometric analysis, when their NP-cell binding was examined for each of the time points (Figure 47). Until the 4 hour time point, the NP-cell binding between the cells with activated or diminished STAT3 activity was displaying similar kinetics. In MDA-MB-231 cell, the kinetics of binding remained comparable within different conditions, with expectably higher binding affinity towards the cells with preserved STAT3 activity. However, in SUM159PT cells, the NP binding to cell with silenced STAT3 expression reached the plateau 4 hours following the treatment. On the contrary, PLE-NPs continued occupying the cells transfected with the non-targeting siRNA control, resulting in approximately 2-fold difference in NP-cell binding.

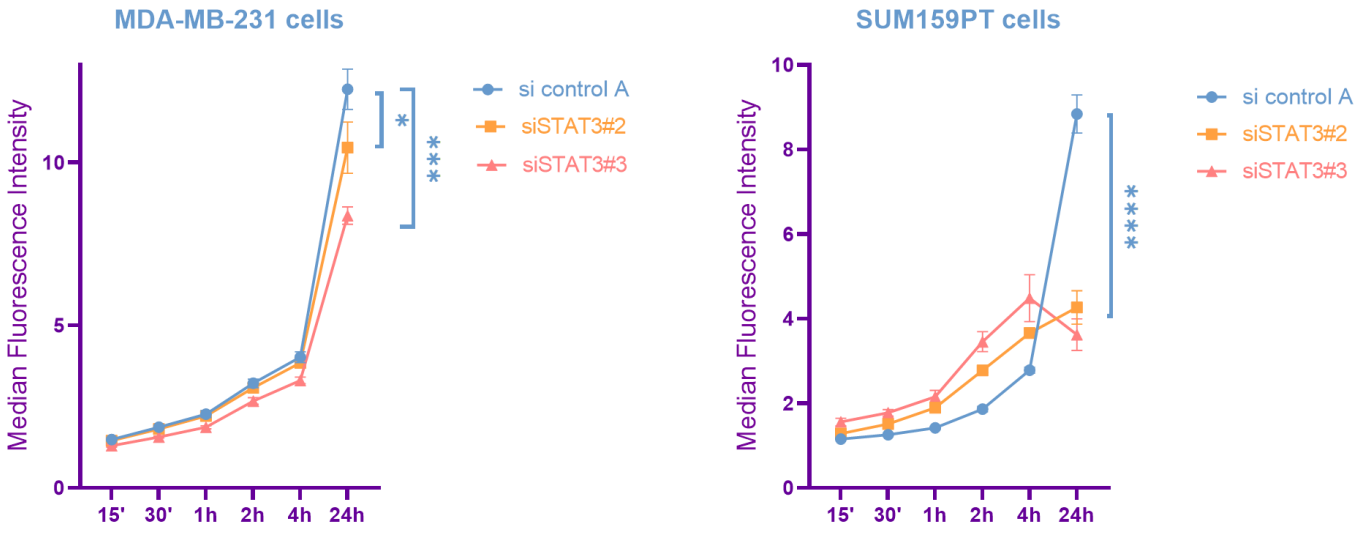

Figure 47. Kinetics of PLE-NP cell binding to TNBC cells. MDA-MB-231 (left) and SUM159PT (right) cells were transfected with two siRNAs targeting STAT3 and a non-targeting siRNA control. The cells were then treated with PLE-NPs or H_2O vehicle control and incubated for indicated time, when the NP-containing media was removed, the cells were washed and replenished with fresh media. The cells were then incubated to a total of 24 hours and NP-cell associated median fluorescence intensity was analyzed by flow cytometry. The NP-cell bound fluorescence medians were normalized to the ones of the vehicle treated controls and the mean values ±SD are presented for each condition (n=4).

4.4.1. Evaluating the cytotoxicity of nanoparticles in TNBC cell lines

In addition, to confirm the safety of these nanoparticles in TNBC cell lines MDA-MB-231 and SUM159PT cells, we evaluated the percentage of viable cells following treatment with the nanoparticles in each of the transfection conditions (Figure 48).

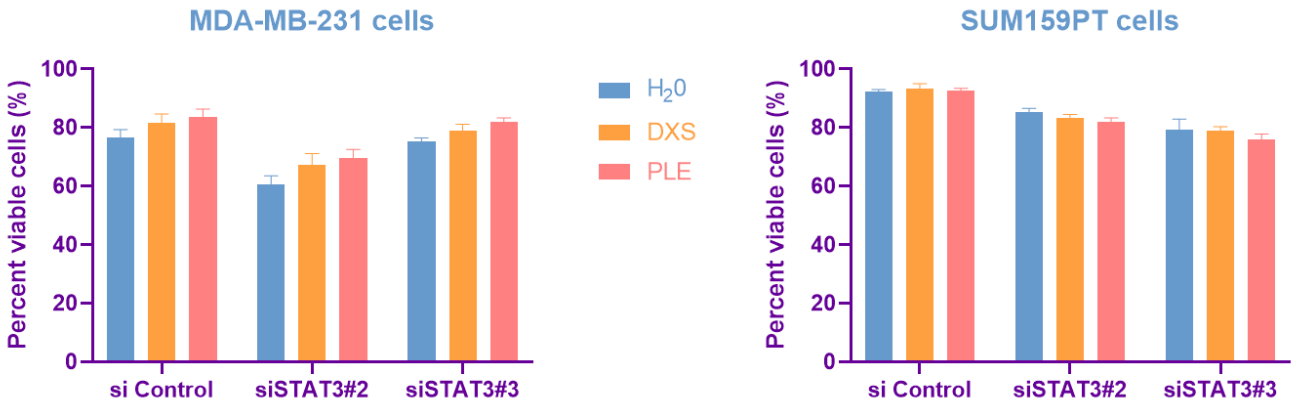

Figure 48. Percent of viable TNBC cells following siRNA transfection and treatment with PLE-NPs and DXS-NPs. MDA-MB-231 and SUM159PT cells were transfected with siRNA control, siSTAT3#2 or siSTAT3#3 and treated for 24 hours with 100 ng/ml DXS-NPs, PLE-NPs or vehicle control, when viability was determined by cell fluorescence of live/dead staining using flow cytometry.

Similarly as in MCF-10A cells, neither DXS- nor PLE-coated nanoparticles displayed cytotoxic effect to TNBC cell lines MDA-MB-231 and SUM159PT, as compared to H_20 treated samples (Figure 48).

4.5. *Characterization of PLE-NP penetration in three-dimensional mammary epithelial cell organoids*

To better model behavior in tumor systems, we characterized PLE-NP accumulation in three-dimensional MCF-10A cell organoids, which more closely recapitulate the architecture of a tumor *in vivo* (189,203,204). STAT3 activation promoted cellular growth and proliferation, resulting in formation of markedly greater number of large colonies (Figure 49) (189). STAT3-transformed organoids also grew at much higher cellular density (Figure 50), which further resulted in greater hypoxia within the organoids (Figure 51) (189).

These findings confirm the potency of STAT3 activation and its capability to induce malignant transformation of a cell as an isolated oncogenic driver.

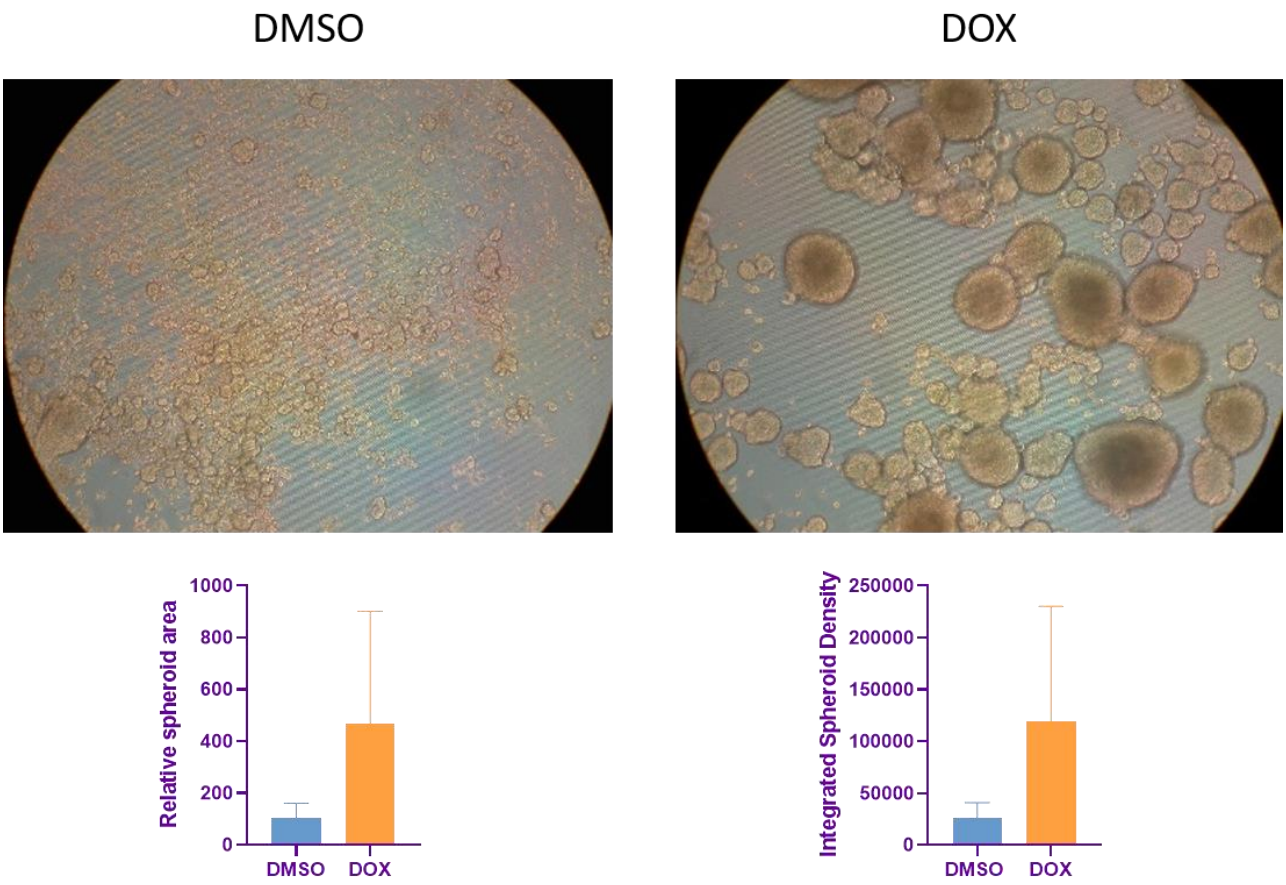

Figure 49. STAT3C induction stimulates growth of MCF-10A cell organoids. MCF-10A cells were cultured for ten days in 3D Nanoculture plates with addition of DOX (or DMSO control). Representative images made using optical microscope are shown in top panel. Spheroid areas of single organoids (bottom left) and integrated spheroid density (bottom right) were analyzed by ImageJ, and presented as mean ±SEM.

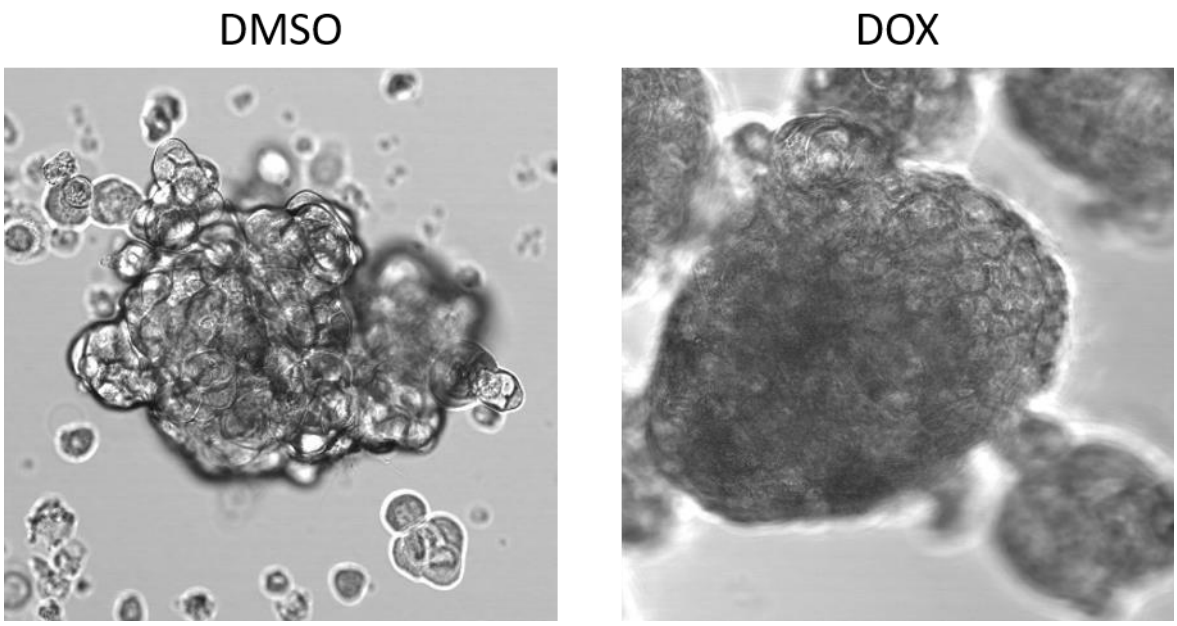

Figure 50. STAT3C induction stimulates growth of dense MCF-10A cell organoid structures. MCF-10A cells were cultured for ten days in 3D Nanoculture plates with addition of DOX (or DMSO control), when imaged by confocal microscopy.

As the other cell lines of interest, such as TNBC cell lines, were unable to form three dimensional structures using this method, we further investigated PLE-NP penetration into the organoids of MCF-10A cells. To determine the accumulation and distribution of PLE-NPs within the organoid structure, we quantified NP fluorescence across three dimensions and compared the mean organoid fluorescence (Figure 51) (189). Recognizing that more voluminous organoids have greater surface area in direct contact with the NP-containing media, we also assessed the mean fluorescence per unit volume of the organoid (189). Despite the substantially higher cellular density of STAT3-transformed organoids, which might have been expected to impede the penetration of NPs, these organoids showed greater quantitative NP fluorescence per organoid (by 40%) as well as per organoid volume (by 73%) (Figure 51) (189). Thus, even in tightly packed three-dimensional organoids, PLE-NPs show preferential penetration and intra-organoid accumulation in the presence of activated STAT3 (189).

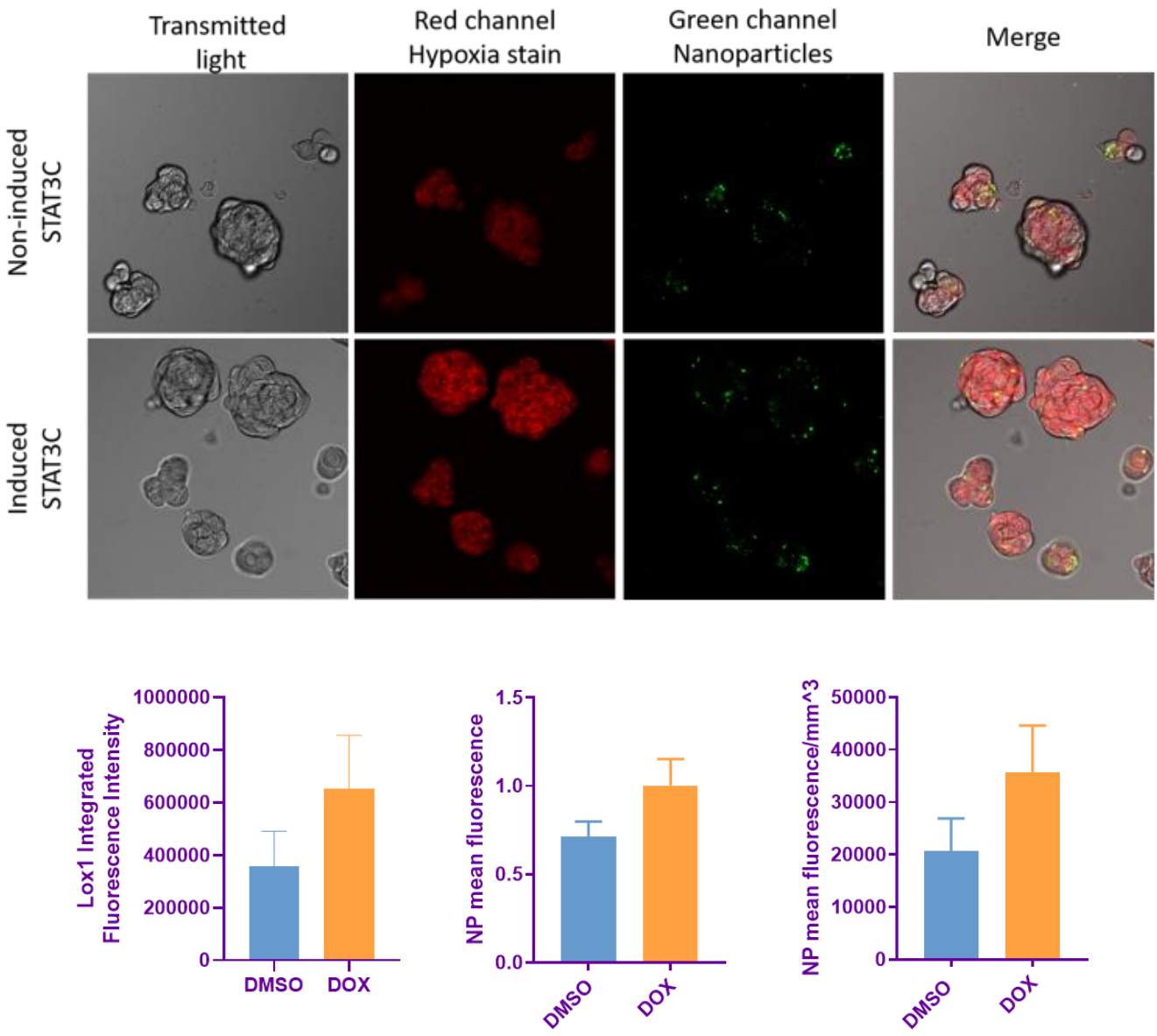

Figure 51. Characterization of PLE-NP penetration in MCF-10A cell organoids. MCF-10A cells were cultured to form three-dimensional organoids in DMSO- or DOX-containing media for three days. Then they were treated with PLE-NPs (green) and stained with Lox1 hypoxia stain (red) for an additional 24 hours, when analyzed with confocal microscopy. Representative images of two independent experiments are shown (top; for DMSO, n=52; for DOX, n=70). Quantification of Lox1 hypoxia staining by ImageJ (bottom left). The accumulation of the nanoparticles across the organoids was quantified using ImageJ and is presented as mean fluorescence per organoid ±SEM (bottom middle) and mean fluorescence per organoid volume ±SEM (bottom right).

In order to confirm the penetration ability of these nanosystems, we prepared the XYZ projection of the PLE-NP treated STAT3-transformed organoid (Figure 52). PLE-NPs expectably congregate on the outer surface of the organoid, however, they display a potent ability to accumulate deep inside the three dimensional cellular structures.

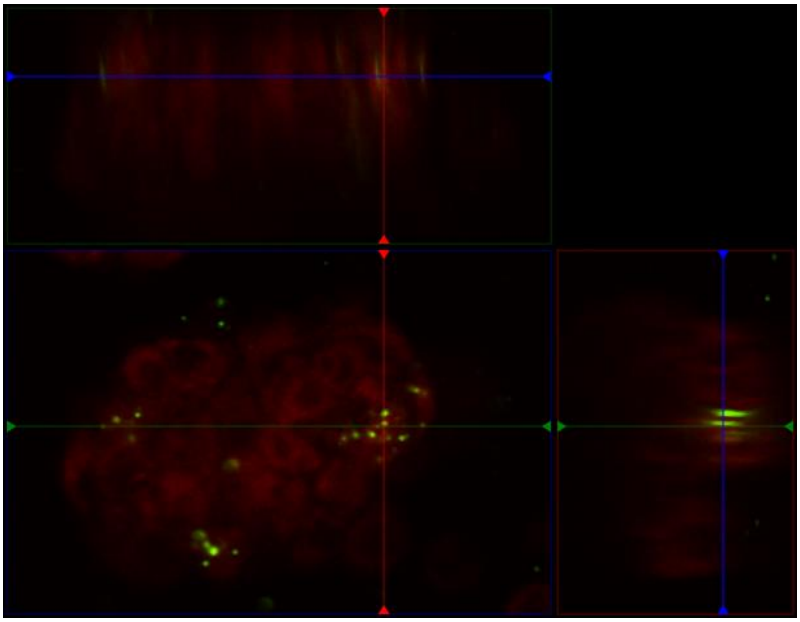

Figure 52. XYZ projection of the PLE-NP distribution in DOX-induced MCF-10A organoid. MCF-10A cells were cultured to form three-dimensional organoids in DOX-containing media for three days. Then they were treated with PLE-NPs (green) and stained with Lox1 hypoxia stain (red) for an additional 24 hours, when analyzed with confocal microscopy. The XYZ projection of PLE-NP distribution across three dimensions was prepared using ImageJ software.

4.6. *Evaluation of translational utility and drug delivery efficacy of PLE-NPs*

To further evaluate the translational utility of these findings, we tested the effect of PLE-NPs incorporating the cytotoxic agent cisplatin (CDDP), as platinum agents are clinically used in TNBC treatment (189,205,206). To evaluate STAT3-dependency of the cytotoxic effect, we used MCF-10A cells with and without induction of STAT3C, as well as triple-negative breast cancer cell line SUM159PT, in which we inhibited STAT3 activity genetically, using two different siRNA molecules (189).

First, we tested these two cellular models for sensitivity to free cisplatin treatment, in order to determine optimal concentrations for CDDP-loaded NP experiments (Figures 53 and 54).

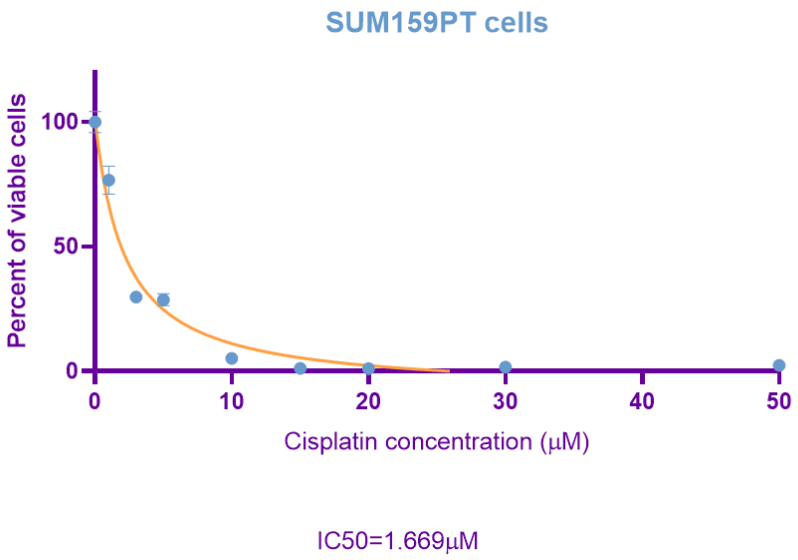

Figure 53. Viability of SUM159PT cells following treatment with indicated concentrations of cisplatin. SUM159PT cells were plated and allowed 24 hours to adhere, when treated with indicated concentrations of free cisplatin for 24 hours. Then the media was changed and the cells were incubated for additional 48 hours, when viability was detected using an ATP-dependent bioluminescence (n=4). IC50 was analyzed using GraphPad Prism software 8.4.

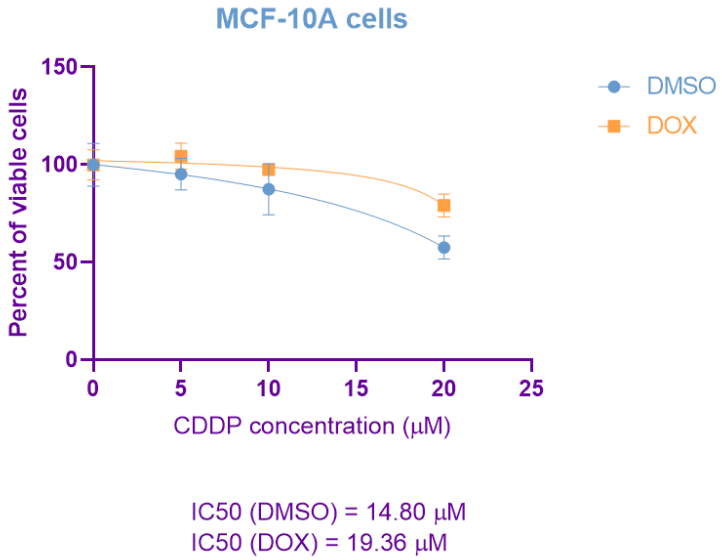

Figure 54. Viability of MCF-10A cells following treatment with indicated concentrations of cisplatin (CDDP). MCF-10A cells were cultured in DMSO- or DOX-containing media for 24 hours, when treated with indicated concentrations of free cisplatin for 24 hours. Then the media was changed and the cells were incubated for additional 48 hours, when viability was detected using an ATP-dependent bioluminescence (n=4). IC50 was analyzed using GraphPad Prism software 8.4.

Based on these results, we determined that the optimal cisplatin concentration range for further CDDP-loaded NP experiments is 1 to 2 µM for SUM159PT, and 10 to 20 µM for MCF-10A cells. It is noteworthy that induction of STAT3C in MCF-10A cells incurred them more resistant to apoptosis induced by CDDP, as opposed to their non-transformed counterparts. Although concentrations below 20 µM appeared as the appropriate concentrations for MCF-10A cell treatment, in further analyses we used slightly lower concentrations, 5 and 10 µM. These parameters were selected in order to maintain the treatment volume below 10% and thus avoid potential effects of high volumes of deionized water to the cells.

Then we tested the effect of PLE-NPs incorporating cisplatin (CDDP-PLE) in these two cellular systems. Induction of STAT3 rendered MCF-10A cells more vulnerable to CDDP-loaded PLE-NPs and significantly increased cell death, whereas MCF-10A cells without activated STAT3 showed greater viability after such treatment (Figure 55) (189). Similarly, the TNBC cell line SUM159PT showed increased apoptotic sensitivity to CDDP delivered via PLE-NPs, and this effect was attenuated when STAT3 was depleted with siRNA (Figure 55) (189).

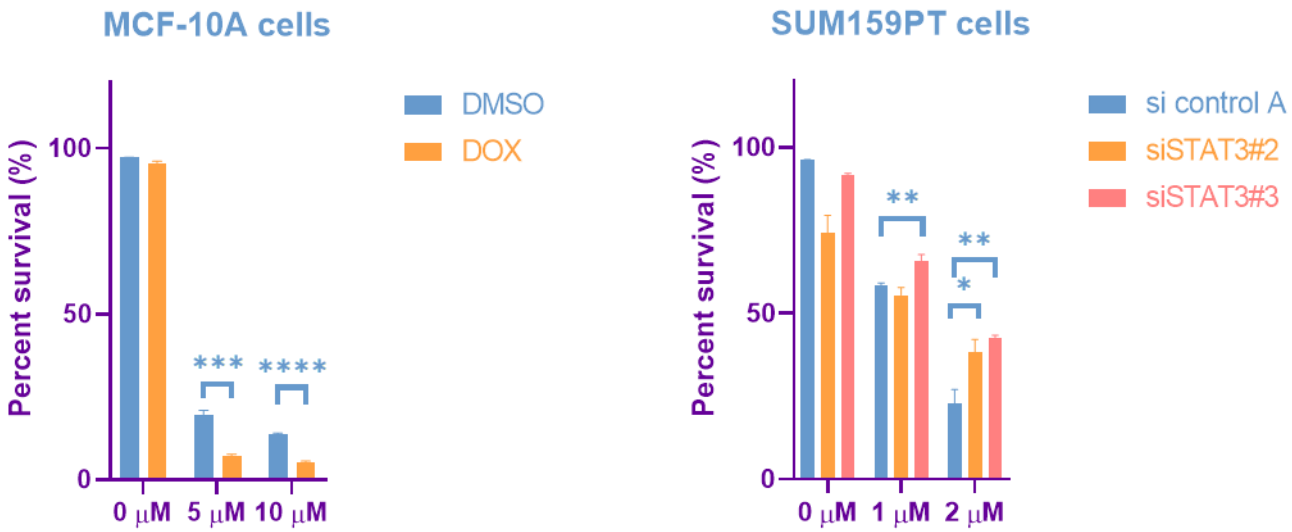

Figure 55. Viability of MCF-10A and SUM159PT cells following treatment with CDDP-loaded PLE-NPs. MCF-10A cells were cultured in DOX- or DMSO-containing media to induce the expression of STAT3C, and SUM159PT cells were transfected with two siRNAs targeting STAT3 (or non-targeting siRNA control), then treated with CDDP- PLE for 4 hours, when the media was changed and the cells were incubated for three days. Viability was detected with flow cytometry using Annexin V/DAPI staining, and presented as percent of viable cells (Annexin V negative, DAPI negative) (n=3).

As both STAT3-transformed and non-transformed MCF-10A cells showed profound apoptotic sensitivity to CDDP-PLE using the previous experimental conditions, we also assessed the effect of both lower treatment concentration and shorter incubation period of 2 hours (Figure 56). By using the concentrations of 1 and 2 µM CDDP-PLE, the cytotoxic effect was expectably less profound on both DOX-primed and non-induced cells, with preserved differential cell killing ability. In addition, similar cytotoxic effects were obtained after 2 and 4 hour treatment with 5 and 10 µM drug-incorporating PLE-NPs, indicating the importance of rapid binding affinity of these systems.

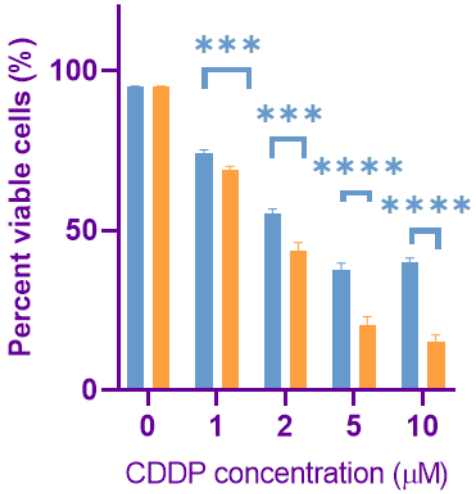

Figure 56. Viability of MCF-10A cells following 2 hour treatment with CDDP-loaded PLE-NPs. MCF-10A cells were cultured in DOX- or DMSO-containing media to induce the expression of STAT3C, then treated with CDDP-loaded PLE-NPs for 2 hours, when the media was changed and the cells were incubated for three days. Viability was detected with flow cytometry using Annexin V/DAPI staining, and presented as percent of viable cells (Annexin V negative, DAPI negative) (n=3).

This differential apoptotic sensitivity did not reflect a general increased sensitivity to cell killing in the cells with activated STAT3, as treatment with non-encapsulated CDDP did not produce a differential effect in these cells (Figure 57).

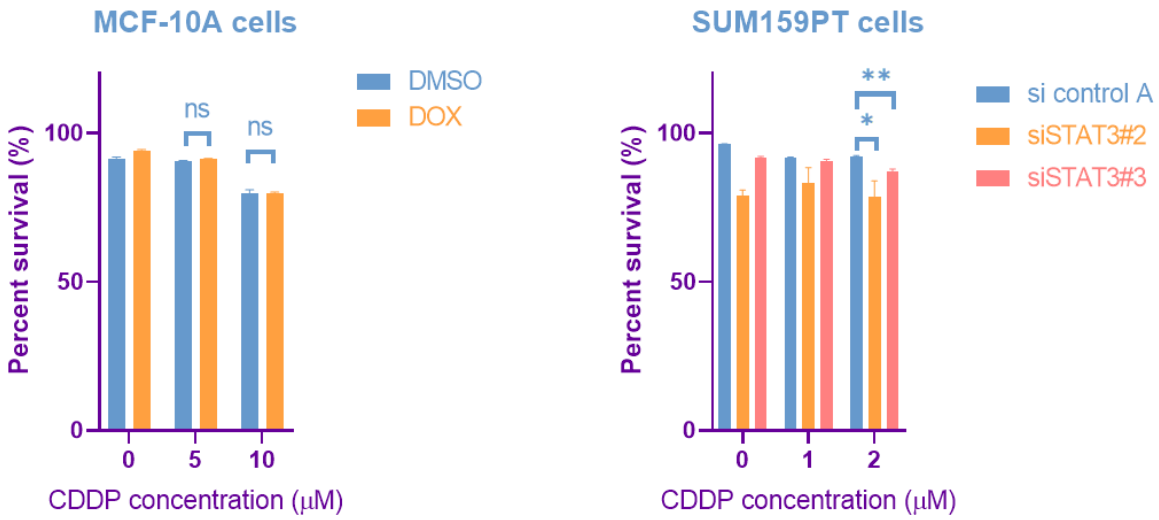

Figure 57. Viability of MCF-10A and SUM159PT cells following treatment with free un-encapsulated cisplatin. MCF-10A cells were cultured in DOX- or DMSO-containing media to induce the expression of STAT3C, and SUM159PT cells were transfected with two siRNAs targeting STAT3 (or non-targeting siRNA control), then treated with free cisplatin for 4 hours, when the media was changed and the cells were incubated for three days. Viability was detected with flow cytometry using Annexin V/DAPI staining, and presented as percent of viable cells (Annexin V negative, DAPI negative) (n=3).

To confirm the targeting potential of PLE coating of these nanosystems, we tested the effects of CDDP-loaded nanoparticles coated with the non-targeting DXS (CDDP-DXS). Whereas SUM159PT cells showed overall low sensitivity to CDDP-loaded DXS-NP treatment, STAT3 induction in MCF-10A cells resulted in greater resistance to this non-targeted form of treatment (Figure 58).

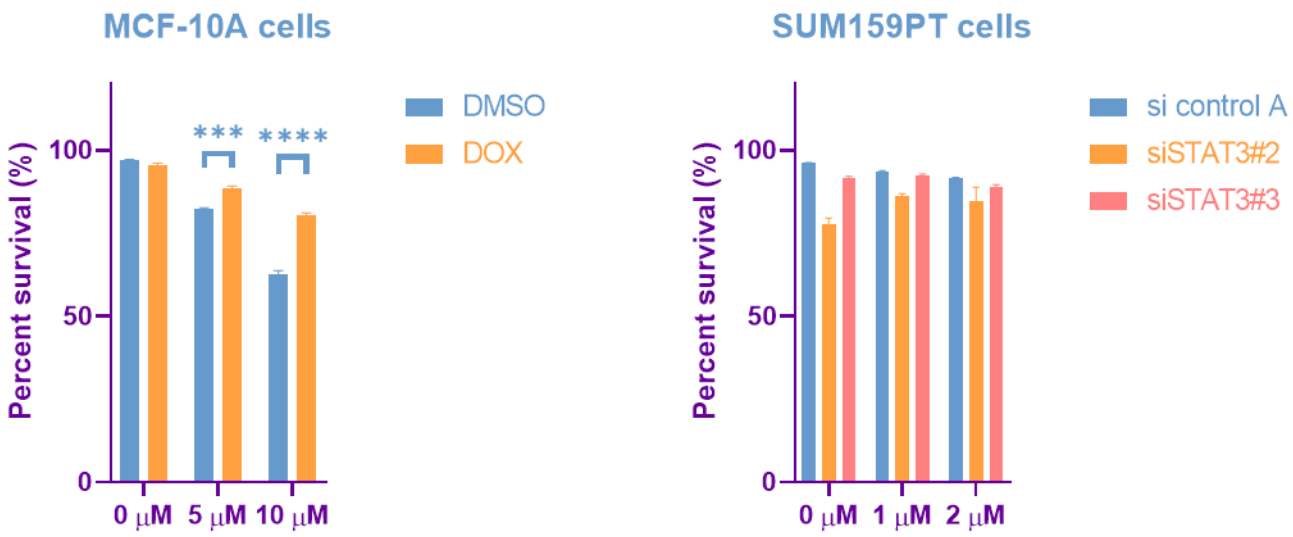

Figure 58. Viability of MCF-10A and SUM159PT cells following treatment with CDDP-loaded DXS-NPs. MCF-10A cells were cultured in DOX- or DMSO-containing media to induce the expression of STAT3C, and SUM159PT cells were transfected with two siRNAs targeting STAT3 (or non-targeting siRNA control), then treated with CDDP-DXS for 4 hours, when the media was changed and the cells were incubated for three days. Viability was detected with flow cytometry using Annexin V/DAPI staining, and presented as percent of viable cells (Annexin V negative, DAPI negative) (n=3).

Similarly, CDDP-loaded NPs that lacked LbL coatings (CDDP-CML) showed less cytotoxic effect on both MCF-10A and SUM159PT cells with activated STAT3, while non-transformed MCF-10A cells showed substantial sensitivity to such a treatment (Figure 59).

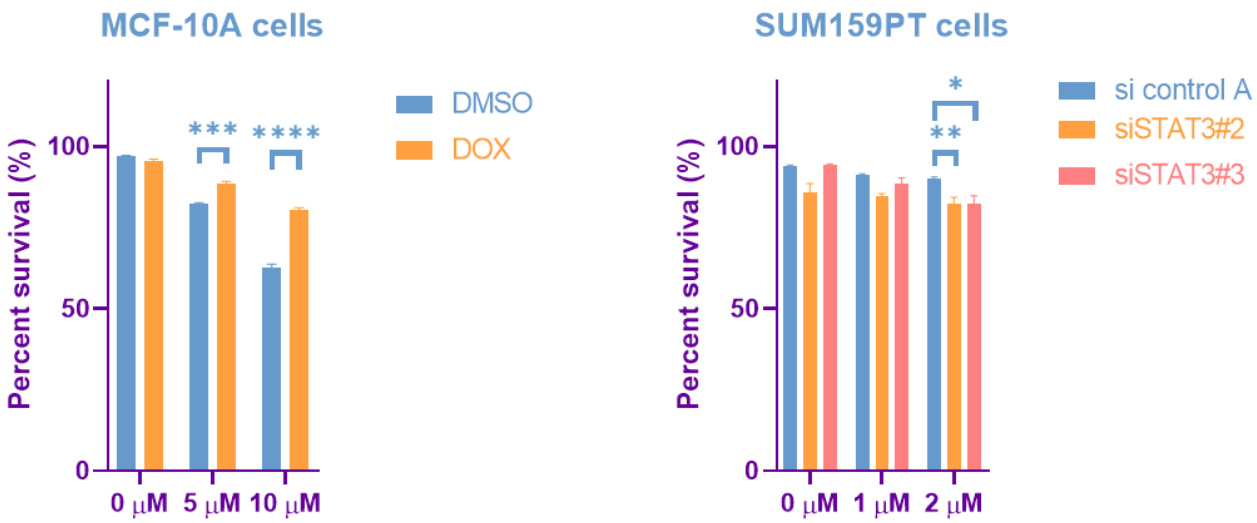

Figure 59. Viability of MCF-10A and SUM159PT cells following treatment with CDDP-loaded NPs lacking the coating layer. MCF-10A cells were cultured in DOX- or DMSO-containing media to induce the expression of STAT3C, and SUM159PT cells were transfected with two siRNAs targeting STAT3 (or non-targeting siRNA control), then treated with CDDP-CML for 4 hours, when the media was changed and the cells were incubated for three days. Viability was detected with flow cytometry using Annexin V/DAPI staining, and presented as percent of viable cells (Annexin V negative, DAPI negative) (n=3).

While MCF-10A cells were generally less sensitive to the 4 hour treatment with both free drug and CDDP-loaded NPs lacking the coating layer, 24 hour treatments further confirmed attenuated sensitivity of STAT3-driven cancer cells compared to non-transformed counterparts, emphasizing the importance of preferential drug delivery via PLE-NPs (Figure 60).

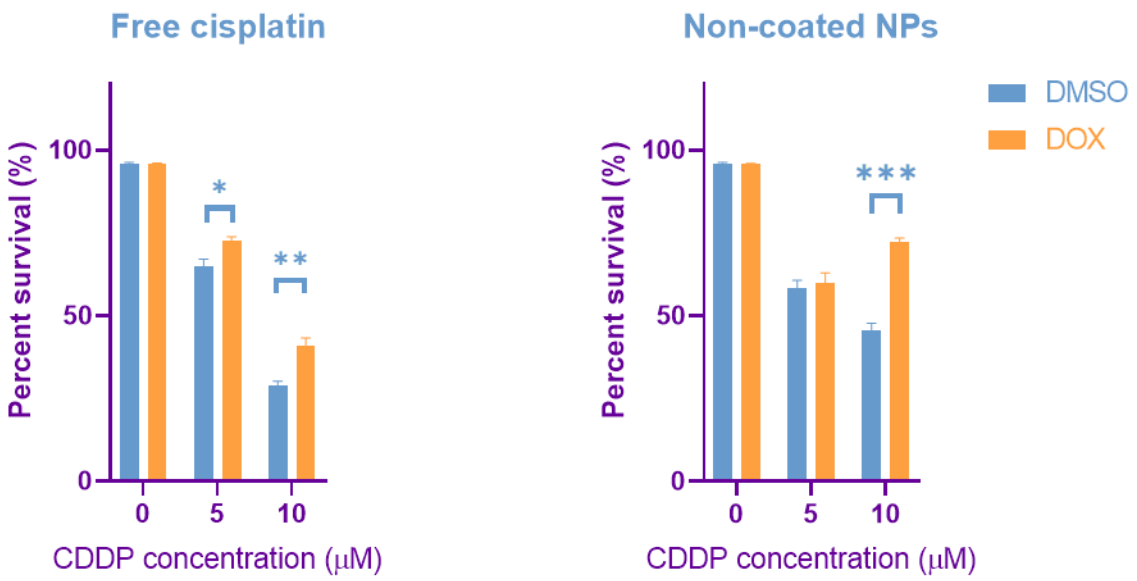

Figure 60. Viability of MCF-10A cells following 24 hour treatment with free CDDP and CDDP-loaded NPs lacking the surface layer. MCF-10A cells were cultured in DOX- or DMSO-containing media to induce the expression of STAT3C, then treated with free cisplatin or CDDP-CML for 24 hours, when the media was changed and the cells were incubated for three days. Viability was detected with flow cytometry using Annexin V/DAPI staining, and presented as percent of viable cells (Annexin V negative, DAPI negative) (n=3).

Since triple-negative SUM159PT cells displayed particular resistance to each of the non-targeted treatments, we assessed their effects on cellular viability using both prolonged treatments and increased concentrations (1; 2; 5 and 15 μM) (Figure 61). Whereas none of the treatments applied at concentration of 5 μM produced a profound cytotoxic effect in this cellular system, 15 μM treatment was more potent at cell killing. This cytotoxicity was primarily related to DXS-coated particles, which was similar between all the tested transfection conditions.

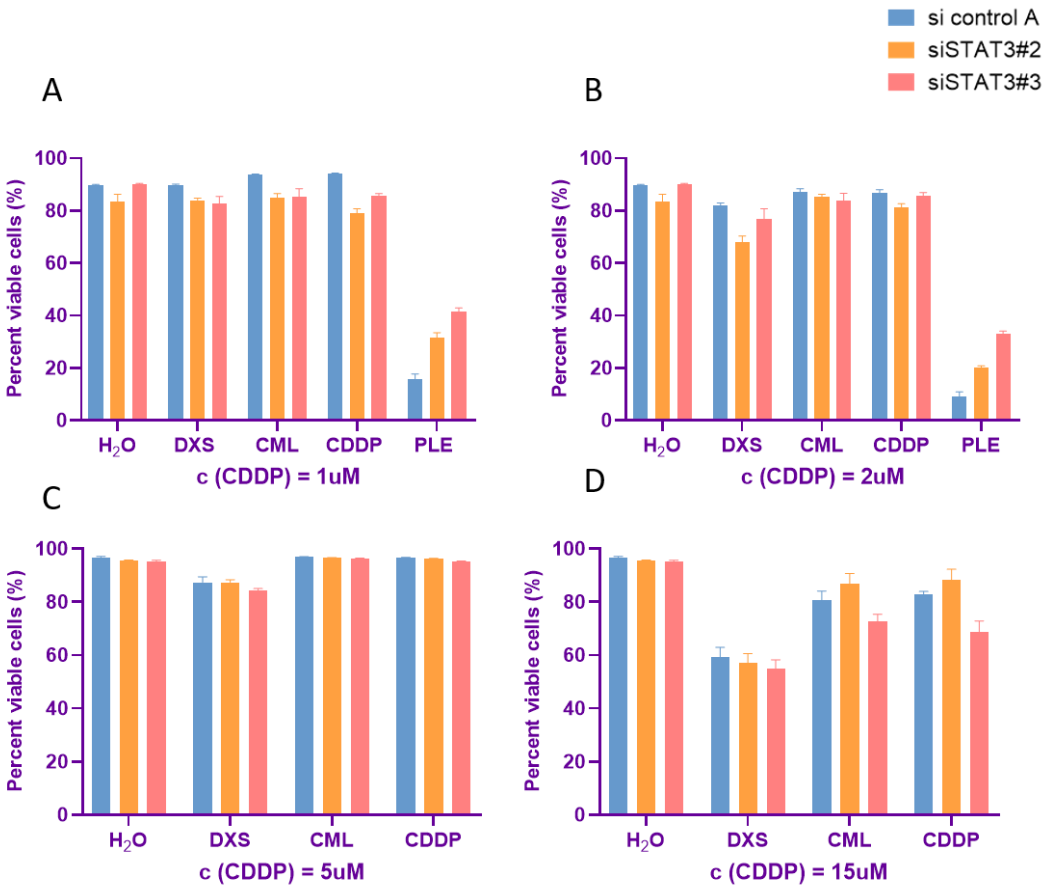

Figure 61. Cytotoxic effect of free cisplatin and CDDP-loaded NPs following 48h treatment in SUM159PT cells. SUM159PT cells were transfected with two different siRNAs targeting STAT3 (or non-targeting siRNA control), then incubated for 48 hours with CDDP-loaded PLE-NP (PLE), DXS-NP (DXS), non-coated liposomes (CML), or non-encapsulated CDDP at concentrations of 1 (A), 2 (B), 5 (C) and 15 µM (D). Cell survival was analyzed by flow cytometry using Annexin V/DAPI staining, and is presented as percent of viable cells (annexin V negative/DAPI negative) (n=3).

Taken together, these data suggest that drug-loaded PLE-NPs could be an effective targeted therapy for STAT3-driven breast cancers, including TNBC, while minimizing toxic effects to normal cells characterized by low and transient STAT3 activation.

4.7. *Evaluation of gamma radiation effect on PLE-NP cell binding*

Gamma radiation is commonly used in the treatment of breast cancer, including TNBC, and is known to alter the properties of the plasma membrane (189,200). Therefore, we tested whether radiation could impact PLE-NP-cell interaction in a STAT3-dependent manner (189). To exclude effects of widespread cell death, we first assessed viable cell numbers of STAT3-transformed and untransformed MCF-10A cells treated over a range of radiation doses (Figure 62) (189). We found that doses below 6 Gy were effective at avoiding a complete proliferation arrest (189).

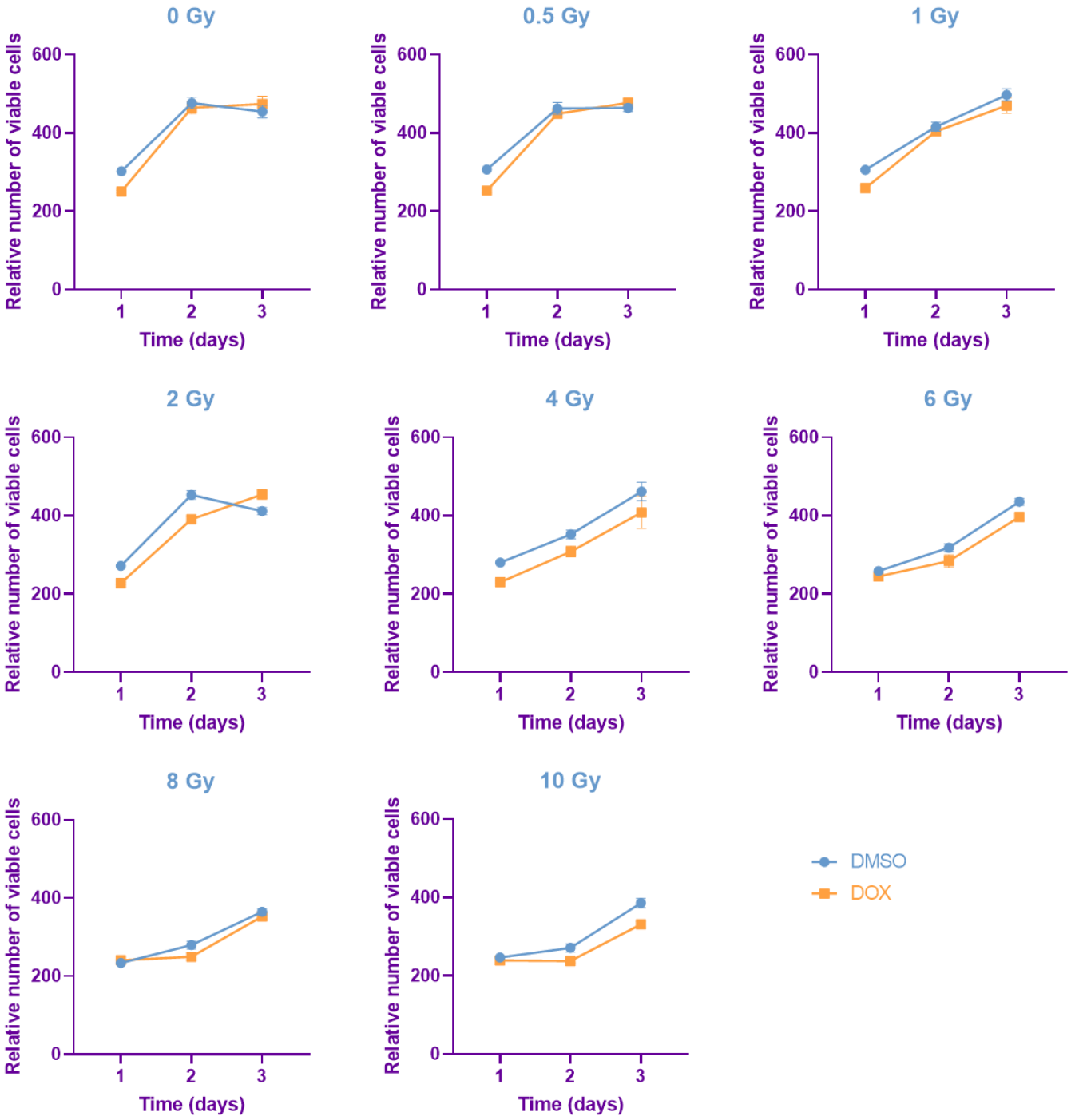

Figure 62. Survival of MCF-10A cells in response to gamma radiation. MCF-10A cells were plated with DOX or DMSO containing media for 24 hours, after which they were irradiated with the indicated dose of gamma radiation. Following incubation for the indicated time period, viable cell number was quantitated using ATP-dependent luminescence (n=4).

Next, we evaluated the effect and dose dependency of acute gamma irradiation on PLE-NP cell binding (Figure 63) (189). Interestingly, gamma radiation reduced the association of PLE-NPs with non-transformed MCF-10A cells in a dose dependent manner. However, binding to STAT3-transformed MCF-10A cells was minimally affected (189). Consequently, the difference in cell-associated PLE-NP fluorescence between non-transformed and STAT3-transformed cells increased from approximately 40% to 80% following 5 Gy irradiation (Figure 63) (189). These findings suggest a potential synergistic effect between radiation and nanoparticle-based targeting of breast cancer cells.

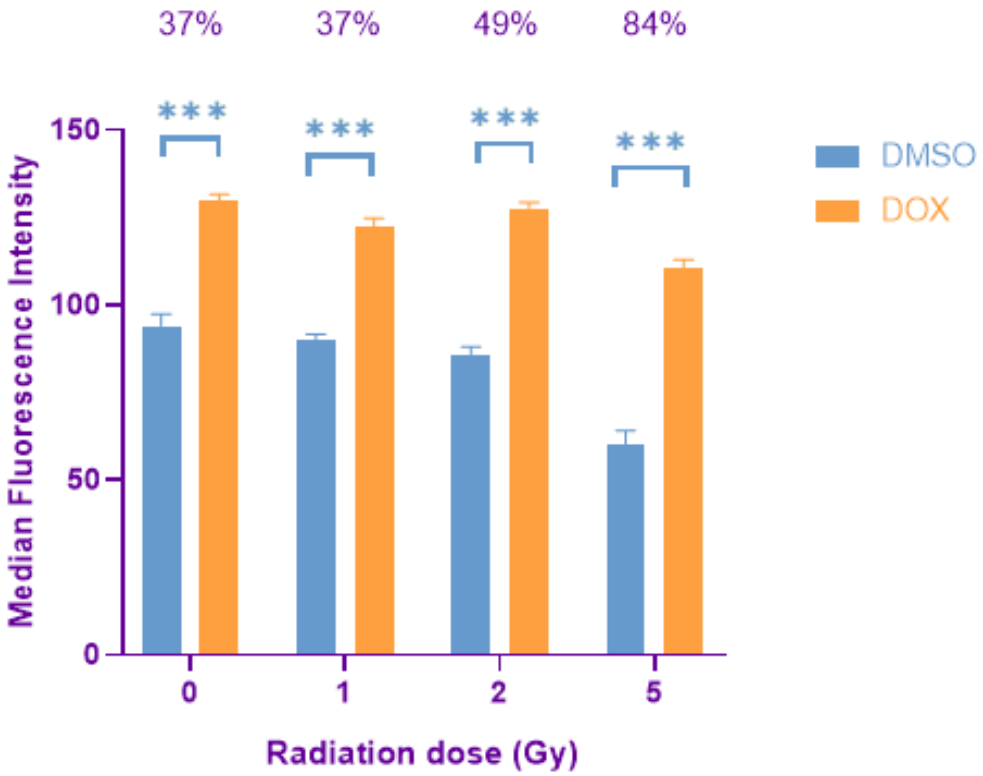

Figure 63. Quantification of PLE-NP binding to MCF-10A cells following gamma irradiation. MCF-10A cells were treated with DOX or DMSO for 24 hours, then irradiated with the indicated dose of gamma irradiation and treated with PLE-NPs (or vehicle (H_2O) control) (n=4). NP-cell association was analyzed by flow cytometry, and the percent difference in NP-cell binding between non-transformed and STAT3-transformed cells is indicated for each of the radiation doses.

4.8. *Analyzing STAT3 activation profile in normal tissue*

When considering targeting tumor cells based on the STAT3 activation profile, it is important to evaluate possible toxicity issues that might arise from such an approach, as STAT3 is ubiquitously expressed protein in human tissues. However, in normal cells STAT3 resides inactivated in cytoplasm, while being constitutively activated in variety of malignant cells. To estimate the level of STAT3 activity in normal cells and its potential limitations to a STAT3-targeted therapy, we analyzed the expression of STAT3-regulated genes between different normal and breast cancer tissue using publicly available gene expression datasets (187). As expected, the expression of STAT3 gene expression signature substantially differs between normal and malignant tissue (Figure 64), indicating a favorable therapeutic index of STAT3-directed treatment approaches.

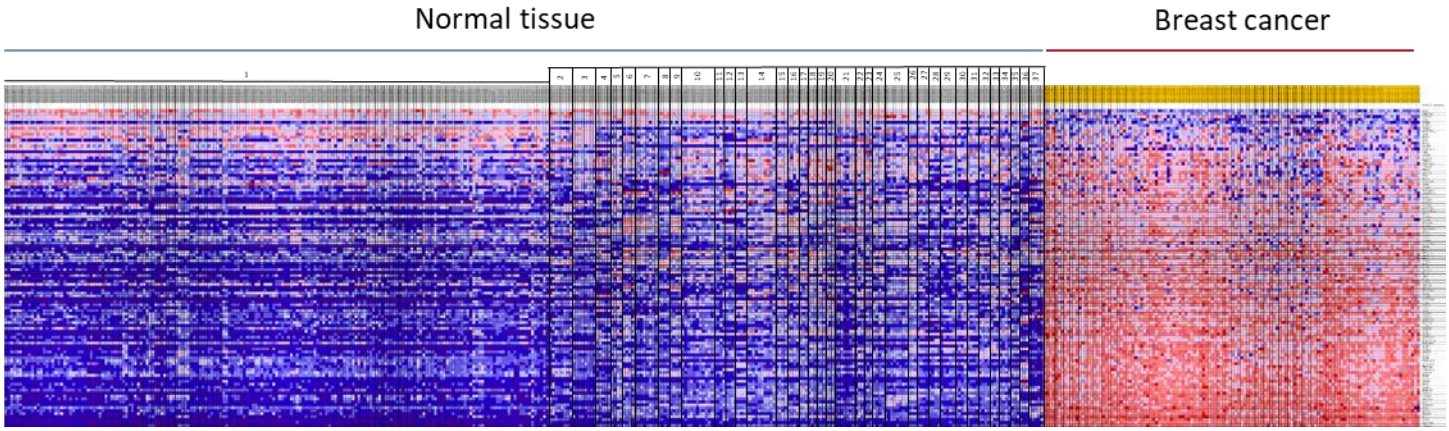

Figure 64. Expression of STAT3 gene expression signature in normal and breast cancer tissue. mRNA expression of STAT3 target gene signature is presented using microarray data of normal tissue (GSE3526, n=353) and breast cancer tissue (GSE5460, n=129). The heatmap was generated using GSEA software.

1. Nervous system (185); 2. Pituitary gland (8); 3. Spinal cord (8); 4. Bone marrow (5); 5. Lymph nodes (4); 6. Oral mucosa (4); 7. Tongue (8); 8. Salivary gland (4); 9. Esophagus (4); 10. Stomach (11); 11. Colon (3); 12. Liver (4); 13. Spleen (4); 14. Adipose tissue (10); 15. Thyroid gland (4); 16. Pharynx (4); 17. Tonsils (3); 18. Trachea (3); 19. Bronchus (3); 20. Lung (3); 21. Heart (7); 22. Coronary artery (3); 23. Saphenous vein (3); 24. Adrenal gland (4); 25. Kidney (8); 26. Urethra (3); 27. Cervix (4); 28. Endometrium (4); 29. Myometrium (5); 30. Ovary (4); 31. Vagina (4); 32. Vulva (4); 33. Breast (3); 34. Nipple (4); 35. Prostate (3); 36. Testes (3); 37. Skeletal muscle (5).

5. Discussion

The incidence of malignant diseases is continuously rising, representing the worldwide public health problem of 21st century. Breast cancer is the most frequently diagnosed malignancy in women, and the second leading cause of cancer-associated mortality accounted for both genders (1). Continuous research and development of new diagnostic and therapeutic modalities has certainly improved patient prognosis and quality of life. However, contemporary medical regimens are yet unable to effectively manage plenty of breast cancer patient cases, resulting in high mortality rates. Triple-negative breast cancer is the most aggressive breast cancer subtype with particularly pronounced metastatic potential, recurrence rate and lower overall survival. In addition, there is no targeted therapy for this subtype, which further emphasizes the need for development of new modalities in treatment of this invasive disease. Better understanding of the biological mechanisms underlying the malignant behavior in this subset of cancers could provide a basis for development of novel therapeutic strategies.

5.1. *Metabolic aspects of breast cancer*

5.1.1. Obesity in tumorigenesis

Malignant transformation is associated with variety of changes in lipid metabolism which have been described in number of malignancies (94). In breast neoplasms particularly, adipose tissue builds up a significant segment of tumor environment, and could influence the tumor growth through secretion of adipokines, cytokines and hormones. An intriguing implication of the metabolic regulation importance in oncogenesis comes from a clear link between obesity and breast cancer (207). In fact, as estimated by the American Cancer Society, approximately 20% of malignancies in general are associated with obesity (208), and one study reported that cancer-related death could be prevented in 14% of men and 20% of women if normal weight was maintained (209). The microenvironment of adipose tissue in obese people displays several similarities with the tumor microenvironment, such as the chronic low degree of inflammation and increased release of reactive oxidative species. On the other hand, adipose tissue functions as an endocrine organ, producing elevated levels of tumor-promoting hormones and cytokines in obese people, such as leptin, estrogen and several members of interleukin family including IL-1β, IL-6, IL-8 and IL-17 (94). As a response, different transcription factors, including STAT3 and NFκB, are continually activated, promoting oncogenic behavior (207). The paracrine IL6/STAT3 signaling and

consequential induction of epithelial to mesenchymal transition, the major factor in aggressive malignant behavior, migration and invasion has been thoroughly described in breast and a number of other malignancies (210-12). Similarly, other components of metabolic syndrome along with associated disorders represent a potent risk factor for development of malignant disease (213). Type 2 diabetes is recognized by insulin resistance of peripheral tissue due to reduced responsiveness of insulin receptor, whose downstream signaling involves PI3K, AKT and mammalian target of rapamycin (mTOR). The pathways regulated by these mediators are ones of the most commonly dysregulated in all cancers (214).

5.1.2. Lipid metabolism of malignant cells

Other than paracrine and endocrine effects of adipocytes to the cancer cells, cellular regulation of metabolic pathways plays a crucial role in cell development and survival, shaping the cell biology and behavior. Alterations in expression of enzymes regulating lipid synthesis, catabolism and storage are abundantly described in breast malignant cells (212). Endogenous lipids are implicated in cellular events such as proliferation, differentiation, inflammation, autophagy, apoptosis and membrane modeling. Thus, their metabolism is tightly regulated through signaling pathways to assure physiological performance of these functions and maintain homeostasis. Under stressful conditions of limited nutrient supply, malignant cell may employ lipid molecules as an alternative source of energy and as membrane building units that facilitate rapid cellular growth (215). Accordingly, many cancer types display abnormally higher level of lipogenesis. For instance, HER2/neu overexpression is commonly accompanied by amplification of peroxisome proliferator-activated receptor gamma (PPARγ) binding protein (*PBP*) gene, possibly due to the co-localization of their genes in the common region on chromosome 17q12–21 (216). Interestingly, STAT3 gene is located in the close proximity of these genetic loci, on chromosome 17q 21.2. Both PBP overexpression and STAT3 activity stimulate PPARγ transcriptional activity, which is one of the major regulators of lipid metabolism and a necessary mediator of adipogenesis and adipocyte differentiation (217-9). It is noteworthy that both fatty acid synthesis (mediated by fatty acid synthase (FASN)), and beta oxidation (FAO) are commonly upregulated in the lipid metabolism of breast cancers (108). FASN-mediated *de novo* fatty acid synthesis and anabolic proliferation, survival and migration can be triggered by its upstream signaling pathways, such as HER/neu overexpression, PI3K/AKT/mTOR and MAPK (94,220). Interestingly, STAT3 activity was shown to correlate with FASN expression (221), with one study indicating FASN as a target of STAT3 transcriptional activity (222). This relation might hold a therapeutic utility for this breast cancer subset, as it has been shown that FAS inhibition reverses previously acquired resistance to trastuzumab (223,224). On the other hand, catabolism of FA through FAO

stimulates tumor growth by providing ATP to support the extensive needs in the conditions of metabolic stress resulting from reduced oxygen and glucose levels (225). JAK/STAT3 signaling induces the expression of carnitine palmitoyltransferase 1B (CPT1B), a rate limiting enzyme in fatty acid oxidation. Given the importance of FAO in breast cancer stem cells (BCSCs) self-renewal and chemoresistance, abolishing this pathway blocks BCSCs aberrant growth and re-sensitizes them to chemotherapy (108,226). In our study, we did not observe significant and consistent alterations in free fatty acid cellular levels following STAT3 activation. However, activation of STAT3 reduced cellular levels of triacylglycerol containing palmitic, stearic and arachidonic acid (Tables 3 and 4 and Figures 18 and 19). This finding might indicate a STAT3-dependent facilitation of fatty acid catabolism through beta oxidation.

5.1.3. STAT3 activity in cellular lipid modeling

Implication of STAT3 signaling in lipid metabolism, including lipolysis, beta oxidation, ferroptosis and membrane lipid raft modeling in various cancer types became intriguingly evident (106-108,227). While such lipid changes may underlie alterations in morphology, motility, and invasion of STAT3-transformed cells, comprehensive evaluation of lipid metabolites modulated by activated STAT3 was lacking. Using an unbiased strategy employing complementary breast cellular models, we identified several metabolites modulated by activated STAT3, including a profound reduction of cellular N-acyl taurine derivates and AA content (Figures 18 and 19). In addition, two metabolites of sphingomyelin, which is shown to drive aggressive behavior of breast cancer cells (228), were significantly increased with STAT3 activation (Figure 18). We also detected STAT3 regulation of other metabolites, such as monoacylglycerol ether and phosphatidylserine; however, this modulation was not observed consistently across all of the tested models and was not accompanied by alterations of more than one member of the molecular class. While these changes may be important, they may also be cell context dependent. Furthermore, using bioinformatics we confirmed these intriguing correlations of STAT3 activity with AA and taurine metabolism in breast cancer patient datasets. Based on the results of the gene set enrichment analysis, it is plausible that STAT3 regulates the content of these metabolites by modulating the expression of enzymes required for the synthesis of taurine and metabolism of arachidonic acid (Figures 20 and 21).

5.1.4. Physiological roles of taurine and correlation with STAT3

Taurine plays a role in various cellular processes exerting antioxidant, membrane

stabilizing, anti-inflammatory effect and regulation of membrane ion transport, particularly Ca^{2+}(229). In addition, tumor suppressing activity of taurine and more specifically N-acyl taurine, was reported in several types of malignancies, including breast cancer (192,193,230,231). Several mechanisms of taurine effect on sustaining the cell membrane integrity and stability have been reported. Taurine directly scavenges hypochlorid acid (HOCl) as a reactive specie, whereas it is incapable of neutralizing other classical ROS. However, by regulating the rate of ROS generation in mitochondria, taurine indirectly alleviates oxidative stress damage and consequent inflammation (232). In addition, ones of the major targets of oxidative stress are unsaturated fatty acids located in the cell membrane. Thus, reactive species-mediated lipid peroxidation causes membrane disruption, and its prevention by antioxidants, including taurine, stabilizes cell membrane (232-4). Furthermore, taurine may stabilize the cellular membrane directly, by forming electrostatic interactions with phosphate and amino groups of the plasma membrane phospholipids (194). While taurine-mediated inhibition of STAT3 phosphorylation has been described (235,236), our findings suggest that activated STAT3 may reduce taurine biosynthesis through transcriptional regulation of CTH and CDO1 enzymes.

5.1.5. Metabolism of arachidonic acid

Our study suggest a role of STAT3 in the metabolism of arachidonic acid, a crucial mediator of inflammation. Arachidonic acid (AA) is a polyunsaturated fatty acid generally esterified to membrane phospholipids ubiquitously distributed in human cells. It is the direct precursor for eicosanoid synthesis, namely prostaglandins, leukotrienes and thromboxane, together with non-classical eicosanoids epoxyeicosatetraenoic acids, endocannabinoids and others, as the bioactive lipid mediators of inflammatory response. AA is released from the plasma membrane phospholipids by the activity of the cytosolic enzyme phospholipase A2 (PLA2G4A) (200), whose expression did not display a correlation with STAT3 activity in our analysis of breast cancer patient's samples (Figure 22). The biosynthesis of eicosanoids from AA is mediated by cyclooxygenases (COX), lipoxygenases (LOX) and cytochrome P450 (CYP450) pathway.

CYP450 is a wide family of enzymes including approximately 60 cytochrome P450 genes in humans that encode different enzymes, some of which convert AA into epoxyeicosatrienoic and hydroxyeicosatrienoic acids. In general, CYP450 enzymes and their products have versatile physiological functions, including synthesis of steroid hormones, cholesterol, fatty acid metabolism and metabolic clearance of xenobiotics. However, due to the wide spectrum of family members and their functions, investigation of CYP450 family of enzymes in breast cancer metabolism and relation to STAT3 activity exceeds the scope of

this study (237).

5.1.6. Biological effects of cyclooxygenases and correlation with STAT3

COX family includes constitutive cyclooxygenase COX-1, inducible COX-2 and a nonfunctional enzyme in humans, COX-3. COX-1 is responsible for different physiological functions, including production of prostaglandins that protect gastric mucosa and kidney, and has not been described in malignant manner as a single oncogenic factor. On the other hand, overexpression of the inducible cyclooxygenase COX-2 promotes tumor initiation, progression, angiogenesis, migration and metastases, and was reported to promote cancer penetration through the hemato-encephalic barrier involved in breast cancer brain metastases (238,239). Among the products of COX-2 enzymatic activity, prostaglandins of E-series are the most relevant and well-described in various pathological disorders, with emphasis on prostaglandin E2 (PGE2). A number of studies indicate that PGE2 is the prevailing product of COX-2 activity responsible for cancer progression by inactivation of host anti-tumor immune cells, stimulation of tumor cell migration, invasiveness, induction of stem-like cell behavior, VEGF-mediated tumor angiogenesis and lymphangiogenesis (200,240). Furthermore, overexpression of COX-2 is observed in 40% of breast cancer patients, and is associated with poor prognosis and unfavorable outcome (241). In addition, Ristimäki et al. showed that breast cancer patients' distant disease-free survival reduces in a linear manner with ascending COX-2 expression (Figure 65), indicating its importance in breast cancer development and progression. Accordantly, selective inhibition of COX-2 was shown to display a potent anti-cancer effect in *in vivo* models of breast cancer, attenuating the migration and invasion capabilities of cancer cells (242). Similarly, data indicating COX-1 implication in cancer development have mostly been based on the observation of tumor apoptosis induction by non-selective inhibition of both COX-1 and COX-2 (243,244).

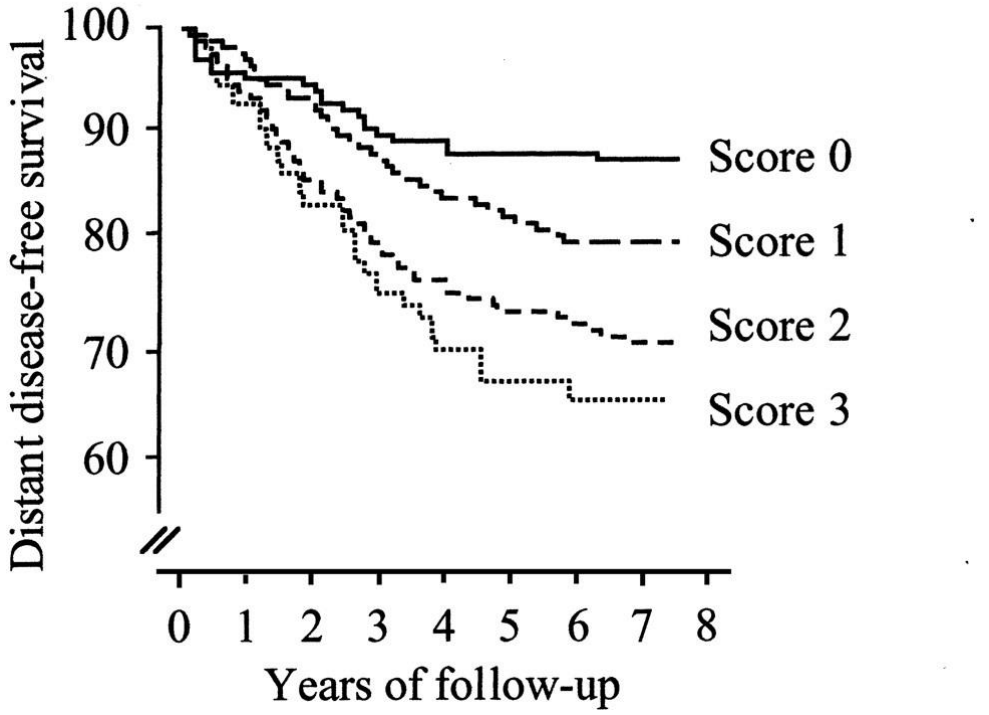

Figure 65. Distant disease-free survival of 1576 breast cancer patients according to COX2 protein expression (241).

Considering STAT3 implication in immune response and concomitant events, one could assume a plausible interplay between this oncogenic driver and COX-2 expression and activity. Reduction of COX-2 protein expression and simultaneous decrease in STAT3 phosphorylation was described in different malignant types, such as prostate cancer and squamous cell carcinoma (197,199). Inversely, Ren et al. showed reversal of IL-6-induced stimulation of COX-2 mRNA and protein expression following treatment with JAK2 inhibitor AG490. In accordance with our findings, these data indicate STAT3-mediated transcriptional regulation of *COX-2* expression (196).

5.1.7. Biological effects of lipoxygenases and correlation with STAT3

Lipoxygenases catalyze the conversion of AA into leukotrienes, commonly associated with asthma and allergic rhinitis. Human genome encodes five genes for *LOX*s, which translates into 5-LOX, 12-LOX (S- and R- conformation) and 15-LOX (isoenzymes 1

and 2). Out of these enzymes, 12-LOX and 15-LOX can metabolize common substrates to produce similar products and are often referred to as 12/15 LOX (245). Aside from catalyzing leukotrienes production, LOXs enzymatic processing of AA results in generation of reactive oxygen species, frequently associated with malignant development (198,246). Taken together with the immunological effects, it is not surprising that each of these three members of lipoxygenases is implicated in oncogenesis. 5-LOX and 12-LOX involvement in cancer development and progression has been well established, whereas conflicting evidence suggests both tumor-repressing and tumor-promoting effects of 15-LOX (247-9). Among these enzymes, 5-LOX is characterized in most details. Under physiological conditions, 5-LOX is mainly expressed in immune cells, however, its expression is detected in malignant cells as well. 5-LOX role in promoting tumorigenesis has been reported in several malignancies, including breast cancer (250,251). Importance of 5-LOX role in breast cancer development is displayed by 50% elevated serum levels of this pro-inflammatory mediator in breast cancer patients. This occurrence is independent of breast cancer molecular subtype, tumor size, stage and menopausal status, indicating the potential of using 5-LOX serum levels as a biomarker for non-invasive early breast cancer detection (252). In accordance, inhibition of 5-LOX led to reduced growth and survival of cancer cells *in vitro* and *in vivo* (253-5).

Role of STAT3 in regulating inflammation and immunity as well as interconnection with AA metabolism is well characterized, however the specific interaction with 5-LOX is so far scarcely described. While Thornber et al. demonstrated reduction of STAT3 phosphorylation following 5-LOX inhibitor treatment in large cell lymphoma cells (198), our findings indicate that STAT3 transcriptional activity might induce the mRNA expression of both 5-LOX and COX-2. Consequently, STAT3 activation enhances eicosanoid synthesis associated with inflammation and cancer progression, while reducing the cellular AA content in breast neoplastic cells (200). Other than the canonical functions of AA in immunity, an interesting finding is that AA also reduces the velocity and migration ability of endothelial cells and modulates the cellular morphology by inducing an elongated cellular shape (256). Thus, STAT3-induced reduction of AA content with associated enhancement of eicosanoid synthesis might promote migration, inflammation and invasive behavior of cancer cells.

The fact that both taurine derivates and arachidonic acid are involved in plasma membrane remodeling (194,195) provides a basis for how changes in the metabolic architecture resulting from aberrant STAT3 activation can provide specificity for a tumor-targeting approach employing surface-directed nanoparticles.

5.2. *Research approaches for targeting oncogenic transcription factor STAT3*

Considering the importance of STAT3 signaling in the pathogenesis of breast cancer and other common tumors, and the high therapeutic index of blocking STAT3 transcriptional function, a number of strategies have been taken to identify inhibitors of this protein (120,257,258). One approach involves large-scale library screenings in identifying STAT3 transcriptional inhibitors. Although they require further investigation of specific mechanism of action, library screens of chemicals may provide an unbiased identification of small molecule inhibitors to oncogenic drivers. With that regard, conduction of a computational screen based on a STAT3 gene expression signature led to the identification of atovaquone, an FDA approved anti-microbial drug, which decreases gp130-dependent phosphorylation of STAT3 (259). Similarly, experimental chemical library screens for specific inhibition of STAT3-dependent gene expression revealed nifuroxazide and pyrimethamine as potent STAT3 transcriptional inhibitors (191,260). These findings led to ongoing clinical trials of pyrimethamine and atovaquone for the treatment of hematological malignancies and lung cancer (ClinicalTrials.gov). Other than small molecule inhibitors, targeted strategies for the inhibition of STAT3 have included the development of molecules designed to bind to specific functional regions of STAT3, including the SH2 and DNA-binding domains. Such targeted approaches include peptidic inhibitors or peptide mimics of pTyr, which bind to the SH2 domain and inhibit the interaction of two STAT3 molecules when forming an active dimer. However, successful engineering of such peptides with high binding affinity to SH2 domain of STAT3 and other signal transducers encounter challenges generally related to insufficient cell penetrating ability and intracellular stability of these compounds (131). Further, antisense oligonucleotide decoys hold promise in inhibiting STAT3 DNA-binding domain. They represent a short double-stranded DNA sequences identical to the ones found in the promoter of the transcription factor target genes. As TFs show high affinity for those sequences, these decoys bind and thus capture TF, disabling its further activity. Although these approaches allow a specific and well defined mechanism, they often display suboptimal potency due to insufficient cell penetration and intracellular stability, as well as unfavorable pharmacokinetic profile when administered *in vivo* (202,261). For instance, Nagel-Wolfrum et al. identified DBD-1, a small peptide aptamer capable of disrupting DNA-binding ability of STAT3 *in vitro*, however, *in vivo* experiments showed only a meek interference with the DNA-binding of STAT3 (262). Thus, it remains to be seen whether these strategies will translate into clinically useful agents for on-target inhibition of STAT3 (59). One of the means to surmount these poor pharmacokinetic properties of biological specimen, such as peptides and oligonucleotides, is by encapsulation into a biodegradable, yet biologically stable nanocarrier with beneficial pharmacokinetic properties. Nanosystems incorporating oligonucleotide decoys to STAT3 molecule have shown promising results *in vitro* and in mouse models of ovarian cancer (263). Another contemporarily favored approach is the

application of nanosystems for delivery of RNA interference, such as short hairpin RNA (shRNA) (264) and much more often small interfering RNAs, to silence the expression of an oncogene. These double stranded oligonucleotides show low capability of permeating through biological barriers including cell membrane. These restrains could be overcome with a nanocarrier that additionally protects them from DNases and serum-mediated degradation (265). Nanosystems carrying siRNA to STAT3 showed encouraging results in targeting breast and other malignancies. Importantly, besides the strong efficacy displayed *in vitro*, the opportunity to modify the nanocarriers to exert advantageous pharmacokinetic properties allows potent cancer killing efficacy *in vivo* (266,267). Nevertheless, due to the genetic alterations caused by siRNA silencing, evaluation of these molecules in humans has been impeded, particularly following first unsuccessful clinical trials (268). Notwithstanding, in the year of 2018, the first siRNA-encapsulating nanoparticle formulation, Givlaari®, gained FDA approval for treatment of a rare hereditary disease transthyretin (TTR) amyloidosis (hATTR), paving the path for the development of new siRNA-derived therapeutics, which may be particularly important in oncology (269). In addition, nanoparticle-based approaches that focus on targeting STAT3 may involve loading a STAT3 small molecule inhibitor into a nano-size carrier, and have shown induction of apoptosis in cancer cells *in vitro* and in mouse models (265,270,271). While many of these approaches hold promise, this is the first study to our knowledge that targets cancer cells based on exploiting STAT3-driven changes in cellular lipid composition. In contrast to direct targeting and inhibition of STAT3, our study focused on utilizing STAT3-driven lipid profile of cancer cells as a promising method of distinction between normal and malignant cells. To further harness these STAT3-dependent metabolic alterations, we examined using Layer-by-Layer nanoparticles that could exploit these lipid differences. To identify the LbL composition with tumor-targeting affinity towards the cells characterized by the STAT3-induced lipid profile, we screened a library of 12 nanoparticles differing in their surface chemistry, which is responsible for NP-cell interaction.

5.3. *Lipidome-based targeting of STAT3-driven breast cancers using Layer-by-Layer nanoparticles*

Our LbL nanoparticle library screen revealed that anionic liposomes coated with PLE as the terminal layer preferentially bind to cells with constitutive STAT3 activation, including TNBC cell lines (Figures 37-41,45,46). This property was unique for PLE-NPs, as NPs with other surface coatings did not show a similar effect (Figures 24-36). Furthermore, abrogation of STAT3 mRNA expression, phosphorylation, or transcriptional activity strongly attenuated cell binding of PLE-NPs, suggesting the specificity of targeting STAT3-driven cells by these nanosystems (Figures 41,45,46). While our study focused on STAT3-dependency of the PLE-NP-cell binding, previous research examined the nature of cell-

association of these particles (164). To examine if cell binding of NPs complemented with PLE and other surface chemistries is specific or non-specific, this study performed a binding saturation evaluation, displayed as the apparent dissociation constant. As control, non-specific coatings of nanoparticles were used, such as DXS and conventionally used poly-ethylene glycol (PEG), together with non-coated carboxy modified latex (CML) core. As expected, they demonstrated linear dose-dependent cell binding, indicating a non-specific NP-cell interaction. In contrast, PLE- along with PLD- and receptor-directed HA-coated particles displayed binding curves characteristic for specific NP-cell interaction, with strong binding affinity even at the lowest concentration, which increases until the binding saturation point (Figure 66). These data indicate a specific mechanism of cell-binding in case of PLD-NPs, PLE-NPs and HA-NPs. While the mechanisms of such interactions with cell membrane remained largely unknown, our study offers an insight into factors modulating PLE-NP cell association.

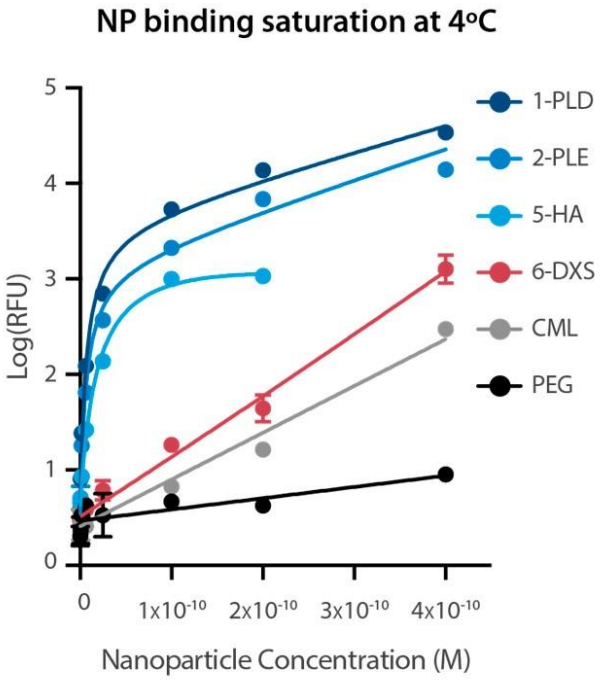

Figure 66. Nanoparticle binding saturation isotherms on OVCAR8 cells. Kd values were calculated for PLD-NPs (6.8 ± 1.6 pM); PLE-NPs (6.2 ± 2.2 pM) and HA-NPs (18.7 ± 18.4 pM). DXS-NPs, PEG-NPs, and CML-NPs could not be fit to the model and appear to act via nonspecific binding interactions. (164)

The tumor-targeting properties of PLE-NPs have been previously demonstrated in

ovarian cancer models, however, the mechanism underlying this phenomenon remained to be elucidated (164). These NPs showed strong ability to bind to different ovarian cancer cell lines, with minimized association to non-malignant cells, such as induced pluripotent stem cell-derived endothelial cells and primary immune and stromal cells isolated from spleens of mice. LbL NPs terminally layered with poly-L-glutamic acid displayed 11-fold greater specificity for cancerous over normal cells, which was to some degree similar to another NP coated with COOH-containing functional groups, PLD. Interestingly, structurally related PLE- and PLD- coatings of the NPs, which do not possess a known ligand-receptor binding ability, displayed stronger tumor-targeting property than hyaluronic acid (HA)-coated particles. HA binds to its cell surface glycoprotein receptor CD44, involved in cell adhesion and migration and commonly overexpressed on malignant cells. Therefore, affinity of HA-NPs for cancer cells was a well anticipated finding. Nevertheless, PLE-coated NPs showed substantial advantage in selectivity and tumor-targeting ability, having occupied 3.5-fold more ovarian cancer cells than the HA-NPs (164). Correa et al. investigated possible mechanisms of such events, however, the underlying principle remained incompletely understood. The binding of PLE-NPs to cell membrane was ATP-, receptor-mediated endocytosis-, caveolar-mediated endocytosis- and macropinocytosis independent, whereas binding of other NPs such as HA- and PLD- were strongly affected by the inhibition of these pathways. The single factor reducing the PLE-NP cell binding found was treatment with methyl-β cyclodextrin, a potent membrane-associated cholesterol removing agent. Thus, methyl-β cyclodextrin disrupts the membrane lipid raft and lipid-associated macromolecules. In conjunction with our findings, it might be possible that this treatment disrupted STAT3-modulated metabolic profile of plasma membrane, attenuating cell binding of PLE-NPs. In addition, STAT3 is commonly aberrantly activated in ovarian cancer and contributes the expression of genes governing malignant behavior in this malignant type, among number of others (273). Taken together with the priory described STAT3-mediated metabolic changes, our study provides a plausible mechanism for high affinity of PLE-NPs towards ovarian cancer cells and its reduction by disruption of STAT3-driven lipid profile of a cancer cell. To evaluate the extent to which this targeting ability was driven by activated STAT3, we compared the previously reported PLE-NP binding affinity in these ovarian cancer cell lines with mRNA expression of the two target genes most specific for STAT3 transcriptional activity, SOCS3 and JUNB (Figure 67). Overall, all of the tested ovarian cell lines showed greater PLE-NP recruitment than other investigated NPs and than non-malignant cells (164) (Figure 67). These cell lines also expressed relatively high levels of the STAT3-regulated genes compared with the other ovarian cell lines. Additionally, cell lines such as JHSO2, COV318, FUOV1, SKOV3 and COV362 showed a positive correlation between PLE-NP binding affinity and STAT3 functional activation. These analyses provide independent confirmation, in a different tumor system, of the affinity of PLE-NPs to tumor cells with activated STAT3.

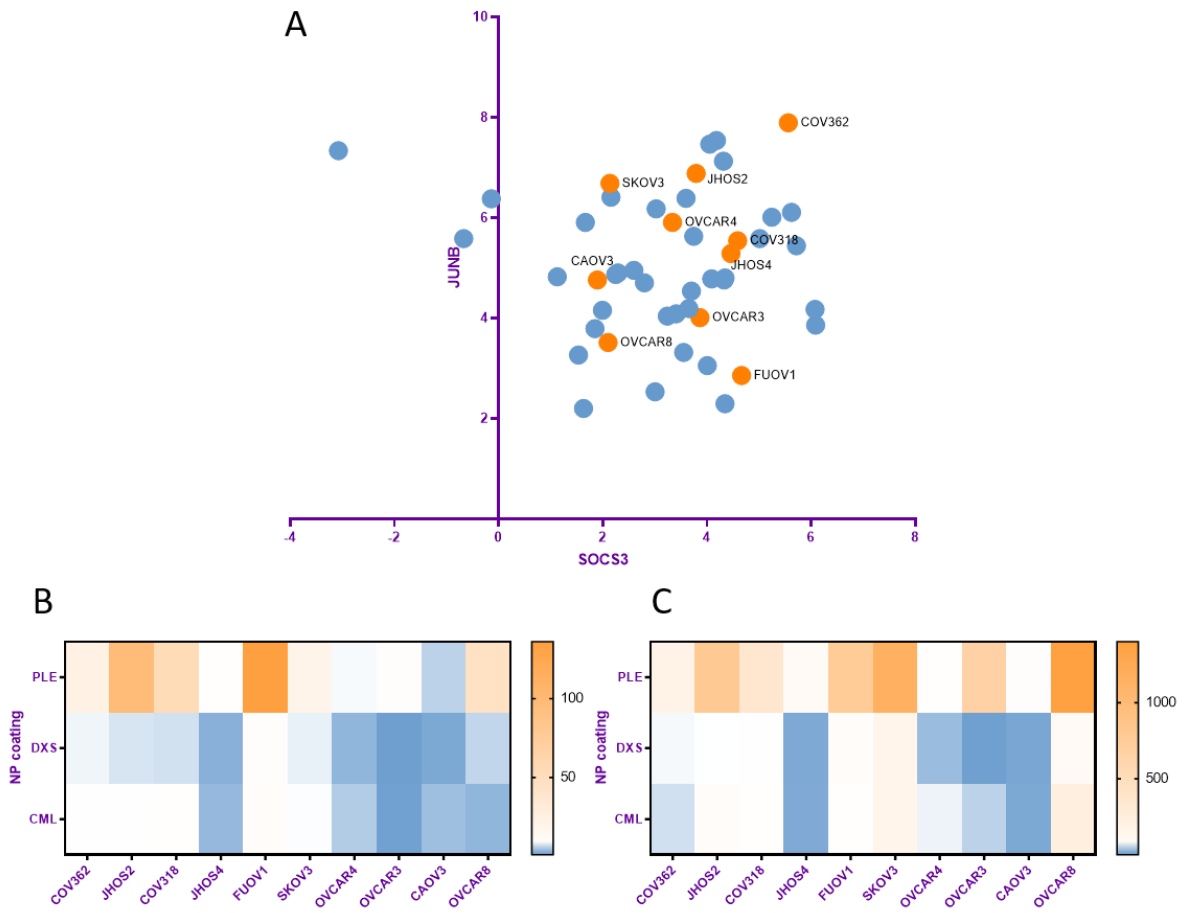

Figure 67. Expression of STAT3-regulated genes JUNB and SOCS3 and their correlation with NP-cell binding in ovarian cancer cells. A. Expression of STAT3 target genes SOCS3 and JUNB was analyzed in 47 ovarian cancer cell lines (Cancer Cell Line Encyclopedia). The cell lines previously tested for NP binding (164, n=10) are presented in orange, and non-investigated are shown in blue. B,C. Cellular binding of NPs coated with PLE, DXS or non-coated carboxy-modified latex core (CML) to indicated ovarian cancer cell lines was previously assessed (164). The NP-cell binding was analyzed following 4 (B) and 24 hour treatment (C) with indicated NPs.

When examining subcellular distribution of PLE-coated nanoparticles, our and previous researches indicate that these particles bind the cellular membrane (Figures 38 and 39, 164). Although they may not necessarily be internalized into the cytoplasm, PLE-NPs show strong capability of preferentially accumulating in tumor tissue *in vitro* and *in vivo* (164,201,202). Consistent with previous findings, our three-dimensional organoid model showed potent penetration ability of these nanocarriers (Figures 51 and 52). Investigating the aspect of PLE-NP accumulation in three dimensional cellular organoids was important for

several reasons. First, we confirmed that these nanocarriers are capable of penetrating into the depth of tumor tissue, which is an essential property necessary for further translational development. Secondly, three dimensional cell cultivating is a better model for mimicking *in vivo* tumor architecture, as it is possible for gene expression and metabolic patterns to show some degree of variability between single cell layer and three dimensional tumor cell growth (203,204). Thus, confirmation of an effect in cancer organoids represents a more precise simulation of behavior in solid tumor. Finally, STAT3 activation is known to induce the malignant cell growth displayed by enhanced growth, proliferation and survival rates (120). Accordingly, induction of STAT3C resulted in formation of greater numbers of massive, dense and hypoxic organoids. While it may have been expected that NPs could hardly penetrate through such a cellular formation, PLE-NPs showed preferential accumulation in organoids characterized by induced STAT3 activity. Our findings were consistent with reports of *in vivo* administration of these unique nanosystems, which successfully avoided premature lymphatic clearance and elimination by liver, and accumulated in tumor tissue of both primary tumors and metastatic lesions (164). Most importantly, analogously to reports of other authors (201,202), we found that PLE-NPs can preferentially deliver therapeutic payloads to malignant cells in a more efficient and specific manner compared to free drug treatment (Figures 55-57).

5.4. *Therapeutic relevance of tumor-targeting by PLE-NPs*

The therapeutic relevance of this finding is reflected by the strong cytotoxic effect of CDDP delivered via PLE-NPs to STAT3-driven cells (Figures 55 and 56). On the contrary, MCF-10A cells lacking constitutive STAT3 activity showed greater survival after this treatment, suggesting a strong therapeutic index. Furthermore, constitutive STAT3 signaling is implicated in aggressive malignant behavior and the development of chemo-resistance patterns in various malignancies, including breast cancers and TNBCs (273). Accordingly, STAT3 expression and activity is upregulated in drug-resistant TNBC cells, as compared to their parental counterparts (108). The most probable manner of STAT3 implication in chemoresistance development is through transcriptional regulation of pro-survival and other genes involved in chemoresistance (274). For instance, STAT3 activation positively regulates the expression of the pluripotency transcription factors octamer-binding transcription factor-4 (Oct-4) and c-Myc, which further mediate resistance to doxorubicin in TNBC. Disruption of this signaling axis by inhibition of STAT3 phosphorylation using WP1066 restored the sensitivity of TNBC cells towards this cytotoxic agent (275). Additionally, previously described target genes of STAT3 are actively involved in development of resistance patterns, such as HIF-1α (276), survivin (277) and BCL-2 family members that inhibit apoptosis, including BCL-2, BCL-xL and MCL-1 (278). By suppressing the chemotherapy-induced cell death, they contribute to acquiring

chemoresistance in cancer cells. Moreover, STAT3 is shown to regulate the expression of multidrug resistance protein 1 (MDR1, ABCB1) and multidrug resistance associated protein 1 (MRP1, ABCC1), responsible for cellular efflux of cytotoxic drugs (279,280). *MDR1* and *MRP1* are shown to be direct STAT3 target genes, as binding to their promoters was verified by chromatin immunoprecipitation (281). As a result, it is well described that STAT3 inhibition sensitizes cancer cells and increases the responsiveness to chemotherapeutic treatment (282). Given the importance of STAT3 signaling in resistance to anti-cancer drugs, our finding that STAT3-driven cancer cells show either greater resistance to non-targeted forms of treatment or display generally low apoptotic sensitivity were well anticipated (Figures 57-61). These findings further emphasize the relevance of the specific cytotoxic effect of PLE-NP-mediated delivery of CDDP, which presumably delivers a higher concentration of drug that can overcome these effects. In addition, LbL NP systems are designed to be biocompatible and have high stability when administered *in vivo*, including a favorable pharmacokinetic profile (181). The affinity of PLE-NPs for STAT3-driven tumor cells could further minimize their off-target effects, facilitating translational and clinical development.

5.5. *Gamma radiation in treatment of breast cancer*

Finally, radiation treatment is an important component of breast cancer management (8,124). Gamma radiation is a form of therapy commonly combined with chemotherapeutic regimen, used for localized ionizing irradiation of tumor tissue. Radiation exerts its activity mainly by inducing production of ROS, primarily hydroxyl and superoxide radicals, which further interact with endogenous molecules to generate free radicals. These highly unstable and reactive ions rapidly interact with biological components, such as DNA and lipids to induce DNA damage and lipid peroxidation (283). In contrast to oxidative stress induction, radiation was shown to reduce the activity of antioxidant enzymes such as superoxide dismutase (SOD), catalase (CAT) and glutathione peroxidase (GPx), together with reduction of glutathione (GSH) a major intracellular free radicals scavenger (284,285). These potent changes in cellular milieu often result in apoptosis of cancer cells, but also adjacent normal cells, resulting in tumor shrinkage. Similarly, we observed proliferation arrest following gamma radiation in a dose-dependent manner (Figure 62). Lipid peroxidation caused by radiation commonly occurs in the lipid bilayer of plasma membrane, consequently altering its properties. Oxidative stress induces the re-organization of the membrane lipid components, peroxiding double bounds and decreasing the number of n-3 and n-6 series of phosphatidylethanolamine fatty acids, and increasing the abundance of their saturated form (286). Thus, irradiation is known to alter the properties of cellular and plasma membrane lipid metabolism. Additionally, inflammatory pathways are being activated in response to gamma radiation, including the stimulation of AA metabolism. Enzymes involved in the

plasma membrane release and metabolism of AA, including PLA2G4A, COX-2 and 5-LOX have all been shown to increase their activity in response to gamma radiation (200).

5.5.1. Effects of gamma radiation on PLE-NPs cell binding

Given the common application of gamma radiation in treatment of breast cancer patients, and its effects on plasma membrane modeling and inflammatory response, we hypothesized that radiation may alter the cell-binding properties of PLE-coated nanoparticles. We found that irradiation led to suppressed binding of PLE-NPs to non-transformed cells, while minimally affecting binding to STAT3-transformed cells (Figure 63). Consequently, the difference in PLE-NP cell binding between non-transformed and STAT3-transformed cells increased 2-fold following 5 Gy irradiation, when compared to non-irradiated baseline cell-binding difference. Although the mechanism of such a finding is not completely understood, one hypothesis to explain this phenomenon is that lipid changes driven by activated STAT3 may be more stable than those in non-transformed cells. Given the role of STAT3 in development of resistance to gamma radiation (287), STAT3 activity might curtail the radiation-induced lipid changes and consequently maintain high binding levels of PLE-NPs to STAT3-transformed cells. On the other hand, cells lacking activated STAT3 might undergo greater lipid changes following radiation, resulting in reduced binding of PLE-coated nanosystems. Multiple approaches are undertaken in development of radio-sensitizing, usually metal-based nanoparticles, containing high atomic mass atoms of peculiar optical, magnetic and mechanical characteristics, including gold, platinum, silver, gadolinium etc (288). Whereas the combination effect of such NPs with radiation therapy is well studied, the combinatory effect with nanosystems that do not possess such a property has not been evaluated thus far. Taken together, these findings raise the possibility of an enhanced therapeutic index in combining PLE-NP-based drug delivery with radiation therapy for breast cancer treatment.

6. Conclusion

Despite the substantial progress in treatment, breast cancer remains the major public health concern, accounting for 600 000 deaths annually at the global level. In particular, treatment of triple-negative breast cancer has been immensely challenging due to the lack of a known target which could enable its distinction from non-malignant tissue. The oncogenic transcription factor STAT3 is abnormally activated in essentially all triple-negative breast cancers and 70% of all breast cancer subtypes. Taken together with the fact that normal cells could endure the absence of STAT3 without major disruptions of physiological performances, STAT3 represents a prominent target in treatment of this pervasive disease. As STAT3 is an intracellular protein which shuttles from cytoplasm to nucleus and does not represent a direct cell surface target, we evaluated using an innovative approach in distinguishing STAT3-driven breast cancers. Therefore, we examined the metabolic aspects of STAT3-driven malignant transformation, and tested using the novel nanoparticle systems, Layer-by-Layer nanoparticles, in exploiting these properties therapeutically.

Based on the results generated and presented in this dissertation, the following conclusions are derived:

1. Qualitative and quantitative analysis of STAT3-driven metabolic profile in breast cellular systems revealed that STAT3 actively modulates the lipid structure of breast cancers. The most consistent and potent metabolic alterations are observed with the cellular abundance of N-acyl taurine and arachidonic acid derivates.
2. STAT3 gene expression signature is highly enriched in the breast cancer patient samples that have low expression of cystathionine gamma lyase (CTH) and cysteine dioxygenase (CDO1), the two enzymes required for taurine biosynthesis from homocysteine. This finding indicate that STAT3 may negatively regulate transcription of these enzymes, resulting in reduction of cellular N-acyl taurine content.
3. STAT3 gene expression signature is highly enriched in the breast cancer patient samples that have high expression of cyclooxygenase 2 (COX-2) and arachidonate 5-lipoxygenase (5-LOX, ALOX-5), the two enzymes that catalyzes the conversion of arachidonic acid into eicosanoids, and does not correlate with the expression of phospholipase A2 (PLA2G4A), the enzyme required for release of arachidonic acid from phospholipid bilayer of cell membrane. These findings indicate that STAT3 may positively regulate transcription of COX-2 and 5-LOX, resulting in reduction of cellular arachidonic acid content.

Both taurine and arachidonic acid are involved in plasma membrane remodeling, providing a plausible distinction between STAT3-driven breast cancer cells and non-malignant tissue.

4. By screening a library of 12 differently coated Layer-by-Layer nanoparticles, we identified poly-L-glutamic acid coated nanoparticles to display targeting affinity towards STAT3-transformed breast cancer cells, while showing attenuated binding to non-transformed counterparts. The specificity of this NP-cell interaction is displayed by absence of similar effect with nanoparticles coated with other surface chemistries.
5. Characterization of PLE-NPs subcellular distribution by high resolution microscopy indicates that these particles primarily bind to the cellular plasma membrane, and may not necessarily be internalized into the cytosol.
6. Quantitative flow cytometry analysis indicates that PLE-NPs preferentially bind to STAT3-transformed MCF-10A cells, displaying 50% greater cell-associated nanoparticle fluorescence compared to their non-transformed counterparts. This event is completely reversed with STAT3 transcriptional (using pyrimethamine) and phosphorylation (using ruxolitinib) inhibition, confirming STAT3-dependency of tumor-targeting properties of these nanoscale systems.
7. PLE-coated nanoparticles could be used as the targeting agent for triple-negative breast cancers, as they show strong binding to TNBC cell lines SUM159PT and MDA-MB-231. The cellular binding is significantly attenuated with genetic inhibition of STAT3 using each of the two different siRNA sequences.
8. Analyses of the PLE-NP effect in three dimensional breast cellular organoids revealed that these nanoparticles potently penetrate in depth of three dimensional cancer structures. Despite the fact that STAT3-transformed organoids grew in denser and massive three-dimensional structures than non-transformed organoids, which may have been expected to impede the NP penetration, these organoids showed greater quantitative PLE-NP fluorescence per organoid (by 40%) as well as per organoid volume (by 73%).
9. The translational potential of this study is presented by significantly stronger cytotoxic effect of cisplatin delivered via PLE-NPs to STAT3-driven cells compared to cells lacking activated STAT3. On the contrary, cells with activated STAT3, including TNBC cells, showed either greater resistance or non-responsiveness to non-specific treatments, including free cisplatin and cisplatin-loaded NPs lacking the surface layer or complemented with non-targeting dextran sulfate.
10. Gamma irradiation significantly reduced the binding of PLE-NPs to non-transformed mammary epithelial cells, while having minimal effect on binding to STAT3-induced cells. This led to radiation dose-dependent increase in differential cell binding of

PLE-NPs, resulting in 2-fold increase in binding difference between non-transformed and STAT3-transformed cells following 5 Gy radiation.

In conclusion, LbL nanoparticles with a terminal poly-L-glutamic acid layer represent a new class of drug carriers that preferentially interact with STAT3-transformed mammary epithelial cells, and may offer synergy with radiation therapy. These findings provide a promising starting point for the development of a rational, targeted approach to treating triple-negative breast cancers, which currently lack such therapeutic options.

1. Uvod

1.1. *Malignitet dojke*

Karcinom dojke je na globalnom nivou najčešće dijagnostikovano maligno oboljenje kod žena i predstavlja drugi vodeći uzrok smrtnosti usled maligniteta (Slika 1) (1,8). Prema procenama na onovu ispitivanja u 185 svetskih zemalja, u 2018. godini je novodijagnostikovano više od 2 miliona pacijenata sa karcinomom dojke, što čini 25-30% ukupne incidencije malignih oboljenja (1). Karcinom dojke je vodeći uzrok mortaliteta usled maligniteta kod žena u većini svetskih zemalja, sa procenjenih 600.000 smrtnih slučajeva u 2018. godini (Slike 2 i 3) (1). Analogna statistička zapažanja su zabeležena u Republici Srbiji, gde karcinom dojke čini 26% obolelih i 17,5% ukupne smrtnosti od maligniteta (4,5). Razvoj novih dijagnostičkih i terapijskih strategija imao je značajan uticaj na rezultate lečenja, o čemu svedoči povećanje procenta petogodišnjeg preživljavanja pacijenta sa karcinomom dojke sa 75% (1975-1977) na 90% (2005-2011) (3,6). Kod pacijenata kod kojih je postavljena dijagnoza u ranoj fazi bolesti postoji značajna mogućnost uspešne terapije i eradikacije malignog tumora. Međutim, na osnovu izveštaja američkog Nacionalnog centra za zdravstvenu statistiku za 2019. godinu, manje od 25% novodijagnostikovanih pacijenata je otkriveno u *in situ* fazi tumora (3,7). Iako kod većine karcinoma dojke u trenutku postavljanja dijagnoze nije došlo do razvoja metastaza, kod skoro trećine pacijenata sa prvobitno dijagnostikovanom *in situ* neoplazmom će tokom kliničkog praćenja doći do pojave metastaza (7,8). Ukoliko je pri postavljanju dijagnoze već došlo do diseminacije malignog tumora u udaljena tkiva, terapijske mogućnosti su ograničene i petogodišnje preživljavanje se smanjuje na samo 26% (3). Najčešći uzrok smrtnosti od karcinoma dojke predstavljaju metastatske diseminacije u limfne čvorove, kosti, jetru, pluća i CNS (8).

1.1.1. Terapijski pristup zbrinjavanju pacijenata sa malignitetom dojke

Terapijski pristup lečenju maligniteta dojke je najčešće multimodalan i uključuje kombinaciju lokalnih tretmana kao što su hirurške metode i radioterapija; i sistemsku terapiju koja se sastoji od hemioterapije, hormonske i ciljane terapije (6). Prilikom određivanja adekvatne medikamentne terapije u savremenoj personalizovanoj onkologiji, najvažniju ulogu ima definisanje molekularnog tipa karcinoma dojke. Maligna proliferacija i preživljavanje ćelija karcinoma često zavisi od specifičnih endogenih molekula koji služe kao onkogeni pokretači, te njihova inhibicija rezultuje ćelijskom smrću. Navedeni tumor-specifični molekuli mogu služiti kao mete za razvoj ciljanje terapije, s obzirom da mogu poslužiti kako za diferencijaciju između normalnih i malignih ćelija, tako i za uspešnu indukciju apoptoze u malignim ćelijama. Usled navedenog, određivanje molekularnog tipa ćelija karcinoma dojke omogućava predviđanje terapije na koju će tumor reagovati (10).

1.1.2. Molekularni tipovi maligniteta dojke

Na osnovu ekspresije hormonskih receptora (HR) za estrogen (ER) i progesteron (PR), kao i receptora humanog epidermalnog faktora rasta 2 (ERBB2, takođe poznat kao HER2), karcinom dojke može se svrstati u tri kategorije: hormon receptor pozitivni (70% pacijenata), ERBB2 pozitivni (15-20%) i trostruko-negativni tumori koji ne eksprimiraju ni jedan od navedenih molekularnih markera (15-20%) (8).

Luminalne karcinome dojke odlikuje ekspresija hormonskih receptora za estrogen i/ili progesteron, i mogu se podeliti u podtipove A i B. Luminalni tip A je najčešći oblik karcinoma dojke i obično se sporo razvija i raste. Podtip B je agresivniji od tipa A, a pored hormonskih receptora može pokazivati i prekomernu ekspresiju HER2 receptora. U skladu sa navedenim, lečenje obe podvrste uključuje hormonsku terapiju, dok se luminalni tip B može dodatno tretirati ciljanim lekovima ka HER2, kao i preventivnom hemioterapijom ukoliko postoji rizik od razvoja metastaza (8,11).

ERBB2 pozitivne ćelije karcinoma dojke su definisane prekomernom ekspresijom ERBB2 transmembranskog receptora tirozin kinaze ili detekcijom amplifikacije genske kopije datog onkogenog pokretača (12). HER2 molekularni tip karcinoma dojke može biti pozitivan ili negativan na hormonske receptore, sa približno jednakom alokacijom (8). Prekomerna ekspresija HER2 dovodi do agresivnog malignog fenotipa, sa većom tendencijom razvoja metastaza u poređenju sa HR pozitivnim karcinomom dojke. Međutim, razvoj ciljanih terapija usmerenih na HER2 je značajno poboljšao prognozu za pacijente, dovodeći do prosečnog preživaljanja pacijenata sa razvijenim metastazama od približno 5 godina, dok 75% svih pacijenata sa HER2 pozitivnim karcinomom dojke postiže potpuni patološki odgovor (8). Najčešće korišćena ciljana terapija protiv HER2 receptora je monoklonsko antitelo trastuzumab (Herceptin®). Ostali korišćeni selektivni inhibitori uključuju pertuzumab (Perjeta®), takođe HER2 antitelo, kao i lapatinib (Tikerb®) i neratinib (Nerlink®) koji su dualni inhibitori tirozin kinaza. Lapatinib i neratinib vrše disrupciju signalnih puteva i receptora HER2/neu i epidermalnog faktora rasta (EGFR), takođe često prekomerno ekspresovanog na malignim ćelijama dojke (13). U skladu sa trenutnim preporukama o lečenju, ciljana terapija se primenjuje zajedno sa nespecifičnom hemioterapijom, koja uključuje taksane (paklitaksel, docetaksel), doksorubicin, ciklofosfamid i antitumorske lekove na bazi platine poput karboplatina (8).

Trostruko-negativni karcinom dojke (engl. *triple-negative breast cancer*, TNBC) predstavlja heterogeni oblik karcinoma dojke u čijim ćelijama postoji izuzetno nizak stepen ekspresije receptora za estrogen, progesteron i humani epidermalni faktor rasta (ER, PR i HER2) (15). Uprkos relativno niskoj prevalenciji (15-20%), TNBC je najagresivniji tip maligniteta dojke i najkomplikovaniji za lečenje, te predstavlja značajan udeo ukupne smrtnosti pacijenata sa karcinomom dojke (13). TNBC imaju izraženu tendenciju metastatskog razvoja, a ukoliko pacijent postigne remisiju, rizik od recidiva je veći u

poređenju sa ostalim molekularnim vrstama. U slučaju metastatskog razvoja TNBC-a, ukupno srednje preživljavanje pacijenata je drastično kraće nego kod drugih podtipova u istom stadijumu, te je približno godinu dana u odnosu na pet godina kod HR i HER2 pozitivnih karcinoma (8). Lečenje TNBC je naročito zahtevno zbog odsustva ekspresije poznatih molekularnih meta kao što su prethodno opisani membranski receptori. Standardni tretman obuhvata nespecifičnu terapiju, kao što su hirurške metode, radioterapija i hemioterapija koja pretežno uključuje taksane, antracikline i ciklofosfamid (15). Stoga, TNBC je tip neoplazme dojke sa najizraženijom potrebom za razvoj novih terapijskih opcija.

Ostale molekularne karakteristike, kao što su ekspresija receptora epidermalnog faktora rasta (EGFR), ekspresija receptora za androgene i folatni α receptor, mutacije *PTEN* ili *PIK3CA* gena, stalno se evaluiraju u cilju razvoja specifične terapije sa ciljanim dejstvom na maligne ćelije (16). Međutim, trenutni prediktivni faktori efikasne ciljane terapije su isključivo prekomerna ekspresija HER2 i status hormonskih receptora. Iako terapijski pristupi poput hormonske terapije i antitela poseduju korisna svojstva ciljanog delovanja i specifičnost, druge pristupe karakteriše nedostatak selektivnosti sa sledstvenom suboptimalnom efikasnošću praćenom sistemskom toksičnošću i oštećenjem zdravog tkiva (17). Stoga, bolje razumevanje etiologije malignih oboljenja dojke i razjašnjavanje njihove biološke i genetske osnove može obezbediti novu metu za razlikovanje malignih ćelija i poslužiti kao osnova za razvoj selektivne terapije. Uporedo sa razvojem novih tehnologija za eksploataciju takvih malignih karakteristika, data istraživanja mogu doprineti unapređenju lečenja ovog visoko rasprostranjenog i često smrtonosnog malignog oboljenja.

1.2. *Etiologija malignih oboljenja*

Etiologija maligniteta je uglavnom multifaktorijalna pri čemu nasledni, faktori životne sredine i načina života međusobno interaguju i zajedno mogu da dovedu do inicijacije i razvoja maligniteta. Poznavanje molekularnih osnova je od značaja za razumevanje biologije malignih ćelija kao i za prepoznavanje pacijenata sa povišenim rizikom za razvoj malignih oboljenja; određivanje personalizovane terapije podešene prema specifičnostima svakog pacijenta i razvoj novih terapijskih i dijagnostičkih modaliteta. Humani genom odlikuje visok stepen diverziteta, što rezultuje specifičnošću genotipa i fenotipa svake individue. Humani genom sadrži 19.116 gena koji kodiraju proteine, 46.932 proizvoda alternativne transkripcije i 562.164 egzona (18). Varijante sekvence genoma mogu rezultovati izmenom sinteze i funkcije konačnog proteina (20). Pored toga, elementi koji regulišu procese transkripcije, translacije i posttranslacione modifikacije značajno utiču na posledične fenotipske manifestacije bez promene u DNK sekvenci. Kontrola ekspresije gena jedna je od osnova za normalan razvoj i funkciju ćelija, a njena disrupcija je čest uzrok raznih patofizioloških manifestacija, uključujući maligna oboljenja (21). Stoga su

epigenetika, transkriptomika, proteomika i metabolomika, tačnije njihova kombinacija koju proučava multi-omika, stekli veliku pažnju pri proučavanju biološke osnove maligne patogeneze (22). Pristup multi-omike je do sada je otkrio veliki broj ključnih mutacija, signalnih puteva, proteina, metabolita i drugih molekula koji bi mogli predstavljati potencijalne mete u razvoju ciljane terapije. Stoga, princip multi-omike može doprineti razvoju personalizovane medicine u terapiji malignih oboljenja, uključujući karcinom dojke.

1.2.1. Faktori transkripcije

Transkripcija genetske informacije sa DNK na mRNK je fundamentalni ćelijski proces, odlikovan kompleksnim mehanizmima i međusobnom interakcijom različitih elemenata potrebnih za manifestaciju transkripcije i obezbeđivanje njene striktne kontrole. Enzim koji katališe transkripciju DNK u mRNK je RNK polimeraza II (Pol II) (30). Da bi ispoljila svoju ulogu, neophodno je da Pol II dobije pristup promoterskoj sekvenci gena, koji predstavlja mesto početka transkripcije odgovorno za njenu inicijaciju (31). Pristup promoteru je ograničen hromatinom, tako da angažovanje Pol II zavisi od promene pozicije nukleozoma i otvaranja hromatina, što je različito regulisano kod različitih promotera i uključuje procese kao što su modulacija hromatina, DNK metilacija, demetilacija, acetilacija i deacetilacija, kao i regulacija posredstvom transkripcionih faktora (19).

Humani genom kodira više od 1600 faktora transkripcije (TFs), čija je funkcija često specifična za ćelijsku vrstu kako bi se osigurala pravilna ekspresija gena na tkivno specifičan način (19). TF su proteini koji interaguju sa *cis*-regulatornim elementima pozicioniranim u 5' regionu promotera uzvodno od gena koje regulišu (32). Promoteri su DNK regioni prisno lokalizovani uz protein-kodirajući region gena, čiju transkripciju regulišu u interakciji sa ostalim elementima regulatornog aparata. Pored vezivanja za promotere gena, transkripcioni faktori mogu regulisati transkripciju i vezivanjem za enhanser region DNK. Dok se sekvenca gen enhansera može naći vrlo udaljena, milion parova baza ili više od njegove sekvence gena u linearnom smislu, ona je prostorno bliska genu zahvaljujući visoko umotanoj i dinamički organizovanoj strukturi DNK (30). Enhanseri sadrže sekvence za vezivanje TF i učestvuju u transkripciji bez direktnog kontakta sa regionom promotera. Osim *trans*-domena potrebnog za vezivanje DNK, TF poseduju domen koji može interagovati sa različitim ko-regulatornim proteinima (CoR), koji stimulišu ili umanjuju njihovu aktivnost (33). Ko-regulatori ne moraju nužno imati afinitet vezanja za DNK, već utiču na stabilnost ili aktivnost DNK-vezanog TF, i tako sadejstvuju u koordinisanju transkripcije (Slika 4). Formiranje kompleksa između koaktivatora i TF dovodi do regrutovanja drugih generalnih faktora transkripcije ili omogućava ispoljavanje ostalih funkcija koaktivatora: određeni ko-regulatori dovode do konformacione promene TF-a, što mu može omogućiti vezivanje za svoju ciljnu sekvencu u promoteru ili enhanseru, dok se brojne poznate funkcije CoR manifestuju direktnom

histonskom aciltransferaznom aktivnošću i remodelovanjem hromatina (34). Vezivanjem za promoter, TF mogu dovesti do lokalnog otvaranja hromatina regrutovanjem kompleksa za modeliranje hromatina i histon acetiltransferaza. Dodatno, otvaranje hromatina nije dovoljan uslov da se Pol II veže na DNK, jer sama polimeraza ne može prepoznati promotersku sekvencu. Umesto toga, vezivanje Pol II za DNK zavisi od TF koji formira most između promotera i polimeraze, i time inicira ili umanjuju regrutovanje Pol II za specifični gen (30,35). Pored klasičnih faktora transkripcije, generalni faktori transkripcije (GTF) regulišu transkripciju vezivanjem za konsenzus sekvencu gena koja se obično nalazi 25-35 baznih parova uzvodno od mesta početka transkripcije velikog broja gena, kao što je TATA region, i samim time generalno regulišu transkripciju većeg broja gena na nespecifičan način (36).

Uzimajući u obzir značaj u regulaciji transkripcije gena i na taj način definisanje osnovnih ćelijskih procesa, logično je pretpostaviti da je poremećaj aktivnosti TF česta pojava u onkogenim procesima (35). Disregulacija aktivnosti TF-a može kako inicirati tako i promovisati manifestaciju malignog fenotipa. Do promene u aktivnosti TF može doći usled mutacija gena koji ih kodira, uz primere mutacija *TP53* (uglavnom supstitucijom jednog nukleotida, SNP; što rezultuje gubitkom funkcije) (37) i *MYC* gena (uglavnom amplifikacijom ili translokacijom) (38), koji su mutirani u različitim malignim bolestima (37). Međutim, disregulacija TF-a se češće manifestuje neadekvatnom aktivacijom, signalizacijom ili posttranslacionom modifikacijom nemutiranog TF (39). Takav poremećaj može biti posledica mutacije na DNA sekvenci za koju se vezuje ili u proteinu odgovornom za njegovu aktivaciju, kao što su kinaze. Fokus ove disertacije je na signalizaciji i terapijskoj upotrebi dostupnih znanja o prenosiocu signala i aktivatoru transkripcije (engl. *signal transductor and activator of transcription*, STAT) 3, čija je abnormalna aktivacija česta pojava i inicijator različitih maligniteta, uključujući većinu karcinoma dojke.

1.3. *Prenosilac signala i aktivator transkripcije 3*

STAT3 je jedan od 7 pripadnika STAT porodice trankripcionih faktora, nazvanih STAT1 do STAT6, uključujući strukturno i funkcionalno slične STAT5A i STAT5B (40). Humani *STAT3* gen je DNK regija od 75.245 parova baza koja se nalazi na hromozomu 17q21.2 sačinjena od 24 egzona i 23 introna. Eksprimiran je ubikvitarno u većini ljudskih tkiva, kao jedna od četiri do sad identifikovane izoforme, STAT3α (92kDa), STAT3β (83kDa), STAT3γ (72kDa) i STAT3δ (64kDa), koji nastaju kao rezultat alternativnog splajsinga (STAT3β) ili proteolitičke obrade (STAT3γ i δ). STAT3α je protein pune dužine i glavna izoforma humanog STAT3 proteina koji se sastoji od 770 aminokiselina (55). Preostale tri izoforme karakteriše nedostatak C-terminus domena usled kojeg su nefunkcionalni i smatraju se dominantno negativnim izoformama (56,57).

1.3.1. STAT3 signalni put

STAT3 signalizacija je stimulisana od strane citokina iz porodice interleukina (IL), uključujući IL-6, IL-10, IL-23, IL-21, IL-11, onkostatin M (OSM), inhibitorni faktor leukemije (LIF), kao i faktora rasta kao što je epidermalni faktor rasta (EGF), trombocitni faktor rasta (PDGF) i drugi (41,50). Vezivanjem za odgovarajući membranski receptor dolazi do oligomerizacije receptora, što dovodi membranski vezane kinaze u neposrednu blizinu kako bi se inicirala njihova transfosforilacija. Porodica takvih kinaza koje dalje fosforilišu STAT su Janus kinaze (JAK), sa JAK2 kao glavnom kinazom STAT3 (58). Jak kinaze zatim fosforilišu intraćelijski domen receptora, formirajući mesto za vezivanje citoplazmatskog STAT3. JAK zatim fosforiliše regrutovani STAT3 na tirozinskoj rezidui 705 (Y705). Pored membranskih receptor kinaza, ne-receptorske citoplazmatske kinaze koje signaliziraju kroz STAT uključuju Abelson leukemija protein (ABL) i Src-kinaze, koje su često prekomerno aktivne u određenim malignitetima kao što je hronična mijeloidna leukemija (CML) (41,59). Fosforilacija STAT3 dalje podstiče formiranje dimera, što pospešuje njegovu translokaciju u jedro i vezivanje za konsenzus sekvencu od devet baznih parova TTCN3GAA u promoteru ciljnih gena kako bi regulisao njihovu transkripciju (Slike 6 i 7) (60). Geni čija je transkripcija regulisana posredstvom STAT3 su ključni medijatori ćelijskog ciklusa i uključuju regulatore ćelijskog preživljavanja i supresore apoptoze, kao što su B-ćelijski limfom (*BCL*)-2, *BCL-6*, *BCL-xL*, *MCL-1*, survivin (član porodice inhibitora apoptoze (IAP)); regulatore proliferacije poput *MYC* i ciklina D1; promotere migracije i metastaze, uključujući matriks metaloproteinaze (*MMP*); posrednike angiogeneze, kao što je vaskularni endotelni faktor rasta (*VEGF*) i pro-inflamatorne citokine kao što je *IL-6* (50,54,59).

1.3.2. Poremećaj funkcije STAT3

S obzirom na svoju ulogu u esencijalnim ćelijskim procesima, aktivnost STAT3 je regulisana endogenim inhibitorima, uključujući supresore citokinske signalizacije (*suppressor of cytokine signaling,* SOCS), proteinske tirozin fosfataze (PTPs) i protein inhibitore aktiviranih STAT (*protein inhibitors of activated STAT,* PIAS) (50). Dok je u normalnim ćelijama fosforilacija STAT3 zavisna od stimulusa, brza i tranzitorna, STAT3 je često konstitutivno aktiviran u različitim malignim poremećajima te podstiče proliferaciju, samo-obnavljanje, angiogenezu i rezistenciju na lekove malignih ćelija. Povećana STAT3 aktivacija može biti rezultat mutacije, koje se najčešće javljaju u SH2 domenu (Slika 8). Međutim, mnogo češći su drugi načini konstitutivne fosforilacije STAT3, kao što je prekomerna stimulacija citokinima parakrinih ili autokrinih izvora u mikro-okruženju tumora; hiperaktivacija JAK kinaza usled genetskih, epigenetskih promena ili prekomerne ekspresije; ili smanjenom aktivnošću STAT3 fizioloških inhibitora (50,59). Poremećaj STAT3 signalnog puta je dovoljan faktor da dovede do maligne transformacije i povezan je

sa agresivnim malignim osobinama i lošom prognozom za pacijente (61). Prvenstveno STAT3, ali i STAT5 su konstitutivno aktivirani u velikom broju solidnih i hematoloških malignih oboljenja, uključujući akutnu i hroničnu mijeloidnu leukemiju, različite oblike limfoma, karcinom dojke, jajnika, prostate, maligniteti glave i vrata, pluća i drugi maligniteti (62). Konstitutivna aktivacija STAT3 je često udružena sa prekomernom IL-6 parakrinom ili autokrinom sekrecijom kod velikog broja maligniteta, kao što su mijelom, karcinom prostate, jajnika, dojke, kolorektalni karcinom i skvamozni maligniteti glave i vrata (63-5). Stepen do kojeg STAT3 stimuliše onkogeni potencijal ćelije može da varira između tipova tkiva, što ukazuje da interakcije sa drugim proteinima, kao što su koregulatori transkripcije i drugi faktori transkripcije koji moduliraju potencijal aktivnosti STAT3 (59).

1.3.3. Efekti aktivacije STAT3 na metabolizam lipida malignih ćelija

Solidne tumore često odlikuje nedovoljna vaskularizacija, te su maligne ćelije hipoksične i imaju manje hranljivih resursa u poređenju sa normalnim ćelijama. Kao kompenzacioni mehanizam, ćelije karcinoma karakterišu promene metaboličkih puteva kako bi zadovoljile svoje povećane metaboličke potrebe. Nedavno je prepoznata ključna uloga regulacije metabolizma glukoze, energije i lipida u razvoju i napredovanju maligniteta (94-6). Novija istraživanja ukazuju na uticaj i međuzavisnost između aktivnosti STAT3 i metabolizma lipida, uključujući lipolizu, beta oksidaciju, feroptozu i modeliranje membranskih lipidnih osobina kod različitih tipova maligniteta (106-8). Pored toga, STAT3 signalni put je povezan sa leptinom, hormonom koji reguliše energetski metabolizam suzbijanjem apetita. Pored vezivanja za svoj receptor OBR na plazma membrani, koji može sam vršiti nishodnu signalizaciju putem STAT3 (109), dokazano je da se leptin vezuje za IL-6 receptor glikoprotein 130 (GP130), inicirajući kaskadu signala koji dovode do fosforilacije STAT3 (110,111). Kontinuirana stimulacija ćelija leptinom dovodi do STAT3-posredovane ekspresije SOCS3, glavnog STAT3 endogenog inhibitora i ciljnog gena. Navedeni signalni put može da dovede do ublažavanja leptin-indukovanog prenošenja signala i izazove rezistenciju na leptin (112). Aktivacija STAT3 leptinom ili drugim medijatorima podstiče ekspresiju karnitin palmitoiltransferaze 1B (CPT1B), ključnog enzima za beta oksidaciju masnih kiselina (FAO, *fatty acids oxidation*). Navedena signalizacija je ključna za samoobnavljanje matičnih ćelija karcinoma dojke i podstiče njihovu hemiorezistenciju (108). FAO rezultira proizvodnjom NADH i FADH2 koji mogu umanjiti oksidativni stres u ovim ćelijama i povećati proizvodnju ATP-a u elektron transportnom sistemu (ETC) (113). Drugi proizvod JAK/STAT3-posredovane FAO je acetil-CoA, koji potom ćelija može iskoristiti za sintezu masnih kiselina, proizvodnju energije kroz Krebsov ciklus i acetilaciju proteina, i neophodan je za rast tumora i preživljavanje matičnih ćelija karcinoma dojke (108).

1.3.4. Uloge STAT3 u karcinomu dojke i ciljano delovanje na STAT3 u terapiji maligniteta

Značaj uloge STAT3 u karcinomu dojke pokazuje njegova aberantna aktivacija u 70% svih slučajeva, koja je zabeležena u svakom od molekularnih tipova (119). Konkretno, STAT3 je konstitutivno aktiviran kod svih TNBC, najagresivnijeg tipa maligniteta dojke koji se karakteriše lošom prognozom i visokom stopom recidiva (8). Aberantna aktivacija STAT3 u TNBC je u velikoj meri povezana sa preživljavanjem ćelija, proliferacijom, invazivnošću, metastatskim potencijalom, angiogenezom i supresijom anti-tumorskog imunološkog sistema (120). Aktivacija STAT3 pokreće date onkogene procese kod karcinoma dojke pre svegaregulacijom ekspresije gena uključenih u prethodno navedene osnovne ćelijske procese. Takođe, interakcijom sa drugim onkogenim faktorima poput PI3K/AKT ili PTEN, STAT3 podstiče malignu ćelijsku proliferaciju (123). Nova istraživanja ispituju dizajniranje terapija usmerenih ka onkogenim faktorima transkripcije, pri čemu STAT3 predstavlja metu visokog potencijala iz više razloga (33). U normalnim ćelijama je aktivacija STAT3 privremena usled delovanja endogenih ćelijskih inhibitora STAT3 kao što su PIAS ili SOCS (289). Samim time, normalne ćelije podnose inhibiciju STAT3 i njegova aktivnost nije neophodna za preživljavanje nemalignih ćelija (125). S druge strane, maligne ćelije sa konstitutivnom aktivacijom STAT3 često pokazuju efekat "zavisnosti od onkogena", te inhibicija STAT3 rezultira zaustavljanjem rasta i ćelijskom smrću. S obzirom da normalne ćelije ne pokazuju takvu zavisnost, ovaj fenomen predstavlja osnovu povoljnog terapijskog efekta STAT3 inhibitora (50). Drugi aspekt ciljanog delovanja na STAT3 se odnosi na činjenicu da predstavlja konvergentnu tačku više onkogenih signalnih puteva. U skladu sa time, ciljano delovanje na jedan protein je povoljnije u poređenju sa inhibicijom više kinaza koje deluju ushodno od datog proteina, jer se može sprečiti razvoj rezistencije na lekove povezane sa aktiviranjem kolateralnih signalnih puteva (50,120). Zbog visokog terapijskog indeksa koji proizilazi iz ovih svojstava, brojni pristupi se ispituju u razvoju terapijskih inhibitora STAT3 (125-7). Neki od molekula su dizajnirani za ciljanje ushodnih posrednika STAT3 aktivacije kao što su Janus kinaze. Takav molekul je ruksolitinib (128), koji se trenutno testira u kliničkim ispitivanjima za lečenje kolorektalnog karcinoma, maligniteta pankreasa i dojke, uključujući TNBC (ClinicalTrials.gov; 126,128). Ograničenja inhibitora kinaza se obično odnose na odsustvo pojedinačne kinaze kao glavnog onkogenog pokretača i razvoj rezistencije mutacijom kinaze ili zaobilaženjem inhibiranog signalnog puta kolateralnim signalizacijama (129). Pored toga, inhibitori kinaza često pokazuju nisku selektivnost te zaustavljaju kako patološku tako i fiziološku signalizaciju, sa mogućnošću blokiranja signalizacije interferona koji podstiče imunološko prepoznavanje i eradikaciju tumora. Dodatno, direktna inhibicija STAT3 je komplikovana usled u nastavku navedenih prepreka u dizajniranju efikasnog i klinički primenjivog STAT3 inhibitora (130):

- STAT3 kao i ostali faktori transkripcije ima relativno veliku i ravnu molekularnu površinu pogodnu za interakcije protein-protein i protein-DNK, premda problematičnu za

direktno vezivanje malih molekula usled nedostatka sterno dostupnog mesta vezivanja u blizini područja od interesa, kao što je Y705 rezidua, SH2 ili DNK-vezujući domen.

- Specifičnost i efikasnost razvijanih molekula je ograničena.
- Peptidni inhibitori se mogu dizajnirati tako da poseduju visoku specifičnost i efikasnost, međutim, karakteriše ih ograničena permeabilnost kroz biološke membrane *in vivo*, a intracelularna stabilnost je često suboptimalna usled fiziološke degradacije (131).
- Različiti oligonukleotidi kao što su DNK-mamci predstavljaju interesantan pristup vezivanju aktivnog STAT3 i sprečavanju njegovog DNK vezivanja. Takođe, dominantno-negativni ekspresioni vektori i kratke interferirajuće RNK (siRNK) pružaju efikasnu inhibiciju STAT3 ekspresije i aktivnosti u ćelijskim kulturama, međutim, njihova *in vivo* bioraspoloživost i ćelijsko preuzimanje su često suboptimalni (132,133).

Usled navedenog, postoji povećana potreba za razvojem novih terapijskih strategija koje bi mogle prevazići navedena ograničenja. Nanomedicina predstavlja jednu od obećavajućih strategija koja ima potencijal da savlada niz navedenih poteškoća (134,135). Mogućnost brojnih strukturnih modifikacija može da obezbedi različite povoljne karakteristike nanosistema (Slika 9). Inkorporiranjem molekula u nanočesticu povoljnih farmakokinetskih (PK) svojstava može se prevazići suboptimalna apsorpcija i permeabilnost kroz biološke membrane, kratak poluživot eliminacije i niska bioraspoloživost, niska biodistribucija u tkivu od interesa i nespecifični efekti sa posledičnim toksičnim efektom po zdravo tkivo. Najvažnija karakteristika nanosistema je da se modifikacijom površinskog omotača može definisati i usmeriti interakcija sa ćelijskom membranom, te je sa razvojem nanomedicine započeto sasvim novo područje razvoja ciljane nanoterapije (136).

S obzirom da je ciljano delovanje direktno na STAT3 kompleksno i zahtevno usled prethodno navedenih ograničenja, u okviru ove disertacije smo razmatrali indirektne metode delovanja na STAT3-aktivirane maligne ćelije. Imajući u vidu da maligne ćelije karakterišu metaboličke promene, ispitali smo kako aktivacija STAT3 utiče kvalitativno i kvantitativno na metaboličku strukturu ćelije. Takođe, jedan od glavnih ciljeva ove studije jeste ispitivanje da li takav STAT3-indukovan metabolički profil može predstavljati vulnerabilnost malignih ćelija koja bi se mogla terapijski iskoristiti. U te svrhe, analizirali smo primenu nanosistema sa ciljem identifikacije nanočestice određenog spoljašnjeg sloja koji pokazuje afinitet vezivanja prema ćelijama metaboličkog profila karakterističnog za STAT3-aktivirane ćelije.

1.4. *Nanomedicina*

Nanomedicina predstavlja savremeni oblik farmaceutskih proizvoda namenjenih lečenju i dijagnostici različitih oboljenja, uključujući dijabetes, kardiovaskularne i infektivne bolesti, a poseban značaj ima u onkologiji (134,137). Primena nanoterapije se sveobuhvatno

ispituje u lečenju karcinoma dojke, sa trenutno aktivnih 76 kliničkih studija i znatno većim brojem ispitivanja u pretkliničkoj fazi (ClinicalTrials.gov). Do sada je nekoliko nanolekova dobilo odobrenje američke Agencije za hranu i lekove (FDA), a većina njih je indikovana za primenu u onkologiji. Tri lipozomske formulacije, Doxil®, Abraxane® i MioCet® su odobrene za adjuvantnu terapiju karcinoma dojke (154). Nanomedicina je definisana kao biomedicinska primena materijala sa najmanje jednom dimenzijom veličine 100-200 nm (138). Trenutno se razvijaju različite vrste nanoformi, a lipozomi i nanočestice predstavljaju dve dominantne grupe nanofarmaceutika (17).

Nanonosači imaju mogućnost enkapsulacije različitih lekova i farmakološki aktivnih jedinjenja, pružajući im povoljna farmakokinetska (PK) svojstva. To omogućava *in vivo* administraciju različitih molekula sa izuzetno lošim PK profilom, kao što su siRNK, miRNK, geni i peptidi, čija sistemska primena drugačije nije moguća (139). Ostali lekovi koji imaju primenljiv, ali nedovoljno povoljan PK profil, uključujući različite hemioterapeutike koje karakteriše uska terapijska širina, takođe mogu imati korist od isporuke lekova posredstvom nanosistema. Time nanonosači štite aktivnu supstancu od degradacije u cirkulaciji i omogućavaju njeno kontrolisano oslobađanje, znatno pospešujući stabilnost leka (140). Kao rezultat izbegavaju se vrlo visoke serumske koncentracije terapeutika i produžava se poluživot eliminacije (141). S tim u vezi, maksimalna tolerisana doza mertansina, hemioterapije klinički korišćene u terapiji TNBC, povećava se 8 puta kada se enkapsulira u nanočesticu (142). Pored toga, ugradnja leka u nanonosač pospešuje endo- i transcitozu inače slabo permeabilnih supstanci, obezbeđujući povećanu intracelularnu koncentraciju leka (143,144). Poseban oblik nanoformulacija koje sadrže određene metale dobre provodljivosti i električnih svojstava kao što su zlato, platina i srebro, koriste se za isporuku senzibilizirajućeg sredstva tokom radioterapije ili kao kontrastna sredstva, usled čega mogu poslužiti za poboljšanje efekta radioterapije ili kao dijagnostička i imidžing sredstva (145). Možda najznačajnija osobina nanomedicinskih preparata je da se modifikacijom površinske strukture omogućava usmeravanje nanosistema prema malignim ćelijama na osnovu diferencijalne ekspresije molekula na plazma membrani (Slika 9). Stoga, nanočestice mogu dostaviti hemioterapijske agense prevashodno malignim ćelijama. Kao posledica se postižu veće koncentracije leka u malignom tkivu, dok se isporuka u zdravo tkivo smanjuje, minimizirajući toksičnost citotoksičnih agenasa (10,149,150). U okviru ove disertacije, ispitivali smo mogućnost korišćenja višeslojnih, takozvanih sloj-po-sloj (engl. *Layer-by-Layer,* LbL) nanočestica (engl. *nanoparticle,* NP), kao novog sistema za dostavu lekova.

1.4.1. Višeslojne LbL nanočestice

LbL nanočestice se sastoje od više ultra-tankih slojeva naizmeničnog naelektrisanja (Slika 10). Njihove komponente su podložne velikom broju različitih modifikacija, pružajući

mogućnost prilagođavanja dizajna i prirode i omogućavajući multifunkcionalnost NP. Slojevi LbL čestica mogu biti izgrađeni od sintetskih polijona i prirodnih biomakromolekula sekvencijalnimređanjem naizmenično naelektrisanih polielektrolita na koloidno jezgro (174). Takav naizmenični sklop stvara jonsko umrežen tanki membranski film koji reguliše otpuštanje leka iz jezgra ili središnjih slojeva. Različiti naboji slojeva omogućavaju enkapsulaciju različitih vrsta molekula sa kontrolisanim oslobađanjem, uključujući lekove, peptide, nukleinske kiseline i dijagnostička sredstva (175,176). Enkapsulacija molekula u različite slojeve ovakvog sistema omogućava ugradnju kombinacije agenasa u jednu nanočesticu, čak i u slučaju inkompatibilnosti datih agenasa. Ovakva jedinstvena struktura pruža visok kapacitet pakovanja terapeutika unutar slojeva, sa enkapsulacijom molekula sa udelom od 10-50% od ukupne mase NP, dok drugi slični polimerni nanosistemi uglavnom omogućavaju 1-10% nosivosti enkapsulirane supstance (174,177).

Koloidno jezgro čestica je karboksi modifikovani lateks (*carboxy modified latex*, CML), koji može nositi terapijski agens ili biti fluorescentno obeležen kako bi omogućio detekciju NP. Okolni slojevi, debljine nekoliko desetina nanometara, sačinjeni su od katjonskih poli-L-arginina (PLR), sa polianjonima kao terminalnim slojem. Površinski sloj NP je odgovoran za interakciju NP sa plazma membranom ćelije, što omogućava dizajn LbL NP-a sa ciljajućim osobinama ka ćelijama tumora (164,174). Da bismo istražili mogućnost korišćenja ovih nanosistema za ciljanju dostavu terapije ćelijama karcinoma dojke sa prekomernom STAT3 aktivnošću, ispitali smo biblioteku od 12 LbL NP-a obloženih različitim modifikacijama površinske strukture. Negativni naboj spoljašnjeg sloja izabran je zbog poboljšane biokompatibilnosti i sistemske cirkulacije u poređenju sa katjonskim NP (178). Pozitivno naelektrisani nanosistemi imaju afinitet prema negativno naelektrisanom luminalnom sloju krvnih sudova, bazalnoj membrani bubrega, membrani epitelnih ćelija i eritrocita, što može prouzrokovati nespecifične efekte NP-a, naročito ukoliko su nosači hemioterapijskog agensa (179). Polianjonske elektrostatički stabilizovane NP imaju relativno dug period cirkulacije u krvi, međutim mogu takođe da interreaguju sa komponentama ekstracelularnog matriksa, poput kolagena tipa I. Površinski sloj ispitivanih NP je izgrađen od polianjona koji sadrže sulfatne ili karboksilne funkcionalne grupe sa prethodno poznatim interakcijama ligand-receptor, kao što su natrijum hijaluronat (HA) i heparin-folat konjugat (HF), ili onih bez poznatih interakcija, uključujući poli-L-glutaminsku kiselinu (PLE) i poli-L-asparaginsku kiselinu (PLD) (Slika 11). Prosečni hidrodinamički prečnik svih NP se kreće od 100 do 155 nm, prosečni indeks polidisperziteta od 0,04 do 0,13 i zeta potencijal <-30 mV (164,180). Pored toga, pokazano je da su ovi NP sistemi sposobni da enkapsuliraju i hidrofobne i hidrofilne supstance, pospešujući ćelijsku isporuku i permeabilnost kroz biološke membrane raznih vrsta molekula (174). LbL NP su sačinjene od biorazgradivih materijala i pokazale su povoljan bezbednosni i PK profil u *in vivo* ispitivanjima (164,181).

2. Cilj istraživanja sa naglaskom na rezultate koje se očekuju

2.1. *Osnovni ciljevi studije*

1. Ispitivanje STAT3-modulirane ćelijske lipidne arhitekture korišćenjem masene spektrometrije nakon indukcije ili inhibicije STAT3 u dva različita sistema ćelijske kulture tkiva dojke, uključujući TNBC ćelijsku liniju.

2. Identifikacija optimalne modifikacije NP sa afinitetom ciljanja prema ćelijama sa aberantnom STAT3 aktivnošću skriningom biblioteke LbL nanočestica pomoću fluorescentne mikroskopije.

3. Kvantifikacija vezivanja STAT3-ciljajućih NP za ćelije protočnom citometrijom i validacija u ukupno tri ćelijske linije dojke.

4. Karakterizacija penetracije NP-a u trodimenzionalne organoide ćelija dojke konfokalnom mikroskopijom.

5. Procena mogućnosti translacije *in vitro* nalaza u potencijalnu terapiju ispitivanjem efekata tretmana NP sa inkorporiranim cisplatinom na ćelijsku apoptozu pomoću Aneksin V/DAPI bojenja i protočno-citometrijske analize.

6. Ispitivanje efekta akutne terapije gama zračenjem na ćelijsko vezivanje NP-a.

2.2. *Osnovni rezultati koji se očekuju (hipoteze)*

1. Procenom ukupno 220 metabolita analizom masene spektrometrije u dva ćelijska sistema aktiviranjem ili supresijom STAT3 i upoređivanjem metabolita sa konzistentnim promenama u različitim uslovima i sistemima očekujemo detekciju lipidnih metabolita na čiju metaboličku i enzimsku regulaciju direktno utiče transkripciona aktivnost STAT3.

2. Skrining biblioteke 12 LbL nanočestica koje se razlikuju u površinskom sloju rezultovaće identifikacijom modifikacije NP sa svojstvima ciljanja STAT3, s obzirom da fluorescentna mikroskopija omogućava procenu stepena ćelijskog vezivanja nanočestica u stvarnom vremenu.

3. Protočna citometrija je metoda izbora za preciznu kvantifikaciju nivoa ćelijskog vezivanja NP, te je očekivano da se primenom ove metode egzaktno utvrdi nivo ćelijskog vezivanja NP sa ciljajućim osobinama prema ćelijama sa povećanom aktivacijom STAT3. Validacija ciljne sposobnosti NP postiže se testiranjem tri ćelijske linije tkiva dojke (nemaligne ćelije sa inducibilnim STAT3 konstruktom, TNBC ćelije) i inhibiranjem STAT3 genetski (pomoću malih interferirajućih RNK, engl. *small interfering RNA*, siRNK) i farmakološki (pirimetamin i ruksolitinib).

4. Trodimenzionalni organoidi omogućuju bolje modelovanje malignog fenotipa karcinoma

dojke. Karakterizacija i kvantifikacija penetracije STAT3-ciljanih NP-a u sve tri dimenzije pruža precizniju simulaciju mehanizma preuzimanja NP-a kod solidnih malignih tumora.

5. Na osnovu prethodnih nalaza, očekuje se da će STAT3-ciljajuće NP konjugovane sa cisplatinom izazvati apoptozu u ćelijama sa povećanom aktivnošću STAT3 u većoj meri nego u ćelijama sa smanjenom aktivnošću STAT3.

6. Očekujemo statistički značajno povećano ćelijsko vezivanje STAT3-ciljajućih NP-a nakon akutnog gama zračenja u dozno-zavisnom smislu.

3. Metode, uzorci i mestro istraživanja

3.1. *Materijal i metode*

MCF-10A ćelije su nemaligne ćelije epitela dojke izmenjene genetskim inženjeringom, te stabilno eksprimiraju STAT3C (sa FLAG oktapeptidnim epitopom) pod doksiciklin (DOX) inducibilnim promoterom, čija indukcija je dovoljan faktor da dovede do ispoljavanja tumorigenskih osobina i maligne transformacije MCF-10A ćelija (190). TNBC ćelijske linije korišćene u ovom istraživanju su MDA-MB-231, MDA-MB-468 i SUM159PT, koje karakteriše konstitutivna fosforilacija STAT3 (127). Biblioteku LbL nanočestica dizajnirala je Hamond grupa, Koch Institut za integrativno istraživanje maligniteta, Masačusets Institut za Tehnologiju (MIT), koristeći prethodno objavljene metode (164,180). Nanočestice su fluorescentno obeležene kako bi se omogućila detekcija protočnim citometrom i fluorescentnim mikroskopom.

1. Ispitivanje STAT3-moduliranog ćelijskog metaboličkog profila

Ćelijski lipidni profil nakon indukcije STAT3 u MCF-10A ćelijama i inhibicije STAT3 siRNK-om i pirimetaminom u MDA-MB-468 TNBC ćelijskoj liniji je određen tečnom hromatografijom kuplovanom sa tandemskom masenom spektrometrijom (LC-MS/MS), koristeći interni standard C12 monoalkilglicerol etar (MAGE) za pozitivno i pentadekansku kiselinu (PDA) za negativno naelektrisane lipide.

2. Skrining biblioteke LbL nanočestica u ćelijama sa inducibilnim STAT3 konstruktom (STAT3C) za određivanje modifikacije NP sa ciljajućim osobinama

Biblioteka od 12 LbL nanočestica različitog spoljašnjeg omotača (Tabela 2) je analizirana u MCF-10A ćelijama u vidu fluorescentne mikroskopske analize na CellObserver mikroskopu. LbL strukture površinskog sloja su sadržale karboksilne ili sulfatne funkcionalne grupe. NP karboksi- omotači su bili sledeći: poli-L-asparaginska kiselina (PLD), poli-L-glutaminska kiselina (PLE), poli-L-glutaminska kiselina – blok - poli-etilen glikol (PLE-b-PEG), poliakrilat (PAA) i natrijum hijaluronat (HA), dok su dekstran sulfat (DXS), sulfatni poli (β-ciklodekstrin) (SBC), heparin sulfat folatni konjugat (HF) i fukoidan (Fuc) korišćeni omotači

sa sulfatnom grupom. Takođe smo testirali tri smeše u razmerama 1:1; 1:3 i 3:1 kombinujući omotače hijaluronske kiseline i poli-L-asparaginske kiseline. Nakon tretiranja sa NP, ćelije su skenirane svakih 30 minuta do ukupno 8 sati, koristeći membransko (aglutinin pšeničnih klica) i nuklearno (Hoechst) obeležavanje bojenjem za određivanje vezivanja NP za membranski i jedarni ćelijski kompartman. Nuklearna i membranska NP kolokalizacija su analizirane korišćenjem pripremljenih automatizovanih modela obrade slika pomoću CellProfiler softvera, zarad uniformne detekcije i kvantifikacije NP.

3. Kvantifikacija diferencijalnog ćelijskog vezivanja najpotentnijih ciljajućih nanočestica i kontrolnih neciljajućih NP u MCF-10A ćelijama, i validacija rezultata u TNBC ćelijskim linijama SUM159PT i MDA-MB-231

STAT3C je indukovan u MCF-10A ćelijama koristeći doksiciklin (ili nosač tj. vehikulum kontrolu) pre tretmana NP. U nezavisnom eksperimentu ćelije su tretirane sa jednim od dva farmakološka STAT3 inhibitora (5 μM primetamina (46706, Sigma Aldrich) ili 2.5 μM ruksolitiniba (ab141356, Abcam) tokom 4.5 sata) pre indukcije STAT3C i tretmana nanočesticama. TNBC ćelijske linije SUM159PT i MDA-MB-231 su transfektovane sa dve različite STAT3 siRNK (D-003544-02-0010 i D-003544-03-0010) ili neciljajućom siRNK kontrolom (sc-37007, Santa Cruz). Zatim su ćelije tretirane sa najpotentnijom STAT3-ciljajućom NP-om, za koje smo prethodno ustanovili da su NP obložene poli-L-glutaminskom kiselinom (PLE-NP), neciljajućom NP obloženom dekstran sulfatom (DXS-NP) kao kontrolom, ili sa H_2O kao nosačem tj. vehikulumom, obeležene bojom za detekciju ćelijske smrti (L34975, Life Technologies) i analizirane protočnom citometrijom da bi se utvrdilo ćelijsko vezivanje NP-a u populaciji živih ćelija.

4. Karakterizacija penetracije NP u trodimenzionalne organoide ćelija dojke

Trodimenzionalna kultivacija ćelija je postignuta upotrebom Nanoculture pločica za formiranje organoida (MBL International) uz korišćenje preporučenih protokola. Ćelijski organoidi su tretirani NP i snimljeni konfokalnim mikroskopom.

5. Procena translacionog potencijala ispitivanjem osetljivosti ćelija sa i bez STAT3 ekspresije na ciljajuće NP ispunjene cisplatinom, i neciljajuće NP i slobodni cisplatin kao kontrolu

Za procenu efekata NP-a ispunjenih cisplatinom (CDDP), ćelije su tretirane tako da se postigne indukcija ili inhibicija STAT3 na prethodno opisan način, nakon čega su tretirane nanočesticama ispunjenim cisplatinom i prekrivenim ciljajućim agensom poli-L-glutaminskom kiselinom (CDDP-PLE, Tabela 2). Kao dodatna kontrola, ćelije su tretirane sa cisplatinom ispunjenim nanočesticama obloženim neciljajućim agensom dekstran sulfatom (CDDP-DXS), nanočesticama bez spoljašnjeg sloja (CDDP-CML), kao i slobodnim cisplatinom. Vijabilnost i apoptoza ćelija su se analizirali primenom protočne citometrije obeležavanjem sa aneksin V/DAPI.

6. Ispitivanje uticaja radioterapije na ćelijsko vezivanje NP

Da bismo utvrdili uticaj gama zračenja na ćelijsko vezivanje NP, prvobitno smo odredili odgovarajuću doza radijacije. U navedene svrhe, MCF-10A ćelije sa i bez STAT3C indukcije smo tretirali različitim pojedinačnim dozama zračenja izvora ^{137}Cs, a njihov uticaj na vijabilnost i proliferaciju smo analizirali nakon jednog do tri dana inkubacije merenjem ATP-zavisne bioluminiscencije uz pomoć luminometra. Doza od 6 Gy dovodi do inhibicije ali je nedovoljna da izazove potpuno zaustavljanje ćelijske proliferacije, stoga je postavljena kao najveća doza za eksperimente ispitivanja kombinovane terapije. Ćelije smo tretirali sa nekoliko doza zračenja (najviša doza je određena pilot eksperimentima), a zatim ih inkubirali sa STAT3-ciljajućim NP, odnosno PLE-NP, (ili kontrolnim vehikulumom). Ćelijsko vezivanje je kvantifikovano protočnom citometrijom.

Paralelno sa svim eksperimentima sa nanočesticama, aktivnost i prisustvo ukupnog i fosforiliranog STAT3 smo određivali imunoblot analizama i qRT-PCR (kvantitativnom lančanom reakcijom polimerizacije u stvarnom vremenu, *quantitative real-time polymerase chain reaction*).

3.2. *Način izbora, veličina i konstrukcija uzorka*

Ćelije su kultivisane u humidifikovanom inkubatoru na 37°C sa 5% CO_2 i subkultivisane manje od tri meseca nakon odmrzavanja. Svim ćelijskim linijama je potvrđena autentičnost putem DNK profilisanja kratkih tandem ponovaka i rutinski su testirane na prisustvo mikoplazme pomoću PCR metode. Za maseno spektrometrijske analize lipida koristili smo tri različita pristupa i dva ćelijska sistema za inhibiciju ili aktivaciju STAT3, pri čemu je svaki od eksperimentalnih uslova testiran u pet replika. Značaj metaboličkih promena je posmatran kroz statističku značajnost i konzistentnost metaboličkih promena među testiranim modelima. Za LbL NP skrining evaluirano je 12 NP sa različitim spoljašnjim omotačem, od kojih je svaki testiran u duplikatu. U cilju isključivanja mogućnosti da je povećano vezivanje NP za STAT3-eksprimirajuće ćelije nespecifična posledica maligne transformacije, paralelno sa STAT3-ciljanim NP koristili smo NP obložene ne-ciljajućom modifikacijom i vršili detekciju protočno citometrijskom analizom. Kako bi se osigurala optimalna detekcija STAT3-zavisnog ćelijskog vezivanja NP, koristili smo tri različita ćelijska sistema. U MCF-10A ćelijama STAT3-zavisnost se procenjuje na tri načina: 1. izvođenjem STAT3C indukcije (konstitutivna aktivacija STAT3), 2. Inhibicijom JAK2-posredovane STAT3 fosforilacije i sledstvene aktivacije (ruksolitinib) (128) i 3. inhibicijom transkripcione aktivnosti (pirimetamin) (60). Za testiranje ćelijskih linija TNBC, dve različite pojedinačne sekvence siRNK-e (i neciljajuća siRNK kontrola) smo koristili za ćelijske transfekcije kako bi se isključila mogućnost nespecifičnih siRNK efekata na ćelijsko vezivanje NP. Svaki od eksperimentalnih uslova testiran je u najmanje tri replike, ukoliko nije drugačije naznačeno. Svaki biološki eksperiment je zasebno izveden najmanje dva puta.

4. Rezultati

4.1. *Uticaj aktivacije STAT3 na promene metabolizma lipida u ćelijama karcinoma dojke*

STAT3 je aberantno aktiviran u najvećem broju karcinoma dojke i predstavlja ključni posrednik u patogenezi ove bolesti. S obzirom da je teško postići direktno farmakološko delovanje na STAT3, ispitali smo da li metaboličke promene uzrokovane konstitutivnom aktivacijom STAT3 mogu pružiti priliku za terapijsku intervenciju. Imajući u vidu da je maligna transformacija povezana sa promenama različitih ćelijskih metabolita, ispitali smo kako STAT3 kvalitativno i kvantitativno utiče na distribuciju lipida u epitelnim ćelijama dojke koristeći dva komplementarna sistema (189). Prvo smo koristili netransformisane MCF-10A ćelije nemalignog epitela dojke u kojima se aktivirani oblik STAT3 može eksprimirati indukcijom sa doksiciklinom (DOX) i dovoljan je da izazove tumorigenezu *in vivo* (190). Indukcija promotera povećala je ekspresiju i fosforilaciju proteina STAT3, praćenu pojačanom mRNK ekspresijom STAT3-ciljnih gena uključujući *SOCS3, BCL-3, BCLAF1* i pozitivnom autoregulacijom sopstvene ekspresije (Slika 16). Takođe smo koristili TNBC ćelijsku liniju MDA-MB-468, koju karakteriše konstitutivna STAT3 fosforilacija tirozina, u kojoj smo inhibirali aktivnost STAT3 genetski (koristeći siRNK) ili farmakološki (sa inhibitorom pirimetaminom (PYR)) (191) (Slika 17).

Metodom tečne hromatografije kuplovane sa tandemskom masnom spektrometrijom (LC-MS/MS) ispitali smo profil ukupno 220 lipidnih molekula koje smo klasifikovali u negativno i pozitivno naelektrisane metabolite. Rezultate smo predstavili kao kumulativne podatke svih metabolita značajno izmenjenih sa STAT3 aktivnošću u bilo kom od eksperimentalnih uslova (Tabele 3 i 4). Zatim smo procenili koje od metaboličkih promena su konzistentne između različitih pristupa aktivacije ili inhibicije STAT3 (sumirano na slikama 18 i 19). Kriterijumi za selekciju metabolita u takav sažetak bili su statistički značajne promene metabolita sa minimalno 20% razlike i istom vrstom alteracije u najmanje dva od testiranih uslova. U navedenoj sumaciji rezultata smo predstavili i metabolite koji pripadaju istoj molekulskoj grupi, ukoliko postoji statistički značajna promena u nekom od eksperimentalnih uslova. Podaci o metabolitima koji ne pokazuju statistički značajne alteracije ni u jednom od tri načina modulacije STAT3 nisu prikazani.

Na ovaj način smo pronašli nekoliko klasa lipidnih molekula koji su značajno promenjeni aktivacijom STAT3 (Slike 18 i 19). Četiri različita, ali slična metabolita N-acil-taurina (NAT) snižena su u MDA-MB-468 ćelijama sa aktiviranim STAT3. Slično tome, prisustvo N-arahidonoil taurina (C20: 4 NAT), za koji je pokazano da indukuje apoptozu ćelija karcinoma prostate (192,193), je smanjeno kada je STAT3C indukovan u MCF-10A ćelijama. Druga dva taurinska derivata, N-palmitoil (C16:0) i N-stearoil (C18:0) taurin,

snažno su redukovani kada je STAT3 konstitutivno aktivan u MDA-MB-468 ćelijama, i pokazuju analogni trend sa STAT3C indukcijom. Zanimljivo je da je nekoliko metabolita lipida koji su negativno modulirani STAT3 aktivnošću, uključujući taurin, konjugovano sa arahidonskom kiselinom (AA, C20:4), prekursorom sinteze eikozanoida (Slike 18 i 19). Metaboliti taurina i AA su aktivno uključeni u remodelovanje plazma membrane (194,195), pružajući potencijalnu molekularnu distinkciju ćelija karcinoma čija je maligna transformacija uzrokovana aktiviranim STAT3. Pored toga, ćelijsko prisustvo ispitivanih triacilglicerola i fosfatidilinozitola je sniženo prilikom STAT3 aktivacije u MDA-MB-468 ćelijama, međutim analogija nije primećena u STAT3-inducibilnom sistemu. Za druge metabolite kao što su lizofosfatidilholin etar, monoacilglicerol etar i fosfatidilserin slične korelacije su utvrđene između inhibicije PYR i stimulacijom STAT3, premda pri utišavanju ekspresije STAT3 nije primećen značajan efekat. Značaj ovih promena je potrebno dalje istražiti, posebno sa aspekta ćelijske specifičnosti.

Navedene konzistentne i značajne redukcije AA i taurina mogu biti direktno povezane sa transkripcionim promenama posredovanim aktiviranim STAT3 (koekspresija drugih gena u genomu, takozvana STAT3 genska signatura). Da bismo dalje istražili da li takva korelacija postoji kod pacijenata sa karcinomom dojke, uradili smo analizu obogaćivanja gena (GSEA) korišćenjem podataka RNK mikromatrica od 129 tumorskih uzoraka pacijenata sa primarnim karcinomom dojke (187). Tom prilikom smo uporedili ekspresiju enzima koji su uključeni u metabolizam AA i taurina sa ekspresijom STAT3 genskih signatura. STAT3 genske signature su značajno obogaćene u uzorcima pacijenata sa niskom ekspresijom cistationin gama-liaze (CTH) i cistein dioksigenaze (CDO1), dva enzima potrebna za sintezu taurina iz homocisteina (Slika 20). Da bismo istražili da li aktivnost STAT3 korelira sa metabolizmom AA, testirali smo korelaciju između ekspresije STAT3 genskih signatura i ekspresije enzima koji su uključeni u oslobađanje i metabolizam AA. STAT3 genske signature značajno pozitivno koreliraju sa ekspresijom mRNK AA metaboličkih enzima ciklooksigenaze 2 (COX-2, PTGS2) i 5-lipoksigenaze (5-LOX, ALOX5) (Slika 21). Suprotno tome, fosfolipaza A2 (PLA2G4A) neophodna za oslobađanje AA iz plazma membrane, nije pokazala značajnu korelaciju (Slika 22). Slično, STAT3 signature nisu pokazale značajnu korelaciju sa kontrolnim genom GAPDH u istom skupu podataka pacijenata obolelih od karcinoma dojke (Slika 23). U skladu sa prethodnim nalazima (196-9), ovi podaci ukazuju na intrigantnu korelaciju između STAT3 signalnog puta i pojačane sinteze eikozanoida povezane sa inflamatornim procesima i razvojem maligniteta (200). Činjenica da su i taurinski derivati i AA uključeni u remodelovanje plazma membrane (194,195) predstavlja osnovu za to kako promene u metaboličkoj arhitekturi kao rezultat aberantne STAT3 aktivacije mogu pružiti mogućnost za razvoj ciljanih terapija prema ćelijama tumora. U te svrhe, koristili smo nanočestice čije površinske modifikacije mogu modulirati interaktivnost sa plazma membranom i time omogućiti dizajn NP sa ciljajućim afinitetom prema ćelijama sa povećanom STAT3 aktivnošću.

4.2. *Skrining biblioteke LbL nanočestica za identifikaciju NP sa ciljajućim svojstvima prema STAT3-aktiviranim ćelijama*

Prilikom ispitivanja mogućnosti translacije u terapiju ovih značajnih metaboličkih promena uzrokovanih STAT3 aktivacijom, koristili smo nov oblik nanočestica koje mogu da iskoriste ove ćelijske osobine, takozvane višeslojne LbL nanočestice (164,174). Tom prilikom smo ispitali biblioteku od 12 LbL NP-a koje se razlikuju u svom spoljašnjem omotaču kako bismo odredili površinsku strukturu koja omogućava najbolje vezivanje za ćelije sa STAT3-indukovanim lipidnim profilom u odnosu na nemaligne ćelije (189). Kvantifikacija membranske i nuklearne kolokalizacije svake od ovih čestica prikazana je na slikama 24-35, a membransko vezivanje je prikazano na slici 36.

Otkrili smo da NP obložene poli-L-glutaminskom kiselinom (PLE-NP) pokazuju značajno izraženije membransko vezivanje za STAT3-aktivirane ćelije u poređenju sa netransformisanim kontrolnim MCF-10A ćelijama (Slike 28 i 36). Reprezentativne mikroskopske slike ćelijskog regrutovanja PLE-NP prikazane su na slici 37. Pored toga, čestice obložene PLE-b-PEG u kojima PEG pokriva glutaminsku kiselinu, nisu pokazale sličan efekat, sugerišući značaj terminalnog PLE sloja u ciljajućim sposobnostima NP (Slika 29). Navedene ciljajuće sposobnosti PLE-NP ne predstavljaju nespecifični efekat neoplastične transformacije, s obzirom da LbL NP obložene drugim modifikacijama nisu pokazale razliku u membranskom vezivanju (Slike 24-36). Diferencijalno vezivanje ovih NP je detektovano u membranskom vezivanju, međutim kolokalizacija sa jedrom je minimalna za sve ispitivane NP u oba stanja (Slike 24-35). Pored toga, nanočestice obložene SBC-om pokazale su statistički značajnu razliku u nuklearnoj kolokalizaciji između netransformisanih i STAT3-transformisanih ćelija, međutim sličan efekat nije primećen u membranskom vezivanju (Slika 25). S obzirom da fluorescentnom mikroskopijom detektujemo sve NP čija je fluorescencija kolokalizovana sa fluorescencijom nuklearnog bojenja, moguće je da je navedeno rezultat nespecifičnog vezivanja nanočestica na membrani neposredno iznad jedra, a ne posledica direktnog vezivanja NP za ćelijsko jedro. Uzimajući u obzir i generalno niske nivoe kolokalizacije sa nukleusom, dalje se nismo fokusirali na detekciju mehanizama i procenu datih efekata SBC nanočestica.

U cilju karakterizacije subcelularne distribucije PLE-NP, izvršili smo dekonvolucionu mikroskopiju u MCF-10A ćelijama nakon 2 ili 24 sata inkubacije sa NP obloženim PLE (Slike 38 i 39). Dok su se PLE-NP vezivale u niskom stepenu za ne-transformisane MCF-10A ćelije, indukcija STAT3 dovela je do regrutovanja znatno većeg broja ovih NP. U skladu s prethodnim izveštajem (164), rezultati mikroskopije visoke rezolucije ukazuju na to da se ove nanočestice vezuju i potencijalno integrišu u plazma membranu (Slike 38 i 39), dodatno odražavajući značaj ćelijskog lipidnog sastava u njihovoj specifičnosti ciljanog ćelijskog vezivanja. Iako nisu nužno internalizovane u citoplazmu, NP obložene sa PLE zadržavaju sposobnost preferencijalne akumulacije u tumorskom tkivu *in*

vitro i *in vivo* (164,201,202). Stoga smo dalje ispitivali STAT3-zavisnost svojstava ciljanja tumora LbL nanočesticama obloženim poli-L-glutaminskom kiselinom, i potencijal njihove upotrebe u lečenju karcinoma dojke.

4.3. *Kvantifikacija STAT3-zavisnog ćelijskog vezanja PLE-NP*

U cilju kvantifikacije diferencijalnog ćelijskog vezivanja PLE-NP u ćelijama karcinoma dojke, prvo smo koristili MCF-10A ćelije sa inducibilnim STAT3 promoterom. Koristeći kvantitativnu protočnu citometriju, otkrili smo da se PLE-NP preferencijalno vezuju za ćelije sa aktiviranim STAT3, pokazujući 50% viši stepen fluorescencije ćelijski vezanih NP u poređenju sa njihovom netransformisanom ćelijskom kontrolom (Slika 40). Da bismo nezavisno procenili da li su ove razlike zavisne od STAT3 konstitutivne aktivacije, inhibirali smo STAT3 fosforilaciju i sledstvenu aktivaciju inhibitorom JAK kinaze ruksolitinibom (RUX) ili transkripcionu aktivnost STAT3 sa pirimetaminom (Slika 41). Oba tretmana dovela su do 50% smanjenja fluorescencije ćelijski vezanih NP-a.

Budući da je STAT3 konstitutivno aktiviran u većini TNBC ćelija, ispitali smo mogućnost korišćenja PLE-NP kao STAT3-ciljajućeg pristupa ovom tipu karcinoma dojke. Koristili smo TNBC ćelijske linije SUM159PT i MDA-MB-231 ćelije s obzirom da obe pokazuju konstitutivnu fosforilaciju tirozinske rezidue STAT3 (Slika 44). Pored navedenog, dugoročni opstanak ovih ćelija je zavisan od STAT3, što potvrđuje činjenica da nije bilo moguće izvesti $STAT3^{-/-}$ klonove datih linija primenom metode promene sekvence gena delovanjem Cas9 enzima na grupisane kratke palindromske ponovke na jednakim rastojanjima (engl. *clustered regularly interspaced short palindromic repeats/CRISPR-associated protein 9,* CRISPR/Cas9). Iz tog razloga, prilikom ispitivanja STAT3-zavisnih efekata koristili smo siRNK utišavanje ekspresije STAT3. Otkrili smo da TNBC ćelijske linije MDA-MB-231 i SUM159PT pokazuju visok stepen vezivanja PLE-NP, koji se značajno redukuje utišavanjem STAT3 ekspresije korišćenjem dve različite siRNK. Navedeni mehanizam je specifičan za PLE-NP, s obzirom da nanočestice obložene DXS-om ili ne pokazuju razliku u vezivanju ili se povećano vezuju za ćelije kojima nedostaje aktivirani STAT3 (Slike 45 i 46).

Dodatno, kako bismo ispitali bezbednost ovih nanočestica i isključili mogućnost njihovog toksičnog efekta, evaluirali smo vijabilnost ćelija nakon 24-časovnog tretmana sa 100 ng/ml PLE-NP i DXS-NP, i uporedili ih sa vijabilnošću ćelija tretiranih sa istim volumenom H_2O kao kontrolnim vehikulumom. Obe nanočestice su pokazale slične efekte po vijabilnost sa vehikulum kontrolom u svim ispitivanim ćelijskim linijama, i nisu dovele do razlike u procentu vijabilnih ćelija (Slike 42,43 i 48).

4.4. *Karakterizacija sposobnosti penetracije PLE-NP u trodiomenzionalne organoide ćelija dojke*

U cilju boljeg uvida u ponašanje ispitivanih nanosistema u solidnim tumorima, ispitali smo akumulaciju PLE-NP u trodimenzionalnim organoidima MCF-10A ćelija, koji približnije simuliraju arhitekturu tumora *in vivo* (203,204). Aktivacija STAT3 je znatno podstakla ćelijski rast i proliferaciju, rezultujući formiranjem znatno većeg broja masivnih kolonija (Slika 49). STAT3-transformisani organoidi su takođe rasli u strukturama primetno veće gustine (Slika 50), što je dalje rezultovalo izraženijim stepenom hipoksije unutar organoida (Slika 51). Dati nalazi potvrđuju potencijal aktiviranja STAT3 i njegovu sposobnost da indukuje malignu transformaciju ćelije kao izolovani onkogeni pokretač. Kako ostale ćelijske linije od interesa poput TNBC ćelijskih linija, nisu mogle da formiraju trodimenzionalne strukture primenom korišćene metode, dodatno smo istražili penetraciju PLE-NP u organoide MCF-10A ćelija. Da bismo odredili akumulaciju i distribuciju PLE-NP kroz strukturu organoida, kvantifikovali smo NP fluorescenciju kroz sve tri dimenzije i uporedili srednju fluorescenciju NP po organoidu (Slika 51). Imajući u vidu da voluminozniji organoidi imaju veću površinu u direktnom kontaktu sa medijumom koji sadrži NP-e, takođe smo analizirali srednju NP fluorescenciju po jedinici zapremine organoida. Uprkos značajno većoj ćelijskoj gustini STAT3-transformisanih organoida, za koju se moglo očekivati da oteža penetraciju NP, ovi organoidi su pokazali veću kvantitativnu fluorescenciju NP po organoidu (za 40%) kao i po zapremini organoida (za 73%) (Slika 51). Stoga, čak i u čvrsto sabijenim trodimenzionalnim organoidima, PLE-NP pokazuju preferencijalnu penetraciju i intra-organoidnu akumulaciju u prisustvu aktiviranog STAT3.

4.5. *Evaluacija terapijske primene PLE-NP*

Kako bismo procenili potencijalnu translaciju laboratorijskih rezultata u kliničku primenu, testirali smo efekat PLE-NP sa enkapsuliranim citotoksičnom agensom cisplatinom (CDDP), kako se agensi na bazi platine klinički koriste u terapiji TNBC (205,206). Indukcija STAT3 učinila je MCF-10A ćelije osetljivim na CDDP dostavljen pomoću PLE-NP (CDDP-PLE) i značajno povećala procenat ćelijske smrti, dok su MCF-10A ćelije bez aktiviranog STAT3 pokazale statistički bolje preživljavanje nakon takvog tretmana (Slike 55 i 56). Slično tome, TNBC ćelijska linija SUM159PT pokazala je veću apoptotsku osetljivost na CDDP isporučen putem PLE-NP, a taj efekat je ublažen kada se STAT3 ekspresija inhibirala primenom siRNK-e (Slika 55). Ovo ne odražava generalnu osetljivost ćelija sa aktiviranim STAT3, pošto je u datim ćelijama indukcija ćelijske smrti primenom slobodnog CDDP bila niža u poređenju sa ćelijama bez aktiviranog STAT3 (Slika 57). Slično tome, CDDP-NP koje nisu obložene LbL slojem ili terminalno sadrže nespecifični agens DXS, uzrokovale su

slabiji citotoksični efekat na ćelije sa aktiviranim STAT3 (Slike 58 i 59). Ovi podaci ukazuju na to da bi PLE-NP sa enkapsuliranim citotoksičnim lekovima mogle biti efikasna ciljana terapija karcinoma dojke koji ispoljavaju povećanu aktivnost STAT3, uključujući TNBC, uz smanjivanje toksičnih efekata na normalne ćelije usled niske i prolazne aktivacije STAT3.

4.6. *Ispitivanje uticaja gama zračenja na ćelijsko vezivanje PLE-NP*

Gama zračenje predstavlja značajan vid terapije maligniteta dojke, uključujući TNBC, a poznato je da menja svojstva plazmalne membrane (200). Stoga smo testirali da li radijacija može uticati na ćelijsku interakciju PLE-NP na STAT3-zavisan način (189). Da bismo isključili efekte prekomerne ćelijske smrti, prvo smo procenili efekat različitih doza radijacije na vijabilnost STAT3-transformisanih i netransformisanih MCF-10A ćelija (Slika 62). Otkrili smo da su doze niže od 6 Gy efikasne u izbegavanju potpunog zaustavljanja proliferacije. Zatim smo procenili uticaj i doznu zavisnost akutnog gama zračenja na ćelijsko vezivanje PLE-NP (Slika 63). Gama zračenje je dovelo do smanjenja ćelijskog vezivanja PLE-NP za netransformisane MCF-10A ćelije u dozno zavisnom smislu. Međutim, uticaj na PLE-NP vezivanje za STAT3-transformisane MCF-10A ćelije je bio minimalan. Shodno tome, diferencijalna PLE-NP fluorescencija između netransformisanih i STAT3-transformisanih ćelija povećala se sa oko 40% na 80% nakon zračenja u dozi od 5 Gy (Slika 63). Ovi nalazi ukazuju na potencijalni sinergistički efekat između gamma zračenja i ciljane terapije malignih ćelija dojke na bazi nanočestica obloženih PLE.

5. Diskusija

Endogeni lipidi su uključeni u ćelijske procese rasta, proliferacije, diferencijacije, inflamacije, autofagije, apoptoze, te je poznato da je maligna transformacija praćena različitim promenama lipidnog metabolizma, koje su opisane u brojnim tipovima maligniteta, uključujući karcinom dojke (94). Dosadašnja istraživanja su prepoznala konekciju između STAT3 aktivnosti i lipidnog metabolizma, uključujući sintezu masnih kiselina, lipolizu, beta oksidaciju i remodelovanje membranskih lipida (106-8,227). Premda takve lipidne alteracije mogu predstavljati osnovu promena u morfologiji, motilitetu i invazivnosti STAT3-transformisanih ćelija, sveobuhvatna procena lipidnih metabolita moduliranih aktiviranim STAT3 nije bila dostupna. Interesantno je da se u malignim ćelijama često primećuje povećan stepen kako sinteze masnih kiselina (zahvajujući enzimu sintazi masnih kiselina, FAS), tako i njihove beta oksidacije (FAO) (108). Prethodno je pokazano da STAT3 aktivnost korelira sa *FASN* genskom ekspresijom (221), uključujući rezultate studije koje je dokazala da je *FASN* ciljni gen STAT3 transkripcione aktivnosti

(222). Sa druge strane, katabolizam masnih kiselina kroz FAO stimuliše rast tumora kroz obezbeđivanje dovoljnih količina ATP-a radi podržavanja povećanih energetskih potreba u uslovima metaboličkog stresa (225). JAK/STAT3 signalizacija indukuje ekspresiju karnitin palmitoiltransferaze 1B (CPT1B), ključnog enzima u beta oksidaciji. Imajući u vidu značaj FAO u proliferaciji i razvoju hemiorezistencije matičnih ćelija karcinoma dojke, inhibicija navedenog puta zaustavlja aberantni rast ovih ćelija i dovodi do ponovnog uspostavljanja osetljivosti na hemioterapiju (108,226). Koristeći sveobuhvatnu i objektivnu strategiju ispitivanjem komplementarnih modela karcinoma dojke, identifikovali smo nekoliko metabolita koji su modulirani aktiviranim STAT3. U okviru date analize, nisu zabeležene statistički značajne i konzistentne alteracije celularnog nivoa slobodnih masnih kiselina nakon aktivacije STAT3. Međutim STAT3 aktivacija je dovela do redukcije triacilglicerola koji sadrže palmitinsku, stearinsku i arahidonsku kiselinu (Tabele 3 i 4 i slike 18 i 19). Navedeni nalazi mogu ukazati na to da STAT3 podstiče katabolizam masnih kiselina kroz beta oksidaciju. Pored triacilglicerola, identifikovali smo nekoliko metabolita koji su modulirani aktiviranim STAT3, uključujući značajnu redukciju ćelijskih derivata N-acil taurina i AA. Korišćenjem bioinformatičkih procedura, utvrdili smo da se navedena korelacija javlja i u tumorima pacijenata obolelih od maligniteta dojke. Ovakvom analizom, ustanovili smo da je STAT3 aktivnost, predstavljena ekspresijom STAT3 genske signature, visoko obogaćena u uzorcima onih pacijenata koji pokazuju visoku mRNK ekspresiju enzima COX-2 i 5-LOX, ključnih enzima u sintezi eikozanoida poreklom od AA, kao i u uzorcima pacijenata koji imaju vrlo nisku ekspresiju enzima koji vrše sintezu taurina, CDO1 i CTH. Na osnovu datih rezultata, moguće je ustanoviti da STAT3 reguliše ćelijski nivo AA i taurina transkripcionim delovanjem na enzime koji ih metabolišu. Pored toga, dva derivata sfingomijelina, za koji je poznato da dovodi do invazivnog fenotipa malignih ćelija dojke (228), su značajno povećana u ćelijama sa aktiviranim STAT3. Otkrili smo i STAT3 regulaciju drugih metabolita, kao što su monoacilgliceroli i fosfatidilserin; međutim, ovakva korelacija je primećena samo kod jednog predstavnika date klase metabolita. Iako je moguće da su navedene promene značajne, postoji mogućnost da su specifične za ispitivani tip ćelijske linije.

Taurin ima ulogu u različitim ćelijskim procesima ispoljavajući antioksidativno i antiinflamatorno dejstvo, uz stabilizirajući efekat na plazmalnu membranu i uticaj na regulaciju jonskog transporta, naročito Ca^{2+}(229). Takođe, tumor supresorna aktivnost taurina, i posebno N-acil taurina, je pokazana kod više vrsta maligniteta, uključujući karcinom dojke (192,193,230,231). Prethodno je opisana inhibicija fosforilacije STAT3 posredstvom taurina (235,236), dok sa druge strane naša studija ukazuje na to da aktivirani STAT3 može smanjiti biosintezu taurina kroz transkripcionu regulaciju CTH i CDO1 enzima. Taurin svoju funkciju na stabilizaciju ćelijske membrane može ispoljiti indirektno, kao antioksidans koji sprečava produkciju ROS u mitohondrijama i neutralizacijom HOCl kao prekursora slobodnih radikala (232). Takođe, taurin se direktno vezuje za amino i fosfatne grupe ćelijske membrane i na taj način dovodi do njene stabilizacije (194).

Naše istraživanje takođe ukazuje na negativnu korelaciju između aktivnosti STAT3 i ćelijskog nivoa arahidonske kiseline, krucijalnog medijatora inflamacije. Arahidonska kiselina predstavlja direktan prekursor sinteze eikozanoida, tj. prostaglandina, leukotriena i tromboksana, kao i drugih neklasičnih eikozanoida kao što su epoksieikozatetraenoična kiselina i endokanabinoidi, kao bioaktivnih lipidnih medijatora inflamatornog odgovora (200). AA se oslobađa iz membrane posredstvom fosfolipaze A2, za koju nismo ustanovili direktnu korelaciju sa STAT3 aktivnošću. Sa druge strane, dalji metabolizam uključuje enzimsku aktivnost ciklooksigenaze 2 i 5-lipooksigenaze, čija mRNK ekspresija pokazuje pozitivnu, statistički značajnu korelaciju sa STAT3 aktivnosti u uzorcima tumora pacijenata obolelih od karcinoma dojke. Prekomerna ekspresija COX-2 promoviše procese inicijacije tumorigeneze, progresiju, angiogenezu, migraciju i metastaziranje i dokazano je da podstiče prolazak tumorske ćelije kroz hematoencefalnu barijeru i formiranje metastaza karcinoma dojke u mozgu (238,239,290). Onkogeni potencijal COX-2 se učestalo povezuje sa njegovim produktom E serije prostaglandina, PGE2, uključenom u većini prethodno opisanih malignih procesa (200,240). U skladu sa time, prekomerna ekspresija COX-2 je primećena kod čak 40% pacijenata sa karcinomom dojke, a selektivna COX-2 inhibicija dovodi do snažnog anti-tumorskog efekta u *in vivo* modelima maligniteta dojke (241,242). Kad je u pitanju međusobna interakcija STAT3 i COX-2, prethodna istraživanja su pokazala uzajamnu relaciju između njihovih aktivnosti, te neka od istraživanja pokazuju inhibiciju fosforilacije STAT3 inhibicijom COX-2 aktivnosti (197,199), dok druga indikuju da STAT3 pozitivno reguliše ekspresiju COX-2 (196), što se zaustavlja JAK2-posredovanom STAT3 inhibicijom. U skladu sa datim istraživanjima i rezultatima naše analize, može se doći do zaključka da STAT3 reguliše ekspresiju COX-2 transkripcionom aktivnošću. Slično COX-2, obilje dokaza govori u prilog onkogenom potencijalu 5-LOX u različitim oblicima maligniteta, uključujući karcinom dojke (250,252-5). Značaj 5-LOX u ovom oboljenju se ogleda činjenicom da pacijenti oboleli od karcinoma dojke pokazuju 50% povišene serumske nivoe ovog proinflamatornog medijatora (252). Dato zapažanje je bilo nezavisno od molekularnog tipa, veličine tumora, stadijuma i menopauzalnog statusa, te ukazuje da bi se 5-LOX serumski nivo potencijalno mogao koristiti kao rani neinvazivni biomarker ovog oboljenja. Iako je povezanost STAT3 signalog puta sa metabolizmom arahidonske kiseline okarakterisana u literaturi, ne postoji dovoljno podataka o direktnoj interakciji STAT3 i 5-LOX. Jedna studija je ukazala na to da 5-LOX aktivira STAT3 transkripcionu aktivnost (198), dok rezultati našeg istraživanja ukazuju na suprotnu interkonekciju i delovanje STAT3 na 5-LOX ekspresiju. Činjenica da su i taurinski derivati i AA uključeni u remodelovanje plazma membrane (194,195) daje osnovu za to kako promene u metaboličkoj arhitekturi kao rezultat aberantne STAT3 aktivacije mogu omogućiti razvoj ciljanih terapija prema ćelijama sa aktiviranim STAT3, uz upotrebu modernih sistema nosača lekova kao što su LbL nanočestice.

S obzirom na značaj STAT3 signalizacije u patogenezi karcinoma dojke i drugih tumora i visok potencijalni terapeutski indeks blokiranja STAT3 transkripcione funkcije,

preduzete su brojne strategije za identifikaciju inhibitora ovog proteina (120,257,258). Neke od nepristrasnih strategija za identifikaciju takvog inhibitora uključuju skrining velikog broja molekula. Na primer, primenom bioinformatičkog skrininga zasnovanog na STAT3 genskoj signaturi došlo je do identifikacije atovakona, antimikrobnog leka odobrenog od strane FDA, koji inhibira fosforilaciju STAT3 putem glikoproteina 130 (GP130), ćelijskog receptora za IL-6 (259). Eksperimentalno testiranje biblioteka molekula zasnovanih na inhibiciji ekspresije STAT3-ciljnih gena doveli su do otkrića nifuroksazida i pirimetamina kao moćnih inhibitora transkripcione aktivnosti STAT3 (191,260). Data otkrića su dovela do trenutno aktuelnih kliničkih ispitivanja pirimetamina i atovakona u lečenju hematoloških maligniteta i karcinoma pluća. Pored toga, ciljane strategije inhibicije STAT3 uključuju razvoj antisens oligonukleotida i molekula dizajniranih da se vežu za specifične funkcionalne regije STAT3, uključujući SH2 i DNK-vezujući domen (131,264). Navedene strategije se relativno sporo razvijaju, te ostaje da se pokaže u budućnosti da li će ovi principi prerasti u klinički korisna sredstva za selektivnu inhibiciju STAT3 (59). Iako mnogi od navedenih pristupa imaju potencijal buduće primene, naše ispitivanje je prva studija prema našim saznanjima koja istražuje primenu ciljane terapije na osnovu STAT3-moduliranih lipidnih osobina maligne ćelije.

Skriningom biblioteke LbL nanočestica utvrdili smo da se anjonske nanočestice obložene poli-L-glutaminskom kiselinom kao terminalnim slojem preferencijalno vezuju za ćelije sa konstitutivnom STAT3 aktivacijom, uključujući TNBC ćelijske linije (Slike 37-41,45,46). Ovakvo svojstvo je bilo jedinstveno za PLE-NP, jer NP sa drugim površinskim slojevima nisu pokazale sličan efekat (Slike 24-36). Pored toga, inhibicija mRNK ekspresije, fosforilacije ili transkripcione aktivnosti STAT3 je značajno umanjila ćelijsko vezivanje PLE-NP, ukazujući na specifičnost ciljanog delovanja ovih nanosistema na ćelije sa aktiviranim STAT3 (Slike 41,45,46). Tumor-ciljajuća svojstva PLE-obloženih nanočestica su prethodno opisana u modelu karcinoma jajnika, mada biološki mehanizam ovog efekta nije bio razjašnjen (164). Kako je STAT3 često aberantno aktiviran kod maligniteta ovarijuma, naše istraživanje pruža verodostojan uzrok datog fenomena. Pored toga, rezultati mikroskopije visoke rezolucije indikuju da se PLE-NP vezuju i potencijalno integrišu u plazma membranu (Slike 38 i 39, 164), dodatno ukazujući na značaj lipidnog sastava ćelije u njihovoj specifičnosti ćelijske interakcije. Iako nisu nužno internalizovane u citosol, PLE-NP zadržavaju sposobnost preferencijalne akumulacije u tumorskom tkivu u *in vitro* i *in vivo* uslovima (164,201,202). U saglasnosti sa prethodno navedenim publikovanim rezultatima, naši eksperimenti u trodimenzionalnim organoidima ćelija dojke dokazali su visoku penetrantnost PLE-obloženih nanošestica. Dodatno, STAT3-transformisani organoidi su pokazali visok stepen proliferacije i ćelijskog rasta, rezultujući hipoksičnim strukturama visoke gustine. Uprkos tome, PLE-NP su ispoljile svoj afinitet ka STAT3-transformisanim ćelijama čak i u uslovima otežanog proslaska kroz ove masivne ćelijske strukture. Dodatno, u skladu sa prethodnim nalazima (201,202), otkrili smo da PLE-NP mogu da preferencijalno isporuče terapijske agense malignim ćelijama na efikasniji i specifičniji način u poređenju sa

primenom slobodnog leka (Slika 55).

Terapijska relevantnost ovog nalaza se ogleda u snažnom citotoksičnom efektu cisplatina (CDDP) dostavljenog putem PLE-NP ćelijama sa aktiviranim STAT3 (Slika 55). Suprotno tome, ćelije kojima nedostaje konstitutivna STAT3 aktivacija pokazuju bolje preživljavanje nakon ovog tretmana, što ukazuje na povoljan terapijski indeks. Pored toga, konstitutivna STAT3 signalizacija dovodi do agresivnog malignog fenotipa i razvoja rezistencije na hemioterapiju u različitim malignim oboljenjima kroz pojačanu ekspresiju gena za ćelijsko preživljavanje i gena zaduženih za efluks lekova iz ćelije (273-80). Shodno tome, ćelije karcinoma dojke sa aktiviranim STAT3 pokazuju veću apoptotsku otpornost na slobodni CDDP i CDDP dostavljen nanočesticama bez ciljajućeg svojstva. Dati rezultati dodatno naglašavaju značaj specifičnog citotoksičnog efekta CDDP isporučenog posredstvom PLE-NP, koje su verovatno u mogućnosti da dostave veću koncentraciju hemioterapeutika, i samim time spreče nastanak hemio-rezistencije. Pored toga, LbL NP sistemi su dizajnirani da budu biokompatibilni i imaju visoku stabilnost aplikovani *in vivo*, uključujući povoljan farmakokinetski profil (181). Afinitet PLE-NP prema ćelijama tumora sa aktiviranim STAT3 može dodatno minimizirati njihove nespecifične efekte i pospešiti translacioni i klinički razvoj.

Radioterapija je značajna komponenta u lečenju pacijenata sa malignitetom dojke (8,124). Gama zračenje ispoljava svoju aktivnost tako što indukuje produkciju ROS, koji dalje interaguju sa endogenim molekulima kao što su DNK i lipidi, te dovodi do oštećenja DNK i lipidne peroksidacije, što rezultuje ćelijskom smrti (283). Shodno tome, u našem eksperimentu je došlo do zaustavljanja ćelijske profileracije nakon akutnog gama zračenja u dozno zavisnom smislu (Slika 62). Ćelije koje prežive radijaciju trpe promene metabolizma lipida i plazma membrane uzrokovane lipidnom peroksidacijom, uzrokujući značajne promene u ćelijskoj membrani (286). Takođe dolazi do indukcije pro-inflamatornih enzima, uključujući oslobađanje AA putem fosfolipaze A2, kao i njen metabolizam posredstvom COX-2 i 5-LOX (200). Prilikom ispitivanja efekta zračenja na ćelijsko vezivanje PLE-NP, otkrili smo da akutna radioterapija dovodi do smanjenog vezivanja nanočestica za netransformisane ćelije, dok minimalno utiče na vezivanje za STAT3-transformisane ćelije (Slika 63). Jedna hipoteza za objašnjenje datog zapažanja je mogućnost da su lipidne promene u STAT3-aktiviranim ćelijama stabilnije od onih u netransformisanim ćelijama. Kao rezultat, diferencijalno vezivanje nanočestica između STAT3-indukovanih i ne-transformisanih ćelija se povećava dva puta nakon akutne radioterapije u dozi od 5 Gy. Navedeni rezultati predstavljaju indikaciju da bi kombinacija isporuke lekova putema PLE-NP i radioterapije mogla dovesti do poboljšanja terapijskog indeksa u lečenju maligniteta dojke.

6. Zaključak

Uprkos znatnom napretku u lečenju, karcinom dojke je i dalje značajan problem javnog zdravlja koji na globalnom nivou dovodi do 600.000 smrti godišnje. Lečenje trostruko-negativnog karcinoma dojke je veoma kompleksno usled nedostatka poznate molekularne mete koja bi mogla omogućiti njegovo razlikovanje od nemalignog tkiva. Onkogeni transkripcioni faktor STAT3 je aberantno aktiviran kod svih trostruko-negativnih karcinoma dojke i 70% svih podtipova maligniteta dojke. Dodatno uzimajući u obzir da normalne ćelije mogu da tolerišu odsustvo STAT3 bez većih poremećaja fizioloških funkcija, STAT3 predstavlja značajnu metu u lečenju ove invazivne bolesti. S obzirom da je STAT3 intracelularni protein koji se translocira iz citoplazme u jedro i ne predstavlja direktnu površinsku metu, ispitali smo korišćenje inovativnog pristupa u razvoju ciljanog mehanizma delovanja naćelije karcinoma dojke sa povišenom STAT3 aktivnošću. Stoga smo ispitali metaboličke aspekte maligne transformacije uzrokovane STAT3 aktivnošću, i ustanovili konzistentnu redukciju ćelijskih metabolita N-acil taurina i arahidonske kiseline. Kako su navedeni metaboliti uključeni u procese modulacije ćelijske membrane, testirali smo primenu novog oblika višeslojnih nanočestica u terapijskoj eksploataciji datih svojstava.

U našem ispitivanju smo identifikovali nanočestice obložene poli-L-glutaminskom kiselinom, kao sisteme dostave lekova koji se preferencijalno vezuju i dostavljaju terapiju ćelijama sa izraženom aktivacijom STAT3. Suprotno tome, ćelije kod kojih je aktivnost ili ekspresija STAT3 inhibirana farmakološki ili genetski, pokazuju niži stepen vezivanja ovih nanosistema, kao i niži terapijski odgovor na nanočestice sa enkapsuliranim citotoksičnim agensom. Takođe, dokazali smo da ovi nanosistemi pokazuju dobru penetraciju kroz organoide malignih ćelija dojke, u kojima zadržavaju STAT3-ciljajuća svojstva. Konačno, radioterapija je doprinela datim ciljajućim svojstvima ovih nanočestica, te ukazuje na poboljšanje terapijske širine i sinergističko delovanje ovako kombinovane terapije.

Na osnovu naših podataka možemo istaći zaključak da LbL nanočestice sa terminalnim slojem poli-L-glutaminske kiseline predstavljaju novu klasu nosača lekova koji pokazuju afinitet interakcije sa STAT3-transformisanim ćelijama epitela dojke, i mogu delovati u sinergiji sa radioterapijom. Rezultati ove doktorske disertacije predstavljaju doprinos u pretkliničkom ispitivanju za dalji razvoj racionalnog, ciljanog pristupa lečenju trostruko-negativnog karcinoma dojke, za koji trenutno ne postoje ciljani modaliteti lečenja.

7. List of abbreviations \ Spisak skraćenica

	English language	Srpski jezik
AA, C20:4	Arachidonic acid	Arahidonska kiselina
ABL	Abelson leukaemia protein	Abelson leukemija protein
AKT, PKB	Protein kinase B	Protein kinaza B
AML	Acute myeloid leukemia	Akutna mijeloidna leukemija
ATP	Adenosine triphosphate	Adenozin trifosfat
BCL	B-cell lymphoma	B-ćelijski limfom
BCLAF1	BCL2-associated transcription factor 1	*BCL2-associated transcription factor 1*
BCR	Breakpoint cluster region protein	*Breakpoint cluster region protein*
BCSCs	Breast cancer stem cells	Stem ćelije karcinoma dojke
BRCA1/2	Breast cancer gene 1 or 2	*Breast cancer gene 1 or 2*
C16:0	Palmitic acid	Palmitinska kiselina
C18:0	Stearic acid	Stearinska kiselina
C18:1	Oleic acid	Oleinska kiselina
C1P	Ceramide -1- phosphate	Ceramid - fosfat
CAT	Catalase	Katalaza
CCD	Charge-coupled device camera	CCD kamera
CD	Cluster of differentiation	Klaster diferencijacije
CDDP	Cisplatin	Cisplatin
CDDP-CML	Cisplatin-loaded NP without coating layer	Cisplatinom ispunjene NP bez spoljašnjeg omotača
CDDP-DXS	Cisplatin-loaded NP coated with DXS	Cisplatinom ispunjene NP obložene sa DXS
CDDP-PLE	Cisplatin-loaded NP coated with PLE	Cisplatinom ispunjene NP obložene sa PLE
CDO1	Cysteine dioxygenase	Cistein dioksigenaza
CML	Chronic myeloid leukemia	Hronična mijeloidna leukemija
CML	Carboxy-modified latex core	Karboksi-modifikovan lateks
CO2	Carbon dyoxide	Ugljen dioksid
CoA	Coenzyme A	Koenzim A
COOH-	Carboxy group	Karboksilna grupa
CoR	Co-regulator protein	Koregulatorni protein
COX-2	Cyclooxygenase 2	Ciklooksigenaza 2
CPT1B	Carnitine palmitoyltransferase 1B	Karnitin palmitoiltransferaza 1B
CRISPR/Cas9	Clustered regularly interspaced short palindromic repeats/CRISPR-associated protein 9	Delovanje Cas9 enzima na grupisane kratke palindromske ponovke na jednakim rastojanjima

CTH	Cystathionine gamma lyase	Cistation gama liaza
CYP450	Cytochrome P450	Citohrom P450
Cτ	Cycle threshold	Broj ciklusa potreban za postizanje praga reakcije
DAG	Diacylglycerol	Diacilglicerol
DAPI	4′,6-diamidino-2-phenylindole	4′,6-diamidino-2-fenilindol
DDTC	Diethyldithiocarbamate	Dietilditiokarbamat
DMEM	Dulbecco's modified Eagle's medium	Dulbecco modifikovani Eagle medijum
DMF	Dimethylformamide	Dimetilformamid
DMSO	Dimethyl Sulfoxide	Dimetil sulfoksid
DNA	Deoxyribonucleic acid	Deoksiribonukleinska kiselina
DNMT	DNA methyltransferase	DNA metiltransferaza
DOX	Doxycycline	Doksiciklin
DSPC	1,2-distearoyl-sn-glycero-3-phosphocholine	1,2-distearoil-sn-glicero-3-fosfoholin
DSPG	1,2-distearoyl-sn-glycero-3-phosphoglycerol	1,2-distearoil-sn-glicero-3-fosfoglicerol
DXS	Dextran sulfate	Dekstran sulfat
DXS-NP	CML core coated with dextran sulfate	CML jezgro prekriveno sa DXS
ECM	Extracellular matrix	Ekstracelularni matriks
EGF	Epidermal growth factor	Epidermalni faktor rasta
EGFR	Epidermal growth factor receptor	Receptor epidermalnog faktora rasta
EMT	Epithelial to mesenchymal transition	Epitelijalno mezenhimalna tranzicija
EPR	Enhanced permeability and retention effect	Efekat povećane permeabilnosti i retencije
ER	Estrogen receptor	Receptor za estrogen
ESI	Electrospray ionization	Elektrosprej jonizacija
ETC	Electron transport chain	Elektron transportni lanac
FAO	Fatty acid beta oxidation	Beta oksidacija masnih kiselina
FASN	Fatty acid synthase	Sintaza masnih kiselina
FBS	Fetal bovine serum	Fetalni goveđi serum
FDA	US Food and Drug Administration	Američka Agencija za hranu i lekove
FFA	Free fatty acid	Slobodna masna kiselina
FITC	Fluorescein isothiocyanate	Fluorescein izotiocijanat
FLT3	FMS-like tyrosine kinase 3	*FMS-like tyrosine kinase 3*
FRα	Folate receptor alpha	Folatni receptor alfa
FSC	Forward scatter	Prednje rasejavanje lasera
Fuc	Fucoidan	Fukoidan
Fuc-NP	CML core coated with fucoidan	CML jezgro prekriveno sa Fuc
GAPDH	Glyceraldehyde 3-phosphate	Gliceraldehid 3-fosfat dehidrogenaza

	dehydrogenase	
GLI1	Glioma-Associated Oncogene Homolog 1	*Glioma-Associated Oncogene Homolog 1*
GM-CSF	Granulocyte macrophage colony-stimulating factor	Granulocitno-makrofagni faktor stimulacije kolonija
GP130	Glycoprotein 130	Glikoprotein 130
GPx	Glutathione peroxidase	Glutation peroksidaza
GSEA	Gene set enrichment analysis	Analiza obogaćivanja gena
GSH	Glutathione	Glutation
GTF	General transcription factor	Generalni faktor transkripcije
HA	Hyaluronic acid	Hijaluronska kiselina
HA-NP	CML core coated with hyaluronic acid	CML jezgro prekriveno sa HA
hATTR	Hereditary transthyretin amyloidosis	Nasledna transtiretin amiloidoza
HBSS	Hank's Balanced Salt Solution	Hank rastvor soli
HDAC	Histone deacetylase	Histon deacetilaze
HDL-C	High-density lipoprotein cholesterol	Lipoproteini visoke gustine
HER2, ERBB2	Human epidermal growth factor receptor 2	Humani epidermalni faktor rasta 2
HF	Heparin-folate conjugate	Heparin folat konjugat
HF-NP	CML core coated with heparin-folate conjugate	CML jezgro prekriveno sa HF
HIF	Hypoxia-inducible factor	Hipoksija-inducibilni faktor
HMT	Histone methyltransferase	Histon metiltransferaza
HOCl	Hypochlorid acid	Hipohloridna kiselina
HPLC	High performance liquid chromatography	Tečna hromatografija visoke efikasnosti
HR	Hormone receptor	Hormonski receptor
HRP	Horseradix peroxidase	Peroksidaza rena
IAP	Inhibitor of apoptosis proteins	Proteini inhibitori apoptoze
IFN	Interferon	Interferon
IL	Interleukin	Interleukin
iNOS	Inducible nitric oxide synthase	Inducibilna sintaza azotoksida
JAK	Janus kinase	Janus kinaza
LbL	Layer-by-Layer	Sloj po sloj
LC-MS/MS	Liquid chromatography coupled to tandem mass spectrometry	Tečna hromatografija kuplovana sa tandemskom masenom spektrometrijom
LDL-C	Low-density lipoprotein cholesterol	Lipoproteini niske gustine
LIF	Leukemia inhibitory factor	Leukemija inhibitorni faktor
lncRNA	Long non-coding ribonucleic acid	Duge nekodirajuće ribonukleinske kiseline
LOX	Lipoxigenase	Lipooksigenaza

LPA	Lysophosphatidic acid	Lizofosfatidna kiselina
LPC	Lysophosphatidylcholine	Lizofosfatidilholin
LPE	Lysophosphatidylethanolamine	Lizofosfatidiletanolamin
LPS	Lysophosphatidylserine	Lizofosfatidilserin
MAG	Monoacylglycerol	Monoacilglicerol
MAGE	Monoalkylglycerol ether	Monoalkilgliceroletar
MCL	Myeloid cell leukemia	*Myeloid cell leukemia*
MDR1, ABCB1	Multidrug resistance protein 1	*Multidrug resistance protein 1*
miRNA	Micro ribonucleic acid	Mikro RNK
MMP	Metalloproteinase	Metaloproteinaza
mRNA	Messenger ribonucleic acid	Informaciona RNK
MRP1, ABCC1	Multidrug resistance associated protein 1	*Multidrug resistance associated protein 1*
mTOR	Mammalian target of rapamycin	*Mammalian target of rapamycin*
NAT	N-acyl taurine	N-acil taurin
ncRNA	Non-coding ribonucleic acid	Nekodirajuća RNK
NES	Normalized enrichment scor	Normalizovan rezultat obogaćenja
NFκB	Nuclear factor kappa B	Nuklearni faktor kapa B
NP	Nanoparticle	Nanočestica
Oct-4	Octamer-binding transcription factor-4	Oktamer-vezujući transkriptioni faktor 4
OSM	Oncostatin M	Onkostatin M
p53	Tumor protein 53	Tumor protein 53
PA	Phosphatidic acid	Fosfatidna kiselina
PAA	Polyacrylic acid	Poliakrilna kiselina
PAA-NP	CML core coated with polyacrylic acid	CML jezgro prekriveno sa PAA
PAGE	Polyacrylamide gel electrophoresis	Elektroforeza na poliakrilamidnom gelu
PBP	PPARγ binding protein	PPARγ vezujući protein
PBS	Phosphate-buffered saline	Fosfatom puferovani fiziološki rastvor
PC	Phosphatidylcholine	Fosfatidilholin
PCp	Phosphatidylcholine plasmalogen	Fosfatidilholin plazmogen
PDA	Pentadecanoic acid	Pentadekanska kiselina
PDGF	Platelet-derived growth factor	Trombocitni faktor rasta
PD-L1	Programmed death ligand 1	Ligand programirane smrti 1
PE	Phosphatidylethanolamine	Fosfatidiletanolamin
PEG	Poly-ethylene glycol	Poli-etilen glikol
PG	Phosphatidylglycerol	Fosfatidilglicerol
PGE2	Prostaglandin E2	Prostaglandin E2
PI3K	Phosphoinositide 3-kinase	Fosfatidilinozitol 3-kinaza

PIAS	Protein inhibitor of activated STAT	Protein inhibitori aktiviranih STAT
PIe	Phosphatidylinositol	Fosfatidilinozitol
PK	Pharmacokinetic	Farmakokinetika
PLA2G4A	Phospholipase A2	Fosfolipaza A2
PLD	Poly-L-aspartic acid	Poli-L-asparaginska kiselina
PLD-NP	CML core coated with poly-L-aspartate	CML jezgro prekriveno sa PLD
PLE	Poly-L-glutamic acid	Poli-L-glutaminska kiselina
PLE-b-PEG	Poly(ethylene glycol-block-poly-L-glutamate)	Poli(etilen glikol-blok-poli-L-glutamat)
PLE-b-PEG-NP	CML core coated with poly(ethylene glycol-block-poly-L-glutamate)	CML jezgro prekriveno sa PLE-b-PEG
PLE-NP	CML core coated with poly-L-glutamic acid	CML jezgro prekriveno sa PLE
PLR	Poly-L-arginine	Poli-L-arginin
Pol II	RNA polymerase II	RNK polimeraza II
PPARγ	Peroxisome proliferator-activated receptor gamma	Peroksizmalni proliferacijom-aktiviran receptor gama
PR	Progesterone receptor	Progesteronski receptor
pS	Serine phosphorylation	Fosforilisana serinska rezidua
PS	Phosphatidylserine	Fosfatidilserin
PTEN	Phosphatase and tensin homolog	Fosfataza i tenzin homolog
PTP	Protein tyrosine phosphatase	Protein tirozin fosfataza
PYR	Pyrimethamine	Pirimetamin
RNA	Ribonucleic acid	Ribonukleinska kiselina
ROS	Reactive oxygen species	Reaktivne oksidativne vrste
qRT-PCR	Quantitative reverse transcriptase polymerase chain reaction	Kvantitativna lančana reakcija polimeraze sa reverznom transkriptazom
RUX	Ruxolitinib	Ruksolotinib
SBC	Sulfated poly(β-cyclodextrin)	Poli-beta-ciklodekstrin sulfat
SBC-NP	CML core coated with sulfated poly(β-cyclodextrin)	CML jezgro prekriveno sa SBC
SD	Standard deviation	Standardna devijacija
SDS	Sodium-dodecyl sulfate	Natrijum dodecilsulfat
SEM	Standard error	Standardna greška
SH2	SRC-homology 2	SRC-homologija 2
shRNA	Short hairpin RNA	*Short hairpin* RNK
siControl	Non-targeting siRNA control	Ne-ciljajuća siRNK kontrola
siSTAT3	siRNA targeting STAT3	STAT3-ciljajuća siRNK
SM	Sphingomyelin	Sfingomijelin
SOCS	Suppressor of cytokine signaling	Supresor citokinske signalizacije

SOD	Superoxide dismutase	Superoksid dizmutaza
SRM	Selective Reaction Monitoring	Selektivni reakcioni monitoring
SSC	Side scatter	Bočno rasejavanje lasera
STAT	Signal transducers and activators of transcription	Prenosilac signala i aktivator transkripcije
STAT3C	STAT3 construct	STAT3 konstrukt
TAG	Triacylglycerol	Triacilglicerol
TF	Transcription factor	Transkripcioni faktor
TGFβ	Transforming growth factor beta	Transformišući faktor rasta beta
TNBC	Triple-negative breast cancer	Trostruko-negativni karcinom dojke
TNFa	Tumor necrosis factor alpha	Tumor nekrozis faktor alfa
Treg cells	T regulatory cells	T regulatorne ćelije
UICC	The Union for International Cancer Control	Međunarodna unija za kontrolu maligniteta
VEGF	Vascular endothelial growth factor	Vaskularni endotelni faktor rasta
WT	Wild-type	Nemutiran
Y705	Tyrosine 705 residue	Tirozinska rezidua 705
1:1 HA/PLD	1:1 blend ratio of hyaluronic and poly-L-aspartic acid	1:1 smeša hijaluronske kiseline i poli-L-asparaginske kiseline
1:3 HA/PLD	1:3 blend ratio of hyaluronic and poly-L-aspartic acid	1:3 smeša hijaluronske kiseline i poli-L-asparaginske kiseline
3:1 HA/PLD	3:1 blend ratio of hyaluronic and poly-L-aspartic acid	3:1 smeša hijaluronske kiseline i poli-L-asparaginske kiseline
3D	Three dimensional	Trodimenzionalni
5-LOX	5-lipoxygenase	5-lipooksigenaza

8. References \ Literature

1. Bray F, Ferlay J, Soerjomataram I, Siegel RL, Torre LA, Jemal A. Global cancer statistics 2018: GLOBOCAN estimates of incidence and mortality worldwide for 36 cancers in 185 countries. CA Cancer J Clin. 2018;68(6):394-424.
2. Krasniqi E, Pizzuti L, Barchiesi G, Sergi D, Carpano S, Botti C, et al. Impact of BMI on HER2+ metastatic breast cancer patients treated with pertuzumab and/or trastuzumab emtansine. Real-world evidence. J Cell Physiol. 2020;235(11):7900-10.
3. Siegel RL, Miller KD, Jemal A. Cancer statistics, 2019. CA Cancer J Clin. 2019;69(1):7-34.
4. Pekmezović T. Epidemiologija raka dojke. U: Milašinović G, urednik. Nacionalni vodič dobre kliničke prakse za dijagnostikovanje i lečenje raka dojke. Beograd: Ministarstvo zdravlja Republike Srbije; 2013. p. 8-9. Serbian
5. Stankov K. Descriptive epidemiology of breast cancer in Vojvodina. Breast. 2011;20(2):192-5. Serbian
6. Greenlee H, DuPont-Reyes MJ, Balneaves LG, Carlson LE, Cohen MR, Deng G, et al. Clinical practice guidelines on the evidence-based use of integrative therapies during and after breast cancer treatment. CA Cancer J Clin. 2017;67(3):194-232.
7. Torre LA, Islami F, Siegel RL, Ward EM, Jemal A. Global Cancer in Women: Burden and Trends. Cancer Epidemiol Biomarkers Prev. 2017;26(4):444-57.
8. Waks AG, Winer EP. Breast Cancer Treatment: A Review. JAMA. 2019;321(3):288-300
9. McDonald ES, Clark AM, Tchou J, Zhang P, Freedman GM. Clinical Diagnosis and Management of Breast Cancer. J Nucl Med. 2016;57 Suppl 1:9S-16S.
10. Tošić IN, Mikov MM, Stankov KM. Application of nanomedical technology in breast cancer treatment. Hospital Pharmacology. 2020;7(1):883-94.
11. Kreutzfeldt J, Rozeboom B, Dey N, De P. The trastuzumab era: current and upcoming targeted HER2+ breast cancer therapies. Am J Cancer Res. 2020;10(4):1045-1067.
12. Loibl S, Gianni L. HER2-positive breast cancer. Lancet. 2017;389(10087):2415-29.
13. Harbeck N, Gnant M. Breast cancer. Lancet. 2017; 10074(389):1134-50
14. Geyer CE, Forster J, Lindquist D, Chan S, Romieu CG, Pienkowski T, et al. Lapatinib plus capecitabine for HER2-positive advanced breast cancer. N Engl J Med 2006;355:2733–43.
15. Alexandrou S, George SM, Ormandy CJ, Lim E, Oakes SR, Caldon CE. The Proliferative and Apoptotic Landscape of Basal-like Breast Cancer. Int J Mol Sci. 2019;20(3):667

16. Nagini S. Breast Cancer: Current Molecular Therapeutic Targets and New Players. Anticancer Agents Med Chem. 2017;17(2):152-63.
17. Pérez-Herrero E, Fernández-Medarde A. Advanced targeted therapies in cancer: Drug nanocarriers, the future of chemotherapy. Eur J Pharm Biopharm. 2015;93:52-79.
18. Piovesan A, Antonaros F, Vitale L, Strippoli P, Pelleri MC, Caracausi M. Human protein-coding genes and gene feature statistics in 2019. BMC Res Notes. 2019;12(1):315.
19. Lee TI, Young RA. Transcriptional regulation and its misregulation in disease. Cell. 2013;152(6):1237-51
20. Stankov K. Biohemija i genetika naslednih bolesti. Medicinski fakultet u Novom Sadu. 2016; ISBN:978-867197-480-6:143-69. Serbian
21. Yoo BC, Kim KH, Woo SM, Myung JK. Clinical multi-omics strategies for the effective cancer management. J Proteomics. 2018;188:97-106
22. Chakraborty S, Hosen MI, Ahmed M, Shekhar HU. Onco-Multi-OMICS Approach: A New Frontier in Cancer Research. Biomed Res Int. 2018;2018:9836256
23. Jovanović D. Osnovi onkologije i palijativna nega onkoloških bolesnika. Medicinski fakultet u Novom Sadu. 2008; ISBN:978-86-7197-292-5:92-141. Serbian
24. Saletta F, Dalla Pozza L, Byrne JA. Genetic causes of cancer predisposition in children and adolescents. Transl Pediatr. 2016;4:67-75.
25. Finch AP, Lubinski J, Møller P, Singer CF, Karlan B, Senter L, et al. Impact of oophorectomy on cancer incidence and mortality in women with a BRCA1 or BRCA2 mutation. J Clin Oncol 2014;32(15):1547-53.
26. Lazzeroni M, Serrano D, Dunn BK, Heckman-Stoddard BM, Lee O, Khan S, et al. Oral low dose and topical tamoxifen for breast cancer prevention: modern approaches for an old drug. Breast Cancer Res. 2012;14(5):214.
27. Kotze MJ, Lückhoff HK, Peeters AV, Baatjes K, Schoeman M, van der Merwe L. Genomic medicine and risk prediction across the disease spectrum. Crit Rev Clin Lab Sci. 2015;52(3):120-37.
28. Barcellos-Hoff MH, Lyden D, Wang TC. The evolution of the cancer niche during multistage carcinogenesis. Nat Rev Cancer. 2013;13(7):511-8.
29. Hilton HN, Clarke CL, Graham JD. Estrogen and progesterone signalling in the normal breast and its implications for cancer development. Mol Cell Endocrinol. 2018;466:2-14.
30. Cramer P. Organization and regulation of gene transcription. Nature. 2019;573(7772):45-54.
31. Danino YM, Even D, Ideses D, Juven-Gershon T. The Core Promoter: At the Heart of Gene Expression. Biochim Biophys Acta. 2015;1849(8):1116-31.
32. Lambert SA, Jolma A, Campitelli LF, Das PK, Yin Y, Albu M, et al. The Human Transcription Factors. Cell. 2018;172(4):650-65.
33. Yan C, Higgins PJ. Drugging the Undruggable: Transcription Therapy for Cancer. Biochim Biophys Acta. 2013;1835(1):76–85.

34. Fischer V, Schumacher K, Tora L, Devys D. Global role for coactivator complexes in RNA polymerase II transcription. Transcription. 2019;10(1):29–36.
35. Bhagwat AS, Vakoc CR. Targeting Transcription Factors in Cancer. Trends Cancer. 2015;1(1):53-65.
36. Thomas MC, Chiang CM. The General Transcription Machinery and General Cofactors. Crit Rev Biochem Mol Biol. 2006;41(3):105-78.
37. Pfister NT, Prives C. Transcriptional Regulation by Wild-Type and Cancer-Related Mutant Forms of p53. Cold Spring Harb Perspect Med. 2017;7(2):a026054.
38. Lee EY, Muller WJ. Oncogenes and tumor suppressor genes. Cold Spring Harb Perspect Biol. 2010;2(10):a003236.
39. Heppler LN, Frank DA. Rare mutations provide unique insight into oncogenic potential of STAT transcription factors. J Clin Invest. 2018;128(1):113–5.
40. Groner B, von Manstein V. Jak Stat Signaling and Cancer: Opportunities, Benefits and Side Effects of Targeted Inhibition. Mol Cell Endocrinol. 2017;451:1-14.
41. Yu H, Jove R. The STATs of cancer--new molecular targets come of age. Nat Rev Cancer. 2004;4(2):97-105.
42. Dudley AC, Thomas D, Best J, Jenkins A. The STATs in cell stress-type responses. Cell Commun Signal. 2004;2:8.
43. Decker T, Kovarik P. Serine Phosphorylation of STATs. Oncogene. 2000;19(21):2628-37.
44. Shih PC. Revisiting the development of small molecular inhibitors that directly target the signal transducer and activator of transcription 3 (STAT3) domains. Life Sci. 2020;242:117241
45. Zhang Q, Raje V, Yakovlev VA, Yacoub A, Szczepanek K, Meier J, et al. Mitochondrial Localized Stat3 Promotes Breast Cancer Growth via Phosphorylation of Serine 727. J Biol Chem. 2013;288(43):31280–8.
46. Stark GR, Cheon H, Wang Y. Responses to Cytokines and Interferons that Depend upon JAKs and STATs. Cold Spring Harb Perspect Biol. 2018;10(1): a028555.
47. Goodman ML, Trinca GM, Walter KR, Papachristou EK, D'Santos CS, Li T, et al. Progesterone Receptor Attenuates STAT1-Mediated IFN Signaling in Breast Cancer. J Immunol. 2019;202(10):3076-86.
48. Zhang Y, Liu Z. STAT1 in cancer: friend or foe? Discov Med. 2017;24(130):19-29.
49. Kaur T, Mukherjea D, Sheehan K, Jajoo S, Rybak LP, Ramkumar V. Short interfering RNA against STAT1 attenuates cisplatin-induced ototoxicity in the rat by suppressing inflammation. Cell Death Dis. 2011;2:e180.
50. Heppler LN, Frank DA. Targeting Oncogenic Transcription Factors: Therapeutic Implications of Endogenous STAT Inhibitors. Trends Cancer. 2017;3(12):816-27

51. Maurer B, Kollmann S, Pickem J, Hoelbl-Kovacic A, Sexl V. STAT5A and STAT5B-Twins with Different Personalities in Hematopoiesis and Leukemia. Cancers (Basel). 2019;11(11). pii: E1726.
52. Walker SR, Xiang M, Frank DA. Distinct roles of STAT3 and STAT5 in the pathogenesis and targeted therapy of breast cancer. Mol Cell Endocrinol. 2014;382(1):616-21
53. Walker SR, Nelson EA, Zou L, Chaudhury M, Signoretti S, Richardson A, et al. Reciprocal effects of STAT5 and STAT3 in breast cancer. Mol Cancer Res. 2009;7(6):966-76.
54. Walker SR, Xiang M, Frank DA. STAT3 Activity and Function in Cancer: Modulation by STAT5 and miR-146b. Cancers (Basel) 2014;6(2):958–68.
55. Aignera P, Justa V, Stoibera D. STAT3 isoforms: Alternative fates in cancer? Cytokine. 2019;118:27-34
56. Ng IHW, Ng DCH, Jans DA, Bogoyevitch MA. Selective STAT3-α or -β expression reveals spliceform-specific phosphorylation kinetics, nuclear retention and distinct gene expression outcomes. Biochem J. 2012;447(1):125-36.
57. Hendry L, John S. Regulation of STAT signalling by proteolytic processing. Eur. J. Biochem. 2004;271:4613-20
58. Reddy EP, Korapati A, Chaturvedi P, Rane S. IL-3 signaling and the role of Src kinases, JAKs and STATs: a covert liaison unveiled. Oncogene. 2000;19(21):2532–47
59. Johnson DE, O'Keefe RA, Grandis JR. Targeting the IL-6/JAK/STAT3 signalling axis in cancer. Nat Rev Clin Oncol. 2018;15(4):234–48.
60. Egusquiaguirre SP, Yeh JE, Walker SR, Liu S, Frank DA. The STAT3 Target Gene TNFRSF1A Modulates the NF-κB Pathway in Breast Cancer Cells. Neoplasia. 2018;20(5):489-98
61. Frank DA. STAT3 as a central mediator of neoplastic cellular transformation. Cancer Lett. 2007;251(2):199-210.
62. Kumari N, Dwarakanath BS, Das A, Bhatt AN. Role of interleukin-6 in cancer progression and therapeutic resistance. Tumour Biol. 2016;37(9):11553-72.
63. Dethlefsen C, Højfeldt G, Hojman P. The role of intratumoral and systemic IL-6 in breast cancer. Breast Cancer Res Treat. 2013;138(3):657-64.
64. Jinno T, Kawano S, Maruse Y, Matsubara R, Goto Y, Sakamoto T, et al. Increased expression of interleukin-6 predicts poor response to chemoradiotherapy and unfavorable prognosis in oral squamous cell carcinoma. Oncol Rep. 2015;33(5):2161-8.
65. Sanguinete MMM, Oliveira PH, Martins-Filho A, Micheli DC, Tavares-Murta BM, Murta EFC, et al. Serum IL-6 and IL-8 Correlate with Prognostic Factors in Ovarian Cancer. Immunol Invest. 2017;46(7):677-88.
66. Desrichard A, Snyder A, Chan TA. Cancer Neoantigens and Applications for Immunotherapy. Clin Cancer Res. 2016;22(4):807-12

67. Lim AR, Rathmell WK, Rathmell JC. The tumor microenvironment as a metabolic barrier to effector T cells and immunotherapy. Elife. 2020;9:e55185.
68. Yu H, Pardoll D, Jove R. STATs in cancer inflammation and immunity: a leading role for STAT3. Nat Rev Cancer. 2009;9(11):798-809
69. Lee H, Herrmann A, Deng JH, Kujawski M, Niu G, Li Z, et al. Persistently activated Stat3 maintains constitutive NF-kappaB activity in tumors. Cancer Cell. 2009;15(4):283-93.
70. Bu LL, Yu GT, Wu L, Mao L, Deng WW, Liu JF, et al. STAT3 Induces Immunosuppression by Upregulating PD-1/PD-L1 in HNSCC. J Dent Res. 2017;96(9):1027-34
71. Kalantari Khandani N, Ghahremanloo A, Hashemy SI. Role of tumor microenvironment in the regulation of PD-L1: A novel role in resistance to cancer immunotherapy. J Cell Physiol. 2020;235(10):6496-506.
72. Ehexige E, Bao M, Bazarjav P, Yu X, Xiao H, Han S, et al. Silencing of STAT3 via Peptidomimetic LNP-Mediated Systemic Delivery of RNAi Downregulates PD-L1 and Inhibits Melanoma Growth. Biomolecules. 2020;10(2):285
73. Wang Y, Shen Y, Wang S, Shen Q, Zhou X. The role of STAT3 in leading the crosstalk between human cancers and the immune system. Cancer Lett. 2018;415:117-28
74. Wang T, Niu G, Kortylewski M, Burdelya L, Shain K, Zhang S, et al. Regulation of the innate and adaptive immune responses by Stat-3 signaling in tumor cells. Nat Med. 2004;10(1):48-54.
75. Yu H, Kortylewski M, Pardoll D. Crosstalk between cancer and immune cells: role of STAT3 in the tumour microenvironment. Nat Rev Immunol. 2007;7(1):41-51.
76. Weinberg RA. The biology of cancer. Yale J Biol Med. 2007;80(2):91
77. Valastyan S, Weinberg RA. Tumor metastasis: molecular insights and evolving paradigms. Cell. 2011;147(2):275-92
78. Kamran MZ, Patil P, Gude RP. Role of STAT3 in Cancer Metastasis and Translational Advances. Biomed Res Int. 2013;2013:421821.
79. Wang Y, Guo W, Li Z, Wu Y, Jing C, Ren Y, et al. Role of the EZH2/miR-200 axis in STAT3-mediated OSCC invasion. Int J Oncol. 2018;52(4):1149–64.
80. Zhang X, Sun Y, Pireddu R, Yang H, Urlam MK, Lawrence HR, et al. A novel inhibitor of STAT3 homodimerization selectively suppresses STAT3 activity and malignant transformation. Cancer Res. 2013;73(6):1922–33.
81. Cao J, Wang X, Dai T, Wu Y, Zhang M, Cao R, et al. Twist promotes tumor metastasis in basal-like breast cancer by transcriptionally upregulating ROR1. Theranostics. 2018;8(10):2739–51.
82. Zhu H, Chang LL, Yan FJ, Hu Y, Zeng MC, Zhou TY, et al. AKR1C1 Activates STAT3 to Promote the Metastasis of Non-Small Cell Lung Cancer. Theranostics. 2018;8(3):676–92.

83. Sullivan NJ, Sasser AK, Axel AE, Vesuna F, Raman V, Ramirez N, et al. Interleukin-6 induces an epithelial-mesenchymal transition phenotype in human breast cancer cells. Oncogene. 2009;28(33):2940-7.
84. Nguyen DX, Bos PD, Massagué J. Metastasis: from dissemination to organ-specific colonization. Nat Rev Cancer. 2009;9(4):274-84.
85. Wang Z, Dabrosin C, Yin X, Fuster MM, Arreola A, Rathmell KW, et al. Broad targeting of angiogenesis for cancer prevention and therapy. Semin Cancer Biol. 2015;35(Suppl):S224–43.
86. Ramjiawan RR, Griffioen AW, Duda DG. Anti-angiogenesis for cancer revisited: Is there a role for combinations with immunotherapy? Angiogenesis. 2017;20(2):185–204.
87. Hanahan D, Weinberg RA. Hallmarks of cancer: the next generation. Cell. 2011;144(5):646-74.
88. Zhang N, Zhang M, Wang Z, Gao W, Sun ZG. Activated STAT3 Could Reduce Survival in Patients with Esophageal Squamous Cell Carcinoma by Up-regulating VEGF and Cyclin D1 Expression. J Cancer. 2020;11(7):1859-68.
89. Wu X, Deng Y, Zu Y, Yin J. Histone demethylase KDM4C activates HIF1α/VEGFA signaling through the costimulatory factor STAT3 in NSCLC. Am J Cancer Res. 2020;10(2):491-506.
90. Pawlus MR, Wang L, Hu CJ. STAT3 and HIF1α cooperatively activate HIF1 target genes in MDA-MB-231 and RCC4 cells. Oncogene. 2014;33(13):1670-9.
91. Gray MJ, Zhang J, Ellis LM, Semenza GL, Evans DB, Watowich SS, et al. HIF-1alpha, STAT3, CBP/p300 and Ref-1/APE are components of a transcriptional complex that regulates Src-dependent hypoxia-induced expression of VEGF in pancreatic and prostate carcinomas. Oncogene. 2005;24(19):3110-20.
92. Tartour E, Pere H, Maillere B, Terme M, Merillon N, Taieb J, et al. Angiogenesis and immunity: a bidirectional link potentially relevant for the monitoring of antiangiogenic therapy and the development of novel therapeutic combination with immunotherapy. Cancer Metastasis Rev. 2011;30(1):83-95.
93. Valle-Mendiola A, Soto-Cruz I. Energy Metabolism in Cancer: The Roles of STAT3 and STAT5 in the Regulation of Metabolism-Related Genes. Cancers (Basel). 2020;12(1):124.
94. Baumann J, Sevinsky C, Conklin DS. Lipid biology of breast cancer. Biochimica et biophysica acta. 2013;1831:1509–17.
95. Sounni NE, Cimino J, Blacher S, Primac I, Truong A, Mazzucchelli G, et al. Blocking lipid synthesis overcomes tumor regrowth and metastasis after antiangiogenic therapy withdrawal. Cell Metab. 2014;20:280–94.
96. Camarda R, Zhou AY, Kohnz RA, Balakrishnan S, Mahieu C, Anderton B, et al. Inhibition of fatty acid oxidation as a therapy for MYC-overexpressing triple-negative breast cancer. Nat Med. 2016;22:427-32.

97. Ying H, Kimmelman AC, Lyssiotis CA, Hua S, Chu GC, Fletcher-Sananikone E, et al. Oncogenic Kras maintains pancreatic tumors through regulation of anabolic glucose metabolism. Cell. 2012;149(3):656-70.
98. Liberti MV, Locasale JW. The Warburg Effect: How Does it Benefit Cancer Cells? Trends Biochem Sci. 2016;41(3):211–8.
99. Demaria M, Giorgi C, Lebiedzinska M, Esposito G, D'Angeli L, Bartoli A, et al. A STAT3-mediated metabolic switch is involved in tumour transformation and STAT3 addiction. Aging. 2010;2:823–42.
100. Yang R, Rincon M. Mitochondrial Stat3, the Need for Design Thinking. Int J Biol Sci. 2016;12(5):532–44.
101. Lee M, Hirpara JL, Eu JQ, Sethi G, Wang L, Goh BC, et al. Targeting STAT3 and oxidative phosphorylation in oncogene-addicted tumors. Redox Biol. 2019;25:101073.
102. Lufei C, Ma J, Huang G, Zhang T, Novotny-Diermayr V, Ong CT, et al. GRIM-19, a death-regulatory gene product, suppresses Stat3 activity via functional interaction. EMBO J. 2003;22(6):1325-35.
103. Tammineni P, Anugula C, Mohammed F, Anjaneyulu M, Larner AC, Sepuri NB. The import of the transcription factor STAT3 into mitochondria depends on GRIM-19, a component of the electron transport chain. J. Biol. Chem. 2013;288:4723–32.
104. Gough DJ, Corlett A, Schlessinger K, Wegrzyn J, Larner AC, Levy DE. Mitochondrial STAT3 supports Ras-dependent oncogenic transformation. Science. 2009;324(5935):1713-6.
105. Wegrzyn J, Potla R, Chwae YJ, Sepuri NB, Zhang Q, Koeck T, et al. Function of mitochondrial Stat3 in cellular respiration. Science. 2009;323(5915):793-7.
106. Babaei R, Schuster M, Meln I, Lerch S, Ghandour RA, Pisani DF, et al. Jak-TGFβ cross-talk links transient adipose tissue inflammation to beige adipogenesis. Sci Signal. 2018;11(527). pii: eaai7838.
107. Dambal S, Alfaqih M, Sanders S, Maravilla E, Ramirez-Torres A, Galvan GC, et al. 27-Hydroxycholesterol Impairs Plasma Membrane Lipid Raft Signaling as Evidenced by Inhibition of IL6-JAK-STAT3 Signaling in Prostate Cancer Cells. Mol Cancer Res. 2020;18(5):671-84.
108. Wang T, Fahrmann JF, Lee H, Li YJ, Tripathi SC, Yue C, et al. JAK/STAT3-Regulated Fatty Acid β-Oxidation Is Critical for Breast Cancer Stem Cell Self-Renewal and Chemoresistance. Cell Metab. 2018;27(1):136-50.e5
109. Banks AS, Davis SM, Bates SH, Myers MG Jr. Activation of downstream signals by the long form of the leptin receptor. J. Biol. Chem. 2000;275:14563–72.
110. Alshaker H, Wang Q, Frampton AE, Krell J, Waxman J, Winkler M, et al. Sphingosine kinase 1 contributes to leptin-induced STAT3 phosphorylation through IL-6/gp130 transactivation in oestrogen receptor-negative breast cancer. Breast Cancer Res Treat. 2015;149(1):59-67.

111. Khandekar MJ, Cohen P, Spiegelman BM. Molecular mechanisms of cancer development in obesity. Nat Rev Cancer. 2011;11(12):886-95
112. Hu W, Lv J, Han M, Yang Z, Li T, Jiang S, et al. STAT3: The art of multi-tasking of metabolic and immune functions in obesity. Prog Lipid Res. 2018;70:17-28.
113. Carracedo A, Cantley LC, Pandolfi PP. Cancer metabolism: fatty acid oxidation in the limelight. Nat Rev Cancer. 2013;13(4):227-32.
114. Yang X, Jia J, Yu Z, Duanmu Z, He H, Chen S, et al. Inhibition of JAK2/STAT3/SOCS3 signaling attenuates atherosclerosis in rabbit. BMC Cardiovasc Disord. 2020;20:133.
115. Zeng Z, He W, Jia Z, Hao S. Lycopene Improves Insulin Sensitivity Through Inhibition of STAT3/Srebp-1c-Mediated Lipid Accumulation and Inflammation in Mice Fed a High-Fat Diet. Exp Clin Endocrinol Diabetes. 2017;125(9):610-7
116. Chen Q, Lv J, Yang W, Xu B, Wang Z, Yu Z, et al. Targeted inhibition of STAT3 as a potential treatment strategy for atherosclerosis. Theranostics. 2019;9(22):6424-42.
117. Wang X, Liu M, Cai GH, Chen Y, Shi XC, Zhang CC, et al. A Potential Nutraceutical Candidate Lactucin Inhibits Adipogenesis Through Downregulation of JAK2/STAT3 Signaling Pathway-Mediated Mitotic Clonal Expansion. Cells. 2020;9(2):331.
118. Yu C, Niu X, Du Y, Chen Y, Liu X, Xu L, et al. IL-17A promotes fatty acid uptake through the IL-17A/IL-17RA/p-STAT3/FABP4 axis to fuel ovarian cancer growth in an adipocyte-rich microenvironment. Cancer Immunol Immunother. 2020;69(1):115-26.
119. Egusquiaguirre SP, Liu S, Tošić I, Jiang K, Walker SR, Nicolais M, et al. CDK5RAP3 is a co-factor for the oncogenic transcription factor STAT3. Neoplasia. 2020;22(1):47–59
120. Qin JJ, Yan L, Zhang J, Zhang WD. STAT3 as a potential therapeutic target in triple negative breast cancer: a systematic review. J Exp Clin Cancer Res. 2019;38:195.
121. Sirkisoon SR, Carpenter RL, Rimkus T, Anderson A, Harrison A, Lange AM, et al. Interaction between STAT3 and GLI1/tGLI1 oncogenic transcription factors promotes the aggressiveness of triple-negative breast cancers and HER2-enriched breast cancer. Oncogene. 2018;37(19):2502-14.
122. Zheng M, Cao MX, Yu XH, Li L, Wang K, Wang SS, et al. STAT3 Promotes Invasion and Aerobic Glycolysis of Human Oral Squamous Cell Carcinoma via Inhibiting FoxO1. Front Oncol. 2019;9:1175.
123. Zhou J, Wulfkuhle J, Zhang H, Gu P, Yang Y, Deng J, et al. Activation of the PTEN/mTOR/STAT3 pathway in breast cancer stem-like cells is required for viability and maintenance. Proc Natl Acad Sci U S A. 2007;104(41):16158-63.
124. Ruddy KJ, Ganz PA. Treatment of Nonmetastatic Breast Cancer. JAMA. 2019;321(17):1716-7

125. Furtek SL, Backos DS, Matheson CJ, Reigan P. Strategies and Approaches of Targeting STAT3 for Cancer Treatment. CS Chem Biol. 2016;11(2):308-18.
126. Stover DG, Gil Del Alcazar CR, Brock J, Guo H, Overmoyer B, Balko J, et al. Phase II study of ruxolitinib, a selective JAK1/2 inhibitor, in patients with metastatic triple-negative breast cancer. NPJ Breast Cancer. 2018;4:10.
127. Ma JH, Qi J, Lin SQ, Zhang CY, Liu FY, Xie WD, et al. STAT3 Targets ERR-α to Promote Epithelial-Mesenchymal Transition, Migration, and Invasion in Triple-Negative Breast Cancer Cells. Mol Cancer Res. 2019;17(11):2184-95
128. Ma JH, Qin L, Li X. Role of STAT3 signaling pathway in breast cancer. Cell Commun Signal. 2020;18(1):33.
129. Yeh JE, Frank DA. STAT3-Interacting Proteins as Modulators of Transcription Factor Function: Implications to Targeted Cancer Therapy. ChemMedChem. 2016;11(8):795-801
130. Orlova A, Wagner C, de Araujo ED, Bajusz D, Neubauer HA, Herling M, et al. Direct Targeting Options for STAT3 and STAT5 in Cancer. Cancers (Basel). 2019;11(12):1930.
131. Cerulli R, Shehaj L, Tosic I, Jiang K, Wang J, Frank D, et al. Cytosolic delivery of peptidic STAT3 SH2 domain inhibitors. Bioorg. Med. Chem. 2020;28(12):115542.
132. Rahmati M, Johari B, Kadivar M, Rismani E, Mortazavi Y. Suppressing the metastatic properties of the breast cancer cells using STAT3 decoy oligodeoxynucleotides: A promising approach for eradication of cancer cells by differentiation therapy. J Cell Physiol. 2020; 235(6):5429-44.
133. Souissi I, Ladam P, Cognet JAH, Le Coquil S, Varin-Blank N, Baran-Marszak F, et al. A STAT3-inhibitory hairpin decoy oligodeoxynucleotide discriminates between STAT1 and STAT3 and induces death in a human colon carcinoma cell line. Mol Cancer. 2012;11:12
134. Wakaskar RR. Promising effects of nanomedicine in cancer drug delivery. J Drug Target. 2018;26(4):319-24.
135. Foster C, Watson A, Kaplinsky J, Kamaly N. Improved Targeting of Cancers with Nanotherapeutics. Methods Mol Biol. 2017; 1530:13-37.
136. Behzadi S, Serpooshan V, Tao W, Hamaly MA, Alkawareek MY, Dreaden EC, et al. Cellular Uptake of Nanoparticles: Journey Inside the Cell. Chem Soc Rev. 2017;46(14):4218-44.
137. Mathavan S, Ionescu CM, Kovacevic B, Mikov M, Golocorbin-Kon S, Mooranian A, et al. Histological effects of pharmacologically active human bile acid nano/micro-particles in Type-1 diabetes. Ther Deliv. 2020; 11(3):157-71.
138. Zhang RX, Wong HL, Xue HY, Eoh JY, Wu XY. Nanomedicine of synergistic drug combinations for cancer therapy - Strategies and perspectives. J Control Release. 2016;240:489-503
139. Yu S, Bi X, Yang L, Wu S, Yu Y, Jiang B, et al. Co-Delivery of Paclitaxel and PLK1-Targeted siRNA Using Aptamer-Functionalized Cationic Liposome for

Synergistic Anti-Breast Cancer Effects In Vivo. J Biomed Nanotechnol. 2019;15(6):1135-48
140. Kamal T, Sarfraz M, Arafat M, Mikov M, Rahman N. Cross-linked guar gum and sodium borate based microspheres as colon-targeted anticancer drug delivery systems for 5-fluorouracil. Pak J Pharm Sci. 2017;30(6(Supplementary)):2329-36.
141. Maranhão RC, Vital CG, Tavoni TM, Graziani SR. Clinical experience with drug delivery systems as tools to decrease the toxicity of anticancer chemotherapeutic agents. Expert Opin Drug Deliv. 2017;14(10):1217-26
142. Ran W, Liu X, Chang L, Cai Y, Zheng C, Liu J, et al. Self-assembling mertansine prodrug improves tolerability and efficacy of chemotherapy against metastatic triple-negative breast cancer. J Control Release. 2019;318:234-45.
143. Mooranian A, Zamani N, Mikov M, Goločorbin-Kon S, Stojanovic G, Arfuso F. Bio Micro-Nano Technologies of Antioxidants Optimised Their Pharmacological and Cellular Effects, ex vivo, in Pancreatic β-Cells. NanotechnolSci Appl. 2020;13:1-9.
144. Mooranian A, Zamani N, Mikov M, Goločorbin-Kon S, Stojanovic G, Arfuso F,et al. A second-generation micro/nano capsules of an endogenous primary un-metabolised bile acid, stabilized by Eudragit-alginate complex with antioxidant compounds. Saudi Pharm J. 2020;28(2):165-71.
145. Her S, Jaffray DA, Allen C. Gold Nanoparticles for Applications in Cancer Radiotherapy: Mechanisms and Recent Advancements. Adv Drug Deliv Rev. 2017;109:84-101.
146. Stankov K, Borisev I, Kojic V, Rutonjski L, Bogdanovic G, Djordjevic A. Modification of antioxidative and antiapoptotic genes expression in irradiated K562 cells upon fullerenol C60(OH)24 nanoparticle treatment. J NanosciNanotechnol. 2013;13(1):105-13.
147. Bogdanović V, Stankov K, Icević I, Zikic D, Nikolić A, Solajić S, et al. Fullerenol C60(OH)24 effects on antioxidative enzymes activity in irradiated human erythroleukemia cell line. J Radiat Res. 2008;49(3):321-7.
148. Mrdanović J, Solajić S, Bogdanović V, Stankov K, Bogdanović G, Djordjevic A. Effects of fullerenol C60(OH)24 on the frequency of micronuclei and chromosome aberrations in CHO-K1 cells. Mutat Res. 2009;680(1-2):25-30.
149. Li B, Wang F, Gui L, He Q, Yao Y, Chen H. The potential of biomimetic nanoparticles for tumor-targeted drug delivery. Nanomedicine (Lond). 2018;13(16):2099-118.
150. Chang DK, Li PC, Lu RM, Jane WN, Wu HC. Peptide-mediated liposomal Doxorubicin enhances drug delivery efficiency and therapeutic efficacy in animal models. PLoS One. 2013;8(12):e83239.
151. Thomas OS, Weber W. Overcoming Physiological Barriers to Nanoparticle Delivery-Are We There Yet? Front BioengBiotechnol. 2019;7:415.
152. Rosenblum D, Joshi N, Tao W, Karp JM, Peer D. Progress and challenges towards targeted delivery of cancer therapeutics. Nat Commun. 2018;9(1):1410.

153. Szczepanowicz K, Bzowska M, Kruk T, Karabasz A, Bereta J, Warszynski P. Pegylated polyelectrolyte nanoparticles containing paclitaxel as a promising candidate for drug carriers for passive targeting. Colloids Surf B Biointerfaces. 2016;143:463-71
154. Wu D, Si M, Xue H, Wong H. Nanomedicine applications in the treatment of breast cancer: current state of the art. Int J Nanomedicine. 2017;12:5879–92.
155. Mikada M, Sukhbaatar A, Miura Y, Horie S, Sakamoto M, Mori S, et al. Evaluation of the enhanced permeability and retention effect in the early stages of lymph node metastasis. Cancer Sci. 2017;108(5):846-52.
156. Velaei K, Samadi N, Barazvan B, Soleimani Rad J. Tumor microenvironment-mediated chemoresistance in breast cancer. Breast. 2016;30:92-100.
157. Wu Q, Yang Z, Nie Y, Shi Y, Fan D. Multi-drug resistance in cancer chemotherapeutics: mechanisms and lab approaches. Cancer Lett. 2014;347(2):159-66.
158. Du JZ, Li HJ, Wang J. Tumor-Acidity-Cleavable Maleic Acid Amide (TACMAA): A Powerful Tool for Designing Smart Nanoparticles To Overcome Delivery Barriers in Cancer Nanomedicine. AccChem Res. 2018;51(11):2848-56.
159. Chen WL, Yang SD, Li F, Qu CX, Liu Y, Wang Y, et al. Programmed pH/reduction-responsive nanoparticles for efficient delivery of antitumor agents in vivo. ActaBiomater. 2018;81:219-30.
160. Dong Y, Liao H, Fu H, Yu J, Guo Q, Wang Q, et al. pH-Sensitive Shell-Core Platform Block DNA Repair Pathway To Amplify Irreversible DNA Damage of Triple-negative Breast Cancer. ACS Appl Mater Interfaces. 2019;11(42):38417-28.
161. Dreaden EC, Morton SW, Shopsowitz KE, Choi JH, Deng ZJ, Cho NJ, et al. Bimodal Tumor-Targeting from Microenvironment Responsive Hyaluronan Layer-by-Layer (LbL) Nanoparticles. ACS Nano. 2014;8(8):8374–82
162. Ravar F, Saadat E, Gholami M, Dehghankelishadi P, Mahdavi M, Azami S, et al. Hyaluronic acid-coated liposomes for targeted delivery of paclitaxel, in-vitro characterization and in-vivo evaluation. J Control Release. 2016;229:10-22.
163. Zhang X, Liu J, Li X, Li F, Lee RJ, Sun F, et al. Trastuzumab-Coated Nanoparticles Loaded With Docetaxel for Breast Cancer Therapy. Dose Response. 2019;17(3):1559325819872583.
164. Correa S, Boehnke N, Barberio AE, Deiss-Yehiely E, Shi A, Oberlton B, et al. Tuning Nanoparticle Interactions with Ovarian Cancer through Layer-by-Layer Modification of Surface Chemistry. ACS Nano. 2020;14(2):2224-37.
165. Peiris PM, Toy R, Doolittle E, Pansky J, Abramowski A, Tam M, et al. Imaging Metastasis Using an Integrin-Targeting Chain-Shaped Nanoparticle. ACS Nano. 2012;10:8783–95.
166. Wang ZH, Yu Y, Dai WB, Cui J, Wu H, Yuan L, et al. A specific peptide ligand-modified lipid nanoparticle carrier for the inhibition of tumor metastasis growth. Biomaterials. 2013;3:756–64.

167. Kim MW, Jeong HY, Kang SJ, Jeong IH, Choi MJ, You YM, et al. Anti-EGF Receptor Aptamer-Guided Co-Delivery of Anti-Cancer siRNAs and Quantum Dots for Theranostics of Triple-Negative Breast Cancer. Theranostics. 2019;9(3):837-52.
168. Roncato F, Rruga F, Porcù E, Casarin E, Ronca R, MaccarinelliF, et al. Improvement and extension of anti-EGFR targeting in breast cancer therapy by integration with the Avidin-Nucleic-Acid-Nano-Assemblies. Nat Commun. 2018;9(1):4070.
169. Shu D, Li H, Shu Y, Xiong G, Carson WE 3rd, Haque F, et al. Systemic Delivery of Anti-miRNA for Suppression of Triple-negative Breast Cancer Utilizing RNA Nanotechnology. ACS Nano. 2015;9(10):9731-40.
170. Lale SV, Kumar A, Prasad S, Bharti AC, Koul V. Folic Acid and Trastuzumab Functionalized Redox Responsive Polymersomes for Intracellular Doxorubicin Delivery in Breast Cancer. Biomacromolecules. 2015;16(6):1736-52
171. Erdoğar N, Esendağlı G, Nielsen TT, Esendağlı-Yılmaz G, Yöyen-Ermiş D, Erdoğdu B, et al. Therapeutic efficacy of folate receptor-targeted amphiphilic cyclodextrin nanoparticles as a novel vehicle for paclitaxel delivery in breast cancer. J Drug Target. 2018;26(1):66-74
172. Ibrahim OM, El-Deeb NM, Abbas H, Elmasry SM, El-Aassar MR. Alginate based tamoxifen/metal dual core-folate decorated shell: Nanocomposite targeted therapy for breast cancer via ROS-driven NF-κB pathway modulation. Int J BiolMacromol. 2020;146:119-31.
173. Ledermann JA, Canevari S, Thigpen T. Targeting the folate receptor: diagnostic and therapeutic approaches to personalize cancer treatments. Ann Oncol. 2015;26(10):2034-43.
174. Correa S, Dreaden EC, Gu L, Hammond PT. Engineering nanolayered particles for modular drug delivery. J Control Release. 2016;240:364-86
175. Deng ZJ, Morton SW, Ben-Akiva E, Dreaden EC, Shopsowitz KE, Hammond PT. Layer-by-Layer Nanoparticles for Systemic Codelivery of an Anticancer Drug and siRNA for Potential Triple-Negative Breast Cancer Treatment. Acs Nano. 2013;7(11):9571-84.
176. Gu L, Deng ZJ, Roy S, Hammond PT. A Combination RNAi-Chemotherapy Layer-by-Layer Nanoparticle for Systemic Targeting of KRAS/P53 with Cisplatin to Treat Non-Small Cell Lung Cancer. Clin Cancer Res. 2017;23(23):7312-23.
177. Westedt U, Wittmar M, Hellwig M, Hanefeld P, Greiner A, Schaper AK, et al. Paclitaxel releasing films consisting of poly(vinyl alcohol)-graft-poly(lactide-coglycolide) and their potential as biodegradable stent coatings. J. Control. Release. 2006;111:235–46.
178. Frohlich E. The Role of Surface Charge in Cellular Uptake and Cytotoxicity of Medical Nanoparticles. Int. J. Nanomed. 2012;7:5577−91.
179. Alkilany AM, Nagaria PK, Hexel CR, Shaw TJ, Murphy CJ, Wyatt MD. Cellular uptake and cytotoxicity of gold nanorods: molecular origin of cytotoxicity and surface effects. Small. 2009;5(6):701-8.

180. Correa S, Choi KY, Dreaden EC, Renggli K, Shi A, Gu L, et al. Highly Scalable, Closed-Loop Synthesis of Drug-Loaded, Layer-by-Layer Nanoparticles. Adv. Funct. Mater. 2016;26(7):991-1003.
181. Poon Z, Lee JB, Morton SW, Hammond PT. Controlling In Vivo Stability and Biodistribution in Electrostatically Assembled Nanoparticles for Systemic Delivery. Nano Lett. 2011;11(5):2096–103
182. Liddle FJ, Alvarez JV, Poli V, Frank DA. Tyrosine phosphorylation is required for functional activation of disulfide-containing constitutively active STAT mutants. Biochemistry. 2006;45(17):5599-605.
183. Bromberg JF, Wrzeszczynska MH, Devgan G, Zhao Y, Pestell RG, C Albanese. Stat3 as an oncogene. Cell 1999;99(2):239.
184. Li L, Shaw PE. Elevated activity of STAT3C due to higher DNA binding affinity of phosphotyrosine dimer rather than covalent dimer formation. J Biol Chem. 2006;281(44):33172-81.
185. Louie SM, Grossman EA, Crawford LA, Ding L, Camarda R, Huffman TR, et al. GSTP1 Is a Driver of Triple-Negative Breast Cancer Cell Metabolism and Pathogenicity. Cell Chem. Biol. 2016;23(5):567–8.
186. Correa S, Boehnke N, Deiss-Yehiely E, Hammond PT. Solution Conditions Tune and Optimize Loading of Therapeutic Polyelectrolytes into Layer-by-Layer Functionalized Liposomes. ACS Nano 2019;13(5):5623-34.
187. Alvarez JV, Febbo PG, Ramaswamy S, Loda M, Richardson A, Frank DA. Identification of a genetic signature of activated signal transducer and activator of transcription 3 in human tumors. Cancer Res. 2005;65(12):5054-62.
188. Walker S, Wang C, Walradt T, Sil Hong B, Tanner JR, Levinsohn JL, et al. Identification of a Gain-Of-Function STAT3 Mutation (p.Y640F) in Lymphocytic Variant Hypereosinophilic Syndrome. Blood. 2016;127(7):948-51
189. Tošić I, Heppler LN, Egusquiaguirre SP, Boehnke N, Correa S, Costa D, et al. Lipidome-based Targeting of STAT3-driven Breast Cancer Cells Using Poly-L-glutamic acid-coated Layer-by-Layer Nanoparticles. Mol Cancer Ther. 2021; doi: 10.1158/1535-7163.MCT-20-0505.
190. Dechow TN, Pedranzini L, Leitch A, Leslie K, Gerald WL, Linkov I, et al. Requirement of matrix metalloproteinase-9 for the transformation of human mammary epithelial cells by Stat3-C. Proc Natl Acad Sci U S A. 2004;101(29):10602-7
191. Takakura A, Nelson EA, Haque N, Humphreys BD, Zandi-Nejad K, Frank DA, et al. Pyrimethamine inhibits adult polycystic kidney disease by modulating STAT signaling pathways. Hum Mol Genet. 2011;20(21):4143-54.
192. Chatzakos V, Slätis K, Djureinovic T, Helleday T, Hunt MC. N-acyl taurines are anti-proliferative in prostate cancer cells. Lipids. 2012;47(4):355-61.
193. Tang Y, Kim YS, Choi EJ, Hwang YJ, Yun YS, Bae SM, et al. Taurine Attenuates Epithelial-Mesenchymal Transition-Related Genes in Human Prostate Cancer Cells. Adv Exp Med Biol. 2017;975(2):1203-12

194. Schaffer SW, Jong CJ, Ramila KC, Azuma J. Physiological roles of taurine in heart and muscle. J Biomed Sci. 2010;17 Suppl 1:S2.
195. Lebrero P, Astudillo AM, Rubio JM, Fernández-Caballero L, Kokotos G, Balboa MA, et al. Cellular Plasmalogen Content Does Not Influence Arachidonic Acid Levels or Distribution in Macrophages: A Role for Cytosolic Phospholipase A2γ in Phospholipid Remodeling. Cells. 2019;8(8). pii: E799
196. Ren M, McGowan E, Li Y, Zhu X, Lu X, Zhu Z, et al. Saikosaponin-d Suppresses COX2 Through p-STAT3/C/EBPβ Signaling Pathway in Liver Cancer: A Novel Mechanism of Action. Front Pharmacol. 2019;10:623.
197. Zhu P, Zhou K, Lu S, Bai Y, Qi R, Zhang S. Modulation of aryl hydrocarbon receptor inhibits esophageal squamous cell carcinoma progression by repressing COX2/PGE2/STAT3 axis. J Cell Commun Signal. 2020; 14(2):175-92.
198. Thornber K, Colomba A, Ceccato L, Delsol G, Payrastre B, Gaits-Iacovoni F. Reactive oxygen species and lipoxygenases regulate the oncogenicity of NPM-ALK-positive anaplastic large cell lymphomas. Oncogene. 2009;28(29):2690-6.
199. Tong D, Liu Q, Liu G, Xu J, Lan W, Jiang Y, et al. Metformin inhibits castration-induced EMT in prostate cancer by repressing COX2/PGE2/STAT3 axis. Cancer Lett. 2017;389:23-32.
200. Kim W, Son B, Lee S, Do H, Youn BH. Targeting the enzymes involved in arachidonic acid metabolism to improve radiotherapy. Cancer and Metastasis Reviews. 2018;37:213–25
201. Liu T, Zhang D, Song W, Tang Z, Zhu J, Ma Z, et al. A Poly(l-Glutamic Acid)-Combretastatin A4 Conjugate for Solid Tumor Therapy: Markedly Improved Therapeutic Efficiency Through Its Low Tissue Penetration in Solid Tumor. Acta Biomater. 2017;53:179-89.
202. Li M, Song W, Tang Z, Lv S, Lin L, Sun H, et al. Nanoscaled poly(L-glutamic Acid)/Doxorubicin-Amphiphile Complex as pH-responsive Drug Delivery System for Effective Treatment of Nonsmall Cell Lung Cancer. ACS Appl Mater Interfaces. 2013;5(5):1781–92.
203. Weeber F, Ooft SN, Dijkstra KK, Voest EE. Tumor Organoids as a Pre-clinical Cancer Model for Drug Discovery. Cell Chem Biol. 2017;24(9):1092-100.
204. Hubert CG, Rivera M, Spangler LC, Wu Q, Mack SC, Prager BC, et al. A Three-Dimensional Organoid Culture System Derived From Human Glioblastomas Recapitulates the Hypoxic Gradients and Cancer Stem Cell Heterogeneity of Tumors Found In Vivo. Cancer Res. 2016;76(8):2465-77.
205. Wahba HA, El-Hadaad HA. Current approaches in treatment of triple-negative breast cancer. Cancer Biol Med. 2015;12(2):106–16
206. Jiang YZ, Ma D, Suo C, Shi J, Xue M, Hu X, et al. Genomic and Transcriptomic Landscape of Triple-Negative Breast Cancers: Subtypes and Treatment Strategies. Cancer Cell. 2019;35(3):428-40.e5

207. Zimta AA, Tigu AB, Muntean M, Cenariu D, Slaby O, Berindan-Neagoe I. Molecular Links between Central Obesity and Breast Cancer. Int J Mol Sci. 2019;20(21):5364.
208. Gallagher E, Novosyadlyy R, Yakar S, LeRoith D. The increased risk of cancer in obesity and type 2 diabetes: potential mechanisms. In: Poretsky L, editor. Principles of Diabetes Mellitus. Springer: US; 2010. p. 579–99.
209. Calle EE, Rodriguez C, Walker-Thurmond K, Thun MJ. Overweight, obesity, and mortality from cancer in a prospectively studied cohort of U.S. adults. N Engl J Med 2003;348:1625–38.
210. He JY, Wei XH, Li SJ, Liu Y, Hu HL, Li ZZ, et al. Adipocyte-derived IL-6 and leptin promote breast Cancer metastasis via upregulation of Lysyl Hydroxylase-2 expression. Cell Commun Signal. 2018;16:100.
211. Gyamfi J, Lee YH, Min BS, Choi J. Niclosamide reverses adipocyte induced epithelial-mesenchymal transition in breast cancer cells via suppression of the interleukin-6/STAT3 signalling axis. Sci Rep. 2019;9:11336.
212. Gyamfi J, Lee YH, Eom M, Choi J. Interleukin-6/STAT3 signalling regulates adipocyte induced epithelial-mesenchymal transition in breast cancer cells. Sci Rep. 2018;8:8859.
213. S O'Neill, L O'Driscoll. Metabolic Syndrome: A Closer Look at the Growing Epidemic and Its Associated Pathologies. Obes Rev. 2015;16(1):1-12
214. Menendez JA. Fine-tuning the lipogenic/lipolytic balance to optimize the metabolic requirements of cancer cell growth: molecular mechanisms and therapeutic perspectives. Biochim Biophys Acta. 2010;1801(3):381-91.
215. Vidavsky N, Kunitake JAMR, Diaz-Rubio ME, Chiou AE, Loh HC, Zhang S, et al. Mapping and Profiling Lipid Distribution in a 3D Model of Breast Cancer Progression. ACS Cent Sci. 2019;5(5):768–80.
216. Kauraniemi P, Bärlund M, Monni O, Kallioniemi A. New amplified and highly expressed genes discovered in the ERBB2 amplicon in breast cancer by cDNA microarrays. Cancer Res. 2001;61(22):8235-40.
217. Kourtidis A, Srinivasaiah R, Carkner RD, Brosnan MJ, Conklin DS. Peroxisome proliferator-activated receptor-gamma protects ERBB2-positive breast cancer cells from palmitate toxicity. Breast Cancer Res. 2009;11(2):R16.
218. Lodhi IJ, Semenkovich CF. Peroxisomes: A Nexus for Lipid Metabolism and Cellular Signaling. Cell Metab. 2014;19(3):380-92.
219. Wang D, Zhou Y, Lei W, Zhang K, Shi J, Hu Y, et al. Signal transducer and activator of transcription 3 (STAT3) regulates adipocyte differentiation via peroxisome-proliferator-activated receptor γ (PPARγ). Biol Cell. 2009;102(1):1-12
220. Menendez JA, Lupu R. Fatty Acid Synthase (FASN) as a Therapeutic Target in Breast Cancer. Expert Opin Ther Targets. 2017;21(11):1001-16.
221. Wu J, Du J, Fu X, Liu B, Cao H, Li T, et al. Iciartin, a Novel FASN Inhibitor, Exerts Anti-Melanoma Activities Through IGF-1R/STAT3 Signaling. Oncotarget. 2016;7(32):51251-69.

222. Gao P, Wang LL, Liu J, Dong F, Song W, Liao L, et al. Dihydroartemisinin Inhibits Endothelial Cell Tube Formation by Suppression of the STAT3 Signaling Pathway. Life Sci. 2020;242:117221.
223. Menendezab JA, Vellon L, Lupu R. Targeting fatty acid synthase-driven lipid rafts: a novel strategy to overcome trastuzumab resistance in breast cancer cells. Med Hypotheses. 2005;64(5):997-1001.
224. Vazquez-Martin A, Colomer R, Brunet J, Menendez JA. Inhibition of fatty acid synthase reverses autoresistance to trastuzumab in breast cancer: Pharmacological blockade of fatty acid synthase (FASN) reverses acquired autoresistance to trastuzumab (Herceptin by transcriptionally inhibiting 'HER2 super-expression' occurring in high-dose trastuzumab-conditioned SKBR3/Tzb100 breast cancer cells. Int J Oncol. 2007;31(4):769-76.
225. Qu Q, Zeng F, Liu X, Wang QJ, Deng F. Fatty acid oxidation and carnitine palmitoyltransferase I: emerging therapeutic targets in cancer. Cell Death Dis. 2016;7(5):e2226.
226. Li J, Zhao S, Zhou X, Zhang T, Zhao L, Miao P et al. Inhibition of lipolysis by mercaptoacetate and etomoxir specifically sensitize drug-resistant lung adenocarcinoma cell to paclitaxel. PLoS One 2013;8:e74623
227. Wu Y, Zhang S, Gong X, Tam S, Xiao D, Liu S, et al. The epigenetic regulators and metabolic changes in ferroptosis-associated cancer progression. Mol Cancer. 2020;19:39.
228. Zheng K, Chen Z, Feng H, Chen Y, Zhang C, Yu J, et al. Sphingomyelin synthase 2 promotes an aggressive breast cancer phenotype by disrupting the homoeostasis of ceramide and sphingomyelin. Cell Death Dis. 2019;10(3):157.
229. Maleki V, Mahdavi R, Hajizadeh-Sharafabad F, Alizadeh M. The effects of taurine supplementation on oxidative stress indices and inflammation biomarkers in patients with type 2 diabetes: a randomized, double-blind, placebo-controlled trial. Diabetol Metab Syndr. 2020;12:9
230. He F, Ma N, Midorikawa K, Hiraku Y, Oikawa S, Mo Y, et al. Anti-Cancer Mechanisms of Taurine in Human Nasopharyngeal Carcinoma Cells. Adv Exp Med Biol. 2019;1155:533-41
231. Zhang X, Lu H, Wang Y, Liu C, Zhu W, Zheng S, et al. Taurine induces the apoptosis of breast cancer cells by regulating apoptosis-related proteins of mitochondria. Int J Mol Med. 2015;35(1):218-26.
232. Seidel U, Huebbe P, Rimbach G. Taurine: A Regulator of Cellular Redox Homeostasis and Skeletal Muscle Function. Mol Nutr Food Res. 2019;63(16):e1800569
233. Schaffer SW, Azuma J, Madura JD. Mechanisms underlying taurine-mediated alterations in membrane function. Amino Acids. 1995;8:231-46
234. Oliveira MWS, Minotto JB, de Oliveira MR, Zanotto-Filho A, Behr GA, Rocha RF, et al. Scavenging and Antioxidant Potential of Physiological Taurine

Concentrations Against Different Reactive oxygen/nitrogen Species. Pharmacol Rep. 2010;62(1):185-93.
235. Li F, Qi J, Qin C, Fu Z, Ren W. Taurolidine promotes cell apoptosis by enhancing GRIM-19 expression in liver cancer. Oncol Rep. 2018;40(6):3743-51.
236. Kim KS, Kim SH. Effect of N-(D-Ribopyranosyl) Taurine Sodium Salt on the Differentiation of Human Preadipocytes and Expression of Adipokines Through Inhibition of STAT-3 Signaling in Differentiated Human Adipocytes. Adv Exp Med Biol. 2017;975:667-74.
237. Yarlaa NS, Bishayeeb A, Sethi G, Reddannae P, Kalle AM, Dhananjaya BL, et al. Targeting arachidonic acid pathway by natural products for cancer prevention and therapy. Semin Cancer Biol. 2016;40-41:48-81.
238. Xu H, Lin F, Wang Z, Yang L, Meng J, Ou Z, et al. CXCR2 Promotes Breast Cancer Metastasis and Chemoresistance via Suppression of AKT1 and Activation of COX2. Cancer Lett. 2018;412:69-80.
239. Bos PD, Zhang XHF, Nadal C, Shu W, Gomis RR, Nguyen DX, et al. Genes That Mediate Breast Cancer Metastasis to the Brain. Nature. 2009;459(7249):1005-9
240. Nandi P, Girish GV, Majumder M, Xin X, Tutunea-Fatan E, Lala PK. PGE2 promotes breast cancer-associated lymphangiogenesis by activation of EP4 receptor on lymphatic endothelial cells. BMC Cancer. 2017;17(1):11.
241. Ristimäki A, Sivula A, Lundin J, Lundin M, Salminen T, Haglund C, et al. Prognostic significance of elevated cyclooxygenase-2 expression in breast cancer. Cancer Res. 2002;62(3):632-5.
242. Denkert C, Winzer KJ, Müller BM, Weichert W, Pest S, Köbel M, et al. Elevated expression of cyclooxygenase-2 is a negative prognostic factor for disease free survival and overall survival in patients with breast carcinoma. Cancer. 2003;97(12):2978-87
243. McFadden DW, Riggs DR, Jackson BJ, Cunningham C. Additive effects of Cox-1 and Cox-2 inhibition on breast cancer in vitro. Int J Oncol. 2006;29(4):1019-23.
244. Farivar-Mohseni H, Kandzari SJ, Zaslau S, Riggs DR, Jackson BJ, McFadden DW. Synergistic effects of Cox-1 and -2 inhibition on bladder and prostate cancer in vitro. Am J Surg. 2004;188(5):505-10.
245. Dobrian AD, Lieb DC, Cole BK, Taylor-Fishwick DA, Chakrabarti SK, Nadler JL. Functional and pathological roles of the 12- and 15-lipoxygenases. Prog Lipid Res. 2011;50(1):115–31.
246. D'Autréaux B, Toledano MB. ROS as signalling molecules: mechanisms that generate specificity in ROS homeostasis. Nat Rev Mol Cell Biol. 2007;8:813–24.
247. Hammamieh R, Sumaida D, Zhang X, Das R, Jett M. Control of the growth of human breast cancer cells in culture by manipulation of arachidonate metabolism. BMC Cancer. 2007;7:138.
248. Orafaie A, Matin MM, Sadeghian H. The Importance of 15-lipoxygenase Inhibitors in Cancer Treatment. Cancer Metastasis Rev. 2018;37(2-3):397-408.

249. Lee SI, Zuo X, Shureiqi I. 15-Lipoxygenase-1 as a Tumor Suppressor Gene in Colon Cancer: Is the Verdict In? Cancer Metastasis Rev. 2011;30(3-4):481-91.
250. Chang J, Tang N, Fang Q, Zhu K, Liu L, Xiong X, et al. Inhibition of COX-2 and 5-LOX Regulates the Progression of Colorectal Cancer by Promoting PTEN and Suppressing PI3K/AKT Pathway. Biochem Biophys Res Commun. 2019;517(1):1-7.
251. Chen EP, Smyth EM. COX-2 and PGE2-dependent immunomodulation in breast cancer. Prostaglandins Other Lipid Mediat. 2011;96(1-4):14-20.
252. Kumar R, Singh AK, Kumar M, Shekhar S, Rai N, Kaur P, et al. Serum 5-LOX: a progressive protein marker for breast cancer and new approach for therapeutic target. Carcinogenesis. 2016;37(9):912-7.
253. Avis I, Hong SH, Martinez A, Moody T, Choi YH, Trepel J, et al. Five-lipoxygenase inhibitors can mediate apoptosis in human breast cancer cell lines through complex eicosanoid interactions. FASEB J. 2001;15(11):2007-9.
254. Chatterjee M, Das S, Janarthan M, Ramachandran HK, Chatterjee M. Role of 5-lipoxygenase in Resveratrol Mediated Suppression of 7,12-dimethylbenz(α)anthracene-induced Mammary Carcinogenesis in Rats. Eur J Pharmacol. 2011;668(1-2):99-106.
255. Chen Y, Hu Y, Zhang H, Peng C, Li S. Loss of the Alox5 gene impairs leukemia stem cells and prevents chronic myeloid leukemia. Nat Genet. 2009;41(7):783–92.
256. Rossen NS, Hansen AJ, Selhuber-Unkel C, Oddershede LB. Arachidonic Acid Randomizes Endothelial Cell Motion and Regulates Adhesion and Migration. PLoS One. 2011;6(9):e25196.
257. Pan L, Chen X, Fu S, Yu W, Li C, Wang T, et al. LLY17, a novel small molecule STAT3 inhibitor induces apoptosis and suppresses cell migration and tumor growth in triple-negative breast cancer. Breast Cancer Res Treat. 2020;181(1):31-41.
258. Khan MW, Saadalla A, Ewida AH, Al-Katranji K, Al-Saoudi G, Giaccone ZT, et al. The STAT3 inhibitor pyrimethamine displays anti-cancer and immune stimulatory effects in murine models of breast cancer. Cancer Immunol Immunother. 2018;67(1):13-23.
259. Xiang M, Kim H, Ho VT, Walker SR, Bar-Natan M, Anahtar M, et al. Gene expression–based discovery of atovaquone as a STAT3 inhibitor and anticancer agent. Blood. 2016;128(14):1845–53.
260. Nelson EA, Walker SR, Kepich A, Gashin LB, Hideshima T, Ikeda H, et al. Nifuroxazide inhibits survival of multiple myeloma cells by directly inhibiting STAT3. Blood. 2008;112(13):5095–102.
261. Wong ALA, Hirpara JL, Pervaiz S, Eu JQ, Sethi G, Goh BC. Do STAT3 inhibitors have potential in the future for cancer therapy? Expert Opin Investig Drugs. 2017;26:883–7
262. Nagel-Wolfrum K, Buerger C, Wittig I, Butz K, Hoppe-Seyler F, Groner B. The interaction of specific peptide aptamers with the DNA binding domain and the

dimerization domain of the transcription factor Stat3 inhibits transactivation and induces apoptosis in tumor cells. Mol. Cancer Res. 2004;2,170−82.
263. Ma Y, Zhang X, Xu X, Shen L, Yao Y, Yang Z, et al. STAT3 Decoy Oligodeoxynucleotides-Loaded Solid Lipid Nanoparticles Induce Cell Death and Inhibit Invasion in Ovarian Cancer Cells. PLoS One. 2015;10(4):e0124924.
264. Liang Z, Wang H, Guo B, Li F, Liu J, Liu Z, et al. Inhibition of prostate cancer RM1 cell growth in vitro by hydroxyapatite nanoparticle-delivered short hairpin RNAs against Stat3. Mol Med Rep. 2017;16(1):459-65.
265. Ashrafizadeh M, Ahmadi Z, Kotla NG, Afshar EG, Samarghandian S, Mandegary A, et al. Nanoparticles Targeting STATs in Cancer Therapy. Cells. 2019;8(10):1158
266. Chen G, Wang Y, Wu P, Zhou Y, Yu F, Zhu C, et al. Reversibly Stabilized Polycation Nanoparticles for Combination Treatment of Early- And Late-Stage Metastatic Breast Cancer. ACS Nano. 2018;12(7):6620-36.
267. Shen J, Xu R, Mai J, Kim HC, Guo X, Qin G, et al. High Capacity Nanoporous Silicon Carrier for Systemic Delivery of Gene Silencing Therapeutics. ACS Nano. 2013;7(11):9867-80.
268. Kleinman ME, Yamada K, Takeda A, Chandrasekaran V, Nozaki M, Baffi JZ, et al. Sequence- and target-independent angiogenesis suppression by siRNA via TLR3. Nature. 2008;452:591–7
269. Setten RL, Rossi JJ, Si-Ping H. The current state and future directions of RNAi-based therapeutics. Nat Rev Drug Discov. 2019;18(6):421-46.
270. Garg SM, Vakili MR, Molavi O, Lavasanifar A. Self-Associating Poly (ethylene oxide)-block-poly (α-carboxyl-ε-caprolactone) Drug Conjugates for the Delivery of STAT3 Inhibitor JSI-124: Potential Application in Cancer Immunotherapy. Mol. Pharm. 2017;14:2570–84
271. Molavi O, Ma Z, Hamdy S, Lavasanifar A, Samuel J. Immunomodulatory and anticancer effects of intra-tumoral co-delivery of synthetic lipid A adjuvant and STAT3 inhibitor, JSI-124. Immunopharmacol. Immunotoxicol. 2009;31:214–21
272. Saini U, Naidu S, ElNaggar AC, Bid HK, Wallbillich JJ, Bixel K, et al. Elevated STAT3 expression in ovarian cancer ascites promotes invasion and metastasis: a potential therapeutic target. Oncogene. 2017;36(2):168-81.
273. Moreira MP, da Conceicao Braga L, Cassali GD, Silva LM. STAT3 as a promising chemoresistance biomarker associated with the CD44(+/high)/CD24(−/low)/ALDH(+) BCSCs-like subset of the triple-negative breast cancer (TNBC) cell line. Exp Cell Res. 2018;363(2):283–90.
274. Zhu X, Shen H, Yin X, Long L, Chen X, Feng F, et al. IL-6R/STAT3/miR-204 feedback loop contributes to cisplatin resistance of epithelial ovarian cancer cells. Oncotarget. 2017; 8(24):39154–66.
275. Cheng CC, Shi LH, Wang XJ, Wang SX, Wan XQ, Liu SR, et al. Stat3/Oct-4/c-Myc signal circuit for regulating stemness-mediated doxorubicin resistance of

triple-negative breast cancer cells and inhibitory effects of WP1066. Int J Oncol. 2018;53(1):339–48.
276. Guo Q, Lu L, Liao Y, Wang X, Zhang Y, Liu Y, et al. Influence of c-Src on hypoxic resistance to paclitaxel in human ovarian cancer cells and reversal of FV-429. Cell Death Dis. 2018;8(1):e3178.
277. Ji T, Gong D, Han Z, Wei X, Yan Y, Ye F, et al. Abrogation of constitutive Stat3 activity circumvents cisplatin resistant ovarian cancer. Cancer Lett. 2013;341(2):231-9.
278. Hu Y, Yagüe E, Zhao J, Wang L, Bai J, Yang Q, et al. Sabutoclax, pan-active BCL-2 protein family antagonist, overcomes drug resistance and eliminates cancer stem cells in breast cancer. Cancer Lett. 2018;423:47-59.
279. Yun M, Lee D, Park MN, Kim EO, Sohn EJ, Kwon BM, et al. Cinnamaldehyde Derivative (CB-PIC) Sensitizes Chemo-Resistant Cancer Cells to Drug-Induced Apoptosis via Suppression of MDR1 and Its Upstream STAT3 and AKT Signaling. Cell Physiol Biochem. 2015;35(5):1821-30.
280. Fang Z, Chen W, Yuan Z, Liu X, Jiang H. LncRNA-MALAT1 Contributes to the Cisplatin-Resistance of Lung Cancer by Upregulating MRP1 and MDR1 via STAT3 Activation. Biomed Pharmacother. 2018;101:536-42
281. Ji L, Liu X, Zhang S, Tang S, Yang S, Li S, et al. The Novel Triazolonaphthalimide Derivative LSS-11 Synergizes the Anti-Proliferative Effect of Paclitaxel via STAT3-Dependent MDR1 and MRP1 Downregulation in Chemoresistant Lung Cancer Cells. Molecules. 2017;22(11):1822.
282. Liu CY, Su JC, Huang TT, Chu PY, Huang CT, Wang WL, et al. Sorafenib analogue SC-60 induces apoptosis through the SHP-1/STAT3 pathway and enhances docetaxel cytotoxicity in triple-negative breast cancer cells. Mol Oncol. 2017;11(3):266-79.
283. Shadyro OI, Yurkova IL, Kisel MA. Radiation-induced Peroxidation and Fragmentation of Lipids in a Model Membrane. Int J Radiat Biol. 2002;78(3):211-7.
284. Prasad NR, Menon VP, Vasudev V, Pugalendi KV. Radioprotective Effect of Sesamol on Gamma-Radiation Induced DNA Damage, Lipid Peroxidation and Antioxidants Levels in Cultured Human Lymphocytes. Toxicology. 2005;209(3):225-35.
285. Srinivasan M, Devipriya N, Kalpana KB, Menon VP. Lycopene: An Antioxidant and Radioprotector Against Gamma-Radiation-Induced Cellular Damages in Cultured Human Lymphocytes. Toxicology. 2009;262(1):43-9.
286. Benderitter M, Vincent-Genod L, Pouget JP, Voisin P. The Cell Membrane as a Biosensor of Oxidative Stress Induced by Radiation Exposure: A Multiparameter Investigation. Radiat Res. 2003;159(4):471-83.
287. Lu L, Dong J, Wang L, Xia Q, Zhang D, Kim H, et al. Activation of STAT3 and Bcl-2 and reduction of reactive oxygen species (ROS) promote radioresistance in breast cancer and overcome of radioresistance with niclosamide. Oncogene. 2018;37(39):5292-304.

288. Liu Y, Zhang P, Li F, Jin X, Li J, Chen W, et al. Metal-based NanoEnhancers for Future Radiotherapy: Radiosensitizing and Synergistic Effects on Tumor Cells. Theranostics. 2018;8(7):1824–49.
289. Verhoeven Y, Tilborghs S, Jacobs J, De Waele J, Quatannens D, Deben C. The potential and controversy of targeting STAT family members in cancer. Semin Cancer Biol. 2020;60:41-56.
290. Fares J, Kanojia D, Rashidi A, Ulasov I, Lesniak MS. Genes that Mediate Metastasis across the Blood-Brain Barrier. Trends Cancer. 2020;6(8):660-76.

План третмана података

Назив пројекта/истраживања

Утицај *in vitro* излагања СТАТ3-активираних малигних ћелија дојке вишеслојним наночестицама обложеним поли-Л-глутаминском киселином.

Назив институције/институција у оквиру којих се спроводи истраживање

а) Department of Medical Oncology, Dana-Farber Cancer Institute, Boston, MA, USA

б) Harvard Center for Biological Imaging, Harvard University, Cambridge, MA, USA

в) Koch Institute for Integrative Cancer Research, Massachusetts Institute of Technology, Cambridge, MA, USA

г) Медицински Факултет Универзитета у Новом Саду

Назив програма у оквиру ког се реализује истраживање

Докторске академске студије, претклиничка испитивања

1. Опис података

1.1 Врста студије

Укратко описати тип студије у оквиру које се подаци прикупљају

Експериментални рад на ћелијским линијама епитела дојке уз примену савремене врсте наночестица и актуелних метода молекуларне биологије.

1.2 Врсте података

а) квантитативни

б) квалитативни

1.3. Начин прикупљања података

а) анкете, упитници, тестови

б) клиничке процене, медицински записи, електронски здравствени записи

в) генотипови: навести врсту _____

г) административни подаци: База података генске експресије узорака тумора 129 пацијената

оболелих од карцинома дојке GSE5460 (*Gene Expression Omnibus*, GEO); база података генске експресије 353 узорка здравог немалигног ткива GSE3526 (*Gene Expression Omnibus*, GEO); база података генске експресије ћелијских линија карцинома оваријума (*Cancer Cell Line Encyclopedia*, CCLE).

д) узорци ткива: нетрансформисана ћелијска линија епитела дојке MCF-10A и троструко-негативне ћелијске линије карцинома дојке MDA-MB-468, MDA-MB-231 и SUM159PT.

ђ) снимци, фотографије: микрографије ћелијских линија култивисаних у једном слоју или у виду тродимензионалних ћелијских органоида и третираних флуоресцентно обележеним наночестицама израђене конфокалним флуоресцентним микроскопом; Western blot слике за анализу експресије и фосфорилације протеина.

е) текст, навести врсту _____

ж) мапа, навести врсту _____

з) остало: Експериментален рад на ћелијским линијама коришћењем метода молекуларне биологије; биоинформатичке методе прикупљања и обраде података.

1.3 Формат података, употребљене скале, количина података

Табеле (4), графикони (105), микрографије и Western blot слике (50). Подаци су приказани као релативни компаративни односи генске експресије, нивоа ћелијског присуства метаболита, степена везивања наночестица и ћелијске вијабилности у виду корелације између контролних и третираних ћелија.

1.3.1 Употребљени софтвер и формат датотеке:

a) Excel фајл, датотека _____

b) SPSS фајл, датотека _____

c) PDF фајл, датотека _____

d) Текст фајл, датотека _____

e) JPG фајл, датотека _____

f) Остало, датотека _____

1.3.2. Број записа (код квантитативних података)

а) број варијабли: Велики број варијабли

б) број мерења (испитаника, процена, снимака и сл.): Сваки биолошки експеримент је независно изведен најмање два пута, у оквиру којих је сваки биолошки узорак припремљен у најмање три реплике уколико није другачије назначено.

1.3.3. Поновљена мерења

а) да

б) не

Уколико је одговор да, одговорити на следећа питања:

а) временски размак између поновљених мера је: најмање две недеље, у зависности од експеримента.

б) варијабле које се више пута мере односе се на реплике биолошких експеримената.

в) нове верзије фајлова који садрже поновљена мерења су именоване као _____

Напомене: _____

Да ли формати и софтвер омогућавају дељење и дугорочну валидност података?

а) Да

б) Не

Ако је одговор не, образложити _____

_____

2. Прикупљање података

2.1 Методологија за прикупљање/генерисање података

2.1.1. У оквиру ког истраживачког нацрта су подаци прикупљени?

а) експеримент, навести тип: квантитативна ланчана реакција полимеразе уз реверзну транскриптазу (*quantitative reverse transcriptase polymerase chain reaction*, qRT-PCR); Western blot; утишавање генске експресије коришћењем малих интерферирајућих РНК, сиРНК; течна хроматографија куплована са тандемском масеном спектрометријом; проточно цитометријско одређивање ћелијског везивања наночестица; тестови ћелијске вијабилности на бази луминисценције зависне од количине ћелијског ATP-а и тестови вијабилности флуоресцентним бојењем помоћу анексин V/пропидијум јодида и анализа проточном цитометријом.

б) корелационо истраживање, навести тип: У свим претходно наведеним експериментима је

анализирана корелација између података добијених за контролни и узорак третиран испитиваним третманом.

ц) анализа текста, навести тип _____

д) остало, навести шта _____

2.1.2 Навести врсте мерних инструмената или стандарде података специфичних за одређену научну дисциплину (ако постоје).

QuantStudio 6 Flex Real-Time PCR System (Applied Biosystems), Agilent 6430 i 6460 QQQ LC-MS/MS (Agilent Technologies), MyECL Imager (ThermoFisher Scientific), HPLC (Agilent), CellObserver (Zeiss), Applied Precision DeltaVision Ultimate Focus Microscope with TIRF Module (Inverted Olympus X71 microscope), BD LRSFortessa (BD Biosciences), LSM 880+ Airyscan (Zeiss), Luminoskan Ascent (ThermoFisher Scientific).

2.2 Квалитет података и стандарди

2.2.1. Третман недостајућих података

а) Да ли матрица садржи недостајуће податке? Да **Не**

Ако је одговор да, одговорити на следећа питања:

а) Колики је број недостајућих података? _____

б) Да ли се кориснику матрице препоручује замена недостајућих података? Да Не

в) Ако је одговор да, навести сугестије за третман замене недостајућих података

_____

2.2.2. На који начин је контролисан квалитет података? Описати

Квалитет података је контролисан коришћењем реплика при сваком биолошком експерименту и применом статистичких тестова. Сваки биолошки експеримент је изведен најмање два пута.

2.2.3. На који начин је извршена контрола уноса података у матрицу?

Подаци су преузимани директно и искључиво са експерименталних инструмената на којима је вршена анализа.

3. Третман података и пратећа документација

3.1. Третман и чување података

3.1.1. Подаци ће бити депоновани у _____ репозиторијум.

3.1.2. URL адреса _____

3.1.3. DOI _____

3.1.4. Да ли ће подаци бити у отвореном приступу?

а) Да

б) Да, али после ембарга који ће трајати до _____

в) Не

Ако је одговор не, навести разлог _____

3.1.5. Подаци неће бити депоновани у репозиторијум, али ће бити чувани.

Образложење

_____

_____

3.2 Метаподаци и документација података

3.2.1. Који стандард за метаподатке ће бити примењен? _____

3.2.1. Навести метаподатке на основу којих су подаци депоновани у репозиторијум.

_____

_____

Ако је потребно, навести методе које се користе за преузимање података, аналитичке и

процедуралне информације, њихово кодирање, детаљне описе варијабли, записа итд.

_____

_____

_____

_____

3.3 Стратегија и стандарди за чување података

3.3.1. До ког периода ће подаци бити чувани у репозиторијуму? _____

3.3.2. Да ли ће подаци бити депоновани под шифром? **Да** Не

3.3.3. Да ли ће шифра бити доступна одређеном кругу истраживача? **Да** Не

3.3.4. Да ли се подаци морају уклонити из отвореног приступа после извесног времена?

Да **Не**

Образложити

_____

_____

4. Безбедност података и заштита поверљивих информација

Овај одељак МОРА бити попуњен ако ваши подаци укључују личне податке који се односе на учеснике у истраживању. За друга истраживања треба такође размотрити заштиту и сигурност података.

4.1 Формални стандарди за сигурност информација/података

Истраживачи који спроводе испитивања с људима морају да се придржавају Закона о заштити података о личности *(https://www.paragraf.rs/propisi/zakon_o_zastiti_podataka_o_licnosti.html)* и одговарајућег институционалног кодекса о академском интегритету.

4.1.2. Да ли је истраживање одобрено од стране етичке комисије? Да **Не**

Ако је одговор Да, навести датум и назив етичке комисије која је одобрила истраживање

Истраживање је спроведено *in vitro* на експерименталним ћелијским линијама, те је на Институту Дана Фарбер, Универзитет Харвард, САД, 20.јануара 2020. издат документ од стране Директора медицинских истраживања, који потврђује да одобрење етичког комитета није потребно за *in vitro* истраживање.

4.1.2. Да ли подаци укључују личне податке учесника у истраживању? Да **Не**

Ако је одговор да, наведите на који начин сте осигурали поверљивост и сигурност информација везаних за испитанике:

а) Подаци нису у отвореном приступу

б) Подаци су анонимизирани

ц) Остало, навести шта

_____

_____

5. Доступност података

5.1. Подаци ће бити

а) јавно доступни

б) доступни само уском кругу истраживача у одређеној научној области

ц) затворени

Ако су подаци доступни само уском кругу истраживача, навести под којим условима могу да их користе:

_____

_____

Ако су подаци доступни само уском кругу истраживача, навести на који начин могу приступити подацима:

_____

_____

5.4. Навести лиценцу под којом ће прикупљени подаци бити архивирани.

Ауторство – некомерцијално – делити под истим условима.

6. Улоге и одговорност

6.1. Навести име и презиме и мејл адресу власника (аутора) података

Исидора Тошић, isidora.tosic@mf.uns.ac.rs

6.2. Навести име и презиме и мејл адресу особе која одржава матрицу с подацима

Исидора Тошић, isidora.tosic@mf.uns.ac.rs

6.3. Навести име и презиме и мејл адресу особе која омогућује приступ подацима другим истраживачима

Исидора Тошић, isidora.tosic@mf.uns.ac.rs